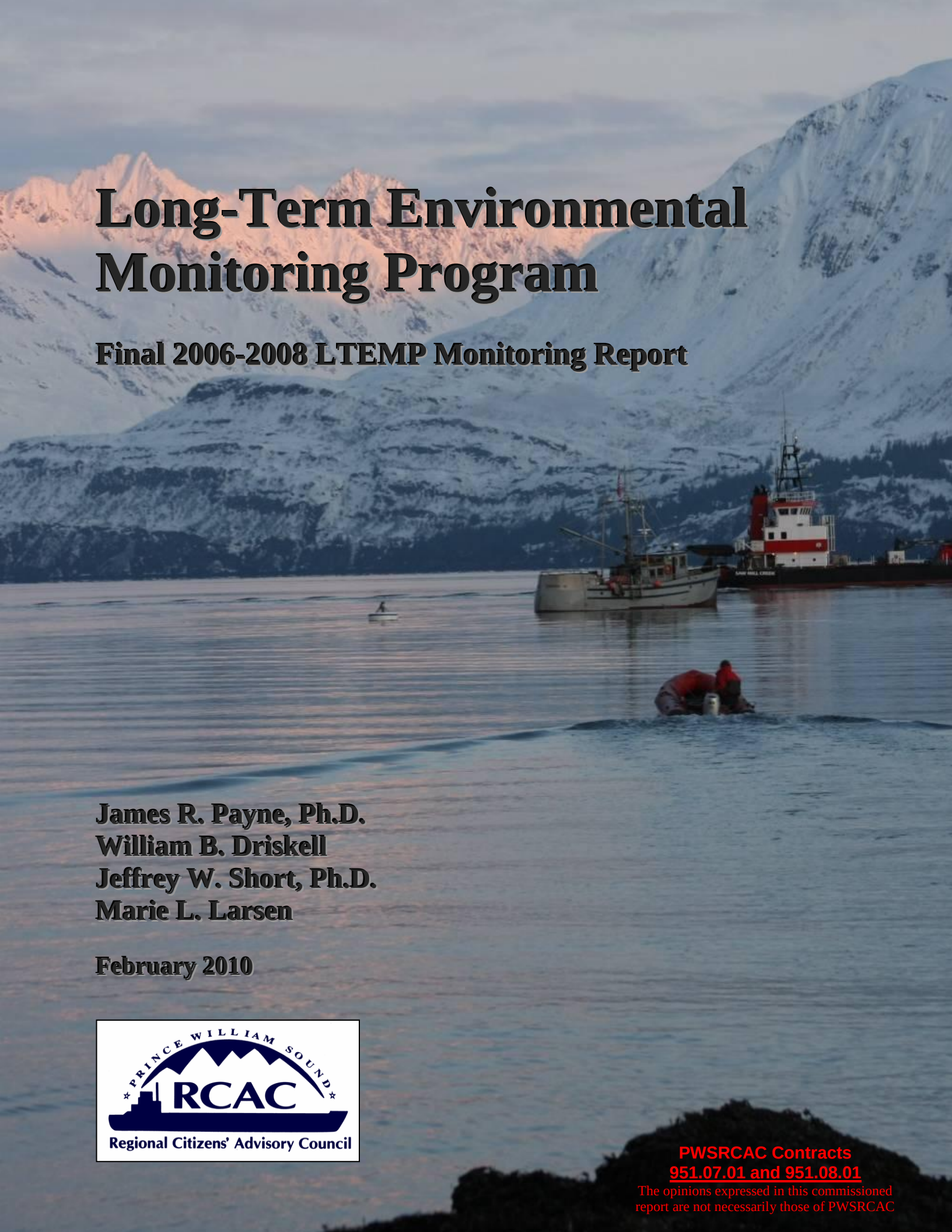

Long-Term Environmental Monitoring Program

Final 2006-2008 LTEMP Monitoring Report

James R. Payne, Ph.D.
William B. Driskell
Jeffrey W. Short, Ph.D.
Marie L. Larsen

February 2010

PWSRCAC Contracts
951.07.01 and 951.08.01

CONTENTS

FIGURES

TABLES

Photo Credits

Cover photo of Port Valdez by Bill Driskell;
Photo on this page by Dave Janka showing Payne and Driskell sampling sediments in Port Valdez.
Figure 23 by Bill Driskell
Appendix E – various by Driskell or Payne

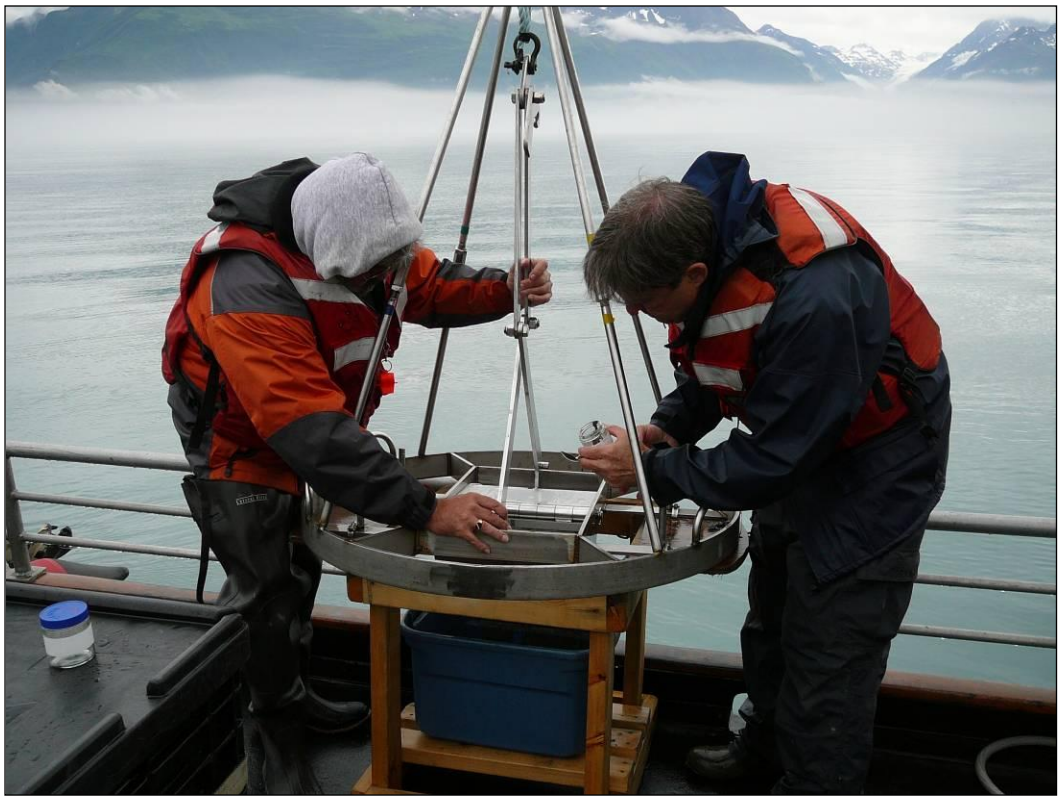

ABBREVIATIONS

Stations:

AMT	Alyeska Marine Terminal, Port Valdez
AIB	Aialik Bay, west of Seward
COH	Constantine Harbor, Hinchinbrook Entrance, PWS
DII	Disk Island, Knight Island Group, western PWS
GOC	Gold Creek, Port Valdez
KNH	Knowles Head, eastern PWS
SHB	Sheep Bay, eastern PWS
SHH	Shuyak Harbor, Kodiak
SLB	Sleepy Bay, Latouche Island, western PWS
WIB	Windy Bay, Outer Kenai Peninsula
ZAB	Zaikof Bay, Montague Island, central PWS

ABL	NOAA/NMFS Auke Bay Laboratory, Juneau AK
AHC	aliphatic hydrocarbons (same as saturated hydrocarbons – SHC)
ANS	Alaskan North Slope
BWTF	Alyeska Terminal's Ballast Water Treatment Facility
DSI	Dissolved Signal Index
EVOS	*Exxon Valdez* oil spill
EVTHD	*Exxon Valdez* Trustees Hydrocarbon Database
EMAP	US EPA Environmental Monitoring and Assessment Program
GC/FID	gas chromatography/flame ionization detector
GC/MS	gas chromatography/mass spectrometry
GERG	Geochemical and Environmental Research Group, Texas A&M University
KLI	Kinnetic Laboratories, Inc., Anchorage AK
MDL	analytic method detection limit
NIST	National Institute of Standards and Technology
NMFS	National Marine Fisheries Service
NOAA	National Oceanographic and Atmospheric Administration
PAH	polycyclic (or polynuclear) aromatic hydrocarbons
PECI	Payne Environmental Consultants, Inc., Encinitas, CA
PGS	particle grain size
PSI	Particulate Signal Index
PWS	Prince William Sound
RCAC	Regional Citizens Advisory Council
SAC	Scientific Advisory Committee for PWSRCAC
SCAT	Shoreline Cleanup Assessment Team
SHC	saturated hydrocarbons (same as AHC: n-alkanes + pristane and phytane)
SIM	selected ion monitoring
SRM	NIST standard reference material
TAHC	total AHC
TIC	total inorganic carbon
TOC	total organic carbon
TPAH	total PAH
TSHC	total saturated hydrocarbons (same as total alkanes)
UCM	unresolved complex mixture

1 EXECUTIVE SUMMARY

This "annual" report is actually a biennial report. After delays in receiving analytical results following Auke Bay Laboratory's facility move, two years of data arrived in one package. Hence, this report encompasses two years of sampling from July 2006 through October 2007 (contractually 2006-2008; the April 2008 sample collections, by PWSRCAC Scientific Advisory Committee (SAC) design, were intentionally skipped).

In overview, oil exposures at the monitoring sites throughout the region are mostly non-existent with a few exceptions. We are still tracking a trace-level, mostly dissolved-phase signal of PAH exposure in mussels across the region, which would suggest a non-oil source. No accidental spills were detected during this reporting period; however, there is a low-level signal of EVOS oil in Disk Island mussels, and the usual low-level, weathered, ANS-crude-oil signal in Port Valdez from Alyeska's Ballast Water Treatment Facility (BWTF) discharge.

At the Alyeska Marine Terminal (AMT) between 2002 and 2006, mussel TPAH concentrations remained steady within a range of 52-65 ng/g, but the relative-phase-composition signals suggest the accumulation of highly variable, particulate/oil-phase and combustion-derived PAH components from the BWTF along with lesser contributions from the dissolved phase. Since October 2006, the mussels at the AMT site have exhibited a dominant dissolved-phase signal. Sediment conditions at the AMT location, are also trending to continuously lower TPAH levels. After a brief plateau in 2003-2004 in the 167-184 ng/g range, since 2005, subtidal sediments have now dropped even lower to 41-86 ng/g. They still show the weathered-ballast-oil signature plus combustion products, along with the usual biogenic marine and terrestrial SHC components, but conditions are definitely improving. These trends most likely reflect the decreased ballast-water throughput from the facility as oil flow through the pipeline and subsequent tanker traffic drops and as double-hulled tankers, carrying segregated, oil-free ballast, come into operation. This facility is currently undergoing a reconfiguration in treatment methods that presumably will maintain or improve current conditions.

Mussel tissue loads at Gold Creek (GOC) had been consistently low (30-116 ng/g) since July 2002, excepting a diesel spill sometime between July and October 2004 that increased the TPAH values to the highest ever observed at the site, 858 ng/g. The diesel signal was still apparent through the following March, but by July 2005, it was no longer apparent. TPAH levels between July 2006 and July 2007 ranged between 45-75 ng/g, but in October 2007, concentrations had dropped to <30 ng/g. Phase assignments suggested a mixture of particulate/oil-phase and combustion-derived components. TPAH concentrations in GOC sediments are still driven primarily by combustion products, as has always been the case at this site, but they are now at all time lows (12-28 ng/g).

The trace PAH levels seen at sites beyond Port Valdez doubtlessly reflect, oil-wise, the currently pristine nature of the environment. Most stations are now showing mussel tissues with less than 60 ng/g TPAH (many with <30 ng/g), and compositionally the near-MDL traces appear primarily as a dissolved–phase signal. Furthermore, while the

dissolved character of the signals points inconclusively to an unknown source(s), the broad-scale similarities suggest incidental geographic input rather than point sources. Using PAH phase-assignments, we have been able to identify temporal and compositional events that characterize three separate regions comprising Port Valdez, central Prince William Sound, and the outer-coast Gulf of Alaska stations. From the magnitude and nature of the PAH signal, the bulk of Prince William Sound and the northern Gulf of Alaska reflect only trace background levels of dissolved-phase PAH. The only exception to this scenario occurs at the Disk Island site where mussels show a very low (23-67 ng/g) but more complex signature that suggests a weathered particulate/whole oil source. Normally, this signature would be too low to identify a source, but double-ratio plots suggest it is linked to residual EVOS oil seen buried above the LTEMP transect in 2007 and 2008 and recently exposed by Trustee remediation assessment teams.

The reported project years also included co-sponsored funding from EVOS Trustees (Restoration Project No. 050763) for tracking down anthropogenic and other sources of hydrocarbons introduced to regions affected by EVOS. Previously, we reported on the results of mussels and intertidal sediments collected in 2005 at heavily oiled sites in the EVOS impacted region (Short et al., 2007a; Payne et al., 2008a). Although there were still persistent buried EVOS residues at a number of the beaches, they are highly sequestered and do not appear to be bioavailable unless disturbed. As a continuation of that effort, stratified random pits were excavated during the 2006 and 2007 summer field programs at ten current or past human habitation sites identified in Appendix G. No visual evidence of any buried oil was observed in any of the 50 pits dug at each of the sites examined in the 2006 and 2007 field programs. Additional reports on those activities are being prepared by Dr. Short. Also as part of the EVOS Trustees studies, a modest scoping experiment was undertaken in July 2007 to examine sediment/seawater partitioning behavior using the PAH-rich intertidal sediments from Constantine Harbor. This effort (described in Appendix E) was intended to identify a possible source for the ubiquitous dissolved-phase signal observed in mussel tissues throughout the LTEMP region. The results suggest that eroded, terrestrial sedimentary material previously believed to only contain non-bioavailable PAH locked within its matrix, may in fact be contributing to the trace dissolved-phase signals.

In summary, the LTEMP program is primed for its main mission of detecting spill events. In Port Valdez, we see the low-level imprint of human activities in addition to discharge from the Terminal, while elsewhere, we see the trace, dissolved-phase, background signal. Any new petroleum hydrocarbon inputs to the system have been and will be easily detected.

Prior to delving into the report's technical details, readers unfamiliar with environmental hydrocarbon chemistry may want to examine Appendix A, a primer on basic hydrocarbon chemistry, weathering patterns, and the utilization of mussels as indicator organisms for environmental monitoring.

2 INTRODUCTION

The primary objective of the ongoing Long-Term Environmental Monitoring Program (LTEMP) is to collect "…standardized measurements of hydrocarbon background in the EVOS region as long as oil flows through the pipeline." Under Federal and State statutes, the unregulated release of oil into the environment is strictly prohibited; the LTEMP data serve as a sentinel indicator and independent quality control check for Alyeska Marine Terminal and tanker operations throughout the region.

Currently measured variables include polycyclic (or polynuclear) aromatic and saturated (or aliphatic) hydrocarbon levels (PAH and SHC) in mussel (*Mytilus trossulus*) tissues from ten stations between Valdez and Kodiak and sediments from two stations in Port Valdez. The Port Valdez sediment samples are also analyzed for particle grain size and total organic carbon content to validate continuity of the site environments. Sampling and analytical methods are patterned after the protocols developed by the National Oceanic and Atmospheric Administration (NOAA) Status and Trends Mussel Watch Program as fully detailed in the annual Monitoring Reports prepared by Kinnetic Laboratories, Inc. (KLI) and the Geochemical and Environmental Research Group (GERG).

Following the first five years of the program, the collective results from the KLI/GERG team were reviewed in a synthesis paper (Payne et al. 1998). At that time, background oil levels were higher, hot spots were identified, large and small spill events were visible in the data set, and identification of weathered sources was important. Subsequent to this assessment, the PWSRCAC reduced the scope of the program to the current biannual sampling of regional mussel tissues and Port Valdez sediments. Fall mussel sampling was added just in Port Valdez (Alyeska Marine Terminal and Gold Creek) to better track the terminal's discharge. Analyses of aliphatic hydrocarbons in mussel tissues, dropped from the original program in 1995 due to results being confounded from lipid interference, were reinstated in 1998. Improved lab methods have essentially eliminated interference issues at this time.

In 2001, another data evaluation and synthesis review was completed on just the LTEMP results from the Port Valdez sites (Payne et al., 2001). Data from Alyeska Marine Terminal and the Gold Creek control site suggested Alaska North Slope (ANS) crude oil residues from the terminal's ballast water treatment facility (BWTF) had accumulated in the intertidal mussels within the Port. Payne et al. (2001) concluded, however, that the PAH and SHC levels measured in sediments and mussel tissues (and the estimated water-column levels) were very low and unlikely to cause deleterious effects. From the analyte signatures, they were able to further discriminate between particulate- (oil droplet) and dissolved-phase signals in the water column and then correlate those signals with seasonal uptake of hydrocarbons in mussels and with absorption in herring eggs (from other studies). These findings gave new insight into the transport and exposure pathways in Port Valdez. The results also suggested a surface microlayer mechanism may be responsible for seasonal transport of ANS weathered oil residues from the BWTF diffuser

to intertidal zones across the fjord. They concluded that the potential for photo-enhanced toxicity of concentrated contaminants in a surface microlayer should be considered in future impact investigations.

In July 2002, Payne Environmental Consultants, Inc (PECI) and the NOAA/NMFS Auke Bay Laboratory (ABL) began conducting LTEMP operations. Detailed discussions of the transitional 2002/2003 LTEMP samples and interlaboratory comparisons of split samples and Standard Reference Materials (SRMs) supplied by the National Institute of Standards and Technology (NIST) analyzed by both GERG and ABL are presented in Payne et al. (2003a). The results from the 2003/2004 LTEMP and a comprehensive review and synthesis of all analyses completed since the beginning of the program are available in Payne et al. (2005a). Results and discussion of the program through 2006 are also published in *Marine Pollution Bulletin* (Payne at al., 2008b).

3 SCOPE

This report examines the 2006-2008 samples and trend analyses of over 924 tissue and 202 sediment samples collected historically within Prince William Sound and the surrounding region (Figure 1) in addition to laboratory quality control results. The reported project years also included co-sponsored funding from EVOS Trustees for tracking down anthropogenic and other sources of hydrocarbons into regions affected by EVOS. As part of that effort, stratified random pits were excavated at ten current or past human habitation sites at the stations identified in Appendix G. In addition to these so-called SCAT VI and VII surveys (as designated by the NOAA/NMFS Auke Bay Laboratory), a scoping study examining sediment/seawater partitioning behavior was also undertaken using the PAH-rich intertidal sediments from Constantine Harbor. This effort (described in Appendix E) was intended to identify a possible source for the ubiquitous dissolved-phase signal observed in mussel tissues throughout Prince William Sound.

4 METHODS

4.1 Sampling Design

For both the tissue and sediment collections, the current sample design followed the previous years' efforts (KLI 2002) with slight modifications. As noted above, mussel tissues are sampled at ten sites and sediments from two sites in Port Valdez on a biannual basis (March-April and July-August) (Figure 1). Mussel tissues are also collected from the two Port Valdez sites in October (inset Figure 1).

For tissues, three replicates were typically taken at haphazard (governed by mussel availability) locations within each 10m section of a fixed, 30m transect at each site. At Zaikof Bay and Knowles Head, the absence of mussels along the transects (starfish predation) necessitated local, off-transect sampling. Each replicate of 25-30 mussels was collected by hand using Nitrile® gloves, wrapped in aluminum foil, Ziplock® bagged, labeled, double-bagged and kept chilled until reaching the nearest freezer. The collection site was photographed and GPS coordinates recorded for documentation. The entire trip collection was eventually air-freighted frozen to the NOAA/NMFS Auke Bay Laboratory in Juneau under chain-of-custody protocols.

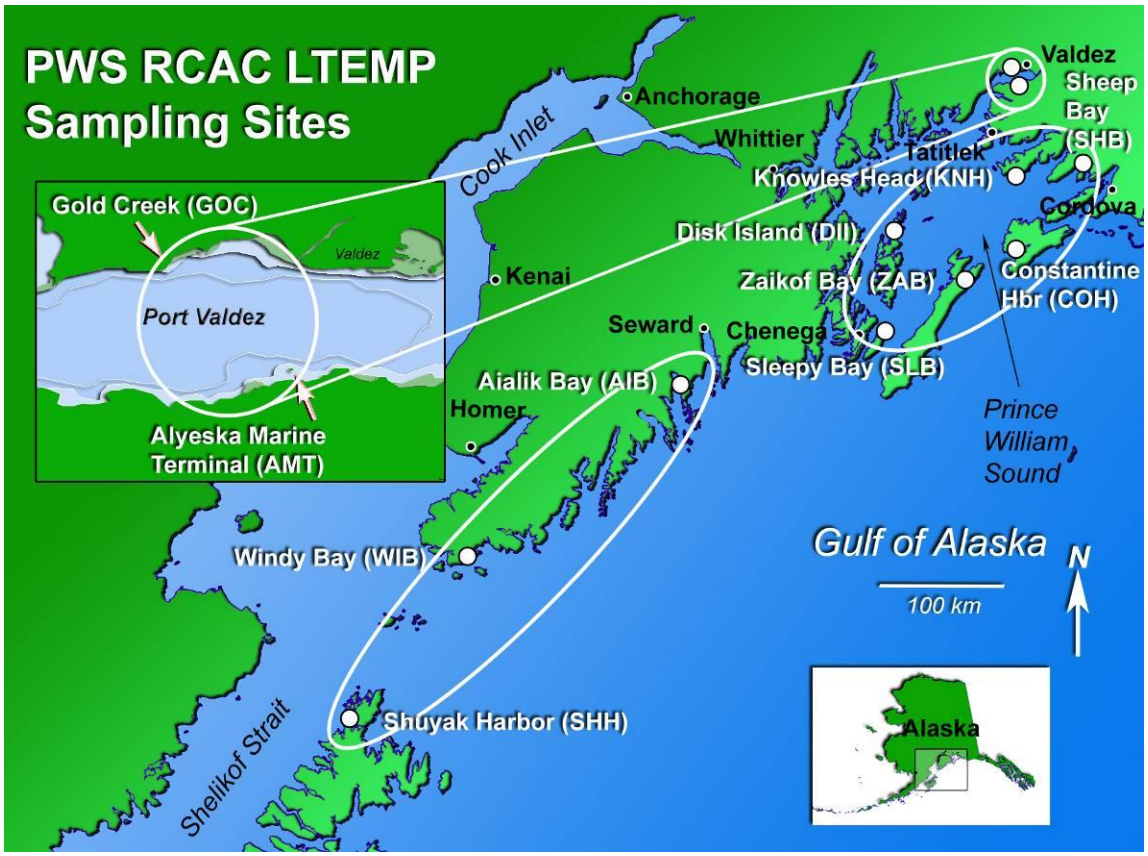

Figure 1 Map of the 2006-2007 LTEMP sites. Circled regions represent sites with similar hydrocarbon signatures and events (discussed later).

Subtidal sediments were collected aboard the support vessel using a modified Van Veen grab sampler, i.e., the standard pincer-jawed, bucket grab commonly augmented with an encircling stabilization frame to theoretically ensure vertical penetration. This sampler was an appropriate choice at the beginning of the program when a variety of benthic habitats were encountered but with the focus on just Port Valdez, it has been a problematic choice as it tends to over-penetrate in the Port's extra-soft, glacial-flour sediments. In use, only the top centimeter of undisturbed sediment is collected from the center of each sample (away from the edges of the grab), scooping with a pre-cleaned spoon into a contaminant-free glass jar. An additional sample is also taken from each grab for particle-grain-size analysis. Water depth and GPS location are recorded for each sample. Prior to beginning sampling at each station, the grab is scrubbed with Alconox® detergent to prevent cross-contamination, rinsed with a previously tested, seawater deck hose, dunked overboard, and the drippings collected as a rinsate blank. The deck hose used for rinsing the grab between samples has also been tested as an equipment blank. The sediment samples are immediately frozen onboard and eventually air-freighted to Auke Bay Laboratory in Juneau.

A combination of vessel and float plane is used to access the sampling sites (Table 1). Typically, during PECI field efforts, the *M/V Auklet* is used for the Port Valdez, Knowles Head and Sheep Bay stations while a float plane is used for sampling all other sites.

Table 1. LTEMP Stations 2006-2007. Station depths are not tidal corrected.

Sediment Sampling

Station Location	Station Code	Matrix	Sampling Date	Depth	Latitude (N)	Longitude (W)
Alyeska Marine Terminal	AMT-S	Subtidal Sediment	7/15/2006	84 m	61.0905	-146.392
			4/5/2007	71 m	61.0901	-146.395
			7/10/2007	70 m	60.0905	-146.393
Constantine Harbor	COH-S	Intertidal Sediment	7/27/2006		60.3510	-146.658
			7/12/2007		60.3460	-146.666
Gold Creek	GOC-S	Subtidal Sediment	7/15/2006	37 m	61.1243	-146.491
			4/5/2007	28 m	61.1240	-146.493
			7/10/2007	27 m	61.1245	-146.491

Mussel Sampling

Station Location	Station Code	Sampling Date	Latitude (N)	Longitude (W)
Aialik Bay	AIB-B	7/27/2006	59.87978	-149.65768
		4/17/2007	59.8797	-149.65772
		7/28/2007	59.87978	-146.6579
Alyeska Marine Terminal	AMT-B	7/15/2006	61.09078	-146.40617
		10/8/2006	61.0908	-146.40628
		4/5/2007	61.09077	-146.40633
		7/10/2007	61.09071	-146.40638
		10/27/2007	61.09083	-146.4064
Constantine Harbor	COH-B	7/27/2006	60.35102	-146.65787
		7/12/2007	60.34602	-146.66558
Disk Island	DII-B	7/27/2006	60.49839	-147.66101
		4/17/2007	60.49895	-147.65857
		7/17/2007	60.49895	-147.65856
Gold Creek	GOC-B	7/15/2006	61.12393	-146.4942
		10/8/2006	61.12447	-146.49422
		4/5/2007	61.12457	-146.49425
		7/10/2007	61.12456	-146.49418
		10/27/2007	61.12453	-146.4942
Knowles Head**	KNH-B	7/7/2006	60.69058	-146.58564
		4/6/2007	60.69487	-146.5965
		7/11/2007	60.69485	-146.59648

Station Location	Station Code	Sampling Date	Latitude (N)	Longitude (W)
Sheep Bay	SHB-B	7/27/2006	60.64658	-145.99537
		4/6/2007	60.6466	-145.99535
		7/11/2007	60.64655	-146.9954
Shuyak Harbor	SHH-B	7/26/2006	58.50195	-152.6193
		4/17/2007	58.50197	-152.62548
		7/28/2007	58.50195	-152.63549
Sleepy Bay	SLB-B	7/11/2006	60.06781	-147.83118
		4/17/2007	60.06782	-147.83112
		7/14/2007	60.06786	-147.8312
Windy Bay	WIB-B	7/25/2006	59.2188	-151.51817
		4/17/2007	59.2189	-166.518
		7/28/2007	59.21886	-151.5184
Zaikof Bay**	ZAB-B	7/27/2006	60.26558	-147.08388
		4/17/2007	60.26555	-147.08402
		7/12/2007	60.26558	-147.08395

*GPS coordinates reflect normal variance in satellite positioning. Intertidal sites are haphazard systematically sampled along fixed location transects.
** Stations temporarily shifted following catastrophic starfish predation.

4.2 Analytic Methods

Sediment samples (~50 g wet weight) or whole mussel tissue samples (~10 g wet weight) were spiked with a suite of 5 aliphatic and 6 aromatic perdeuterated hydrocarbon surrogate standards (identified in Table 2) and then extracted with dichloromethane at 100°C and 2,000 psi for 10 min in a Dionex ASE 200 accelerated solvent extractor. The dichloromethane solutions were exchanged with hexane over steam, and separated into aliphatic and aromatic fractions by column chromatography (10 g 2%-deactivated alumina under 20 g 5%-deactivated silica gel; columns for sediments also contained 20 g granular elemental copper and 8 g anhydrous sodium sulfate for removal of sulfur and water, respectively). Aliphatics eluting with 50 mL pentane were analyzed by gas chromatography with a flame ionization detector (GC/FID) following concentration to ~ 1 mL hexane over steam and addition of dodecylcyclohexane as an internal standard to evaluate recoveries of the surrogate standards. The PAH fraction eluting with 250 mL of a 1:1 solution of dichloromethane and pentane was reduced in volume to ca. 0.8 mL and was further purified by gel-permeation high performance liquid chromatography (HPLC). The injection volume was 0.8 mL into dichloromethane flowing at 7 mL/min through two size-exclusion gel columns (Phenomenex, phenogel, 22.5 mm x 250 mm, 100 Å pore size) connected sequentially. The initial 110 mL eluate was discarded, and the following 50 mL was collected and concentrated over a 60–70^{o} C water bath and exchanged with hexane to a final volume of *ca*. 1 mL, then spiked with hexamethylbenzene as an internal standard for estimating recoveries of the initially added perdeuterated aromatic hydrocarbon surrogate standards.

Table 2. Polycyclic aromatic hydrocarbon (PAH) and saturated hydrocarbon (SHC) analytes measured in this study, along with analyte abbreviations, internal and surrogate standards.

Analytes	Abbreviation	Internal Standard	Surrogate Standard
PAH			
Naphthalene	N	A	1
C1-Naphthalene	N1	A	1
C2-Naphthalene	N2	A	2
C3-Naphthalene	N3	A	2
C4-Naphthalene	N4	A	2
Biphenyl	BI	A	2
Acenaphthylene	AC	A	2
Acenaphthene	AE	A	2
Fluorene	F	A	2
C1-Fluorenes	F1	A	2
C2-Fluorenes	F2	A	2
C3-Fluorenes	F3	A	2
Dibenzothiophene	D	A	3
C1-Dibenzothiophene	D1	A	3
C2-Dibenzothiophene	D2	A	3
C3-Dibenzothiophene	D3	A	3
C4-Dibenzothiophene	D4	A	3
Anthracene	A	A	3
Phenanthrene	P	A	3
C1-Phenanthrene/Anthracene	P/A1	A	3
C2-Phenanthrene/Anthracene	P/A2	A	3
C3-Phenanthrene/Anthracene	P/A3	A	3
C4-Phenanthrene/Anthracene	P/A4	A	3
Fluoranthene	FL	A	3
Pyrene	PYR	A	3
C1-Fluoranthene/Pyrene	F/P1	A	3
C2-Fluoranthene/Pyrene	F/P2	A	3
C3-Fluoranthene/Pyrene	F/P3	A	3
C4-Fluoranthene/Pyrene	F/P4	A	3
Benzo(a)Anthracene	BA	A	4
Chrysene	C	A	4
C1-Chrysenes	C1	A	4
C2-Chrysenes	C2	A	4
C3-Chrysenes	C3	A	4
C4-Chrysenes	C4	A	4
Benzo(b)fluoranthene	BB	A	5
Benzo(k)fluoranthene	BK	A	5
Benzo(e)pyrene	BEP	A	5
Benzo(a)pyrene	BAP	A	5
Perylene	PER	A	6
Indeno(1,2,3-cd)pyrene	IP	A	5
Dibenzo(a,h)anthracene	DA	A	5
Benzo(g,h,i)perylene	BP	A	5
Total PAH	**TPAH**		**5**

Analytes	Abbreviation	Internal Standard	Surrogate Standard
n-Alkanes			
n-Decane	C10	B	7
n-Undecane	C11	B	7
n-Dodecane	C12	B	7
n-Tridecane	C13	B	7
n-Tetradecane	C14	B	8
n-Pentadecane	C15	B	8
n-Hexadecane	C16	B	8
n-Heptadecane	C17	B	8
Pristane	Pristane	B	8
n-Octadecane	C18	B	9
Phytane	Phytane	B	9
n-Nonadecane	C19	B	9
n-Eicosane	C20	B	9
n-Heneicosane	C21	B	9
n-Docosane	C22	B	10
n-Tricosane	C23	B	10
n-Tetracosane	C24	B	10
n-Pentacosane	C25	B	10
n-Hexacosane	C26	B	10
n-Heptacosane	C27	B	10
n-Octacosane	C28	B	10
n-Nonacosane	C29	B	11
n-Triacontane	C30	B	11
n-Hentriacontane	C31	B	11
n-Dotriacontane	C32	B	11
n-Tritriacontane	C33	B	11
n-Tetratriacontane	C34	B	11
Total n-Alkanes	TALK		

Calibrated analytes are identified by boldface. Internal standards:
A = hexamethylbenzene; B = dodecylcyclohexane.

Surrogate standards: 1 = naphthalene-d8, 2 = acenaphthene-d10,
3 = phenanthrene-d10, 4 = chrysene-d12, 5 = benzo[a]pyrene-d12,
6 = perylene-d12, 7 = dodecane-d26, 8 = hexadecane-d34, 9 = eicosane-d42,
10 = tetracosane-d50, and 11 = triacontane-d62.

PAHs in extracts were separated and analyzed with a Hewlett-Packard 6890 gas chromatograph equipped with a 5973 mass selective detector (MSD). The injection volume was 1 µL into a splitless injection port at 300° C. The initial oven temperature was 60° C, increasing at 10° C per minute immediately following injection to a final temperature of 300° C, then held for 12 min. The chromatographic column was a 25 m fused silica capillary (0.20 mm ID) coated with 5% phenyl methyl silicone. The helium carrier gas was maintained at 70 kPa inlet pressure. The gas chromatographic column was eluted into the 70 eV electron impact MSD through a 240° C transfer line. The ionizer temperature and pressure were 240° C and 10^{-5} torr, respectively. The MSD was operated in the selected-ion-monitoring (SIM) mode. The MSD was tuned with mass 69, 102, and 512 fragments of perfluorotributylamine before each batch of samples was analyzed.

Calibrated PAHs were identified based on retention time and ratio of two mass fragment ions characteristic of each hydrocarbon. Calibrated PAHs are identified by bold typeface in Table 2, and include dibenzothiophene and the aromatic hydrocarbons in SRMs supplied by NIST. Chromatographic peaks were identified as a calibrated aromatic hydrocarbon if both ions were co-detected at retention times within ±0.15 minutes (9 seconds) of the mean retention time of the hydrocarbon in the calibration standards, and if the ratio of the confirmation ion to the quantification ion was within ±30% of the expected ratio. In addition, the signal-to-noise ratio for the primary and confirmation ions in the SIM run had to be greater than five. If all three of these criteria were not met, the analyte of interest would be reported as non-detect, and a zero (0) ng/g dry weight value would be entered in the database. All of these determinations were made by the laboratory chemist, Marie Larsen, at the NOAA Auke Bay Laboratory.

Uncalibrated PAHs include the alkyl-substituted isomers of naphthalene (except the 1- and 2-methyl-substituted homologues), fluorene, dibenzothiophene, phenanthrene/ anthracene, fluoranthene/pyrene, and chrysene. Uncalibrated PAHs were identified by the presence, within a relatively wide retention time window, of a single mass fragment ion that is characteristic of the uncalibrated PAH sought. Wider retention time windows were necessary for the uncalibrated PAH because of the range of retention times of the various isomers that are included in an uncalibrated PAH homologue grouping (e.g. C3-phenanthrene).

Concentrations of calibrated PAHs in extracts were estimated by a method employing multiple internal standards and a five-point calibration curve for each calibrated PAH. The deuterated surrogate standards that were initially spiked into each sample are treated as internal standards, where each surrogate compound is associated with one or more calibrated PAHs. A calibration curve for each calibrated PAH and batch of samples analyzed was based on five different hexane dilutions of the PAH standard run before each sample batch or "laboratory string." Each calibration curve was derived from linear regression of (1) the ratio of MSD/SIM quantification ion response of the calibrated PAH and the associated deuterated surrogate standard and (2) the ratio of the amount of calibrated PAH and the amount of deuterated surrogate in the calibration standards. This approach effectively means that all reported analytes are corrected for the appropriate surrogate recoveries.

Concentrations of uncalibrated PAHs in extracts were determined with calibration curves and procedures for the most similar calibrated PAH. The MSD/SIM response to the quantification ion of each uncalibrated PAH homologue isomer were summed; this sum was used in place of the calibrated PAH response in the procedure described above for calculating concentrations of calibrated PAHs. For example, the fluorene calibration curve and procedure was used for all the alkyl-substituted fluorenes identified, but 2,6-dimethylnaphthalene, 2,3,5-trimethylnaphthalene and 1-methylphenanthrene calibration curves were used for C2-naphthalenes, C3-naphthalenes, and for all the alkyl-substituted phenanthrenes, respectively.

Alkanes in extracts were separated and analyzed with a Hewlett-Packard 5890 gas chromatograph equipped with a flame ionization detector (FID). The injection volume was 1 µL into a splitless injection port at 300° C. The 60° C initial oven temperature was maintained for 1 minute, then increased at 6° C per minute to a final temperature of 300° C, then held for 25 min. The detector temperature was 320° C. The chromatographic column was the same as that used for PAH analysis (see above). The helium carrier gas flow rate was 0.80-2.0 mL per minute, and the column effluent was combined with 34 mL per minute nitrogen make-up gas before entering the FID. The FID was operated with hydrogen- and air-flow rates of approximately 33 and 360-410 mL per minute, respectively. Alkane hydrocarbons were identified based on their retention times. Any peak detected above the integrator threshold within ±0.25% of the mean retention time of the alkane in the calibration standards was identified and quantified as that alkane.

Concentrations of calibrated alkanes (Table 2) were determined by an internal-standard method employing a five-point calibration curve for each alkane. The deuterated surrogate standards that were initially spiked into each sample were treated as internal standards, where each surrogate compound was associated with a group of calibrated alkanes. A calibration curve for each calibrated alkane and batch of samples analyzed was based on five different hexane dilutions of the alkane standards. Each calibration curve was derived from linear regression of (1) the ratio of FID response of the alkane and the associated deuterated surrogate standard, and (2) the ratio of the amount of calibrated alkane and the amount of deuterated surrogate in the calibration standards. As with PAH, reported n-alkane concentrations are surrogate-recovery corrected.

Amounts of uncalibrated alkane hydrocarbons and the cumulative amount of hydrocarbons in the unresolved complex mixture (UCM) were based on detector responses and the calibration curve for hexadecane. Flame ionization detector response due to the UCM was determined as the difference of the total FID response and the response due to distinguishable peaks using valley-to-valley baseline integrations.

4.3 Quality Assurance

Quality control samples were analyzed with each batch of 12 samples to assess the analytic accuracy and precision, and to verify the absence of laboratory-introduced contaminants. Two quality control samples for accuracy assessment were prepared from hydrocarbon standards prepared by NIST (for PAH) or by ABL (for aliphatics), and run with each batch. Precision was assessed by analysis of two NIST standard reference material (SRM) samples analyzed with each batch: SRM 1974a for mussels and SRM 1944 for sediments. The mussel reference is especially appropriate for these analyses because the PAH concentrations are quite low, with many of the PAH analytes present at concentrations near the method detection limits (MDLs). In addition, lab duplicates of field or reference samples are run with each batch to further assess analytical precision. Absence of laboratory contaminants was verified by analysis of one method blank sample with each batch. Field blanks were analyzed to document the lack of any contamination from collection equipment or procedures utilized in the field.

Method detection limits (MDLs) were estimated for each calibrated alkane and PAH analyte following the procedure described in Appendix B, 40 Code of Federal Regulations, Part 136. Method detection limits for uncalibrated PAHs were not experimentally determined. Consequently, detection limits for these analytes were arbitrarily assumed as the MDL of the most closely related calibrated PAH analyte. In PAH and SHC bar chart plots throughout this report, MDLs are depicted by a dashed blue line with blue diamonds when appropriate. They are included for the reader's benefit in assessing the significance of the data particularly where concentrations are at trace levels. When all of the constituents are below the MDLs, they are so-noted in the figure legends and the MDL line may or may not be shown for clarity in presenting other data in the chart. As described below, we are primarily interested in detecting expected multi-analyte patterns rather than the quantifying absolute levels of single analytes. Note that the published PAH MDLs in this report are from a 1996 study at ABL; new MDLs released by the laboratory in 2010 are all sub-ng values. All quantified values of PAH (even if they were below the old – 1996 levels) are summed in calculating total PAH (TPAH). In the NOAA Status and Trends (Mussel Watch) Program, less-than MDL PAH values are reported, but they are not summed in calculating TPAH.

4.4 Determination of Moisture Content

Weighed aliquots of wet mussel homogenates or of sediments were dried at 100^{o} C for 24 h and re-weighed to determine the moisture content, and the ratio of these wet and dry weights was used to convert PAH and SHC concentrations to a dry weight basis.

4.5 Particle Grain Size Determination

Measurement of sediment particle grain sizes was determined by a combination of sieving and pipette methods (Folk 1974). Implementation of these procedures at ABL (Larsen and Holland 2004) is almost identical with the method described in SOP-8908 at GERG. The ABL procedure differs from the GERG procedure in the sample pre-treatment. At ABL, a somewhat smaller sample aliquot is used (8 – 12 g instead of 15 – 20 g sediment), the minimum amount of hydrogen peroxide is used to oxidize organic matter (typically 30 – 60 mL of 30% H_2O_2 instead of 50 – 100 mL), the sample is not washed with distilled water to remove soluble salts at ABL because of the risk of losing sediment fines, and only ~ 100 mL of sodium hexametaphosphate solution is used to disperse the sample at ABL instead of 400 mL at GERG. These changes were implemented at ABL because they were specifically optimized for the samples analyzed for the LTEMP program. The effects of these minor procedural differences on the estimates of particle grain size distributions in comparison with results produced at GERG are almost certainly negligible.

4.6 Determination of Total Organic and Total Carbon

Analytical measurements of total organic and total carbon are determined on oven dried and pulverized sediment samples using a Dohrmann DC-85A TOC catalytic combustion (oxygen at 200 mL/min and cobalt oxide on alumina) furnace. The carbon dioxide produced is passed through an acidified liquid sparger (scrubs out entrained water vapor and corrosive species), two scrubbers (copper and tin) and linearized non-dispersive infrared detection, by comparison with results from a calibration curve based on

potassium acid phthalate. Total organic carbon (TOC) and total carbon (TC) are determined using samples treated with and without 10% HCl in methanol. Total inorganic carbon is calculated as the difference between TC and TOC.

4.7 Data Analysis

For data analysis, we favor using the standard accepted practices of forensic pattern recognition, which involves subjectively assessing the analyte levels and composition patterns to identify sources and weathering/transport processes (Wang and Stout, 2007). Bar chart PAH and SHC plots for each sample, ordered by increasing molecular weight (number of aromatic rings and degree of alkylation), are scrutinized for relevant details relating to weathering or dissolution behavior. Each replicate is examined separately in order to assess fidelity of the triplicate patterns and avoid any potentially confounding amalgam from replicates with radically differing profiles; identifying a potential anthropogenic oil source is initially more important than the average quantification. Standard errors of the mean are displayed graphically, where practical, for averaged index trends (also tabulated in the appendices).

An issue exists with the pattern recognition process in how we utilize hydrocarbon data that fall below laboratory method detection limits (MDLs). As defined by the US Environmental Protection Agency (EPA) (Federal Register, 1986), an MDL calculation provides the lower limit for a 95% confidence in a single analyte's quantification. But since we look at whole patterns of multiple analytes rather than single analytes, we take added confidence that false positive identifications of the complex hydrocarbon profiles are minimized based both on prior knowledge of expected multi-analyte patterns (primarily ANS crude, diesel or pyrogenic sources) and on laboratory use of secondary ion confirmations in the SIM analyses. This <MDL practice is an acknowledged conundrum in pattern analysis but is widely practiced among forensic analysts. Although it has evoked much discussion among PWSRCAC program reviewers, it elicited no comments from peer reviewers and editors at *Marine Pollution Bulletin* (Payne et al., 2008b). We conclude that it is theoretically and empirically justified for holistically assessing multi-analyte source patterns and is completely adequate for the primary goal of this project. We refer here to monitoring for anthropogenic hydrocarbon releases; events that typically spike multi-analyte signals at magnitudes well above the MDLs and the current trace background levels. As noted above, when this report was going to press (2010), new sub-ng PAH MDLs were announced to replace the previous (1996) values.

In water, oil partitions by physical equilibrium into two phases, the dissolved phase (also called the water-soluble fraction) and the particulate or whole-oil droplet phase. The ability to discriminate between the dissolved- and particulate/oil-droplet phases, particularly as clues to fate and transport processes, has been essential in our data interpretations. Filter-feeding mussels may acquire waterborne oil signatures from both phases in addition to combustion products (soot) as finely suspended, pyrogenic particles (Baumard et al., 1998; Payne and Driskell, 2003). Note that there is a bias when directly comparing a mussel's dissolved-phase PAH levels (absorbed via equilibrium dynamics) versus an ingested oil microdroplet (or contaminated suspended-particulate matter) in that mussels can accumulate particle-bound PAH some 80-fold more effectively than they do

with an equivalent aqueous concentration of dissolved PAH (Short, 2005). The presence and pattern of insoluble n-alkanes plus phytane along with alkylated fluoranthenes/ pyrenes and chrysenes can also be used to confirm a sample's particulate/oil-phase burden.

In addition to reviewing individual or triplicate samples, data overviews are created using a custom Excel application developed to plot all sets of replicate samples (by station and sampling date) along with the relevant lab method blank. Thus plotted, with all samples from a single site serially on single worksheet, spotting trends (and issues) becomes greatly simplified. For more detailed comparisons, another Excel application quickly retrieves and graphs both PAH and SHC analytes with phase assignments and any relevant indices from any three samples plus a reference standard (typically, reference ANS crude or BWTF outfall).

One-way, randomization paired t-tests were performed to compare seasonal phase data for Port Valdez sites using Resampling software available online from David C. Howell (www.uvm.edu/~dhowell/StatPages/Resampling/Resampling.html). Correlation p-values were then calculated online using a utility by Center Space Software by Daniel Soper (www.danielsoper.com/statcalc/calc44.aspx). All other statistics were calculated with Excel formulas and standard analytic add-ins.

4.7.1 Hydrocarbon Indices

In prior LTEMP studies, several indices, both published and *ad hoc*, have been used with varying degrees of utility to describe LTEMP data trends. Because we use pattern recognition to interpret the data, most of the previously cited indices have become less germane to interpreting the data; we're primarily looking for ANS oil signals and can readily distinguish it through a progression of weathering states. We presently rely on our three derived indices (Table 3) which quantify the dissolved-, particulate/oil-phase-, and pyrogenic-source signals in a sample signature in addition to the summary TPAH and TSHC values. We have found the other indices previously used in this project to encompass varying degrees of ambiguity relative to assigning sources or to be superseded by newer approaches and insights (see method comparison in Appendix F).

Double-ratio plots are another diagnostic approach we use for comparing an oil sample to a reference source. Perhaps the most commonly used are the ratios of the conservative alkylated homologues of dibenzothiophene to phenanthrene, D2/P2 versus D3/P3. These ratios are not a precise measure but do tend to vary in predictable trend lines as the PAH differentially weather from the reference source.

During a different 2004/2005 study of the Alyeska Marine Terminal Ballast Water Treatment Facility (BWTF), Payne et al. (2005b,c) utilized a Portable Large Volume Water Sampling System (PLVWSS) to separate (via filtration through a 0.7 µm glass fiber filter) the dissolved- and particulate/oil-phase fractions (Payne et al., 1999) in a sample of the BWTF effluent just before discharge into Port Valdez. The less water-soluble, higher-molecular-weight PAH (Figure 2 top) and SHC (Figure 3 top)

Table 3. Hydrocarbon Parameters Used in the LTEMP Data Analysis.

Parameter	Relevance
DSI (mussel tissues and sediments)	Dissolved Signal Index sums the soluble PAH fractions of an oil signature (see accompanying text) DSI = dissolved (naphthalenes + fluorene + C1-fluorene) + dissolved (phenanthrenes) + dissolved (dibenzothiophenes)
PSI (mussel tissues and sediments)	Particulate Signal Index sums the less soluble PAH fractions plus any water-washed groups (see accompanying text) PSI = (C2- + C3-fluorene) + particulate (anthracenes & phenanthrenes) + particulate (dibenzothiophenes) + particulate (fluoranthene/pyrenes) + particulate (chrysenes)
Pyrogenic index (mussel tissues and sediments)	Pyrogenic Index = pyrogenic fraction + pyrogenic (phenanthrenes) + pyrogenic (dibenzothiophenes) + pyrogenic (fluoranthene/pyrenes) + pyrogenic (chrysenes) Where: Pyrogenic fraction = benzo(a)anthracene + benzo(b)fluoranthene + benzo(k)fluoranthene + benzo(e)pyrene + benzo(a)pyrene + indeno(1,2,3-cd)pyrene + dibenzo(a,h)anthracene + benzo(g,h,i)perylene
TPAH (mussel tissue and sediments)	Total PAH as determined by high resolution GC/MS with quantification by selected ion monitoring; defined as the sum of 2- to 5-ring polycyclic aromatic hydrocarbons: Naphthalene + fluorene + dibenzothiophene + phenanthrene/anthracene + chrysene, and their alkyl homologues + other PAHs (excluding perylene); useful for determining TPAH contamination and the relative contribution of petrogenic, pyrogenic, and diagenic sources
TSHC (sediments)	Total Saturated Hydrocarbons quantifies the total n-alkanes (n-C_{10} to n-C_{34}) + pristane and phytane; represents the total resolved hydrocarbons as determined by high resolution gas chromatography with flame ionization detection (GC/FID); includes both petrogenic and biogenic sources
UCM (sediments)	Unresolved Complex Mixture – petroleum compounds represented by the GC-FID signal for total resolved peaks plus unresolved area under the peaks minus the total area of the resolved peaks quantified with valley-to-valley baseline integration; a characteristic of some fresh oils and most weathered oils.

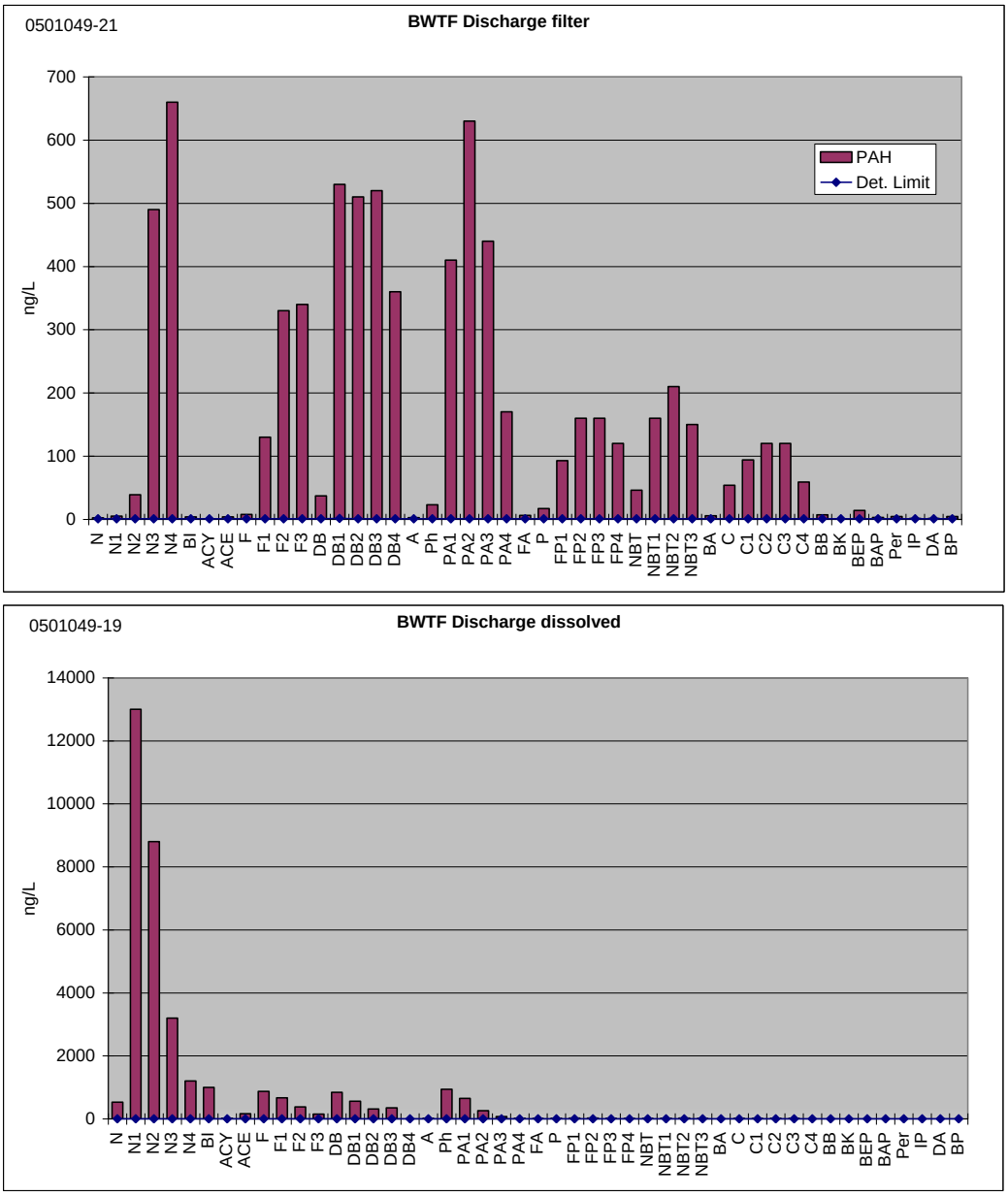

Figure 2 PAH profiles of oil droplets removed by filtration (upper) and the dissolved-phase (lower) of the AMT BWTF effluent, January 2005 (from Payne et al. 2005b).

components appear as the fine particulate phase and finite oil droplets trapped on the glass-fiber filter of the PLVWSS. In the dissolved phase (filtrate – Figure 2 bottom) sample, however, the naphthalenes clearly predominate over all the other PAH, and the presence of the declining but slightly water-soluble C1- and C2-alkylated homologues is in direct contrast to the water-washed pattern (also see Appendix A) obtained for the higher-molecular-weight particulate/oil phase PAH trapped on the filter. Also, almost all of the n-alkanes (Figure 3 bottom) are just barely above (or in most cases below) the MDL in the filtrate (dissolved phase) because of their limited water solubility.

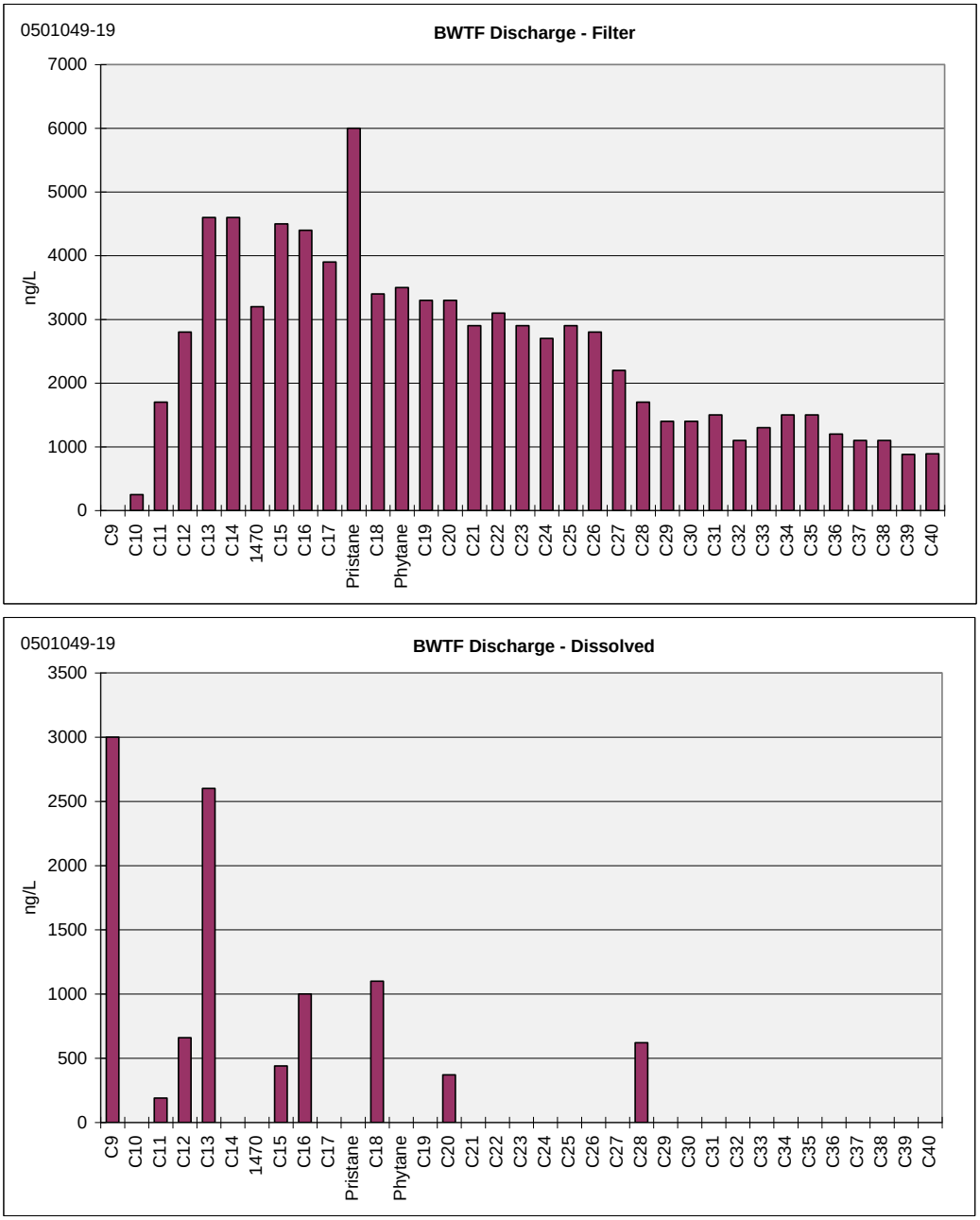

Figure 3 SHC profiles of oil droplets removed by filtration (upper) and the dissolved-phase (lower) of the AMT BWTF effluent, January 2005 (from Payne et al. 2005b).

This partitioning behavior is controlled both by the concentration of a given component in the initial oil phase as well as the solubility of that component in both the oil and water phases (i.e., the oil/water partition coefficient). The kinetics of this partitioning are controlled by the oil droplet surface-area-to-volume ratio, the interphase mass-transfer coefficient, and the distance from equilibrium concentrations of a given water-soluble component in the oil and water phases (Payne et al., 1984; NRC 1985, 2003, 2005).

When oil is spilled at sea, a true equilibrium of oil and water-column concentrations is rarely attained because of the continuing dilution of dissolved components with fresh seawater. Thus, at any given moment, a dynamic (rather than static) equilibrium exists between the oil and water phases.

When filter-feeding organisms (in this case, mussels) are exposed to water containing oil, the resulting PAH profile of the mussel-tissue extracts will reflect the physical state of the oil in the water (dissolved versus particulate/oil phase) plus any non-soluble pyrogenic (combustion) products (Baumard et al., 1998; Payne and Driskell 2003; also see Appendix A). These signatures are easily differentiated by their plots (examples in Figure 4) although mixtures can be more tricky to tease out. To better illustrate a pyrogenic source, we have included an LTEMP sediment sample. Combustion products generally make up only 20% or less of the total PAH signal in most LTEMP mussel samples (i.e., there are other components present at higher concentrations).

In 2005, Driskell et al. presented original algorithms for discerning the relative portions of dissolved PAH versus particulate versus pyrogenic phases in a crude oil sample (further refined in Payne et al., 2006). Note that the formulations presented here describe the general model but do not represent the complete algorithms (see Driskell et al., 2005; Payne et al. 2006). Briefly, the dissolved-signal index (DSI) is summed from the PAH analytes that display water-soluble patterns, which primarily comprise the lighter-molecular-weight analytes (left side of the PAH profiles, e.g., bottom Figure 2 and top Figure 4).

Dissolved Signal Index =

Dissolved (naphthalenes + fluorene + C1-fluorene) + dissolved phenanthrenes + dissolved dibenzothiophenes

The particulate index (PSI) is similarly formulated using less-water-soluble, mid-molecular-weight PAH (e.g., Figure 4 middle).

Particulate Signal Index =

(C2- + C3-fluorene) + particulate (anthracenes & phenanthrenes) + particulate dibenzothiophenes + particulate fluoranthene/pyrenes + particulate chrysenes

A pyrogenic signal is characterized by the higher-molecular-weight PAH plus the suites of middle (3-4 ringed) PAH when they display descending stair-step patterns and are not part of the dissolved signal (e.g., Figure 4 bottom).

Pyrogenic Index =

Pyrogenic fraction + pyrogenic phenanthrenes + pyrogenic dibenzothiophenes + pyrogenic fluoranthene/pyrenes + pyrogenic chrysenes

Where:

Pyrogenic fraction = benzo(a)anthracene + benzo(b)fluoranthene + benzo(k)fluoranthene + benzo(e)pyrene + benzo(a)pyrene + indeno(1,2,3-cd)pyrene + dibenzo(a,h)anthracene + benzo(g,h,i)perylene

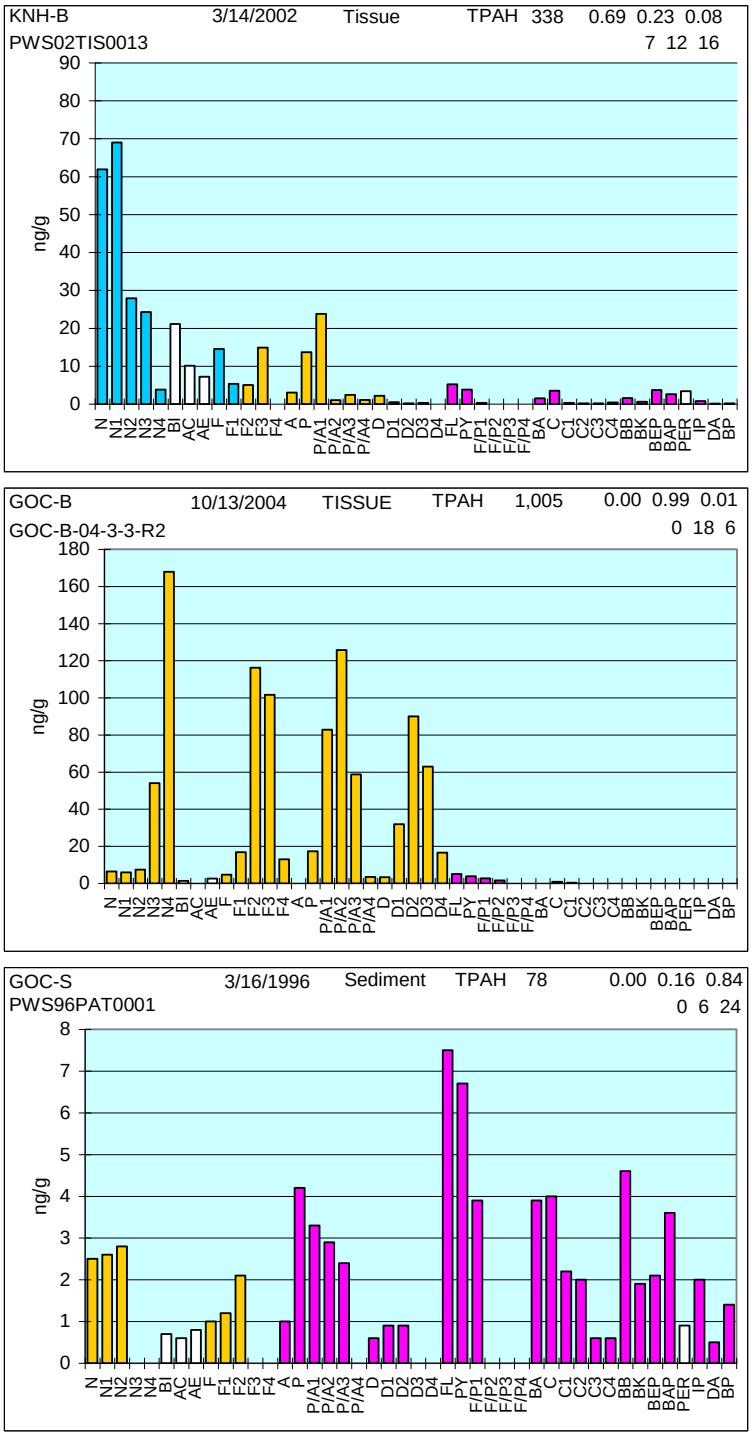

Figure 4 Examples of PAH profiles from LTEMP mussels containing primarily background dissolved-phase components (analytes colored turquoise; top – Knowles Head) and particulate/oil-phase components from a diesel spill (colored gold; middle – Gold Creek), and LTEMP sediments containing primarily low-level combustion products (colored fuchsia; bottom – Gold Creek). White colored analytes are indeterminate. The fractional proportions of each phase (soluble, particulate/oil, and pyrogenic) are shown by the numbers in the upper right-hand corner of each plot with the number of analytes assigned to each group just below (e.g., the bottom replicate was 84% pyrogenic from the 24 fuchsia-coded analytes).

For batch processing the PAH data, algorithms assigning the five multi-state PAH families to dissolved, particulate, or pyrogenic fraction are formulated as Excel logic statements. The logic assigns analytes to a phase based on expected patterns relative to their known dissolution characteristics in water. For example, phenanthrenes would be assigned depending upon both the relative amounts of the parent and alkylated homologues and diagnostic traits from other analyte groups (see Payne et al., 2006 for full description). For example, phenanthrenes in tissues are allocated as dissolved, particulate, or pyrogenic by:

IF
Tissue phenanthrene > max (phenanthrene homologues)
THEN
IF
Naphthalenes are dissolved
THEN
Dissolved phenanthrenes = sum (all phenanthrenes + anthracene)
ELSE
IF
Pyrogenic fraction > 0
or
Fluoranthene or pyrene or chrysene are pyrogenic
THEN
Pyrogenic phenanthrenes = sum (all phenanthrenes + anthracene)
ELSE
Particulate phenanthrenes = sum (all phenanthrenes + anthracene)

Since dissolved phenanthrenes are unlikely to occur in sediments, sediment phenanthrenes and fluorenes are only attributed as pyrogenic or particulate based on:

IF
Sediment phenanthrene > max (phenanthrene homologues)
and
(Pyrogenic fraction > 0
or
Fluoranthene or pyrene or chrysene are pyrogenic)
THEN
Pyrogenic phenanthrenes = sum (all phenanthrenes + anthracene)
ELSE
Particulate phenanthrenes = sum (all phenanthrenes+ anthracene)

Similar logical constructs assess each analyte family (Payne et al., 2006). As each replicate sample is processed through the logic, the individual analytes are plotted color-coded to represent their assignment to a particular phase (plotted in three colors, Figure 4). Phase proportions and number of analytes in each phase appear as labels in the upper right of the plot. This graphic style greatly improves the efficiency of evaluating the 15 years of triplicate LTEMP samples (n>800). In practice, the computer phase assignments

are not considered final interpretations. If circumstances suggest mixed sources or small critical differences, we may overrule the assignments based upon other evidence (e.g., similarity to other replicates or SHC patterns suggesting either petrogenic or biogenic components).

4.7.2 Data Anomalies

In the years since LTEMP's inception, analytical chemistry methods and instrumentation have improved. Regrettably, some of the early data with low-level TPAH contain obvious anomalies; lower-concentration samples were incorrectly integrated and merely reflect the laboratory method blanks. Newer GC/MS instrumentation was introduced circa 1997, which resulted in more detections of lower-concentration analytes and more accurate data. To avoid misinterpretations, we have chosen to begin our time series analysis with 1998, although some earlier data that we felt reliably report moderate-to-high TPAH levels are presented. Further details are available in previous annual reports (Payne et al., 2003a, 2005a, 2006).

One issue with early program data occurred with exceptionally clean or low-PAH-level tissue samples when laboratory artifacts were inadvertently reported as real PAH components. We report the data here but flag them as unreliable (discussed below). The problem is detailed in Payne et al. (1998, 2003a, 2005a) but briefly, the issue arose when the early software for the laboratory's GC/MS instrumentation did not automatically integrate all the alkylated PAH homologues (08/07/03 personal communication with Dr. Guy Denoux, GERG Laboratory Director). Most parent PAH components (and methylnaphthalenes) were automatically integrated, but quantification of the remaining C_2-, C_3-, and C_4-alkylated homologues had to be done manually by the GC/MS operator, and then only when a recognizable signal was first observed. As a result, PAH patterns identical to those shown in Figure 5 were often obtained on tissue samples from the cleaner areas and in many of the laboratory procedural blanks (Figure 5). Fortunately, this issue does not appear with sediment chemistry data or with mussel tissue results from later (post 1997) years of the program.

Another procedural artifact discussed at length by Payne et al. (2003a) was anomalously high fluorene and alkylated-fluorene (F, F1, F2, F3) concentrations being reported as a result of incomplete sample cleanup and lipid interference. This was particularly problematic in tissue samples analyzed by GERG from the July 1994, July 1996, and July 1999 sample collections. For reasons presented in Payne et al. (2006), we elected to simply drop the fluorene contribution to the TPAH and other diagnostic indices for the July 1994, July 1996, and July 1999 tissue samples to eliminate the mega-spikes. Where there was a significant real signal from other PAH, the loss would be minimal and characterization mostly unaffected.

In the July 1997 samples from Disk Island (DII), Gold Creek (GOC), Knowles Head (KNH), Sheep Bay (SHB), and Sleepy Bay (SLB), we noticed that the PAH patterns were remarkably similar (if not identical) and characterized by one or two additional naphthalenes at higher concentrations plus all the other procedural artifacts (Figure 5). In

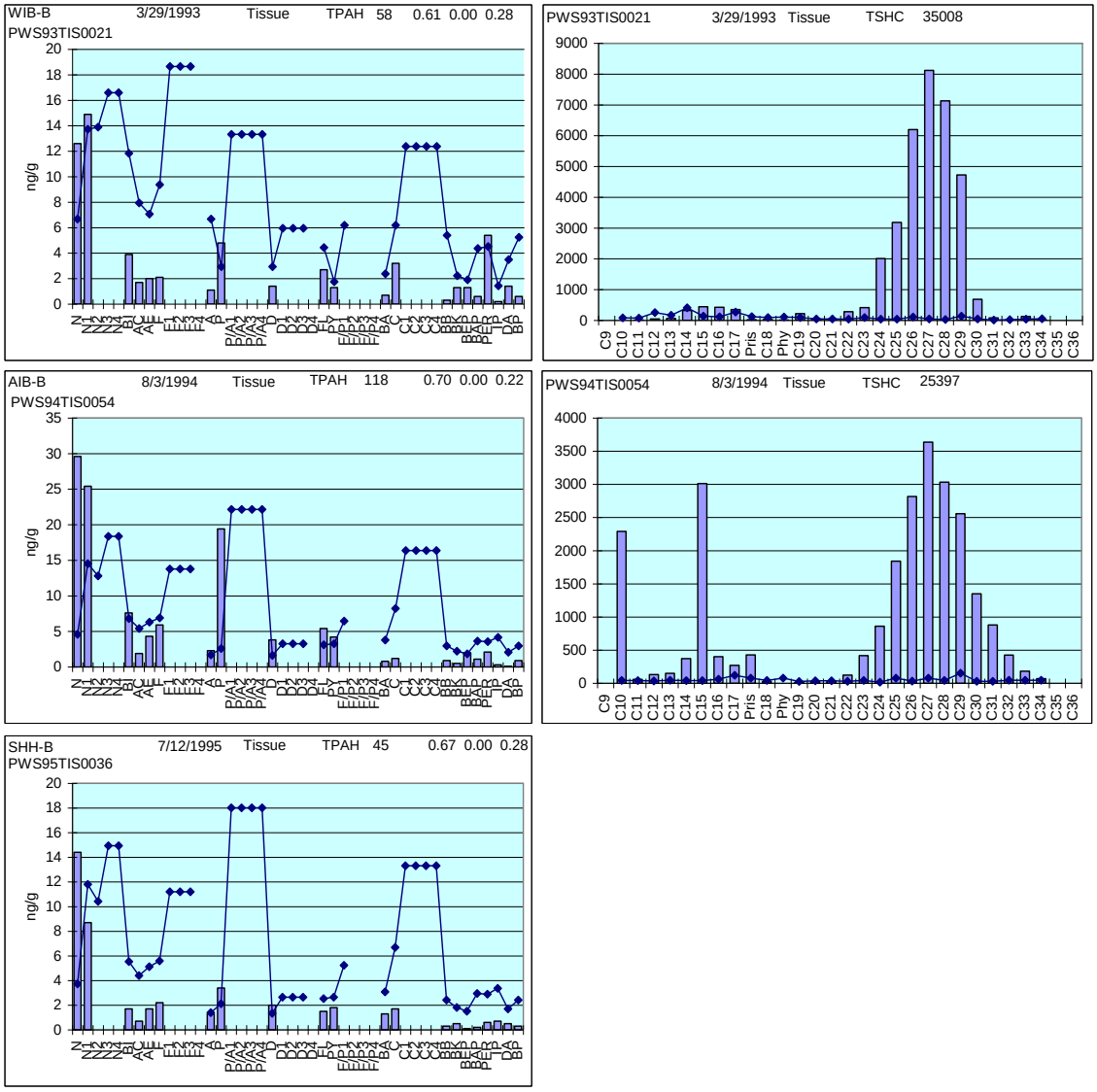

Figure 5 PAH procedural artifact patterns (left graphs) common in early LTEMP samples between March 1993 and March 1997. For these samples, homolog data are incomplete. The overlaying solid lines with the blue diamonds represent reported MDLs. Line gaps indicate analytes not reported at the time. SHC analyses (right graphs) were discontinued between 1995 and 1998 due to lipid interference problems.

these instances, there were no other alkylated components detected (except for the extra naphthalenes) to suggest that the observed patterns were in fact real (Figure 6), and we concluded that the laboratory may have again erroneously reported concentrations for procedural artifacts plus additional naphthalenes that were manually integrated. For additional details, see Payne et al. (2006).

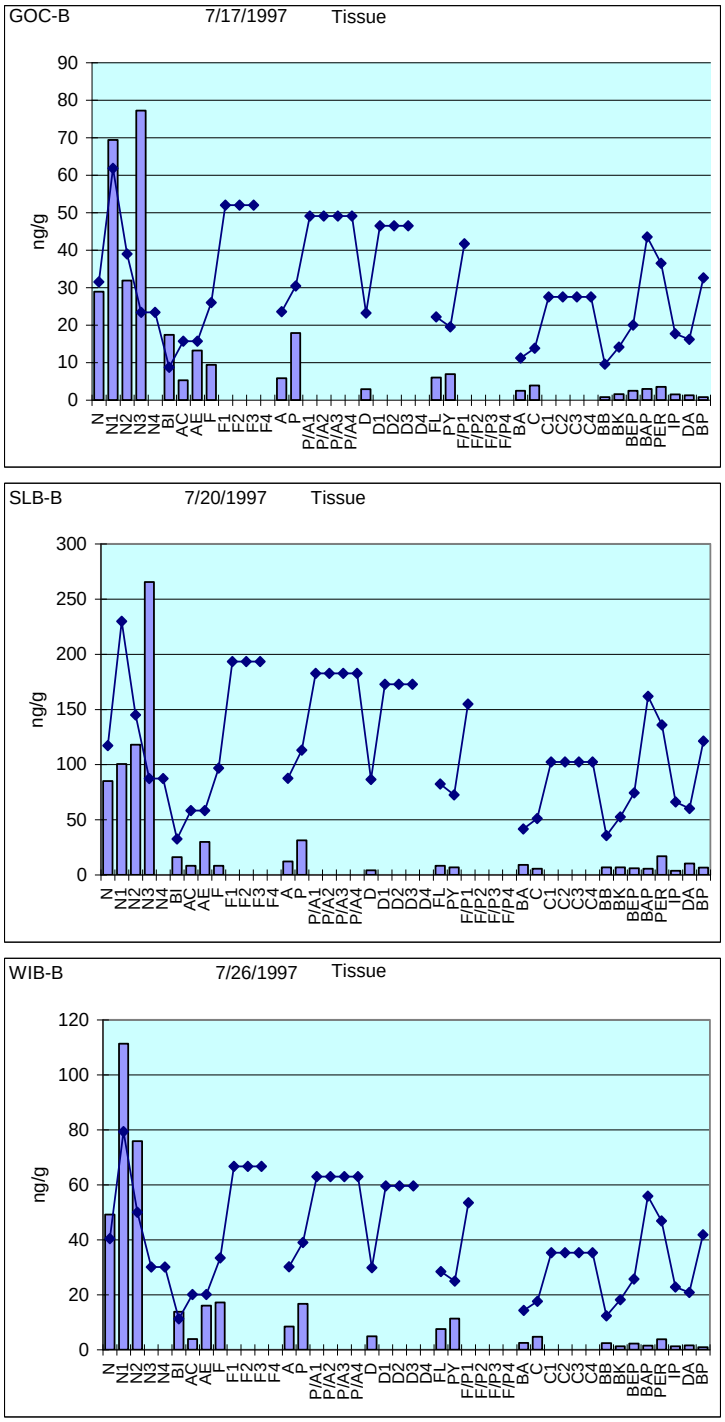

Figure 6 Representative PAH profiles and method detection limits (solid lines with blue diamonds) from July 1997 tissue samples from Gold Creek, Sleepy Bay, and Windy Bay showing highly similar procedural patterns (GC/MS integration artifacts – see Figure 5) plus additional naphthalenes.

These elevated naphthalenes lead to an apparent region-wide spike in TPAH levels in 1997 with major contributions from the dissolved phase. However, we have little confidence in those data and suspect instead that this apparent trend is really nothing more than an anomaly introduced by changing laboratory integration procedures.

Finally, in reviewing these data, we noted that many of the major TPAH peaks in serial plots of early tissue data tended to correlate with extracted sample weights below 1.0 g dry weight (and frequently below 0.5 g). This becomes an issue when the laboratory quantifies the instrument's response on a per gram dry weight of extracted-sample basis because below-normal-sample-weight adjustments arithmetically amplify the results (i.e., a small denominator for the sample dry weight amplifies the final concentration calculation). For this project, we chose to conservatively eliminate only obvious outliers (e.g., samples with half the other triplicates sample weights but twice their concentrations) and address the ramifications in the discussion. Note that even when inflated, there may still be useful information; the analytes' relative concentrations in a low-weight sample may be accurate enough to review phase assignments and source identification, particularly as a confirming signature for the samples' triplicates.

For this year's report, we have once again flagged those samples that were characterized by one of the four patterns discussed above. Then, to avoid propagating questionable data, any questionable data points were excluded in our PAH time series plots. For these plots, the averaged values in which we have confidence are represented by symbols on the connecting lines; questionable data have dashed connecting lines between sampling intervals but no symbols. With this approach, legitimate data are easily identified while questionable values are only presented for displaying the complete data set.

4.8 Data Management

Data received in spreadsheet format from ABL were combined with historic data from the LTEMP Microsoft Access database archives. Data processing and calculations (described above) occur in pre-formulated Microsoft Excel spreadsheets; pivot tables are used for most data compilations. Data retrieval and graphing routines were custom programmed for Excel using Microsoft Visual Basic for Applications (VBA) code.

5 RESULTS AND DISCUSSION

5.1 Sampling and Data Quality

5.1.1 ABL Quality Assurance Chemistry Results

The 2006-2008 field samples were processed with a set of quality assurance samples designed to verify analytical accuracy, precision, method cleanliness, and method efficiency. Analysis of the thirty accuracy-check, instrumental-stability samples (i.e. SRM 1491 or the ABL aliphatic standard) indicated that accuracy for the calibrated compounds were within ABL's targeted range of 85% to 115% of certified or expected

values in 98.8% of the observations. Analysis of the six spiked blanks showed that accuracy for the aromatic and aliphatic calibrated compounds were within ± 15% of the expected value in 94% of the observations and analysis of the eight SRM 1944 sediment samples showed that accuracy for the PAH were within ± 15% of the certified values in 93% of the observations. The median precision of the PAH (including the uncalibrated compounds) in the nine SRM 1974b tissue samples analyzed with the mussel batches, expressed as the coefficient of variation, was 20%. The precision for the certified, calibrated analytes above the 1996-defined MDL ranged from 17% to 42%. The median precision of the PAH (including the uncalibrated compounds) in the eight SRM 1944 samples analyzed with the sediment batches, expressed as the coefficient of variation, was 16%. The precision for the certified, calibrated analytes above the MDL ranged from 14% to 24%. The method blanks analyzed with each batch of samples for this report were lower than or near respective MDLs for analytes verifying the absence of positive interferences introduced at the laboratory.

Recoveries of surrogate standards were between 30% and 113% for 97.4% of all surrogate hydrocarbons. These values are within the accepted ranges published in the standard operating procedures (SOP's) for the ABL laboratory and those recommended in NOAA Status and Trends protocols. In accordance with those protocols and to be consistent with procedures utilized at GERG, all individual and total PAH and SHC concentrations have been corrected for surrogate recoveries and are reported on a dry weight basis.

5.1.2 Mussel Populations

One issue of moderate concern is the availability of mussels at some of the sites (Table 4). Some locations have but patchy remnants of former colonies so boldly obvious in earlier KLI photos. At most sites, there is normal attrition in the dominant 6-7 year old mussel age class (based on growth rings) with a 3-4 year old class maturing to fill the space. There are also new 0-3 year old recruits at most locations. The size and robustness of mussels differ substantially among the sampling sites, most likely natural variation from available food resources, predation and physical disruption. The Sleepy Bay site is a chronically impoverished location but in 2009 is finally showing good signs of progressive recovery. Both Knowles Head and Zaikof Bay transects have been stripped by starfish (*Pisaster)* predation in late 2004. Nearby off-transect populations have been selected for continued monitoring. As of April 2009, the Knowles Head and Zaikof Bay sites remain impoverished, but sampling off-transect has ample abundance.

5.2 Port Valdez Sediments

The primary purpose of the Port Valdez sites is to monitor the regulated discharges (or accidental spills) from the tanker operations at the Alyeska Marine Terminal (AMT), the terminus of the Trans-Alaska oil pipeline. Nearby mussels and subtidal sediments are sampled that have been chronically exposed to the diluted discharge of the Alyeska

Table 4. Field notes on mussel populations, July 2006-October 2007*.

Station	Field notes
Aialik Bay	Very good population. Dense, 5-6 yr old, plump and healthy crop of recruits. No predators visible.
Alyeska Marine Terminal	Excellent pickings!
Disk Island	Healthy, plump, vivid blue shells. Fluid oil seen in upper intertidal sediments. Site was visited by RPI crew in lingering oil surveys.
Gold Creek	Colony in eroded patchy strips, slippery, silt-covered with reduced shell volume. Suboptimal niche?
Knowles Head	In July 2006, they were completely removed by *Pisaster* predation at established transect. Still missing as of 2008. New outcrop location at north end of bay has sustainable population free of starfish.
Sheep Bay	Harvestable mussels discontinuous in mid transect. Shells small but increasing by 2008. Still a depressed population.
Shuyak Harbor	Mussels patchy near right end. But healthy and aged 5-6 yr old. Less patchy near left end but slightly smaller. Good recruitment.
Sleepy Bay	Mussels are only in broken shale above the marker and at left end beyond marker. Mostly very small 3-5 yr olds. Mussels in mid-section are small but beginning to return. Small healthy group found on back side of outcrop beyond left end marker.
Windy Bay	Good site. Beds dense and continuous. Mussels healthy, plump and mature. Good recruitment. No visible predators.
Zaikof Bay	The colony is still depleted of mussels after being completely stripped by *Pisaster*. Sampling was shifted slightly northwest of site. Abundant, robust mussels.

* Note: Additional information obtained in July 2008 is included as appropriate.

Ballast Water Treatment Facility (BWTF). A reference station is also sampled 6 km across the port at Gold Creek (GOC). Again, the April 2008 sampling event was intentionally skipped by SAC design as a program cost-saving measure. The July and October 2008 samplings will be reported under the 2008-09 program.

The BWTF treats and discharges oil-contaminated ballast water offloaded from the tankers prior to refilling them with Alaska North Slope (ANS) crude oil. The ballast-water treatment uses both physical and biological methodologies, which remove most of the BTEX and partially degrade the PAH and SHC components. The treated ballast water is subsequently released through a 63 m-long diffuser, approximately 400 m offshore at a depth of 62-82 m. During the 2006-2008 period, an average of 3.09 million gallons per day (MGD) (Figure 7, range 0-12) was discharged, a significant reduction in

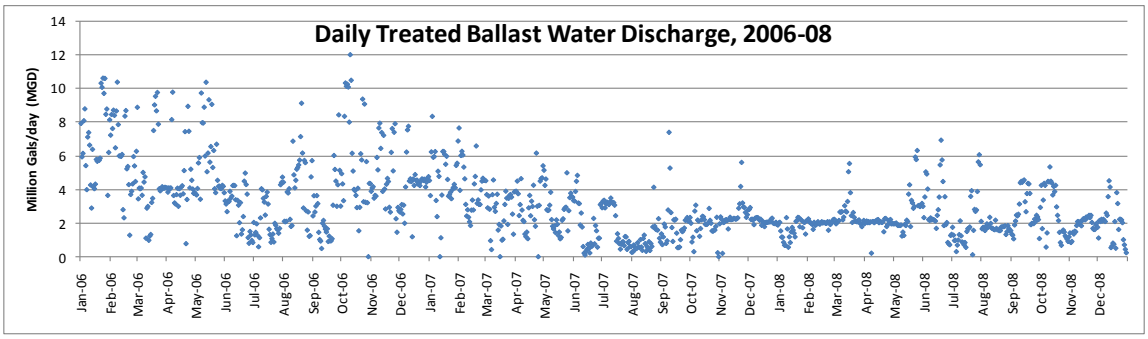

Figure 7 Effluent flow from Ballast Water Treatment Facility, 2006-2008, from NPDES Discharge Monitoring Reports.

total flow compared to the 16-18 MGD treated in the early 1990s. Furthermore, since September 2007, there appears to be a reduced variability in flow with an average discharge of 2.2 MGD. In 2009, the facility is undergoing a redesign to better process the reduced flow.

During warmer months, SHC biodegradation within the facility is very rapid while PAH biodegradation is only partially complete before the effluent is discharged into Port Valdez. During colder months, the biodegradation process is less efficient for both SHC and PAH (Payne et al., 2005b,c). In both seasons, the effluent signature is low level (usually < 100 ppb), but PAH and SHC constituents still appear in local sediments within the mixing zone sampled by the Alyeska Environmental Monitoring Program (EMP) (Blanchard et al., 2005; Shaw et al., 2005) and in mussel and sediment samples historically collected by LTEMP and other PWSRCAC studies (KLI, 2000 and references therein; Payne et al., 2001, 2003a,c,d, 2005a; Salazar et al., 2002). Despite the excellent processing efficiency at the BWTF, the sheer volume processed results in an estimated 0.5-0.7 barrels of highly diluted oil (both as finely dispersed free oil-droplet and dissolved phases – Figure 2 and Figure 3) being discharged daily during the study period into the Port. Based on past measurements of the dissolved and particulate phases, it is estimated that 10-20% of the TPAH is contributed by the oil-droplet phase (Payne et al., 2005c).

5.2.1 Sediment Particle Grain Size

Sediment grain size plots (Figure 8) show that sediment compositions from the last two samplings are within the range of previous years. The 2002-2003 LTEMP report (Payne et al. 2003a) discusses sources and relevance of this variance. To summarize, the PGS data serve two main purposes to the LTEMP program. First, they ensure that the monitored location has not undergone drastic changes, e.g., slope failures, dredge spoils deposits, etc. Secondly, the silt + clay value allows a rough confirmation or calibration of TPAH levels should it ever become necessary.

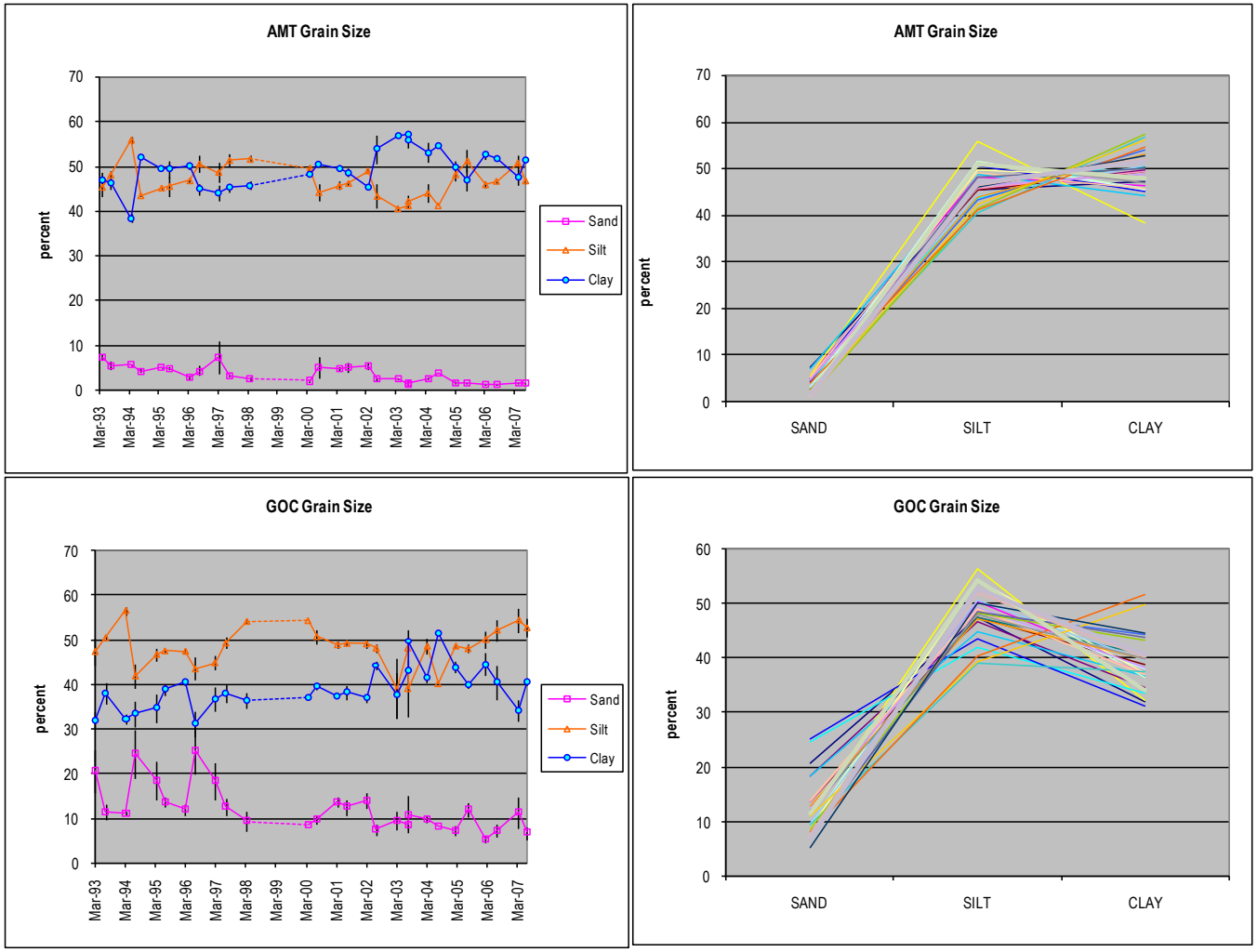

Figure 8 Time series and time overlays of grain size composition at Alyeska Marine Terminal and Gold Creek, 1993-2007. Sediments were not collected in 1998-99.

From the past and current data, we have noted outlier samples and their effect on the chemistry data but conclude that the outliers represent spatial heterogeneity rather than site changes and more importantly, have not affected the trends nor the interpretation of results. In last two reports, we noted the recent cyclic trend of fines at GOC (Figure 9) seem to reflect seasonal silt deposition. This phenomenon is also observed in the intertidal; the GOC intertidal bedrock site occasionally becomes slippery with a noticeable cover of silt. Examining the total fines (silt + clay), there appear to be increasing trends over time at both sites (Figure 9) but the sampling design is too confounded to draw any real conclusions (e.g., variance in site location, change in soil labs, consistency in obtaining surface PGS sample). Results do suggest that AMT is a less dynamic regime than GOC, but the sites have always yielded similar soft fines at every sampling and thus represent a good comparative site pairing.

5.2.2 Total Organic and Inorganic Carbon

Although suspended sediment loads are visibly high in the eastern portion of the Port Valdez basin, the carbon contents (Table 5 and Figure 10) are typical of the predominate, organically-poor glacial flour common throughout the Port Valdez and Prince William Sound Basin. At Constantine Harbor (COH), values are similarly low but do show a presumed bump from spring blooms. Even though this site has exposure to oceanic input from Gulf of Alaska, it is often visibly within the diluted, yet still turbid plume of the Copper River.

Table 5 Total organic and inorganic carbon in sediment replicates at Port Valdez and Constantine Harbor stations.

	Jul-06			Apr-07			Jul-07		
	% TC	% TOC	% TIC	% TC	% TOC	% TIC	% TC	% TOC	% TIC
AMT	0.65	0.56	0.09	0.47	0.43	0.04	0.70	0.65	0.05
AMT	0.62	0.54	0.09	0.48	0.42	0.06	0.56	0.49	0.07
AMT	0.50	0.45	0.05	0.48	0.43	0.05	0.64	0.46	0.18
mean	0.59	0.52	0.07	0.48	0.43	0.05	0.63	0.53	0.10
std dev	0.08	0.06	0.02	0.01	0.01	0.01	0.07	0.10	0.07
GOC	0.66	0.60	0.06	0.55	0.50	0.05	0.62	0.55	0.07
GOC	0.50	0.47	0.03	0.47	0.47	0.00	0.52	0.47	0.06
GOC	0.62	0.53	0.08	0.63	0.51	0.12	0.62	0.56	0.06
mean	0.59	0.54	0.06	0.55	0.49	0.06	0.59	0.53	0.06
std dev	0.09	0.07	0.03	0.08	0.02	0.06	0.06	0.05	0.01
COH	1.05	0.32	0.73				1.14	0.98	0.15
COH	2.53	0.70	1.83				2.81	2.27	0.54
COH	1.97	0.66	1.31				1.00	0.60	0.40
mean	1.85	0.56	1.29				1.65	1.29	0.36
std dev	0.75	0.21	0.55				1.01	0.88	0.19

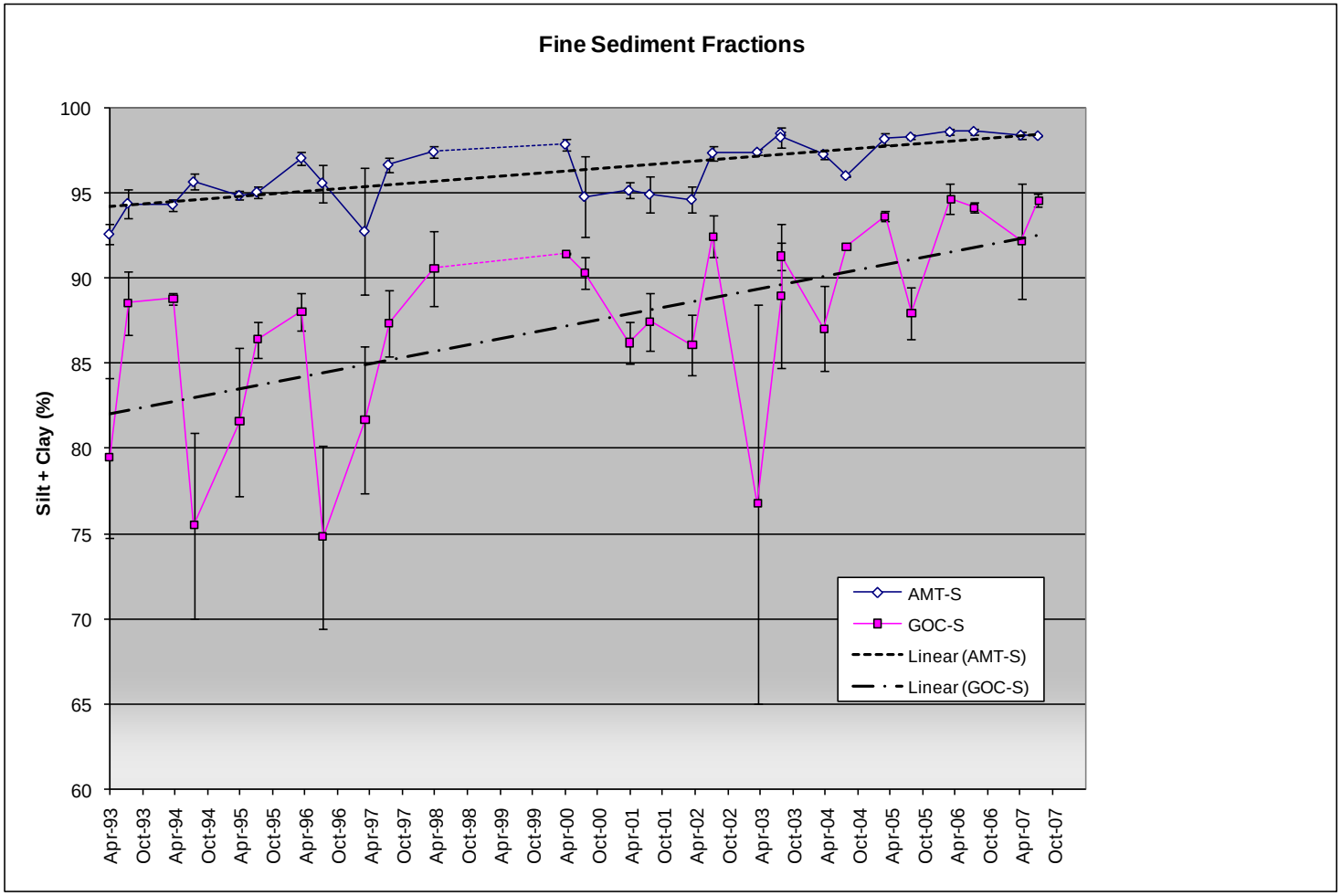

Figure 9 Average fine sediment fractions (silt + clay) time series trends from GOC and AMT surficial sediment grabs (±standard error of means). Note y-axis scale has been clipped for detailed viewing. Sediments were not collected in 1998-99

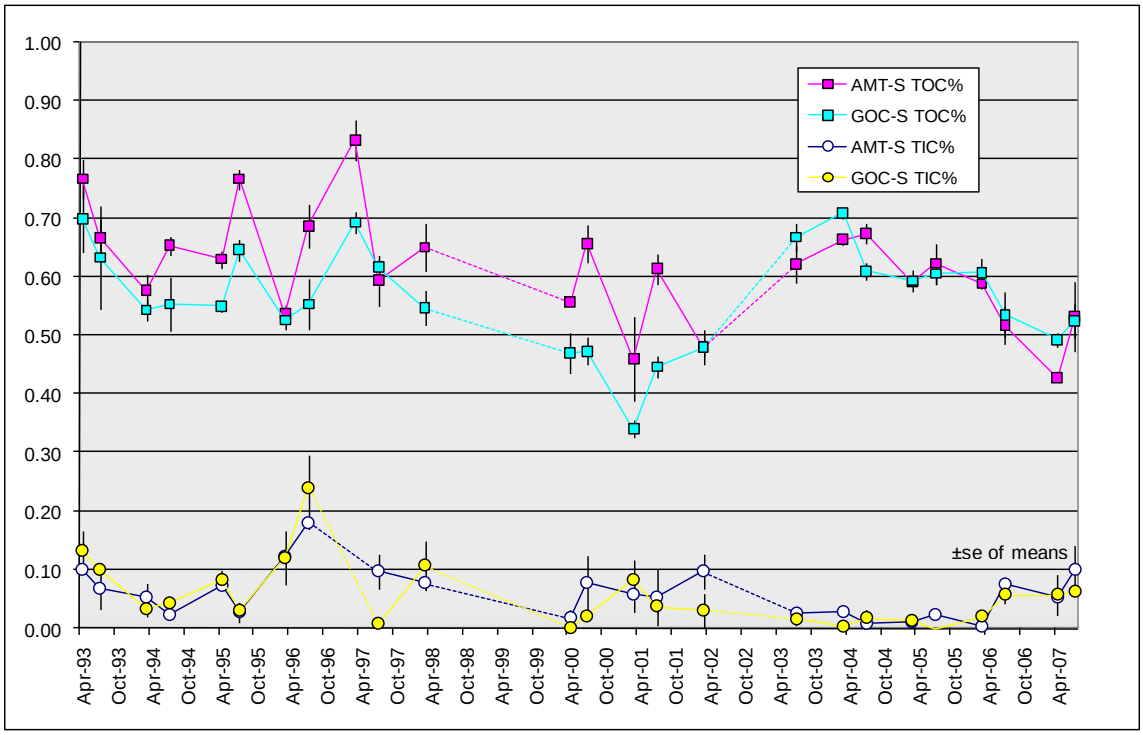

Figure 10 Time series of total organic and inorganic carbon in AMT and GOC sediment. Dotted lines indicate data gaps.

5.2.3 Sediment Chemistry

For a historic recap of the summary sediment chemistry data, Appendix B-1 tabulates the total SHC and PAH values of individual samples, seasonal averages, and the associated coefficients of variation for the replicate measurements completed between 1993 and 2007. In the following sections, these data are discussed for each site separately utilizing a graphical technique first introduced in the 2004-2005 LTEMP report (Payne et al., 2006).

Using the three phase indices presented in Section 4.7.1 plus TPAH, we developed a graphic style (Figure 11) that presents averaged time-series data. The dual-axis, left-hand panels show the relative portions of the TPAH from the three phases (scaled by the left axis) as well as the actual TPAH value (by the logarithmic right axis). The right-hand panels present the same data but scaled as total concentrations (ng/g dry weight on a linear scale) for each phase. Here, the sum of the phases equals the total PAH. This dual-presentation format allows overall trends to be easily identified with the absolute phase magnitudes shown in the right-hand panels, while finer details on relative phase contributions are tracked in the left-hand panels. As a convention, the early samples where procedural artifacts are suspected (1993-1997) are left in context represented by finely-dashed lines; data that we consider reliable have solid symbols. Error bars are omitted for visual clarity.

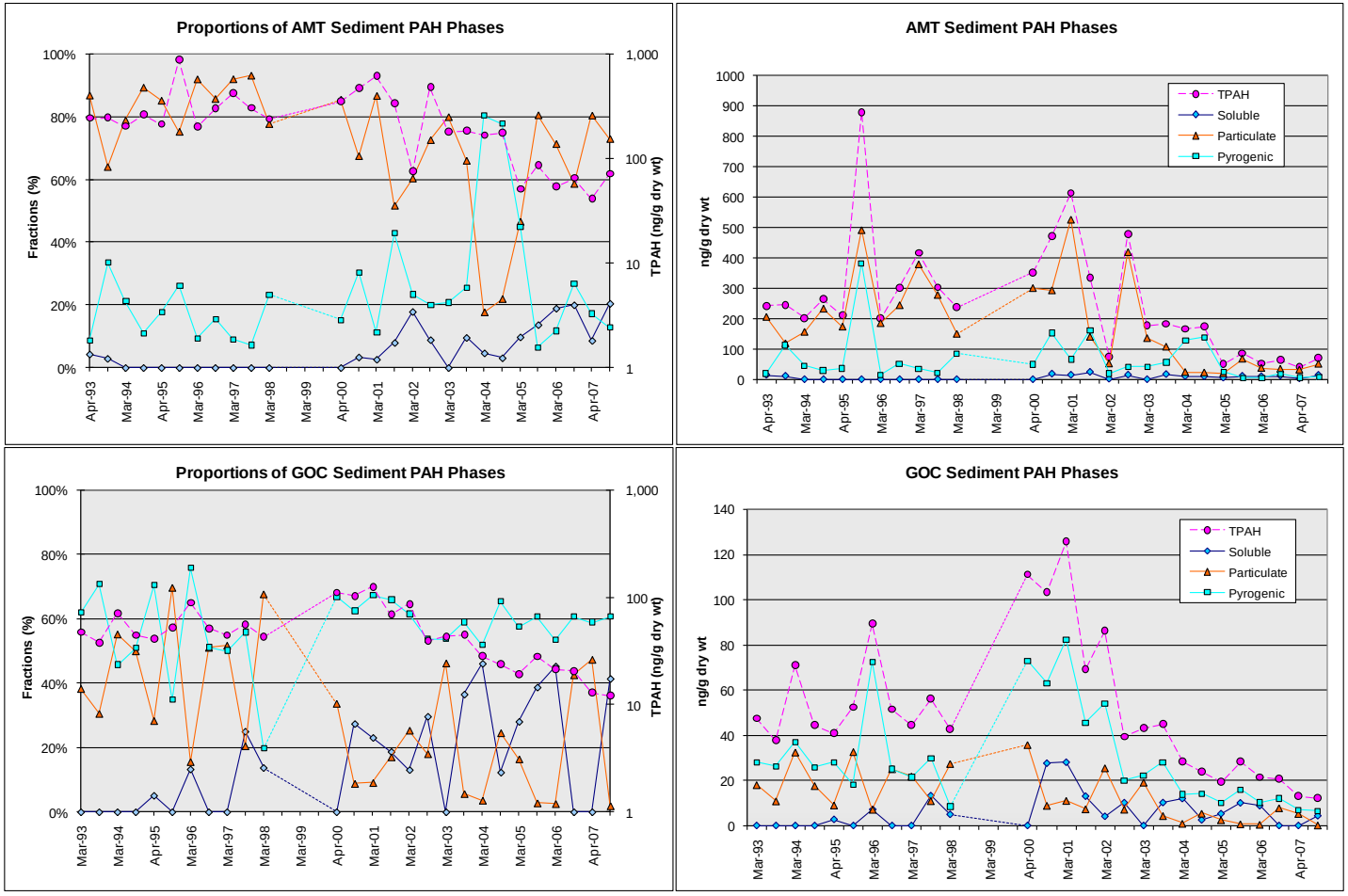

Figure 11 Time series TPAH and relative phase composition of PAH profiles in AMT and GOC sediment samples. Sediments were not collected in 1998-99 or in April 2008.

5.2.3.1 Alyeska Marine Terminal

While there has historically been a lot of variability in the sediment TPAH values at this site (top panels in Figure 11), the concentrations have been less variable over the last four years, and since March 2005 have markedly declined compared to the historical range. Also, it is clear that except for the period of March 2004 through March 2005, the majority of the TPAH signal has been associated with the particulate/oil-droplet phase with lesser contributions from pyrogenic components (Figure 11). This is probably the result of free oil droplets from the diffuser interacting with suspended particulate material (SPM, primarily glacial flour) followed by near-field sedimentation (Payne et al. 1989, 2003b; ETC 1999). In between March 2004 and 2005, pyrogenic components were dominant (Figure 11 upper panels), but a more typical, very low, and heavily biodegraded, particulate oil signal has been consistently observed since July 2005 (Figure 12). The decline in TPAH in the AMT sediments presumably reflects lower levels of free oil droplets in the BWTF discharge from reduced discharge volumes, or improvements in the ballast water treatment process efficiency at removing free oil droplets, or both.

As pointed out in previous LTEMP reports (Payne et al., 2003a, 2005a, 2006), we cannot tell from these data if the water-soluble fraction (primarily naphthalenes, which are apparently increasing in proportion to other components over the last four years) is truly bioavailable or simply tied up in the sedimentary matrix. Naphthalenes make up a major component in the deepwater sediments throughout Port Valdez, Prince William Sound, and offshore areas in the Gulf of Alaska from the Copper River to the Shelikof Straits (Short and Babcock 1996; Short et al., 1999, 2007b; Page et al., 1995; Payne et al., 1998, 2006; Saupe, 2004). Our phase-assignment model assigns a dissolved characterization to the naphthalenes because of their decreasing trend with increasing levels of alkylation and their abundance relative to the fluorenes and the phenanthrenes/anthracenes (see Section 4.7.1), but their ubiquitous nature suggests that they are largely tied up in the internal matrix of the mineral phase (discussed later).

5.2.3.2 Gold Creek

Just as in the sediment samples from the Alyeska Marine Terminal, there has been considerable variability in the TPAH values at GOC in the past, but the overall TPAH concentrations are generally five-to-ten times lower at GOC (lower panels Figure 11). And just like AMT, the GOC sediments show declining TPAH levels since July 2003 (right-hand graphs Figure 11); however, the overall TPAH levels appear to track primarily with the decreasing pyrogenic (combustion) fraction at GOC, whereas they were almost exclusively driven by the particulate/oil-phase at AMT. The relative composition data (lower left Figure 11) show that while the combustion-derived constituents in Gold Creek sediments appear to be fairly consistent (around 60%) since March 2002, the relative contributions from more soluble, lower-molecular-weight constituents and particulate/oil-phase components have been more variable, particularly since March 2006.

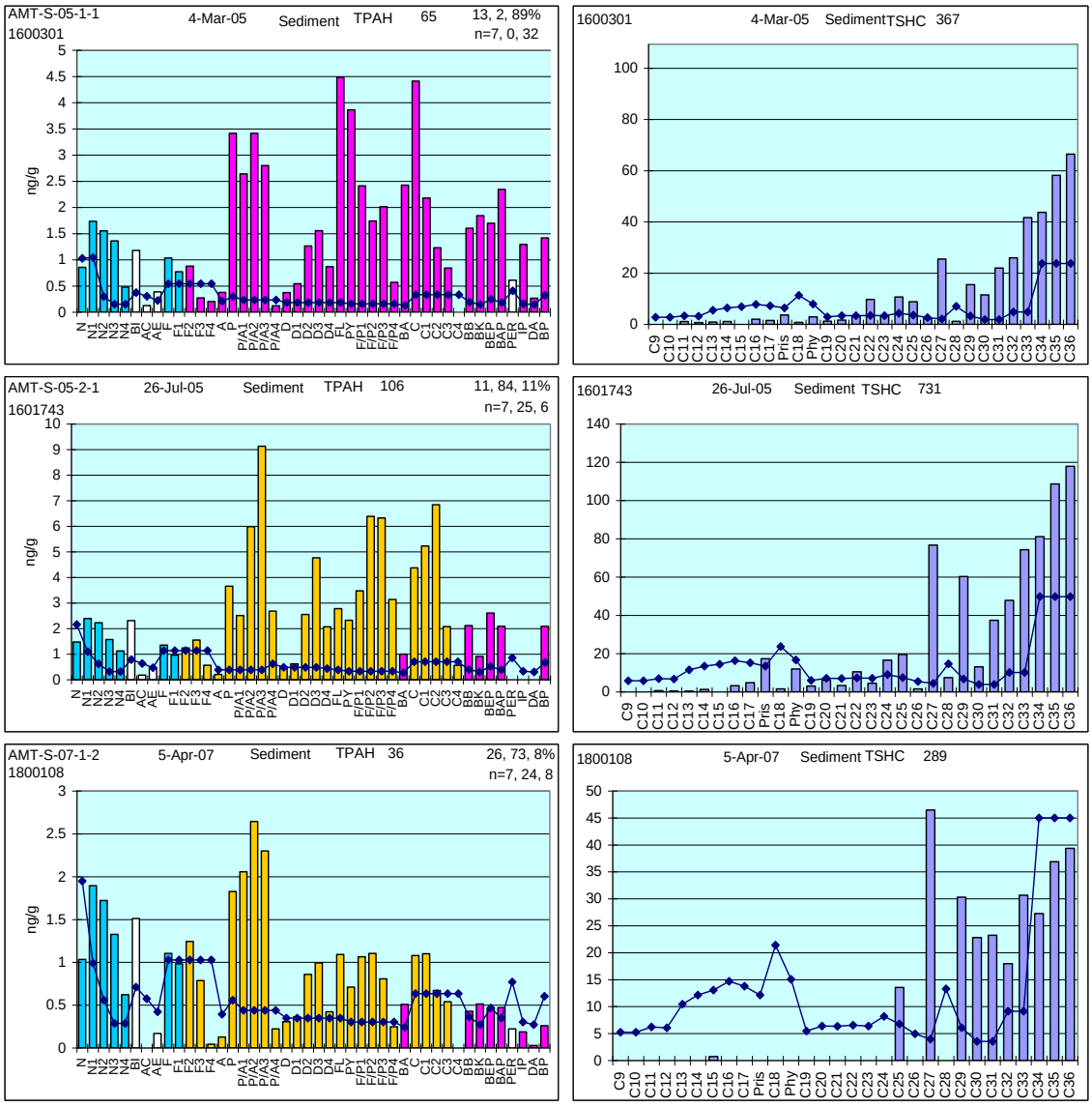

Figure 12 PAH and SHC profiles from representative AMT sediments from 2005 to 2007 showing the transition from a combustion product dominated signal to complex, biodegraded oil/particulate-dominated signatures. 1996-era MDLs indicated with dotted solid line.

From the histogram plots (Figure 13), it is clear that the phase-assignment model attributes PAH to both particulate/oil and combustion products in July 2006 and April 2007, whereas the July 2007 components are assigned to dissolved-phase naphthalenes and combustion products. In all three samples, the SHC fractions show primarily biogenic input reflected by higher-molecular-weight, odd-carbon numbered n-alkanes from terrestrial plant waxes, with traces of below MDL petrogenic components suggested (at least in the July 2006 sample). In this context, however, it is important to note that the

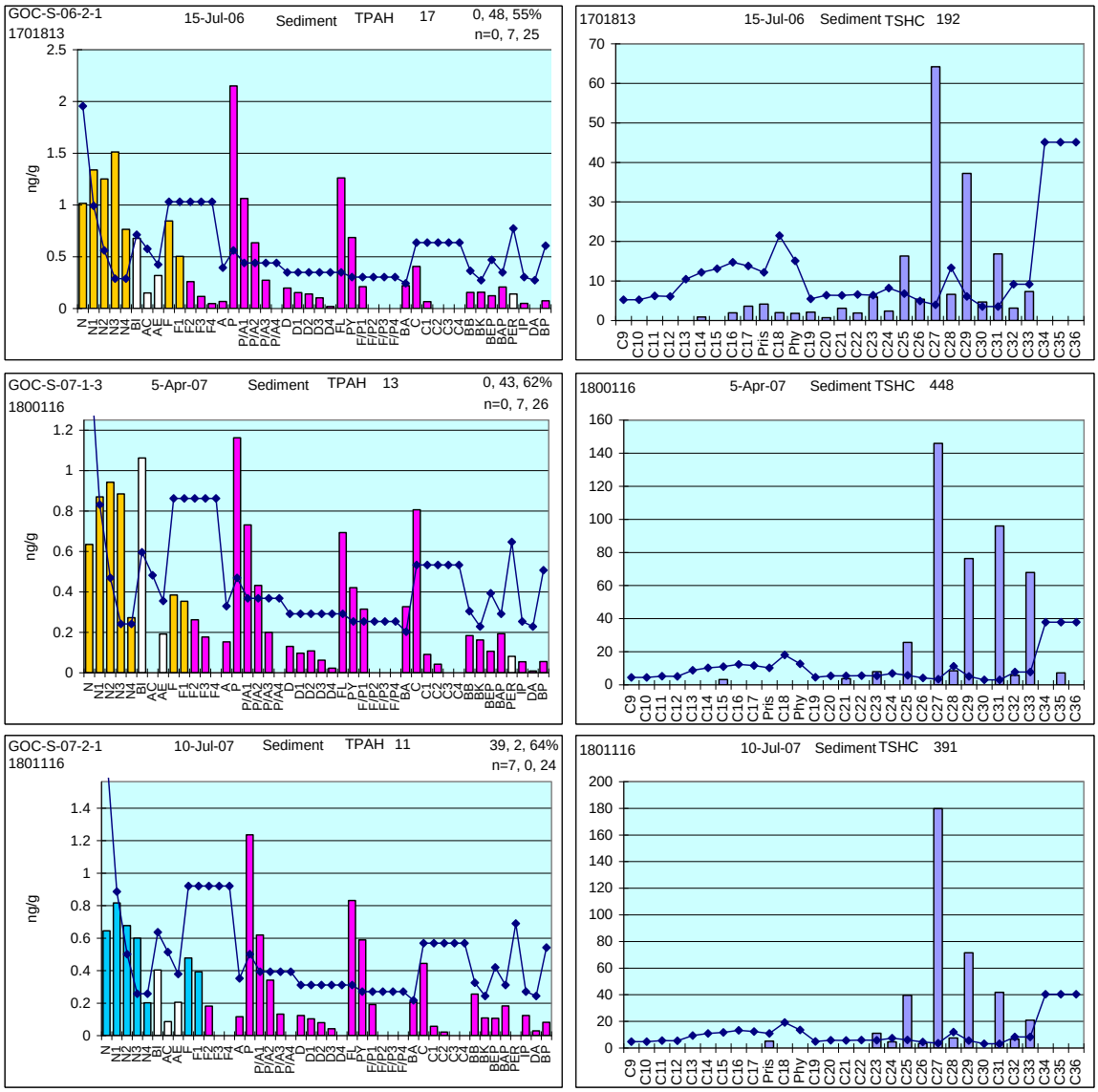

Figure 13 Representative PAH and SHC profiles for 2006-2007 Gold Creek sediments.

overall TPAH levels are very low (generally above the MDLs but still < 50 ng/g dry weight since July 2002), and we should caution that at very low levels the relative proportional signals can become pretty noisy. In these examples, the individual naphthalene homologues are each present at concentrations below 1.5 ng/g dry weight, and a 0.1 ng/g dry weight change in absolute concentration in just one component can trigger a switch from a particulate/oil- to a dissolved-phase assignment (see Section 4.7.1). As will be discussed further below, this has become particularly problematic with low-concentration tissue samples, and for those samples we have observed that our phase-assignment algorithm has become less reliable requiring manual evaluation of the data from each sample.

Without additional sterane and triterpane data, it is impossible to determine if the very minor petrogenic signal observed in the sediments at Gold Creek can be attributed to input from the Alyeska Marine Terminal; however, Shaw et al. (2005) concluded from their triterpane data that the sediment profiles at EMP Stations 40 and 50 (near Gold Creek but at greater depths in the Port) contained petrogenic components derived from Alaska North Slope crude oil.

5.2.3.3 Constantine Harbor

The Constantine Harbor site was added to the program in support of the EVOS Trustees' expanded program objectives. It serves as a non-EVOS oiled, sediment reference site primarily influenced by the plume of coastal Gulf of Alaska longshore transport as it sweeps through the Hinchinbrook Entrance (Short and Babcock 1996). TPAH concentrations have ranged from 30 to 86 ng/g dry weight, and possible sources identified by a number of investigators include suspended sediments, pulverized coal, organic material (e.g., kerogen), and natural oil seeps introduced to the Alaska Coastal Current by numerous rivers and glaciers along the Gulf of Alaska coastline southeast of the Sound (Karinen et al., 1993, Page et al., 1995; Short and Babcock 1996; Short et al., 2007b). In the PAH plots (Figure 14), the naphthalenes in these sediments are algorithmically assigned as particulate/oil-phase since they don't descend in a smooth N1>N2>N3 pattern. In that their concentrations are significantly higher than the subtidal Gold Creek sediments, these phase assignments are believed to truly reflect their physical state albeit even here a 0.5 ng/g dry weight shift in N1 can switch the phase assignment to a dissolved-phase pattern (as was observed in several samples collected in March 2006).

In corroborating evidence, the presence of naphthalenes throughout sediments from the Copper River to Shelikof Strait (EMAP program, S. Saupe, 2004) suggests that they are bound up in the solid sedimentary phase, apparently particulate and not easily leached out. And yet, a naphthalene signal appears in tissues across our LTEMP stations. Could these transported sediments be the source? We tested for a leaching effect during the 2007 summer LTEMP/EVOS Trustees SCAT program by collecting interstitial water samples from Constantine Harbor and experimentally mixing intertidal Constantine Harbor sediments with clean seawater samples collected from the Hinchinbrook Entrance (see Appendix E). The results showed that the three most water-soluble PAH (naphthalene, biphenyl, and C1-naphthalene) increased linearly in the filtered seawater (i.e., dissolved phase) with increasing sediment loads. These data support the hypothesis that sedimentary materials previously believed to only contain sequestered and non-bioavailable PAH, may in fact be contributing to the ubiquitous dissolved-phase signals observed in mussel-tissue samples throughout the region. This effect is discussed further in Section 5.3.3.5, and additional details are provided in Appendix E.

We do not have time-series data from Constantine Harbor as part of the LTEMP program, but data from Karinen et al. (1993) and Short and Babcock (1996) showed higher, and relatively invariant TPAH concentrations (~560 ng/g dry weight) in intertidal

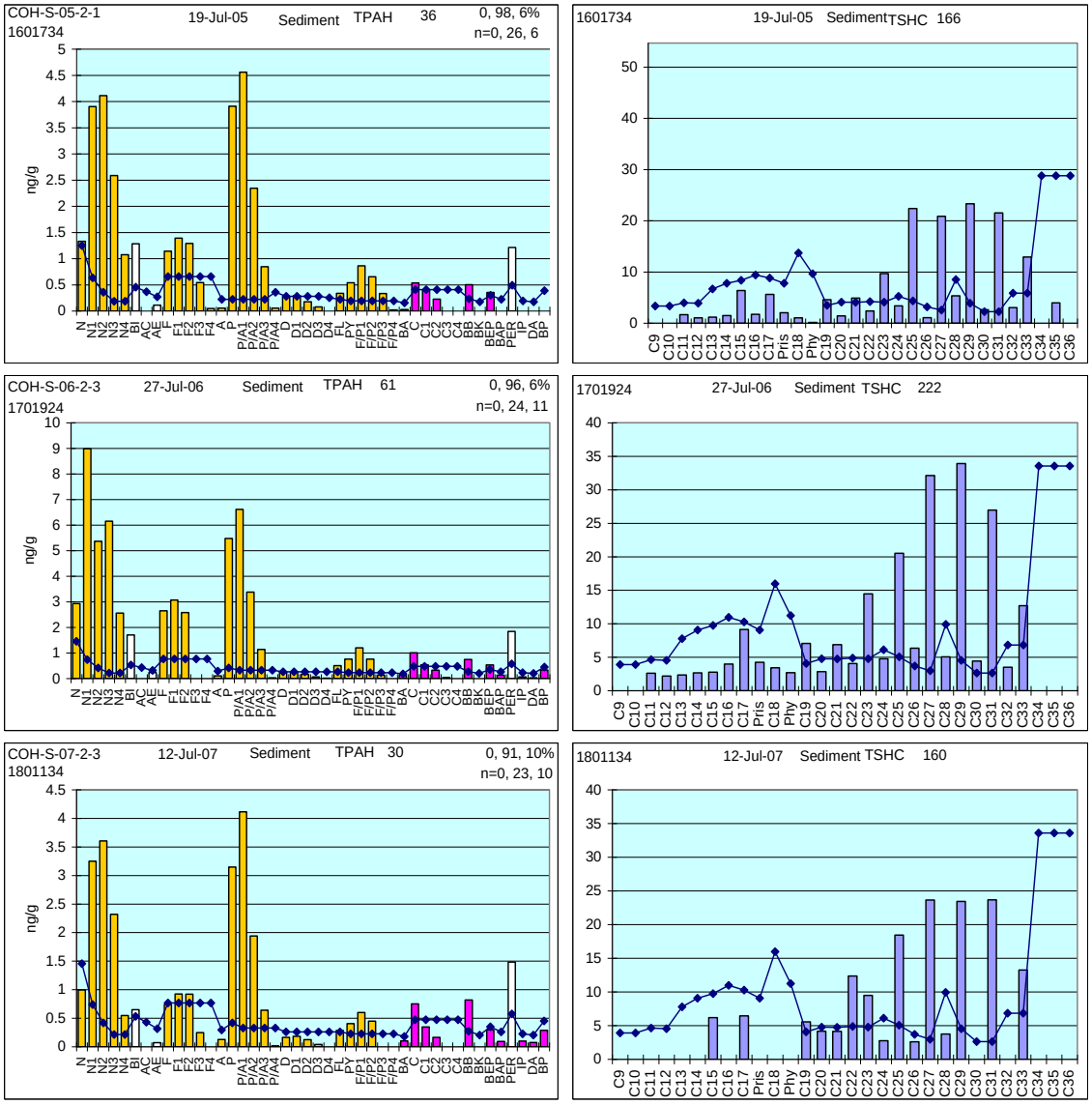

Figure 14 PAH and SHC profiles from representative 2005-2007 Constantine Harbor intertidal sediments.

sediments collected in 1977-1980 and 1989-1991, respectively. The intertidal sediments collected as part of the LTEMP sampling were obtained from a slightly different area within Constantine Harbor, but the PAH composition was very similar to data reported in earlier studies. The lower concentrations presumably reflect spatial heterogeneity within the Harbor and dilution by local sediments introduced from the surrounding watershed. The SHC profiles reflected terrestrial plant wax components, and a general absence of fresh petroleum (very low or non-detectable levels of phytane). As described by Short and his colleagues, there was no evidence of EVOS oil in the sediments collected as part of this program.

5.2.4 Summary and Discussion of Sediment Chemistry Results

From the Port Valdez subtidal sediment-sampling sites, it is clear that the sediments adjacent to the Alyeska Marine Terminal are primarily contaminated by a weathered ANS oil signal, which would be consistent with BWTF-diffuser-sourced, dispersed oil-droplet/suspended-particulate-material (SPM) interactions and subsequent sedimentation (Payne et al. 1989; 2003a,b; ETC 1999). In recent years, the combustion (pyrogenic) components in the sediments at AMT have been variable and appear to be reaching all time lows. The Gold Creek sediments, on the other hand, show generally declining PAH contamination from combustion sources (since March 2001) with lesser contributions from low-level petrogenic sources. These declining combustion product assignments are highly qualified since the TPAH values are so low but may, in fact, reflect lower exhaust emissions from reduced tanker traffic or the concerted local efforts to modify idling tanker operations to mitigate air pollution within the Port.

It is not possible to tell from LTEMP data alone if the low-level petroleum source in the subtidal sediments at Gold Creek is from the BWTF and other activities at Alyeska Marine Terminal, or other sources (boat traffic, sewage and wastewater discharges from the City of Valdez). It may be possible to identify this source through sterane/triterpane analyses of Gold Creek sediments and comparisons to Alyeska Marine Terminal sediments and Alyeska BWTF discharges as part of future LTEMP or other PWSRCAC research activities. Triterpane data from the Alyeska EMP indicate that PAH from their station 40 (deeper and further offshore from the LTEMP GOC station) are consistent with weathered Alaska North Slope crude oil released from the terminal (Shaw et al., 2005).

The SHC patterns observed for the subtidal sediments at Alyeska Marine Terminal (Figure 12) show a combination of biogenic and very weathered ANS oil signals, again consistent with terrestrial and marine copepod fecal-pellet sources along with substantial oil-droplet/SPM interactions given the elevated levels of dispersed oil droplets introduced to the region from the BWTF diffuser (Payne et al. 2001; 2003a,b; 2005b,c; Salazar et al. 2002; Short 2005). In contrast, the SHC profiles from the subtidal sediments at Gold Creek (Figure 13) show a combination of marine and terrestrial biogenic input, with very little weathered-oil signal in keeping with the extremely low TPAH values observed at the site.

The intertidal sediments from Constantine Harbor had lower TPAH values than those reported in previous studies (Karinen et al., 1993; Short and Babcock, 1996), but the PAH and SHC compositional patterns (Figure 14) were consistent with previous findings and represented a non-oiled sediment primarily influenced by the plume of coastal Gulf of Alaska longshore transport as it sweeps through the Hinchinbrook Entrance. Dissolution of water-soluble PAH from these sediments, a potential source for the dissolved-phase PAH pattern observed in mussel tissues throughout the region, is described in detail in Appendix E.

5.3 Mussel Tissue Chemistry

5.3.1 Regional Trends and Approaches

The time series of TPAH concentrations (Figure 15) using the consistently reliable post-1997 data shows generally decreasing trends with a subseries of somewhat synchronous peaks along the timeline. The generally simultaneous TPAH maxima occurred in July 1999, March 2001 (excluding Aialik Bay, Shuyak Harbor, and Windy Bay), March 2002 (again except for Shuyak Harbor and Windy Bay), and March 2004 (except for Knowles Head). These events have been discussed in previous reports couched as possibly ambiguous results or perhaps laboratory artifacts. The large spike in October 2004 for Gold Creek was from an unreported diesel spill, which still manifest itself as a recognizable signal in March 2005 (Payne et al., 2006). Using the recently-developed PAH indices to further evaluate these trends, we have noted that not only were there synchronous peaks, but in many of the stations, the composition of the trace-level signatures were also similar. After further exploration, three regional patterns became apparent; the Port Valdez, Prince William Sound, and Gulf of Alaska regional stations were each trending in similar fashion (Figure 16) and often with regionally similar, low-level dissolved- and particulate/oil-phase signals. These trends and similarities will be discussed further below, but their discovery prompted us to organize the following sections on mussel tissue chemistry by regions (Figure 16).

This report again emphasizes the importance of examining TPAH data from the perspective of dissolved-, particulate/oil-phase and combustion-product signals. Specifically, when analyzing the LTEMP mussel tissue samples, it is important to recognize that as filter feeders, mussels can accumulate an oil signature from both the dissolved- and particulate/oil-droplet phases, in addition to combustion products (soot) present as finely suspended pyrogenic particles in the water column (Baumard et al. 1998; Payne and Driskell 2003; Short and Springman, 2007). Using the dissolved-, particulate-, and pyrogenic indices described in Section 4.7.1, we graphically review in this section the mussel-tissue, time-series trends for each site (as shown in Figure 17 for Alyeska Marine Terminal and Gold Creek), and augment that discussion with PAH and SHC plots to further elucidate source signatures as necessary. Recall from Section 4.7.2, higher-concentration data in which we have confidence are represented by solid symbols in Figure 17 and corresponding figures for other stations, while the early, low-concentration samples where procedural artifacts are suspected (1993-1997) are left in context but represented only by finely-dashed lines.

The dual-axis data in the left-hand panels (Figure 17) show the relative percentages of the total PAH (TPAH) from the soluble, particulate (oil phase), and pyrogenic fractions (left axis) as well as the TPAH value (on a logarithmic scale – right axis). The right-hand panels present the same data simply as total concentrations (ng/g dry weight on a linear scale) for each fraction. In the right-hand panels, the sum of the soluble, particulate, and pyrogenic fractions equals the total PAH (dark fuchsia-colored circles). This dual-

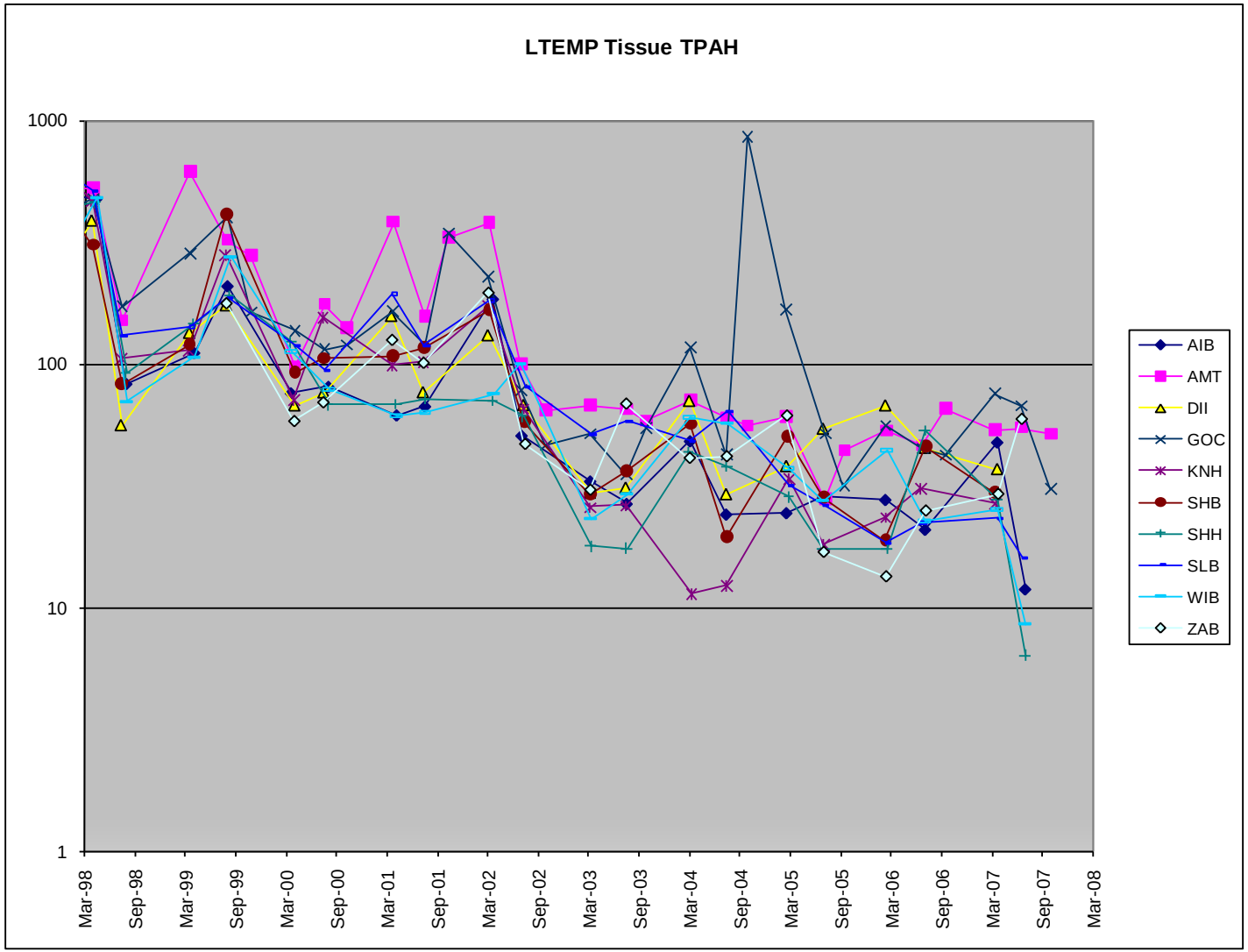

Figure 15 ***Mytilus*** **TPAH time series (triplicate averages) for all LTEMP stations, 1998-2007.**

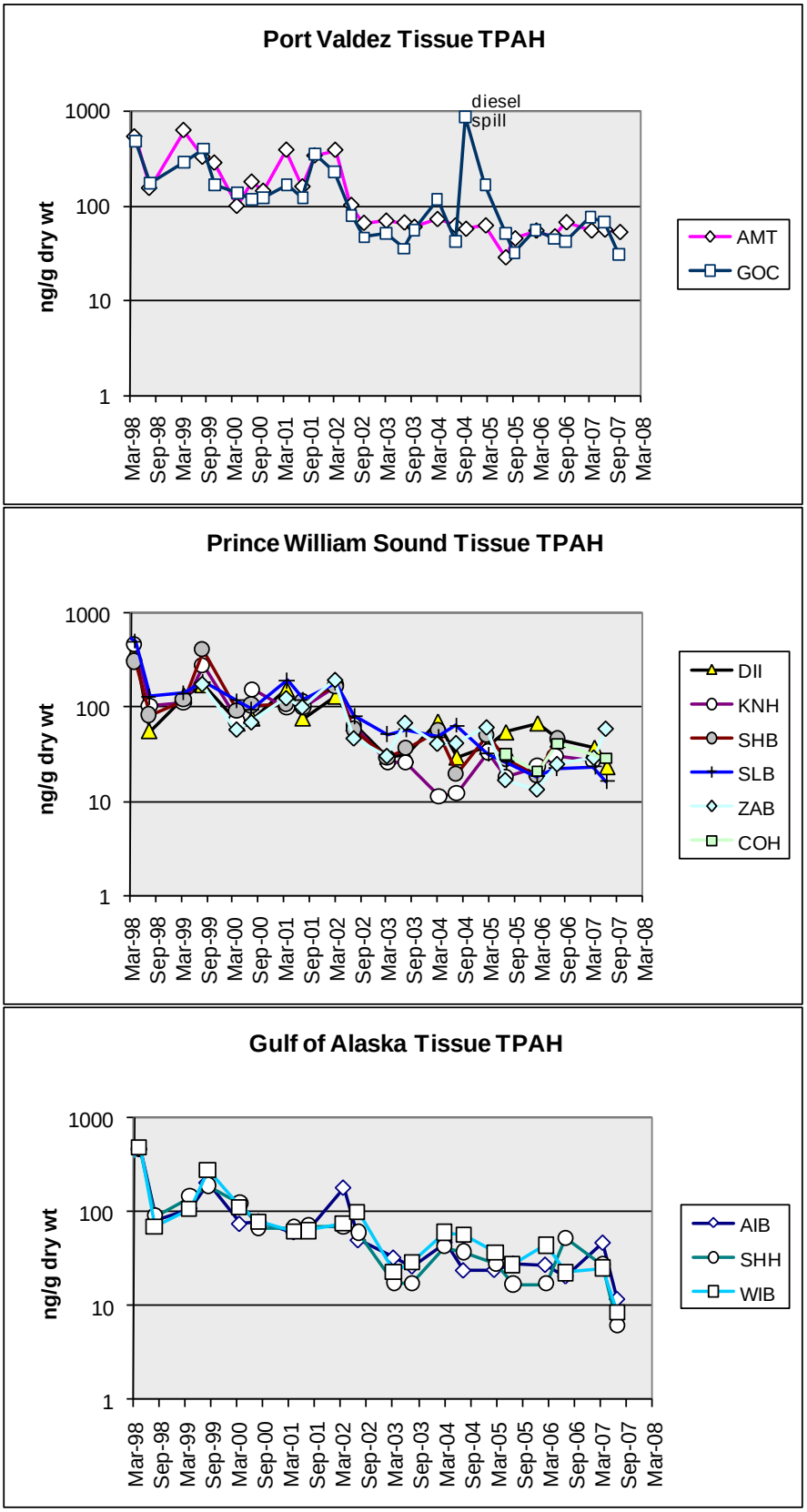

Figure 16 Regional LTEMP *Mytilus* TPAH time series, 1998-2007.

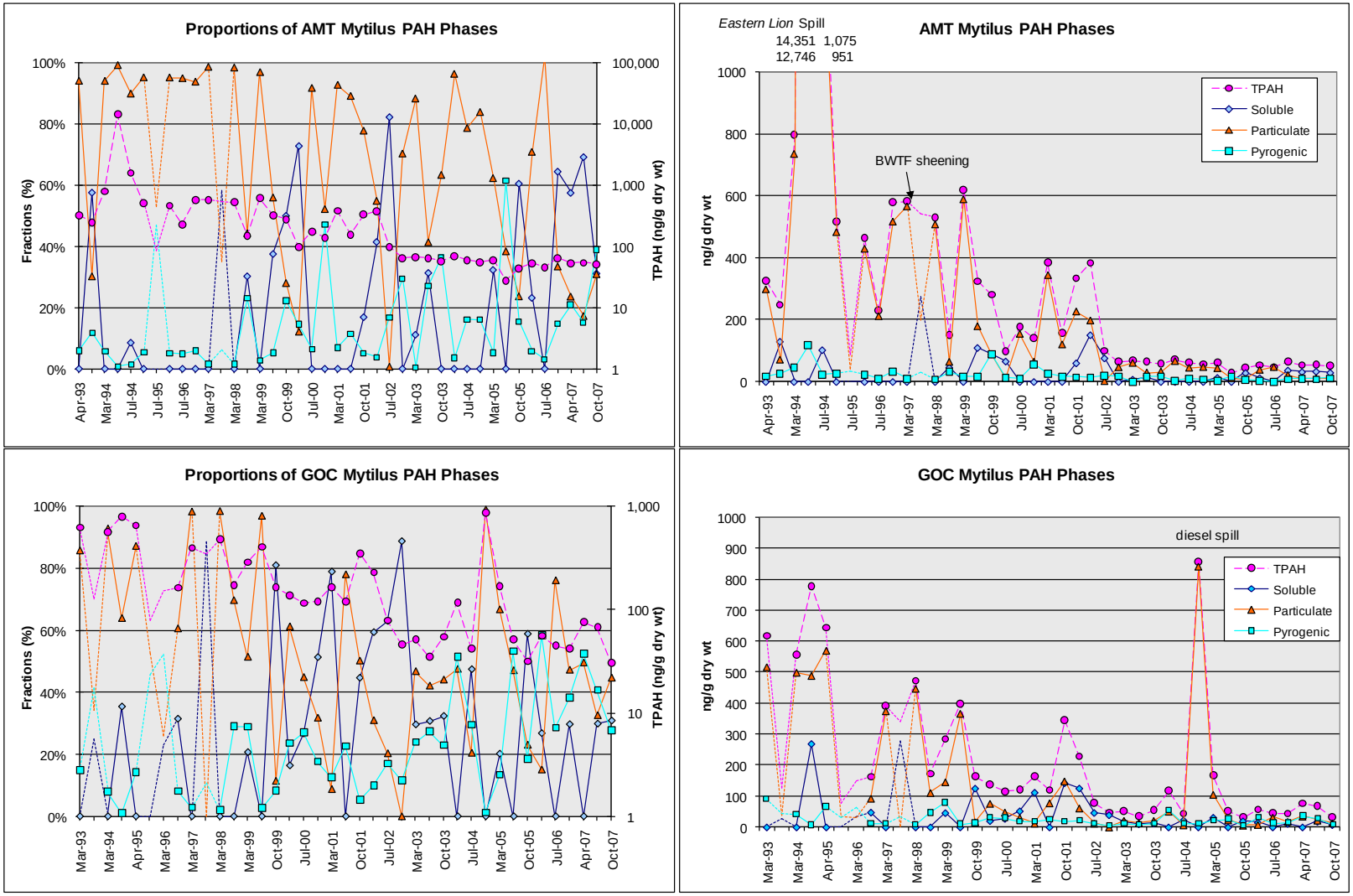

Figure 17 Time series TPAH and relative phase composition of PAH profiles in Alyeska Marine Terminal (AMT) and Gold Creek (GOC) *Mytilus* tissues. Dotted connecting lines without symbols indicate questionable data.

presentation format allows overall trends to be easily identified with the absolute magnitude of each fraction shown in the right-hand panels, while finer details on relative contributions from the different fractions can be tracked in the left-hand panels.

In our report for the 2003-2004 program (Payne et al., 2005a), a complete review and detailed discussion of the tissue chemistry data from all stations sampled over the first eleven years of the program was presented in Appendix A-3 – Station Accounts for Tissue Samples; the interested reader is directed to that report for additional information. Appendix B-1 of this document tabulates the total SHC and PAH values of individual tissue samples, sampling averages, and the associated coefficients of variation for the replicate measurements completed between 1993 and 2007. Appendix B-2 does the same for the PAH indices, and Appendix D presents PAH histogram plots for all the tissue analyses from the 2006-2008 program (actually through October 2007 since the April 2008 sampling effort was eliminated as a cost-saving measure by the PWSRCAC Science Advisory Committee – SAC). The following three sections briefly consider the time-series trends noted for the three geographic regions (Figure 15 and Figure 16): Port Valdez, Prince William Sound, and the Gulf of Alaska (see also Figure 1).

5.3.2 Port Valdez Stations

5.3.2.1 Alaska Marine Terminal Mussel Tissue Chemistry

Mussels collected from Saw Island, adjacent to berth 5 at the Alyeska Marine Terminal (AMT), have historically contained the highest and most variable TPAH concentrations of any site in the program (top panels Figure 17). These values reflect input from the daily discharge of treated ballast water from the terminal as well as known spill events, such as the *T/V Eastern Lion* oil spill in May 1994 and the BWTF spill/sheening event in January 1997. In addition to these known events, there also appear to be uncorrelated incidences of increased particulate/oil-phased TPAH loadings in the adjacent mussels collected in March 1998, March 2001, and March 2002. Details tracking the descent of TPAH levels to the current low, background levels and source-phase variability are described at length in Payne et al. (2006, 2008). In the most recent samples, there appears to be more source variability in the low-level TPAH signals (Figure 17), with particulate/oil-phase, dissolved-phase, and low-level combustion components observed in July 2006, April 2007, and July 2007, respectively (Figure 18). Although phase assignments can be tenuous at these extremely low TPAH values, the PAH patterns for these samples are not ambiguous, and they clearly show the shift from particulate/oil-phase sources to a more dominant dissolved-phase as BTWF flow has decreased in recent years. The final data point in this series, October 2007, is misclassified as particulate phase by the algorithm due to ng-level critical differences in characteristics. Other evidence suggests it is dissolved.

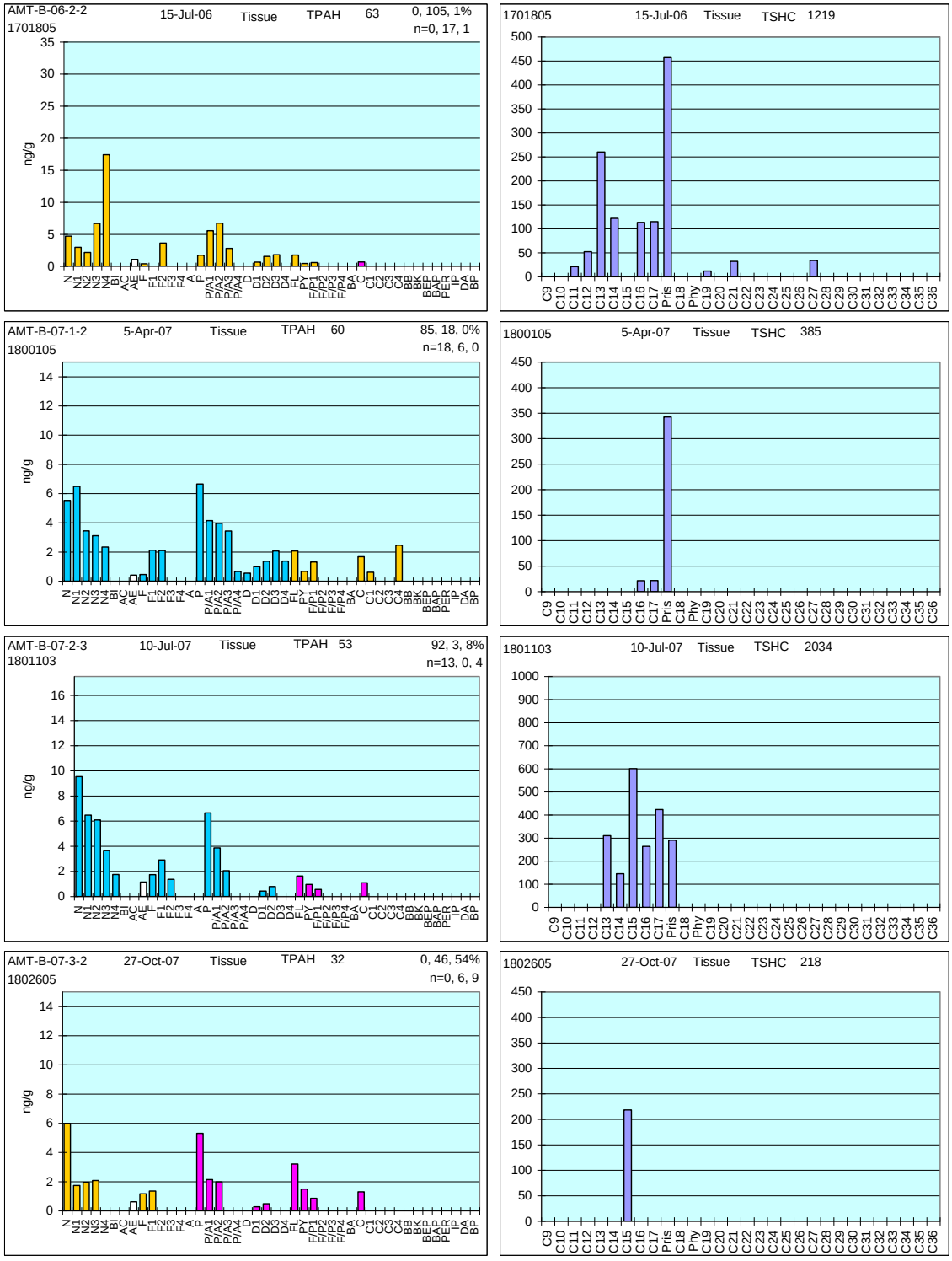

Figure 18 PAH and SHC profiles showing low-level TPAH with variable source signals (particulate/oil-, dissolved-phase, and trace-level combustion products) in AMT mussel samples from 2006-2007. MDL line omitted for scaling perspective (all PAH values are below 1996 MDL but above the sub-nanogram 2010 MDL level).

A striking feature of the early AMT data is the alternating saw-tooth pattern described in previous reports with the particulate/oil phase dominating in the spring, and the soluble phase in the summer (excluding the *Eastern Lion* oil spill) (Figure 19, subset of Figure 17 left panel). To facilitate visualization of the seasonal comparisons within the Port, these data have been re-plotted for both the Alyeska Marine Terminal and the Gold Creek (GOC) reference station 6 km across the Port (Figure 19) with all of the other information removed Testing these patterns using randomization, paired-t tests show, as reported in last year's report, that in the period 1993-2005, particulate phases dominate in spring at both sites while dissolved and pyrogenic phases tend to be higher in summer (Table 6). But apparent in this year's data, around 2002, the relationship breaks down. Considering just the 2002-2007 data, there are spikes but there is no significant pattern (p= ~0.5 for all phases). We do not know from these data if the observed decreases in tissue and sediment TPAH burdens reflect reduced BTWF discharge volumes as more double-hulled tankers are brought into the tanker fleet, the decreased flow of ANS crude oil through the pipeline to the terminal, or improved BWTF efficiency at removing particulate/oil-phase PAH, or a combination of all these factors. As more data become available from the newly redesigned BTWF, the answer may become more apparent

Table 6 Exact one-tailed probabilities* of showing loss of seasonal phase dominance in mussels at AMT and GOC.

	Particulate (%)	**Dissolved (%)**	**Pyrogenic (%)**
	Spring>Summer	**Summer > Spring**	**Summer > Spring**
1993-2005 (n=13) **			
AMT	0.003	0.074	0.046
GOC	0.054	0.107	0.122
2002-2007 (n=6)			
AMT	0.493	0.476	0.502
GOC	0.496	0.499	0.506

*randomization paired t-tests (2000 trials)

**comparison 1993-2005 data from Payne et al. 2008

To us, the historic alternating pattern (Figure 19) suggests three contributing processes: water-column stratification, oil/SPM agglomerate sedimentation, and microbial activity. Relative to the receiving seawater, the BWTF effluent is warmer and less saline, so its behavior and dilution are controlled by the physical oceanography and water-column structure in the Port (Colonell 1980a,b; Woodward Clyde Consultants and ENTRIX 1987). During the period of stable water-column stratification in the Port (late spring, summer, and fall), we believe that the dispersed oil droplets released from the BWTF effluent are primarily entrained beneath the pycnocline (stratified layer) in the middle-water-column regions where they are advected and diluted into the receiving Port waters allowing them to interact with SPM to form agglomerates and sink without ever reaching the upper water column to any significant extent (Payne et al, 2001, 2003b,d). Thus, lower overall TPAH levels with higher dissolved-phase signals are often observed in the AMT and GOC intertidal mussels collected in the summer period. During the winter and early spring,

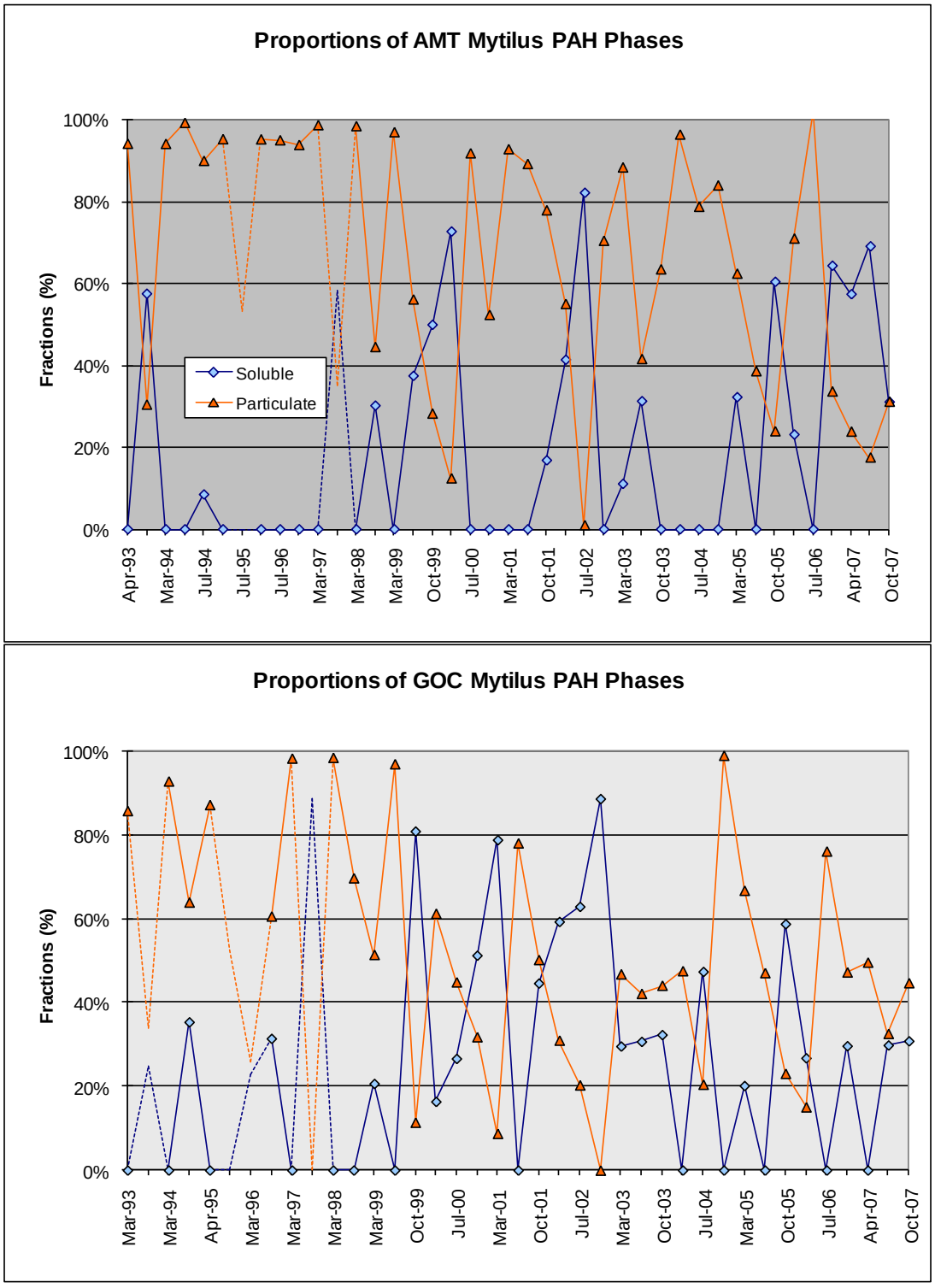

Figure 19 PAH Phase assignments for AMT and GOC mussel showing alternating seasonal (winter vs. summer) spikes in dissolved and particulate phases. Beginning in 2002, the pattern decouples.

however, when the water column is not stratified, the warmer and less-saline BWTF effluent can reach the water surface where it is likely to form a surface microlayer (Hardy 1982; Hardy et al., 1987a,b, 1990; Cross et al., 1987) containing higher levels of weathered oil-droplet-phase SHC and PAH components. Since mussels feed from the surface and upper few meters of the water column, this effect results in the predominance of the particulate/oil-phase signals observed in the intertidal mussels at AMT and (to an even greater extent) GOC during the spring LTEMP collections.

Adding to the stratification effect would be the increased levels of SPM (mostly glacial flour) brought by spring rains and summer glacier melting that would result in increased scavenging and settling of the oil droplets. With the Port's sedimentation rates estimated at 0.4-1.5 cm yr^{-1} (Savoie et al., 2006), one would expect a fairly efficient removal of dispersed oil droplets. And finally, during the warmer months with added insolation, increased surface temperatures, and nutrients from spring blooms, microbial degradation rates might also be expected to increase thus removing more of the particulate/oil phase. In summary, during warmer months, stratification reduces transport to the surface while increased sedimentation and enhanced microbial degradation augment the removal rate of oil droplets before they are acquired by mussels. Starting with the significantly lower TPAH levels observed in the mussels at both AMT and GOC in 2002 (Figure 17), the source signal is much weaker, and the seasonal trend appears to disappear. Without additional supporting data, we make no attempt to tease out the relative effects of these processes, but the combined results are plainly visible (albeit variable) in the data.

A potential negative aspect to this seasonal phenomenon is that concentrated contaminants in an upper layer or surface microlayer would also increase risks from photo-enhanced toxicity to near-surface, planktonic biota (Barron and Ka'aihue 2001; Pelletier et al., 1997; Duesterloh et al., 2002; Barron et al., 2003). Supporting this conjecture, Carls et al. (2006) show that within Port Valdez, particle-feeding, *Neocalanus* copepods are capable of concentrating PAH from trace levels in water to detectable levels in tissue, and they had PAH profiles both similar to the BWTF effluent and to the low levels seen in mussels. Furthermore, copepod samples from sites at the western end of the Port and mid Prince William Sound, like the LTEMP mussels, showed a transition from a particulate/oil-phase signature to just a dissolved-phase background signal.

5.3.2.2 Gold Creek Mussel Tissue Chemistry

In general, the overall levels of TPAH measured at GOC (Figure 17, bottom graphs) are slightly lower than those at AMT, but the observed peaks and valleys (concentration maxima) track with those at AMT, particularly during the early years of the program when spills or other discharges from the terminal were more frequent. Also, the same seasonally-dependent, saw-tooth pattern of alternating soluble- and particulate/oil-phase signals observed at AMT is apparent (Figure 17, bottom left panel and Figure 19). While many of the lower-TPAH level samples (July 1993, July 1995, March 1996, and July 1997) were subject to the procedural artifact issues discussed in Section 4.7.2 (shown as

dashed lines without solid data points in Figure 17), the data for the elevated PAH levels were judged to be of good quality and appear to be related to the known spill events at the terminal across the Port.

In October 2004, the TPAH concentration spikes to the highest levels ever recorded at GOC (830 ng/g), due to an unreported diesel spill which occurred sometime between the July and October 2004 sampling events (Payne et al., 2006). One possible source might be fishing vessels, which before openings, anchor at GOC instead of Valdez Harbor; in July 2005, fishing vessels were observed anchored in the bight east of GOC Point.

Evidence of the residual diesel signal persisted in the mussel tissues through the sample collections in March 2005 (Payne et al., 2006). There was no evidence of the diesel spill in any of the AMT mussel samples collected in July or October 2004, and there was no evidence of the diesel signal in the subtidal sediments collected at Gold Creek in March 2005 (Payne et al., 2006). This latter observation is in line with findings after other oil spills on similar gravel/cobble beaches (including the *Exxon Valdez* oil spill in 1989) where there was very little evidence of oil transfer to near-shore subtidal ($\geq$40 m) sediments (O'Clair et al., 1996).

In the most recent tissue samples collected between July 2006 and October 2007 (Figure 17), mussel TPAH levels continue to be extremely low (<100 ng/g dry weight), although there appeared to be a slight rise in concentrations in April and July 2007. The PAH phase signatures (Figure 20) were a mixture of trace-level particulate/oil-phase components and combustion products plus dissolved naphthalenes in several samples. The SHC profiles reflect dominant marine and terrestrial biogenic components (NRC 1985) in all samples except July 2006 where petrogenic phytane was also observed (Figure 20).

5.3.3 Prince William Sound Stations

In our 2004/2005 LTEMP report, we presented extended discussions of the 1993-2005 time-series trends for each of the five Prince William Sound stations (Payne et al., 2006). The time-series phase plots for each site were discussed in detail with representative PAH and SHC profiles to illustrate the context of the phase assignments. In our 2005/2006 report (Payne et al., 2008), we noted that with the exception of Disk Island (DII), the TPAH levels at the other four Prince William Sound stations continued to be extremely low and variable, if not decreasing (generally <60 ng/g dry weight). That trend has continued in the samples collected from these stations between July 2006 and July 2007. Furthermore, except for an apparent region-wide increase in the relative proportion derived from a trace particulate/oil-phase signal (also below the MDL; range 12-63 ng/g dry weight) in July 2004, the PAH profiles at these other four sites have been generally dominated by below-MDL, background, dissolved-phase signals since April and July 2000.

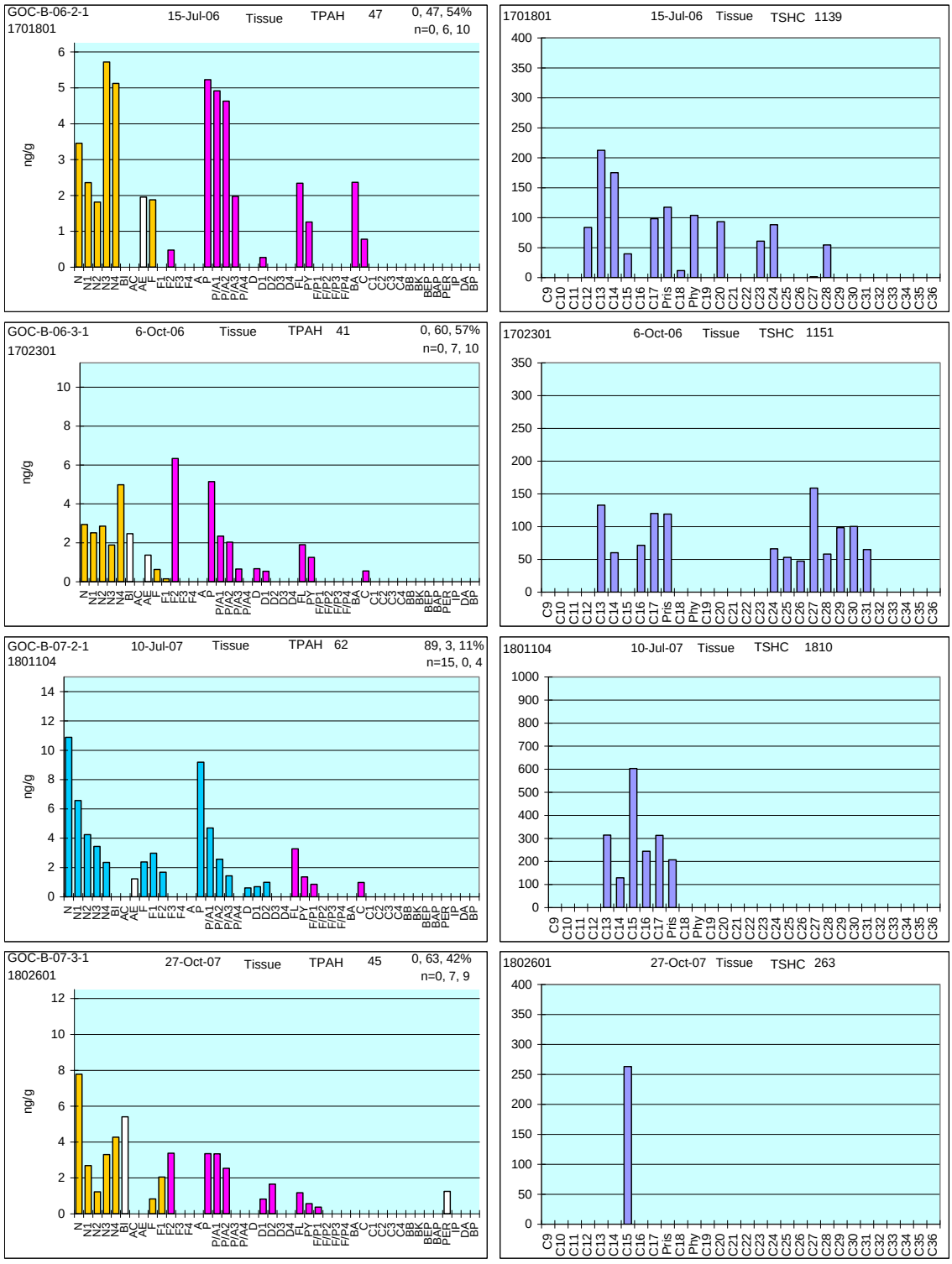

Figure 20 Gold Creek mussel PAH and SHC profiles from July 2006 – October 2007 showing low-level TPAH with variable, mixed-source signals (dissolved- and particulate/oil-phase naphthalenes plus combustion products). The SHC patterns reflect exclusively marine and terrestrial biogenic components with the exception of phytane in July 2006. MDL line omitted for scaling perspective (all PAH values are below 1996 MDL but above the sub-nanogram 2010 MDL level).

At Disk Island, the PAH signals have been more variable over time, and while they were dominated by a dissolved-phase pattern between April 2000 and March 2004, there was an increasing trend in particulate/oil-phase TPAH from July 2004 through March 2006 (Payne et al., 2008). Since the March 2006 maxima, the TPAH concentrations are declining again but they are still primarily dominated by a particulate/oil-phase signal. As a result, we will examine that station in more detail for this report. PAH profiles for all of the 2006/2008 tissue samples are presented in Appendix D.

PAH-phase-differentiated, time-series plots for the Prince William Sound stations are presented alphabetically: Disk Island (DII), Knowles Head (KNH), Sheep Bay (SHB), Sleepy Bay (SLB), and Zaikof Bay (ZAB). Representative PAH and SHC profiles from the Prince William Sound stations are presented where appropriate to elucidate the time-series plots. Constantine Harbor mussels from the EVOS Trustees SCAT program are presented along with intertidal sediment results from that site to illustrate the relationships in hydrocarbon signals between mussel tissues and the surrounding sediment (also see Appendix E).

5.3.3.1 Disk Island Mussel Tissue Chemistry

Although the TPAH levels are low (<75 ng/g dry weight), there has been a monotonic increase since July 2004 with petrogenic/oil-phase signals dominating in July 2004, March 2005, and March 2006 (Figure 21, left panel). After reaching a maximum in March 2006, the TPAH levels then decreased to < 25 ng/g dry weight through July 2007, but they were still dominated by a particulate oil/phase signal. The PAH and SHC profiles (Figure 22) show a mixed dissolved-phase and particulate/oil-phase pattern characteristic of weathered EVOS oil in March and July 2006 while in April and July 2007 the petrogenic profile is augmented by trace-level combustion products.

Diagnostic double-ratio plots of the conservative dibenzothiophene to phenanthrene homologues (Figure 23) confirm the samples resemble the ANS reference. The recent data (orange symbols) fall along a loose trend line from the origin to upper right representing various weathering states of the original oil (center red symbol).

Even though the TPAH levels are below the sample-weight-adjusted MDLs, there is no doubt that the site is still releasing oil from near-surface EVOS deposits. Surface sheens and free oil have been observed above the LTEMP transect beginning in July 2007 (Figure 24). Earlier data suggest that bioavailable oil was being released at this site as far back as July (and possibly March) of 2004. The elevated dissolved-phase signals observed between July 1998 and March 2004 may have been from lower-molecular-weight components leaching from this buried oil but it is it is impossible to confirm with just these data.

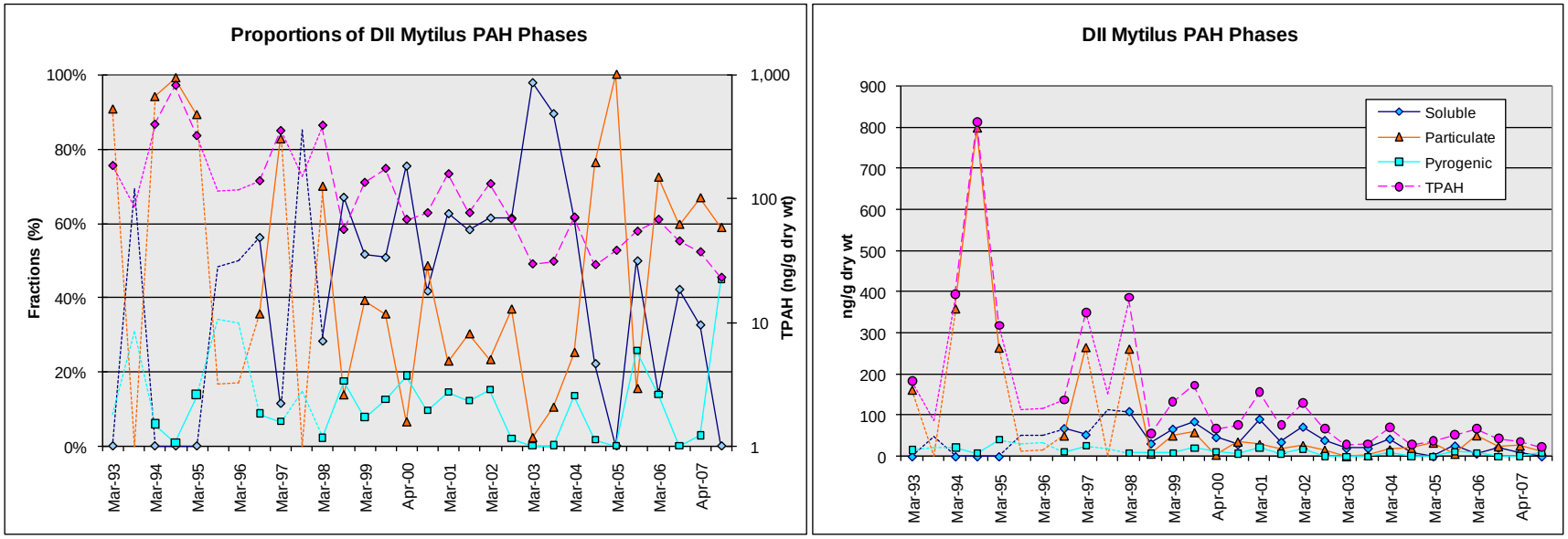

Figure 21 Time series TPAH and relative phase composition profiles in Disk Island (DII) Mytilus tissues. Dotted connecting lines without symbols indicate earlier questionable data.

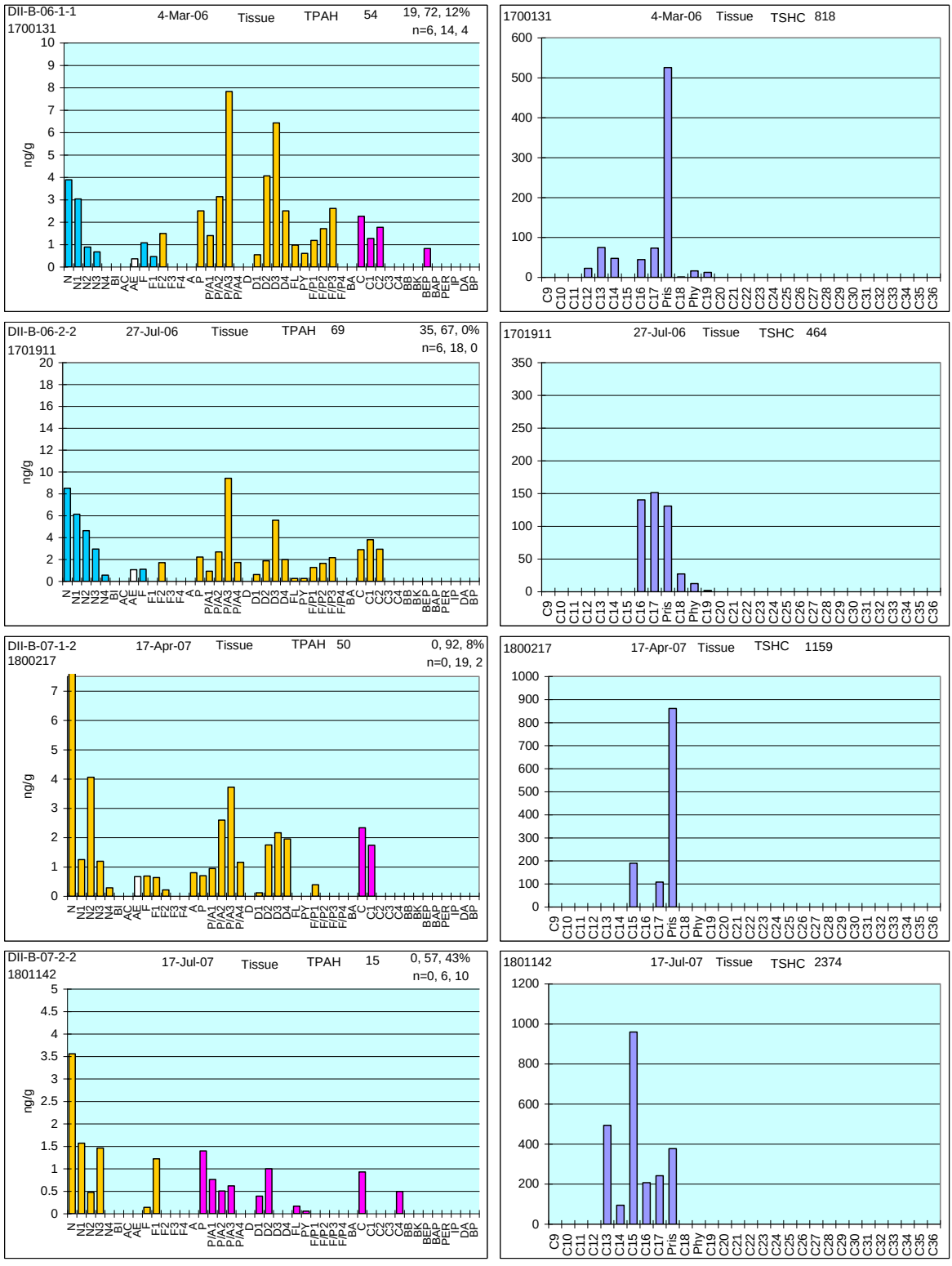

Figure 22 Disk Island *Mytilus* PAH profiles showing mixed low-level dissolved-, particulate/oil-phase, and combustion components in 2006 – 2007 samples. SHC profiles reflect a dominant marine biogenic influence and only traces of petrogenic phytane in 2006. MDL lines omitted for scaling perspective (all PAH values are below 1996 MDL but above the sub-nanogram 2010 MDL level).

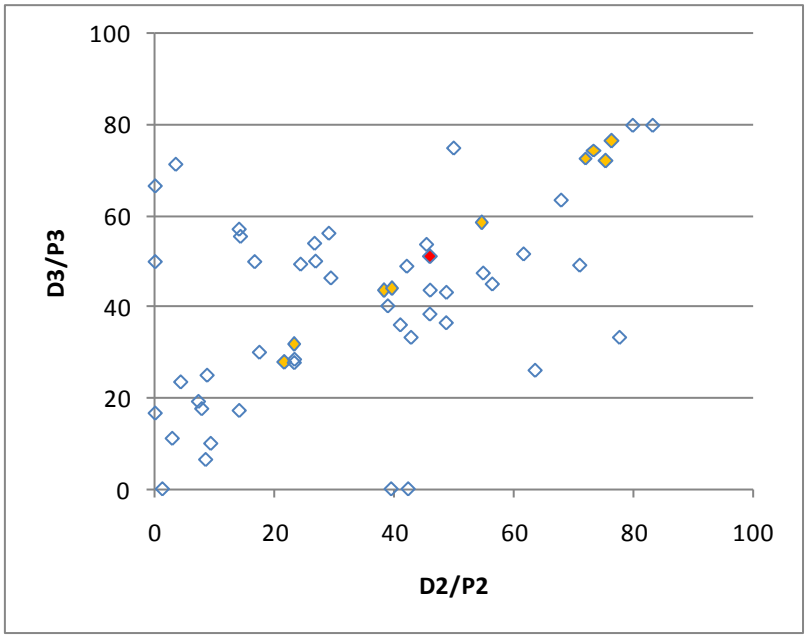

Figure 23 Double ratio plot of Disk Island replicates, 1998-2007. Recent samples (July 2005-2007) indicated by orange symbols, ANS reference by red symbol. Trend from lower left to upper right is typical of oil weathering behavior.

Figure 24 Trace of EVOS oil from disturbed sediments on Disk Island (above the LTEMP transect), April 2009.

5.3.3.2 Knowles Head and Sheep Bay Mussel Tissue Chemistry

Because of their geographic proximity (Figure 1) and their similar TPAH and phase shifts trends since July 1998 (Figure 25, left panels), these two sites are presented together.

Early lower-concentration data from Sheep Bay and Knowles Head are mostly unreliable as discussed in Section 4.7.2. Since March 2002, however, the TPAH levels at both sites have dropped steadily, and although they are currently very low (<40 ng/g dry weight and below laboratory MDLs), the phase assignments based on those low-level PAH signatures show remarkable detrended correlations (Figure 26).

For example in July 2004, the PAH and SHC profiles from both stations show dramatic shifts from a primarily dissolved-phase pattern to extremely low petrogenic profiles (Figure 25, Figure 26, Figure 27). After that, the patterns are generally dominated by dissolved phase signals through April 2007 (Figure 26, Figure 28, and Figure 29). While we have a lot of confidence in the distinctive particulate/oil-phase signal from Knowles Head (Figure 27 where the PAH were just below MDLs), the Sheep Bay PAH profiles and phase assignments at that time are more tenuous because the concentrations are so low. However, the corresponding SHC pattern at Sheep Bay (Figure 27 right panel) shows a mixture of biogenic and trace-level petrogenic hydrocarbons which, as separate lines of evidence, support this assignment. In March 2005, there was a synchronous return to the background dissolved-phase signal (Figure 26), and this is clearly supported by the PAH and SHC histogram plots obtained through April 2007 (Figure 28, Figure 29). In addition to the synchrony shown in the phase assignment plots (Figure 26), the PAH and SHC patterns for the two stations paired by sampling dates (Figure 28 and Figure 29) also show remarkable fidelity. As noted earlier, however, phase assignments at these low TPAH concentrations can be very tentative. Only the long series of correlation (20 sampling events at two sites using two different laboratories) provides the authority for these trace-level interpretations. PAH and SHC profiles for the rest of the 2006-08 collections are shown in Appendix D.

5.3.3.3 Sleepy Bay Mussel Tissue Chemistry

During the early sample collections at Sleepy Bay, the low concentration data are sketchy, but the higher concentration signals (Figure 30, right panel) were dominated by distinctive particulate/oil-phase patterns as buried EVOS oil, released from the intertidal substrate following spring storm/wind events, gradually diminished. Since March 1998, Sleepy Bay TPAH levels have generally trended lower with a dissolved-phase signal largely dominating, with lesser contributions from particulate/oil-phase and pyrogenic components. In our 2005-6 LTEMP report (Payne et al., 2008), we showed that the Sleepy Bay phase signals appeared to loosely follow those observed at Knowles Head and Sheep

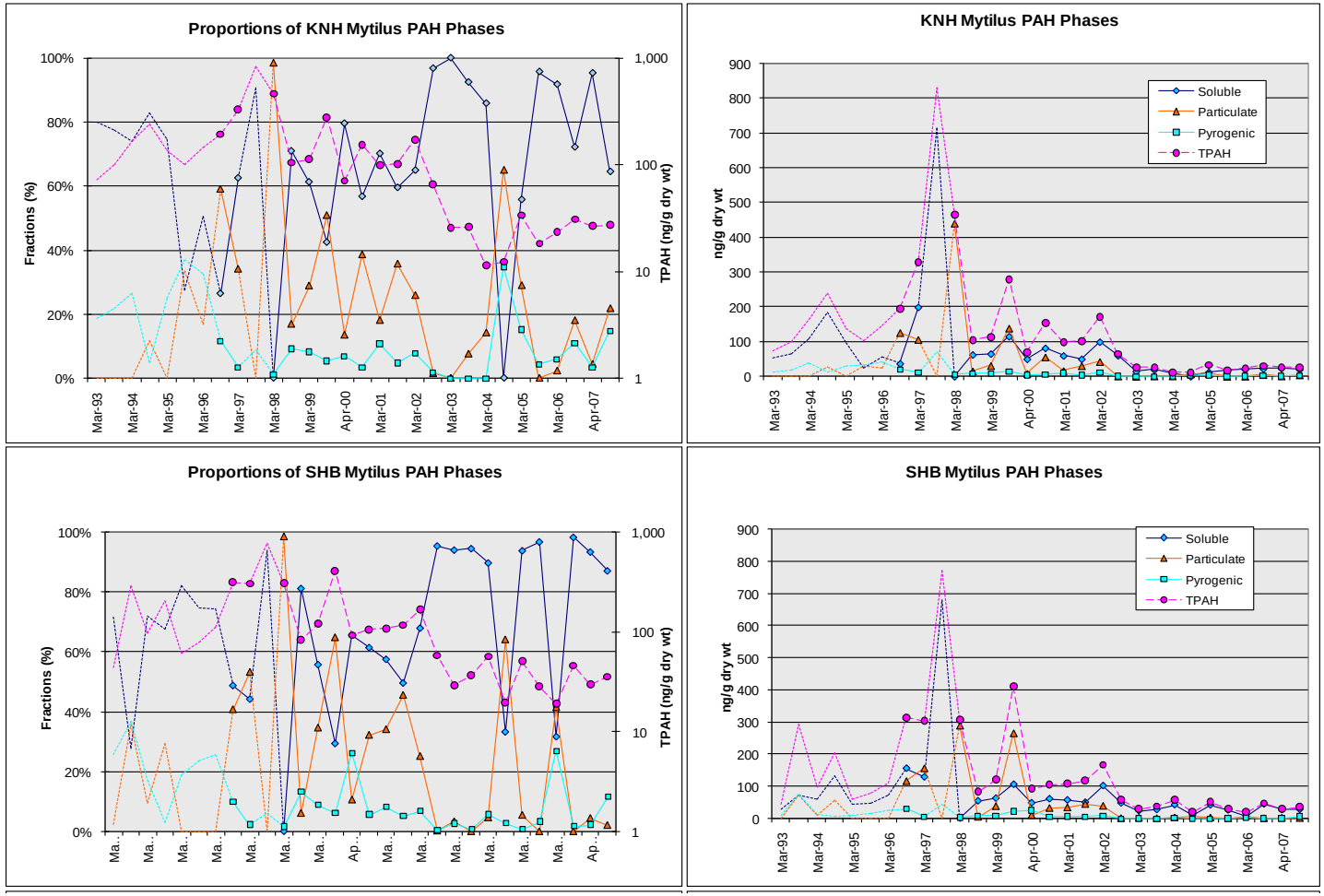

Figure 25 Time series TPAH and relative phase composition profiles in Knowles Head (KNH) and Sheep Bay (SHB) Mytilus tissues. Dotted connecting lines without symbols indicate earlier questionable data.

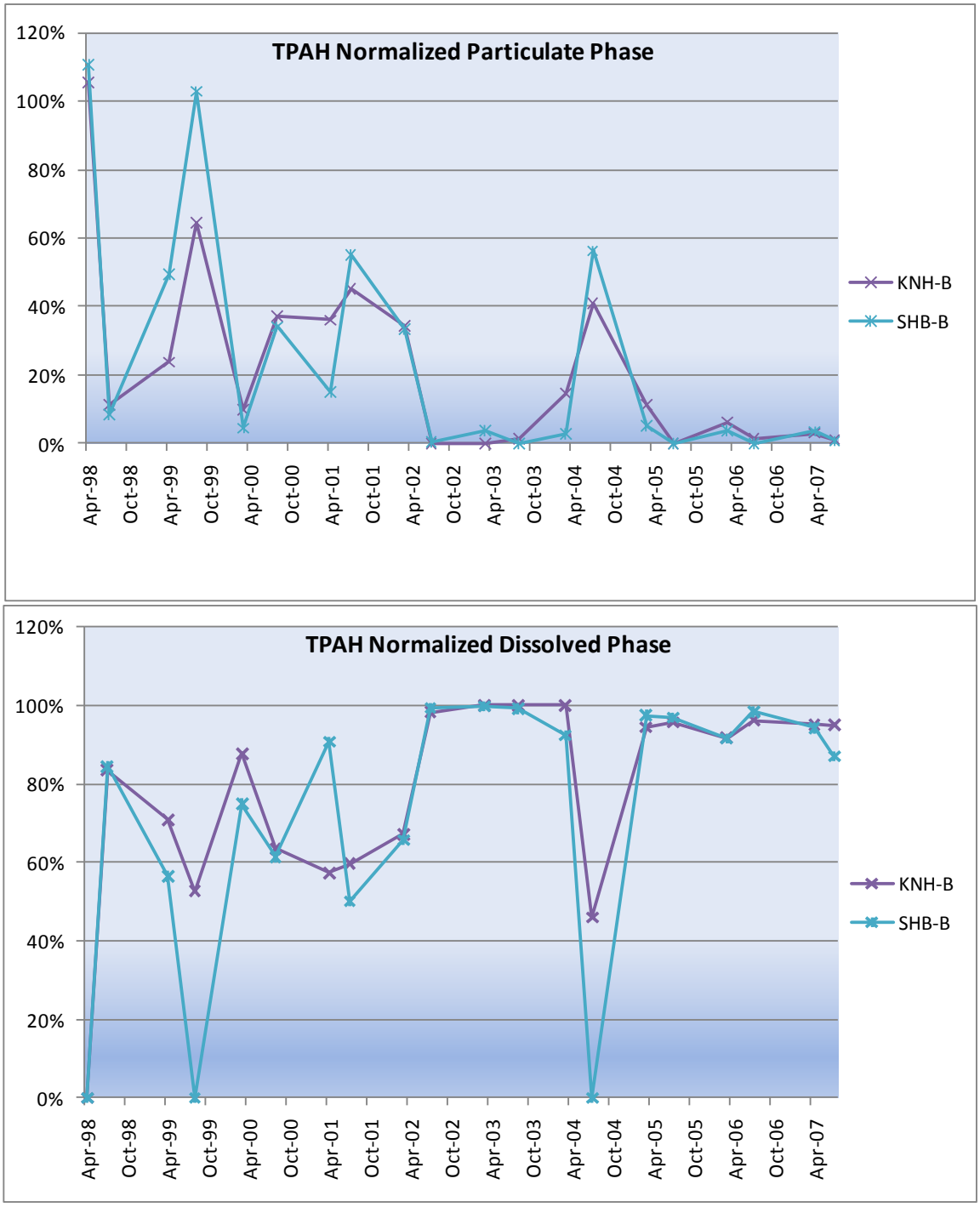

Figure 26 Synchrony in average phase portions between Sheep Bay (SHB) and Knowles Head (KNH) Mytilus PAH since July 1998. Particulate-phase correlation = 0.94; Dissolved-phase correlation = 0.87.

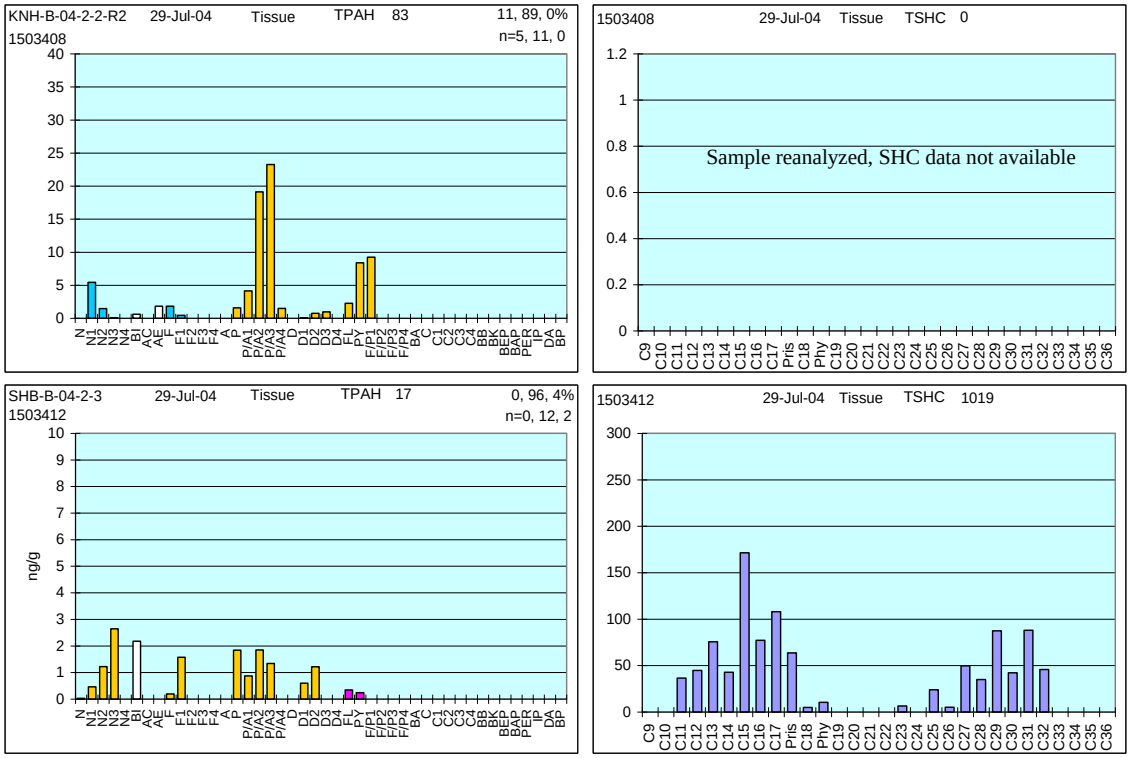

Figure 27 Representative Knowles Head and Sheep Bay Mytilus PAH and SHC profiles showing low-level particulate/oil-phase components in July 2004. MDL lines omitted for scaling perspective (all PAH values are below 1996 MDL but above the sub-nanogram 2010 MDL level). Also, note the different concentration scales.

Bay (with the notable exception of a strong particulate/oil-phase signal in July 2003), but now the trend has apparently broken down with particulate/oil-phase spikes in March 2006 and July 2007 that are not observed at the other two stations (Figure 25 and Figure 30).

The PAH and SHC profiles observed in Sleepy Bay *Mytilus* tissues since July 2004 show occasional spikes of particulate/oil-phase components against a background of dissolved-phase naphthalenes and occasional combustion products (Figure 31). These mixed-phase patterns are in direct contrast to those observed at Knowles Head (KNH) and Sheep Bay (SHB) over the same time period (Figure 28 and Figure 29). As in the other central Prince William Sound stations, the overall TPAH levels are extremely low (< 30 ng/g dry weight) and presumably only represent background components.

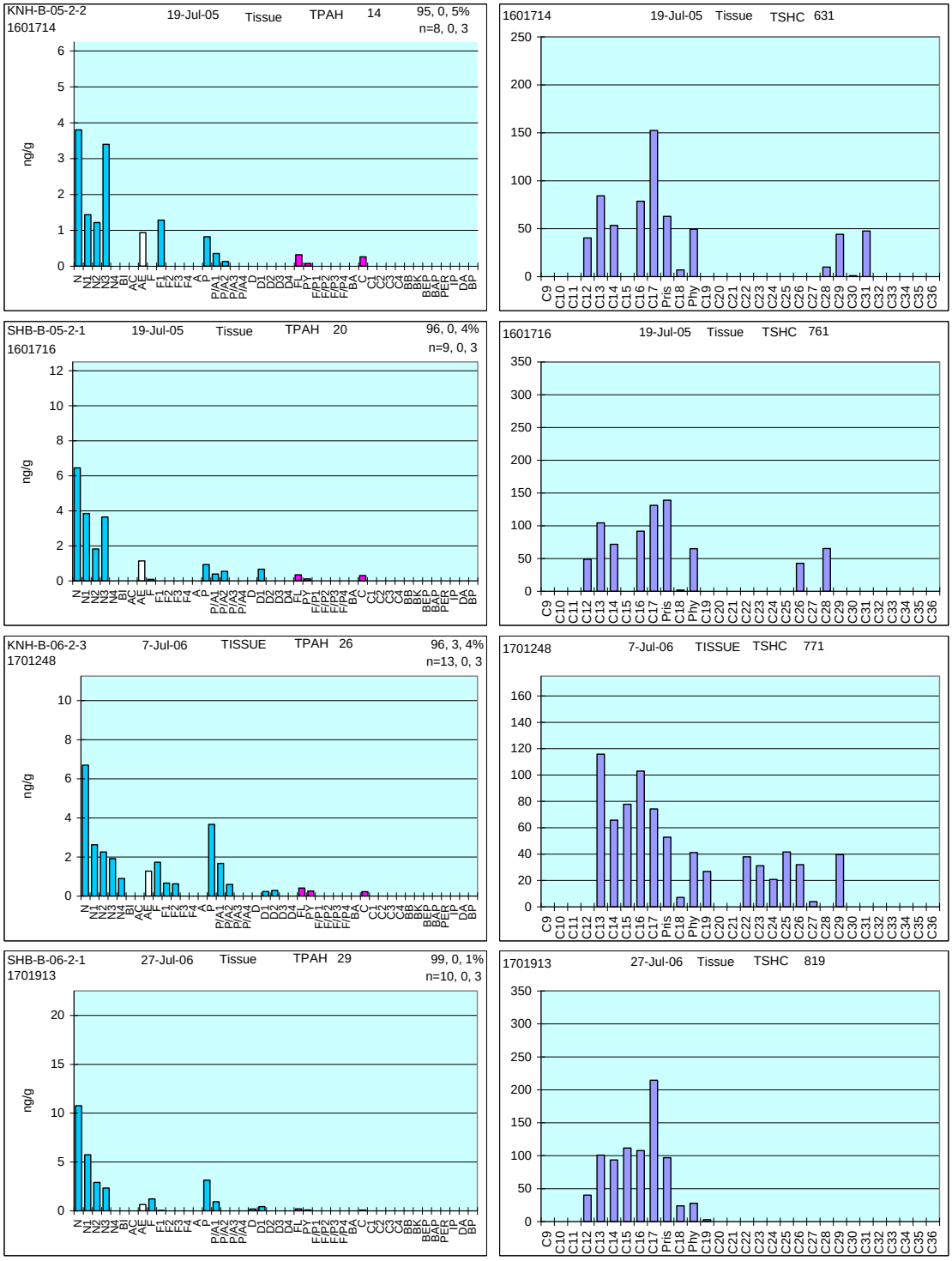

Figure 28 Representative Knowles Head and Sheep Bay *Mytilus* PAH and SHC profiles (paired by years for July 2005 and 2006) showing similarities in dissolved-phase PAH and primarily biogenic SHC patterns. MDL lines omitted for scaling perspective (all PAH values are below 1996 MDL but above the sub-nanogram 2010 MDL level).

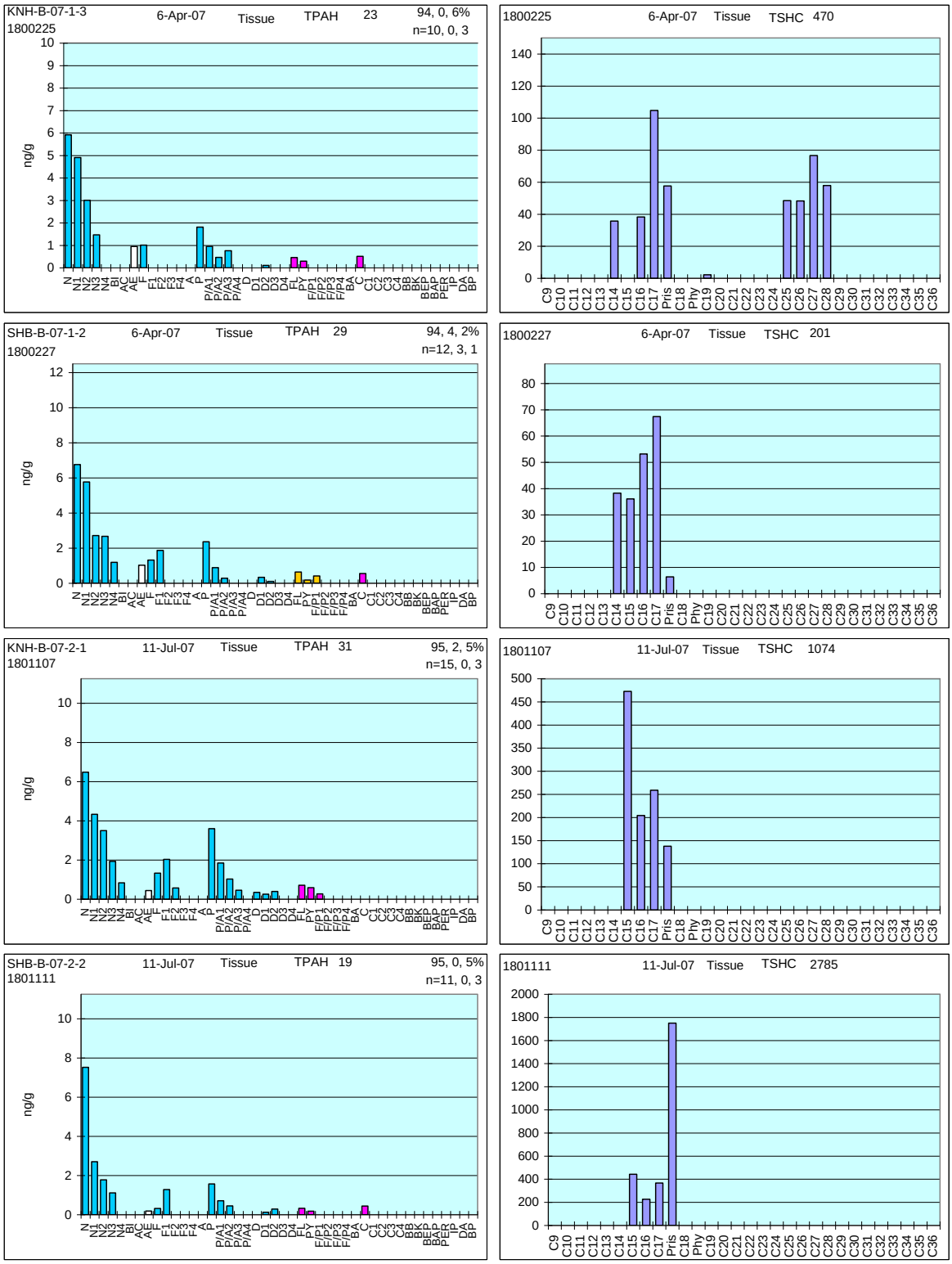

Figure 29 Representative Knowles Head and Sheep Bay *Mytilus* PAH and SHC profiles (paired by collections in April and July 2007) showing similarities in dissolved-phase PAH and primarily biogenic SHC patterns. MDL lines omitted for scaling perspective (all PAH values are below 1996 MDL but above the sub-nanogram 2010 MDL level).

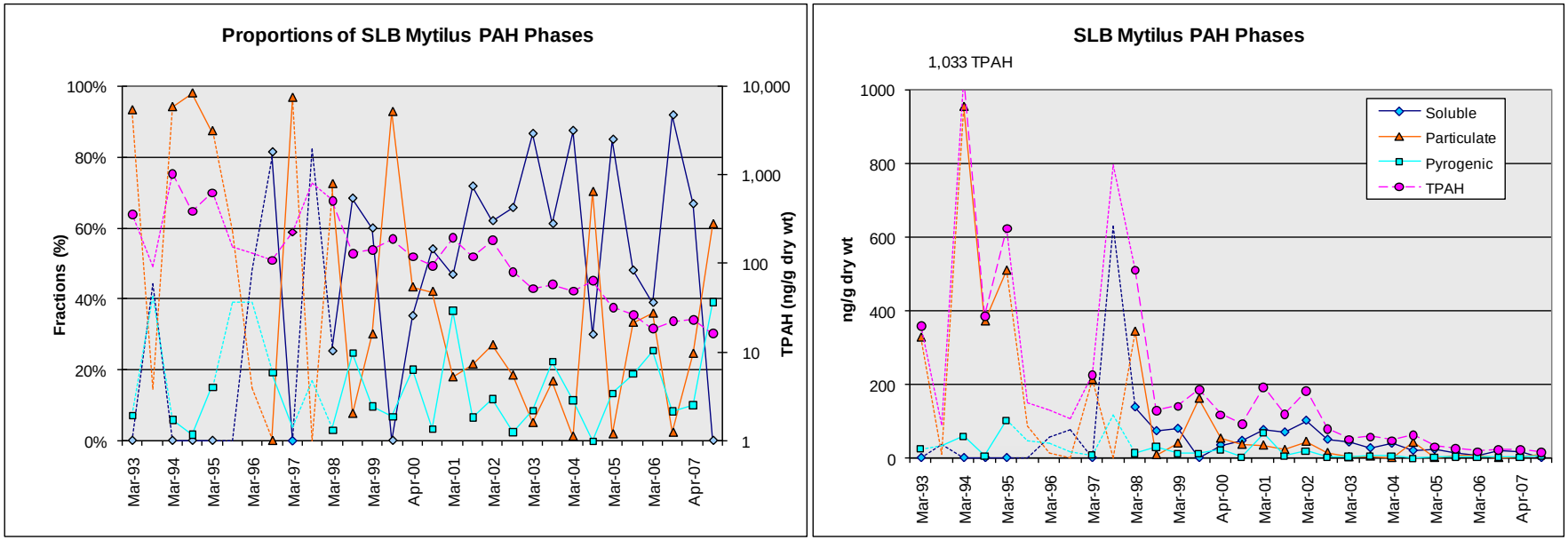

Figure 30 Time series TPAH and relative phase composition profiles in Sleepy Bay (SLB) *Mytilus* tissues. Dotted connecting lines without symbols indicate earlier questionable data.

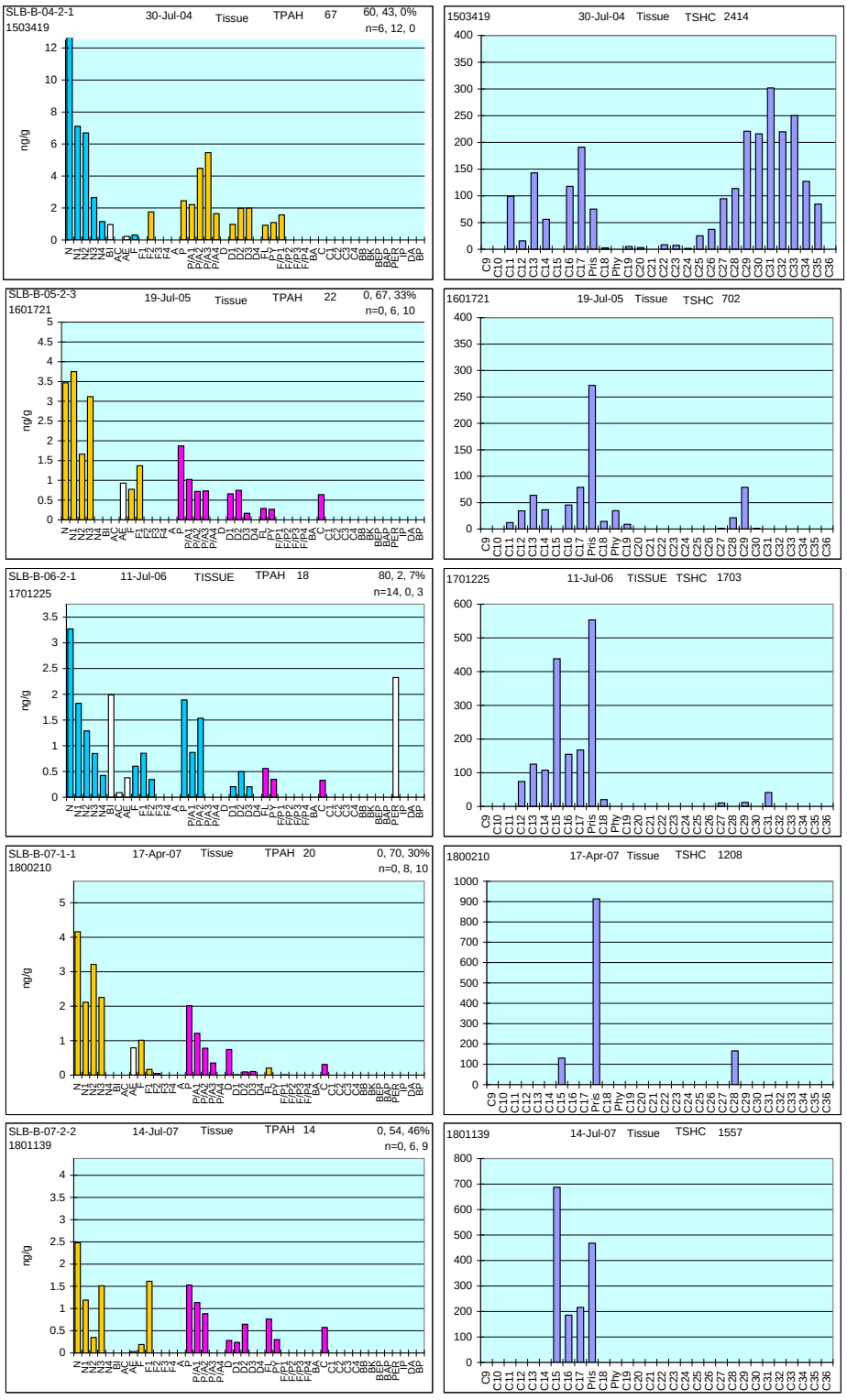

Figure 31 Representative Sleepy Bay (SLB) *Mytilus* PAH and SHC profiles from July '04, '05, '06, and April and July '07 showing the more mixed-phase signals in contrast to the dominant dissolved-phase signals at Knowles Head (KNH) and Sheep Bay (SHB). MDL lines omitted for scaling perspective (all PAH values are below 1996 MDL but above the sub-nanogram 2010 MDL level).

5.3.3.4 Zaikof Bay Mussel Tissue Chemistry

This station was added to the program in 1999 to better assess petroleum hydrocarbon inputs from tanker traffic passing through the Hinchinbrook Entrance to Prince William Sound. TPAH concentrations have been low (less than MDL) and variable over the eight-year sampling period at this site (Figure 32), but over this time frame, the signals have been consistently derived from the dissolved phase (Figure 32, right panel). The maximum TPAH level (197 ng/g dry weight) observed in March 2002 dropped to an all-time low (13 ng/g dry weight) in March 2006, and since then, the dominant dissolved-phase TPAH concentration has increased to 60 ng/g dry weight. Phase patterns at this site do not correlate well with either the nearby central PWS sites or the Gulf of Alaska sites; it behaves uniquely. Representative PAH and SHC profiles from July 2004 through July 2007 show the low-level mixed dissolved- and particulate/oil phase PAH patterns characteristic of this site (Figure 33). The contributions of trace-level particulate/oil-phase components in July 2004, March 2005, and July 2005 (Figure 33) are reflected in the PAH histograms, while the SHC profiles show both marine and terrestrial biogenic components with occasional traces of petrogenic phytane. PAH and SHC profiles from the entire suite of 2006/2008 samples are shown in Appendix D.

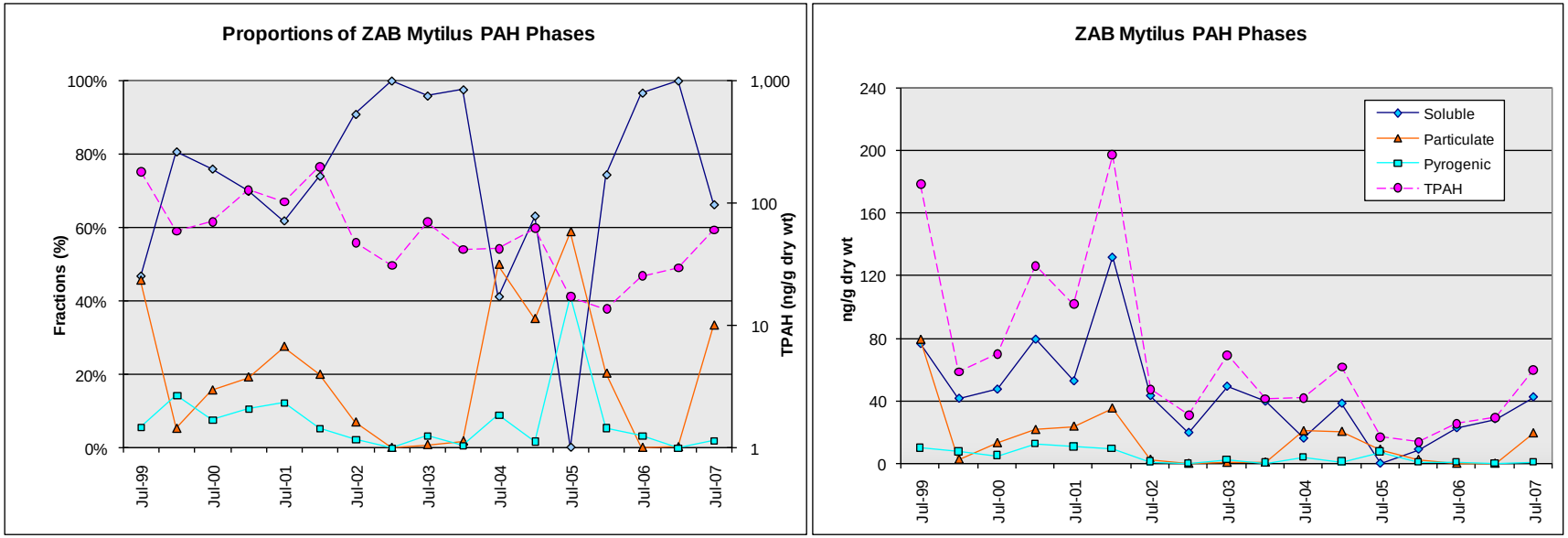

Figure 32 Time series TPAH and relative phase composition profiles in Zaikof Bay (ZAB) *Mytilus* tissues. Dotted connecting lines without symbols indicate questionable data.

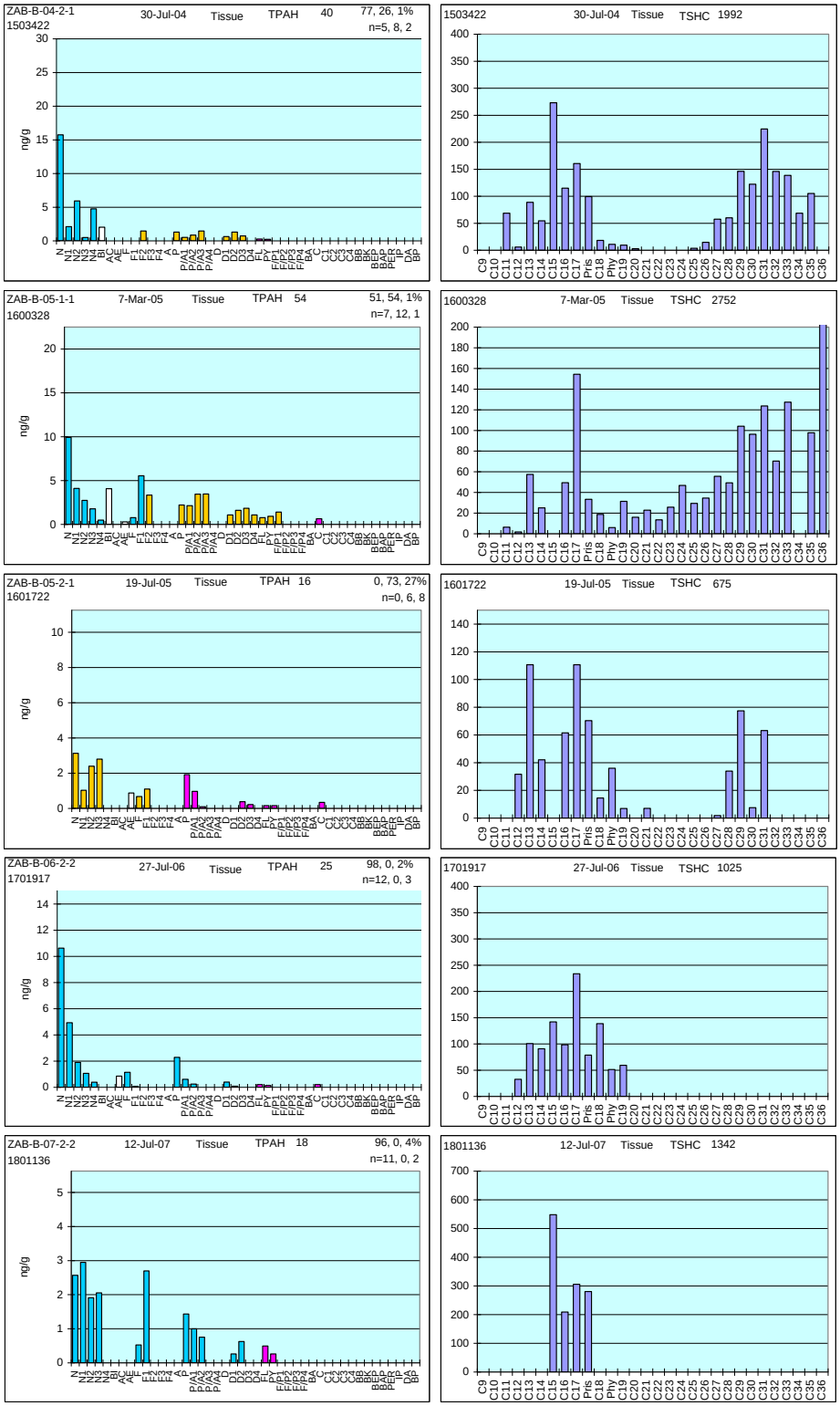

Figure 33 Representative Zaikof Bay (ZAB) *Mytilus* PAH and SHC profiles from July 2004, March and July 2005, July 2006, and July 2007 showing a mixture of dissolved-, particulate/oil-phase, and pyrogenic components during the first three sampling events reverting to a more dominant dissolved-phase signal in 2006 and 2007. MDL lines omitted for scaling perspective (all PAH values are below 1996 MDL but above the sub-nanogram 2010 MDL level).

5.3.3.5 Constantine Harbor Mussel Tissue Chemistry

This site was added to the 2005/2006 LTEMP as part of the EVOS Trustees SCAT Program undertaken by Auke Bay Laboratory. The location was selected as a reference site because it is known to receive PAH-bearing sedimentary deposits from suspended particulate material introduced to Prince William Sound by the Alaskan Coastal Current sweeping the Gulf of Alaska coastline southeast of the Sound (Karinen et al., 1993, Page et al., 1995; Short and Babcock 1996; Short et al., 2007b). These PAH dominate the background signal, particularly in the deep sediments of PWS (except in Port Valdez). Also, it was not impacted by oil released from the *Exxon Valdez* oil spill. Along with the mussel samples, intertidal sediments were collected from this site (previously discussed in Section 5.2.3.3). Representative sediment PAH and SHC profiles are re-plotted here along with the corresponding profiles for the mussel tissues (Figure 34) to compare the tissue burdens against the surrounding sediments.

Mussels have been sampled historically, even pre-spill, at this site by Auke Bay Lab but unfortunately, those data are from a slightly different part of the spit and thus, although similar, are not exactly comparable. From June 1989 samples, Short and Babcock (1996) reported TPAH levels of ~650 ng/g dry weight and, similar to the recent samples, with over 50% of the TPAH signal derived from naphthalenes.

Like most of the other LTEMP tissue samples discussed in this report, individual PAH concentrations are all below MDLs while the intertidal sediment profiles are well above (Figure 34). The sediments show the dominant particulate/oil-phase PAH input of particulate material introduced to the Alaska Coastal Current by numerous rivers and glaciers along the Gulf of Alaska coastline east of the Sound. The sediment SHC profiles show the dominant higher-molecular-weight (n-C21 to n-C35) odd-carbon number contribution from terrestrial plant waxes (NRC 1985) introduced by those rivers and the local watershed. In contrast, the mussel tissues show only trace levels of dissolved-phase naphthalenes and phenanthrenes/anthracenes. Likewise, the tissues do not reflect the higher-molecular-weight, odd-carbon-number n-alkanes, indicating very little direct uptake of particulate-phase material from the immediately adjacent sediments.

This ubiquitous background signal of dissolved-phase lower-molecular-weight components (e.g., naphthalenes, fluorenes, and phenanthrenes/anthracenes) has been observed throughout Prince William Sound, and it has become more dominant as PAH signals from EVOS and other sources have decreased over time (see Sections 5.3.3.2 through 5.3.3.4 and Figure 28, Figure 29, Figure 31, and Figure 33). While it is clear from the Constantine Harbor data that the mussels are not taking up higher-molecular-weight PAH or SHC from the sediments directly, it is not known if they may be accumulating dissolved-phase components from selective dissolution (either *ex situ* or *in situ*) of the sparingly water-soluble constituents associated with those sediments. Up to

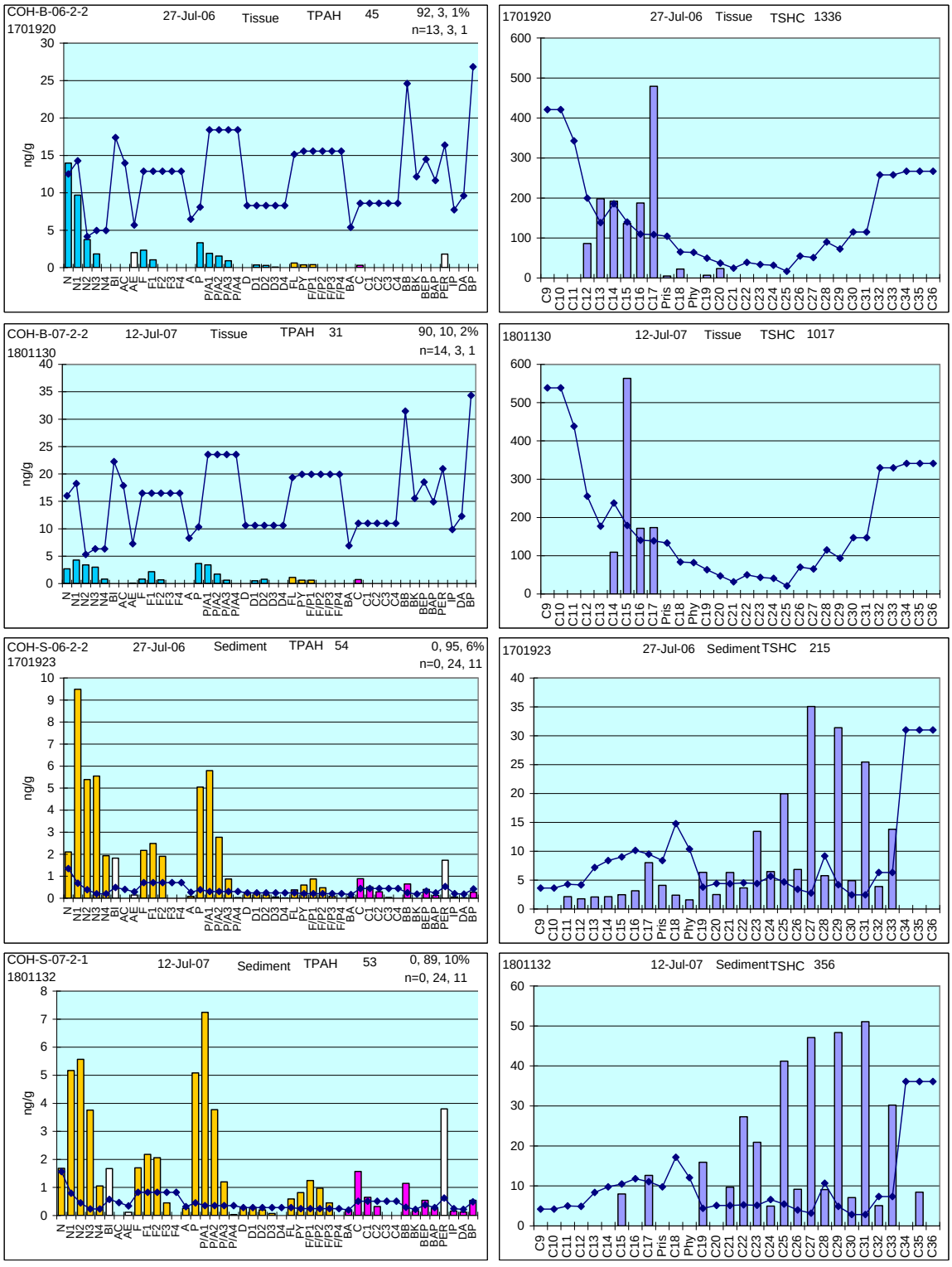

Figure 34 Representative Constantine Harbor *Mytilus* and adjacent intertidal sediment PAH and SHC profiles, 2006-2007. The 1996-generated MDLs are indicated with dotted line; all PAH values are above the sub-nanogram 2010 MDL level.

this time, these particulate/sediment-bound PAH have not been generally considered to be bioavailable, and they were not believed to be a possible source for the dissolved-phase components observed in the mussels.

In an effort to evaluate the possibility that water soluble constituents may in fact be leaching from the water-borne sedimentary materials themselves, a modest experiment was conducted as part of the EVOS Trustees-sponsored SCAT VII Program in July 2007. The complete experimental design and results are presented in Appendix E, but to briefly summarize, when clean seawater was partitioned against increasing amounts of intertidal sediment and then filtered through 0.7-µm glass fiber filters, linear increases in dissolved-phase naphthalene, C1-naphthalene, and biphenyl were measured. The results were highly significant (Appendix E) and suggested that the sediments themselves were the source of these three more water-soluble PAH in the filtered seawater extracts. Furthermore, the resulting PAH profiles from the filtered seawater samples closely resembled the patterns observed in the LTEMP mussels from Constantine Harbor and elsewhere in the Sound.

5.3.4 Gulf of Alaska Stations

This section presents the tissue chemistry data from the Gulf of Alaska LTEMP stations, and includes: Aialik Bay (AIB), Shuyak Harbor (SHH), and Windy Bay (WIB). In our 2004/2005 LTEMP report, we presented extended discussions of the 1993-2005 time-series trends for each of Gulf of Alaska stations, and the time-series phase plots for each site were discussed in detail with representative PAH and SHC profiles to illustrate the context of the phase assignments (Payne et al., 2006). Rather than repeat that narrative in this year's report, the findings can be briefly summarized as follows: The below-MDL TPAH concentrations in the mussels from the 2006-2008 collections at all three sites remain very low (<50 ng/g dry weight), and the PAH-phase differentiated, time-series plots show variable trace-level dissolved-phase contributions at all three sites with a slight swing to a particulate/oil- phase signal at WIB in July 2006.

5.3.4.1 Aialik Bay Mussel Tissue Chemistry

Between July 2004 and July 2006, the TPAH levels at Aialik Bay appear to have stabilized around 21-28 ng/g dry weight with a modest increase to 48 ng/g dry weight in April 2007 (Figure 35). In July 2007, the TPAH was at an all-time low at 12 ng/g dry weight. Over this time, the signals have been dominated by a dissolved-phase pattern with additional pyrogenic input in March 2006 and more of a mixed-phase pattern with dissolved-, particulate/oil-, and pyrogenic components noted in the April 2007 maximum. SHC patterns reflect both marine and terrestrial biogenic input. All of the measured components are well below the laboratory's sample-specific MDL, so these phase assignments, while supported by the PAH and SHC profiles (Figure 36), should be considered as provisional. The rest of the PAH and SHC profiles from the 2006/2008 collections are shown in Appendix D.

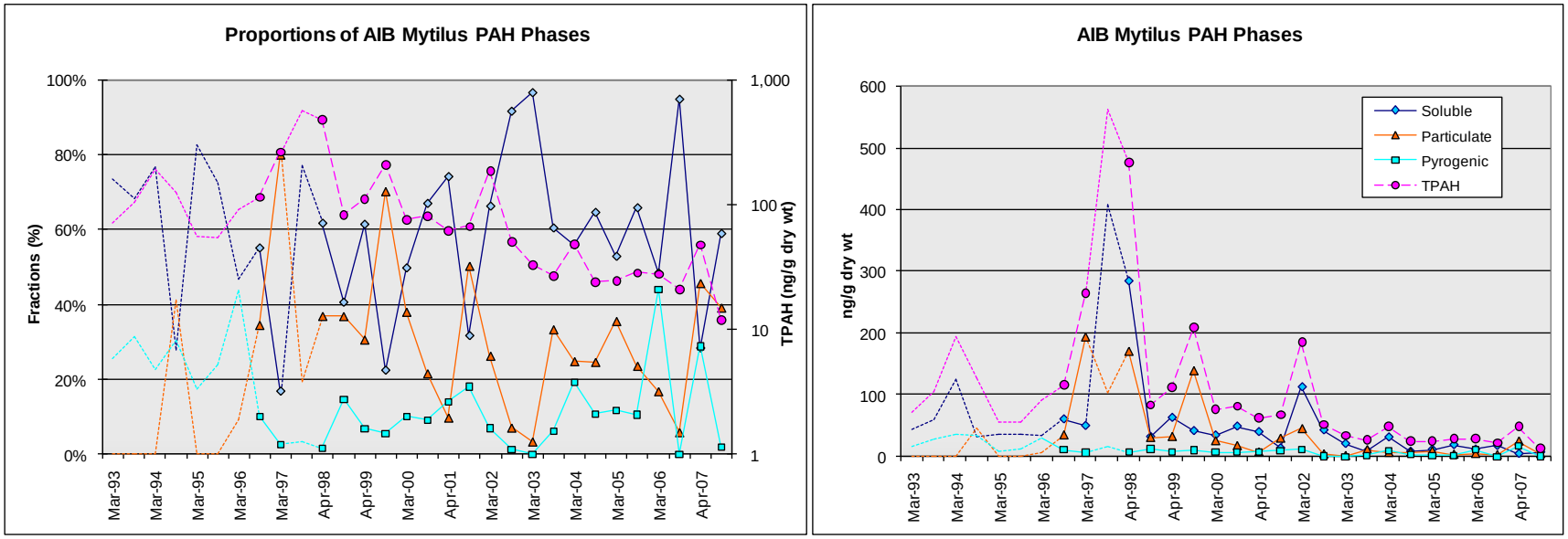

Figure 35 Time series TPAH and relative phase composition profiles in Aialik Bay (AIB) *Mytilus* tissues. Dotted connecting lines without symbols indicate questionable data.

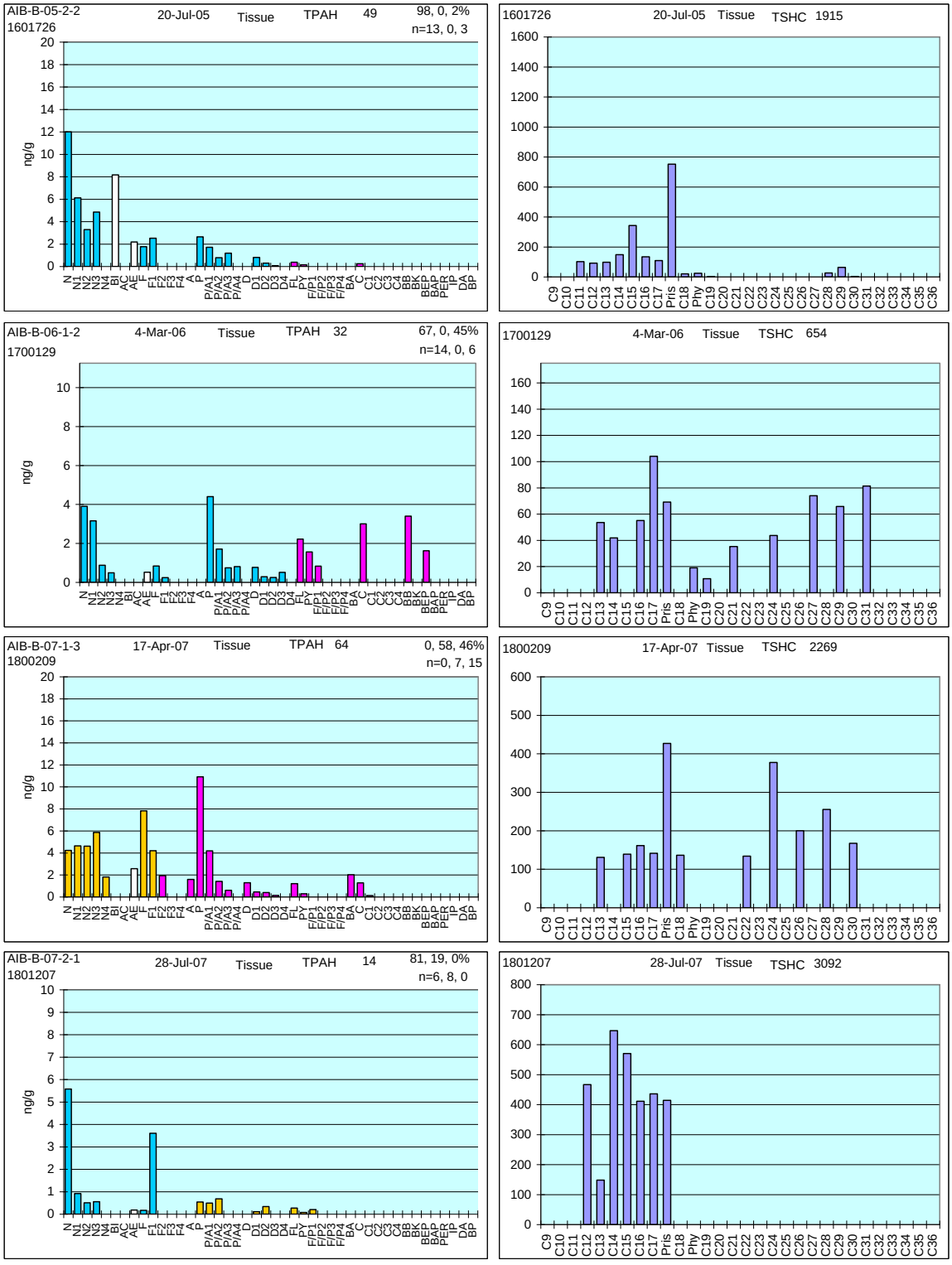

Figure 36 Representative 2005 through 2007 Aialik Bay *Mytilus* PAH and SHC profiles. MDL lines omitted for scaling perspective (all PAH values are below 1996 MDL but above the sub-nanogram 2010 MDL level).

5.3.4.2 Shuyak Harbor and Windy Bay Mussel Tissue Chemistry

These stations are considered together because of their regional proximity (Figure 1); however, their PAH phase trends do show several notable differences (Figure 37). Both stations show generally decreasing TPAH concentrations since March 2004, but there was an apparent increase in TPAH at Shuyak Harbor (SHH) in July 2006 and April 2007, while Windy Bay (WIB) levels have decreased more monotonically over this time frame. Both stations showed a particulate/oil-phase spike in August 2004, but since then, SHH has been dominated by a dissolved-phase signal plus an increase in pyrogenic components in April 2007. WIB, on the other hand, showed another apparent particulate/oil-phase spike in July 2006. In July 2007, both stations showed dissolved-phase signals at all time-low TPAH levels below 10 ng/g dry weight. The below-MDL PAH profiles at both sites generally support the phase assignments discussed above in that both stations show a dominant particulate/oil-phase PAH pattern in August 2004, while the SHC profiles suggest both biogenic and petrogenic contributions (Figure 38 and Figure 39). The PAH patterns for both stations suggest a particulate/oil-phase fraction in addition to the dissolved-phase signal in July 2006, with a slightly higher (42% vs. 28%) petrogenic contribution at WIB compared to SHH. In the April 2007 PAH profiles, the two stations are drastically different with only biphenyl and several combustion products noted at SHH while WIB reflects the common dissolved-phase pattern observed elsewhere in the program. Interestingly, in April 2007 all three Gulf of Alaska stations show drastically different PAH profiles (Figure 36, Figure 38, and Figure 39). In July 2007, the PAH patterns from all three stations again reflect a dominant dissolved-phase pattern.

Lacking more detailed data, it is not possible to speculate on sources or events driving the divergence in the phase assignments at Shuyak Harbor and Windy Bay (Figure 37) and the different PAH patterns observed between March 2005 and April 2007 (Figure 38 and Figure 39); however, at these incredibly low concentrations, these differences may simply reflect nothing more than analytical artifacts. These limited findings do point out the need for additional laboratory studies to better define and improve MDLs, and this is being explicitly addressed as part of the 2009/2010 LTEMP effort. Additional PAH and SHC profiles from the 2006/2008 collections are shown in Appendix D.

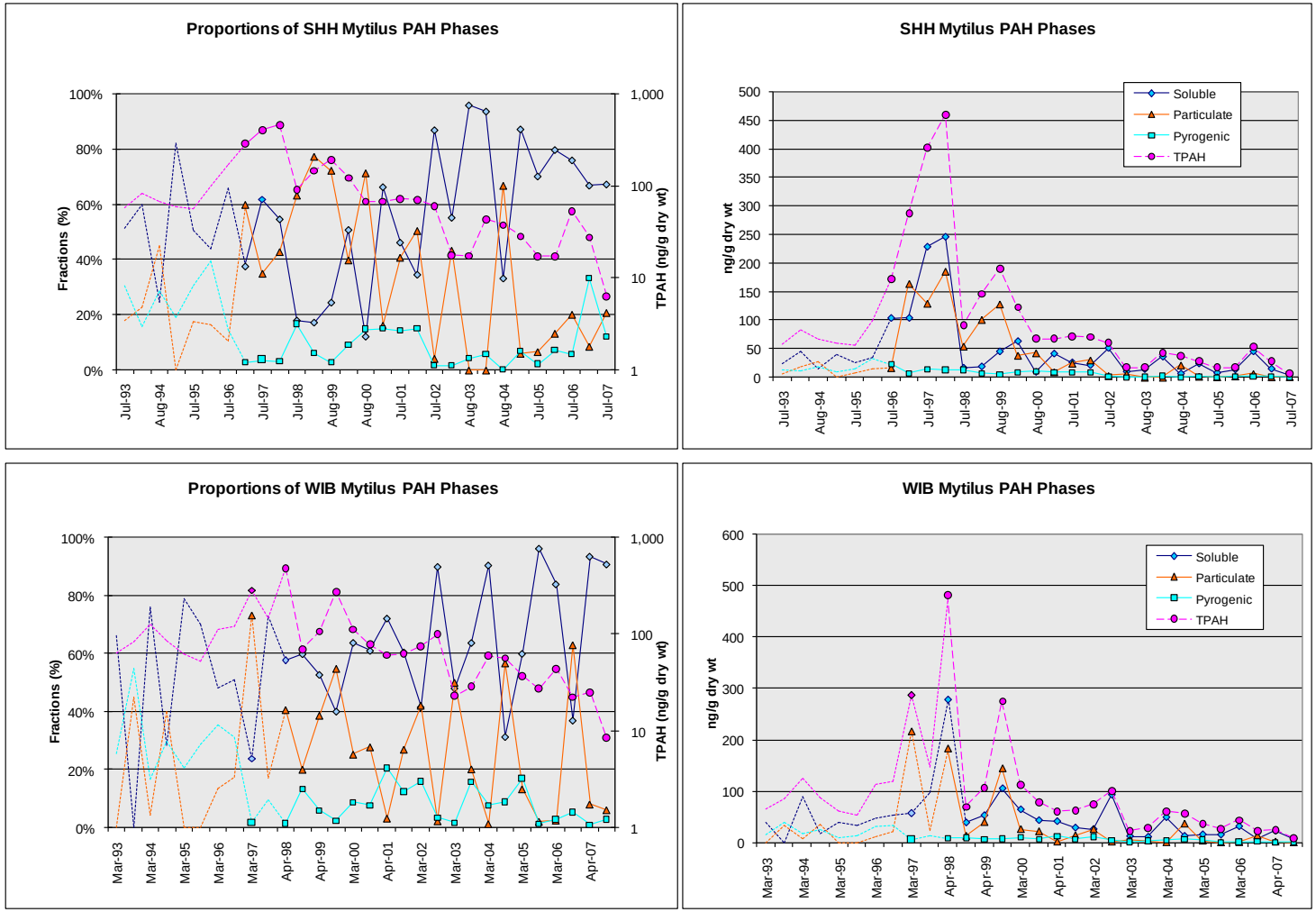

Figure 37 Time series TPAH and relative phase composition profiles in Shuyak Harbor (SHH) and Windy Bay (WIB) *Mytilus* tissues. Dotted connecting lines without symbols indicate questionable data from earlier sample analyses.

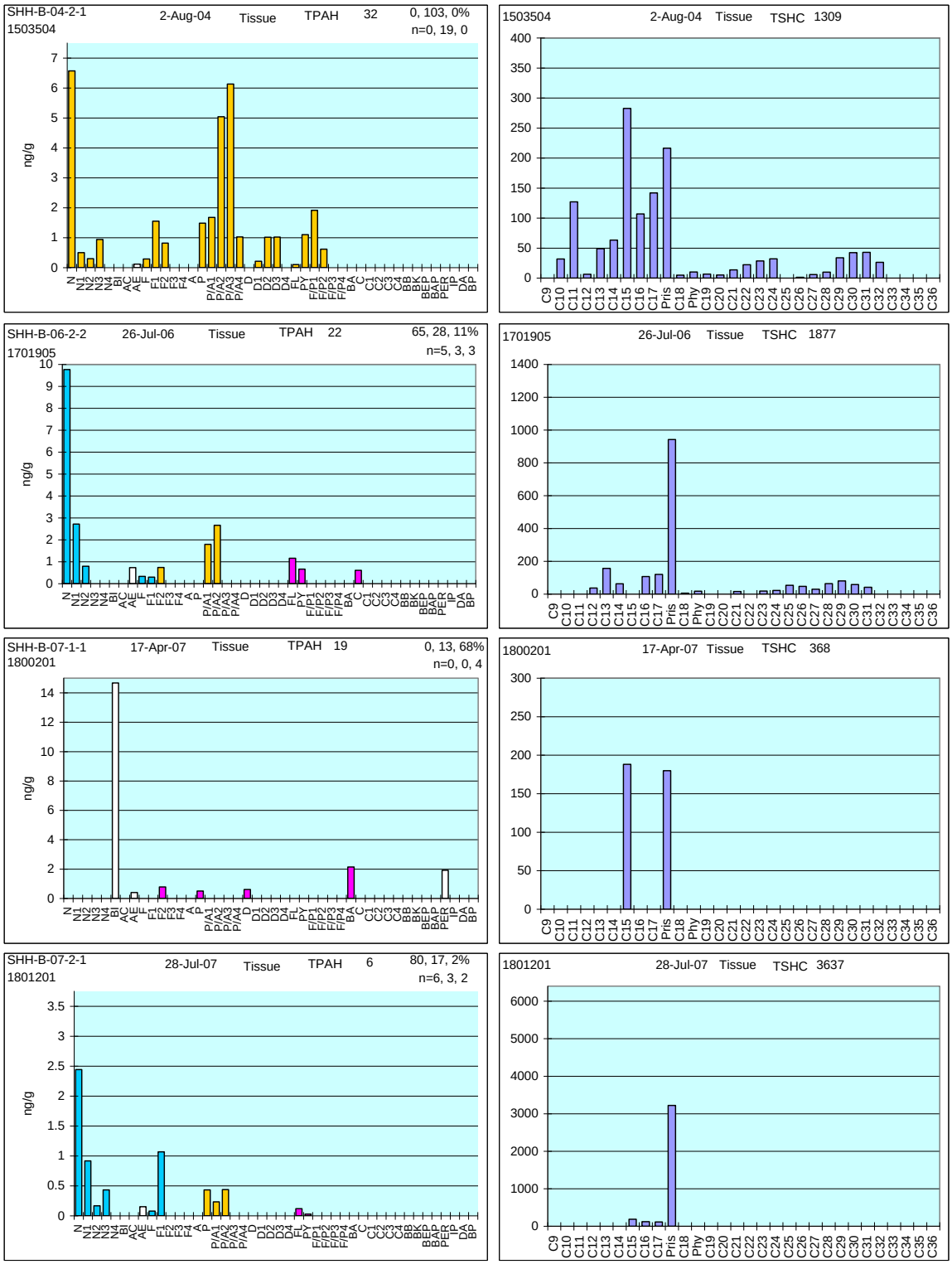

Figure 38 Representative 2004-2007 Shuyak Harbor *Mytilus* PAH and SHC profiles. MDL lines omitted for scaling perspective (all PAH values are below 1996 MDL but above the sub-nanogram 2010 MDL level).

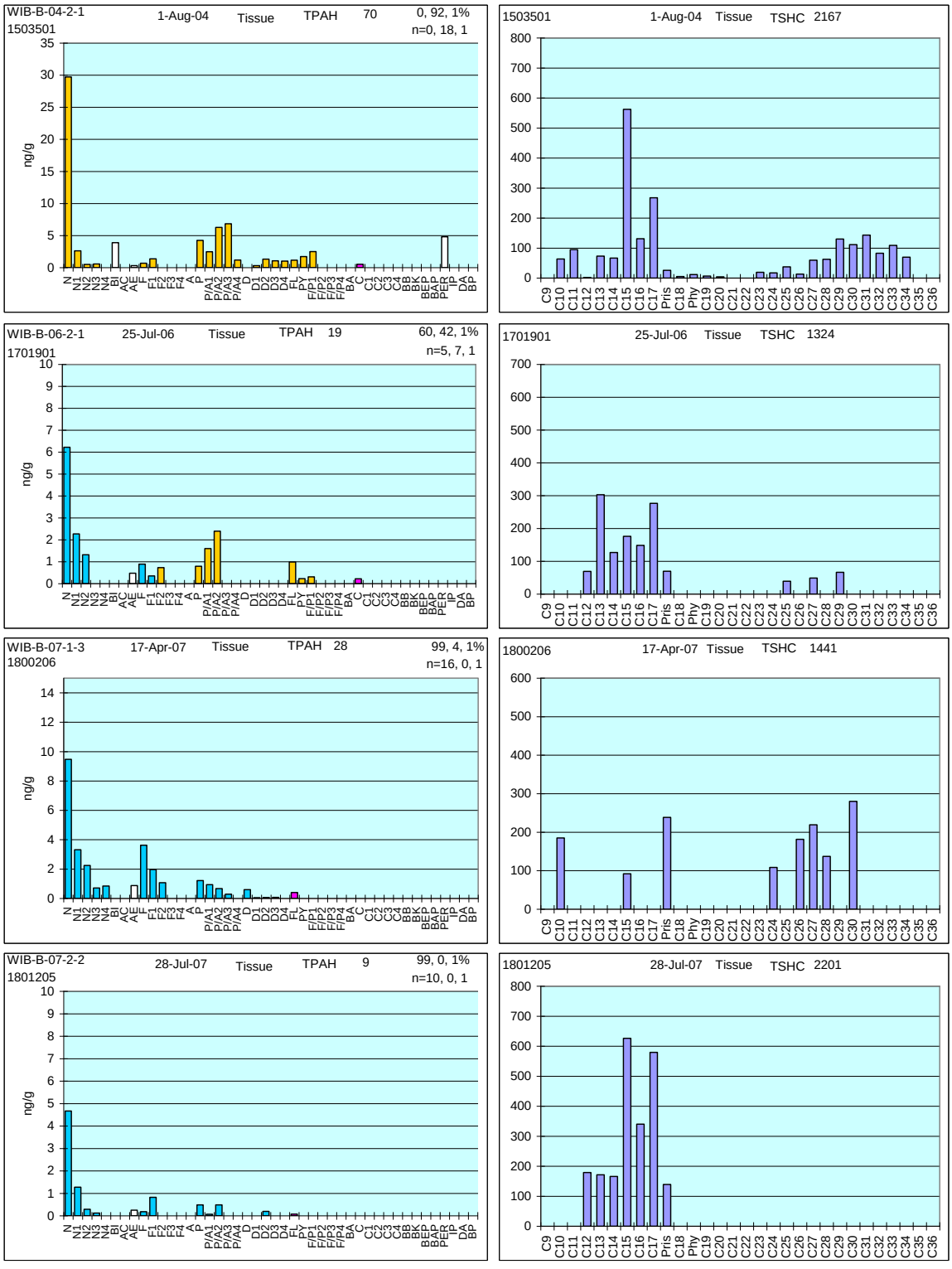

Figure 39 Representative 2004-2007 Windy Bay *Mytilus* PAH and SHC profiles. MDL lines omitted for scaling perspective (all PAH values are below 1996 MDL but above the sub-nanogram 2010 MDL level).

5.3.5 Summary and Discussion of Tissue Chemistry Results

In Port Valdez, *Mytilus* tissues exhibit persistent, but very low and declining levels of hydrocarbons directly attributable to the BWTF discharge and terminal/tanker operations. Except for samples collected after major spill events (e.g., the *Eastern Lion* spill in May 1994, the BWTF sheening event in January 1997, and a diesel spill at Gold Creek between July and October 2004), the PAH patterns in Port Valdez tissues largely have been seasonally controlled. At AMT, a particulate/oil-phase signal is almost always dominant, but in earlier years (prior to 2002) there was generally a saw tooth pattern of increased dissolved-phase proportions during the warmer summer/fall period when the water column is more stratified. Since October 2006, a dissolved-phase PAH signal has been dominant at AMT with TPAH levels holding steady around 52-64 ng/g dry weight. At GOC, the dominant particulate/oil- and dissolved-phase patterns roughly paralleled the trends observed at AMT until October 1999, with increasing dissolved-phase and combustion product contributions observed after that. Since October 2006, the TPAH levels at GOC have ranged from 30-75 ng/g dry weight, with the lowest reported concentrations measured in July 2007.

Since July 2002, TPAH levels in the AMT mussel tissues have been steadily decreasing. The decreases likely reflect either reduced BTWF discharge volumes as both North Slope oil production decreases and more double-hulled tankers with segregated ballast tanks are brought into the tanker fleet, or improved BWTF efficiency at removing particulate/oil-phase PAH, or a combination of these factors. In mussel tissues, pyrogenic inputs at both AMT and GOC have historically been low, but recently their relative contributions to the overall TPAH levels have become higher and much more variable. One might expect these results as the historic primary source from terminal operations diminishes and minor inputs become more visible, but this suggestion is guarded by the phase-assignment ambiguities with the TPAH values currently averaging around 50 ppb.

For comparison, mussels from a clean reference site used for a similar monitoring program near Sullom Voe, Scotland, one of the major oil terminals in the UK usually have four-fold or higher TPAH burden (Widdows et al., 1995) than mussels immediately adjacent to the Alyeska Marine Terminal (the most consistently contaminated LTEMP monitoring site). We conclude that the very high efficiency of oil removal in the BWTF and effective dispersion at the diffuser combined with reduced tanker traffic, have resulted in remarkably little impact on the robust-appearing, mussel populations from the discharged PAH within the Port, particularly over the last six years.

In the Sound, with the bulk of EVOS oil either dissipated or the remnants buried and sequestered, regional sites that are physically remote from the chronic input of BWTF discharge are currently looking very clean. Only Disk Island shows what appear to be low (<MDL) but consistently observed particulate/oil-phase components in mussels over the last seven sample collections (July 2004 through July 2007). The TPAH levels increased from 29 ng/g dry weight in July 2004 to 67 ng/g dry weight in March 2006, but since then, concentrations have dropped to an all-time low of 23 ng/g dry weight. Double

ratio plots of alkylated phenanthrenes/anthracenes and dibenzothiophenes have confirmed the source as residual EVOS oil that has been observed as pockets of occasional free oil droplets and sheen above the LTEMP sampling transect in July 2007 and 2008.

Overall the region is getting cleaner. Regressions of log-transformed, average TPAH time series from the five PWS and three GOA stations show parallel decreasing trends (Figure 40). TPAH levels in both regions are dropping at nearly identical rates. This parallelism suggests the decreases are influenced by similar (oceanographic-scale?) processes, but the occasional asynchrony of peak events also suggests regional variation in the dynamics. So what broad-scale sources might appear as an ambient background dissolved signal? Possibilities include atmospheric deposits, forest fires, leaching of water-soluble constituents from the pervasive source-rock (oil shale or coal that constitutes much of the SPM being transported through the region), some upwelling/climate-driven events, a combination of these or some novel mechanism relating to decadal oscillations and/or global warming. Based on a limited-scale partitioning experiment with clean seawater and intertidal sediment from Constantine Harbor (Appendix E), we now posit that sedimentary materials previously believed to only contain sequestered and non-bioavailable PAH, may be contributing to the ubiquitous dissolved-phase signals observed throughout Prince William Sound.

Another question is how low will this generally declining trend in TPAH values go? Obviously, at some point, the trend must level out. Follow-up sampling in 2004 for oil residues from the 1997 *M/V Kuroshima* grounding on the Aleutian Chain found TPAH levels between 25 and 85 ng/g dry wt, with an average of 57 ng/g dry wt (Table 7, Helton et al., 2004). This compares favorably with LTEMP's July 2007 range of 13-76 ng/g inside the Sound and 12-53 ng/g at the Gulf of Alaska sites. These data also suggest a natural dissolved-phase background TPAH somewhere below 50 ng/g—a range in which analytical sensitivity is highly susceptible to procedural artifacts. It might easily be the case that the LTEMP data are currently tracking subtle variations in the background PAH, and that we are near or at the minimum.

For relative comparisons, data from the National Status and Trends, Mussel Watch Program (MW) (Table 7) show the average PAH concentration in mussels (summing only 24 of the 44 LTEMP analytes) for the remainder of the West Coast is nearly 30 times higher at 1,982 ng/g dry wt. The highest level reported on the West Coast was 46,700 ng/g dry wt at a site in Elliot Bay (Seattle, Washington). The lowest, with 41 ng/g, was from mussels collected on Santa Cruz Island, a National Park 20 miles offshore of Santa Barbara in Southern California. Nationwide from 1986-1996, the 15th, 50th, and 85th percentiles were at 77, 230, and 1,100 ng/g (O'Connor, 2002). In 2001, the state-wide average TPAH concentration in mussels from the five Alaskan MW sites (Ketchikan, Skagway, Port Valdez, Unakwik Inlet, and Cook Inlet) was 86.6 ng/g dry wt with levels ranging from 52.5 to 144 ng/g. Considering LTEMP results sum nearly twice the number of analytes, the region is exceptionally clean. New results from MW (Kimbrough, 2008) summing 38 analytes from 2004-05 samplings report 441 ng/g in Port Valdez. LTEMP results had similar values following the 2004 GOC diesel spill. In 2005, the five Alaska MW sites ranged from 152-441 ng/g, all considered low values.

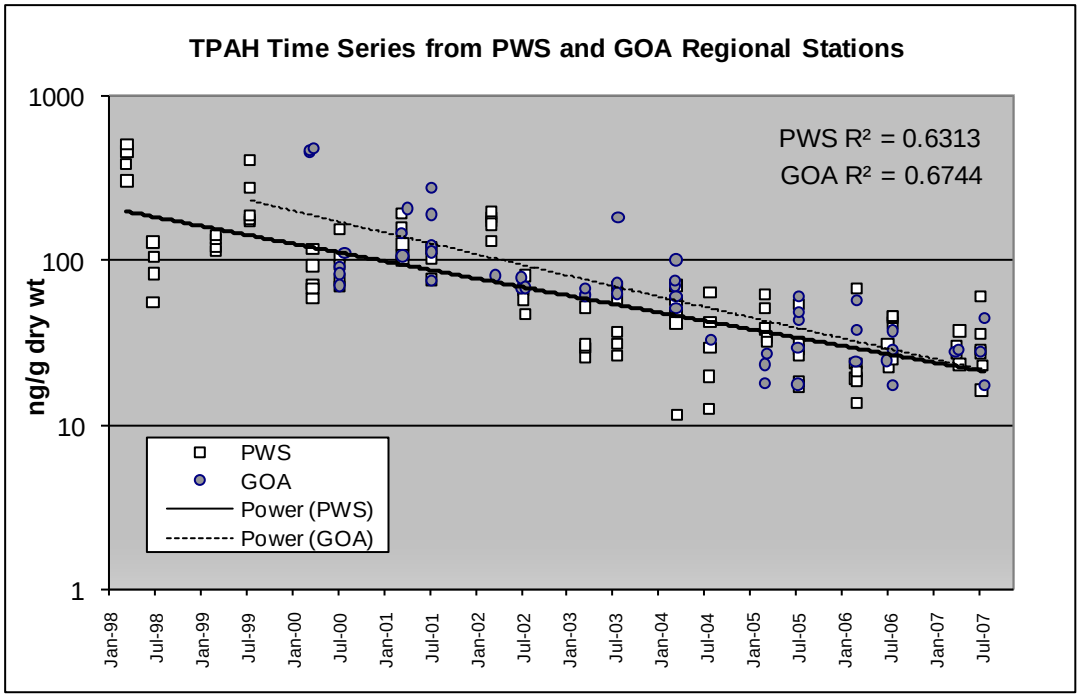

Figure 40 Average *Mytilus* TPAH time series and trend lines comparing Prince William Sound and Gulf of Alaska stations' trends.

Table 7 Current TPAH concentrations in mussel tissues (ng/g dry wt) relative to recent NOAA Mussel Watch monitoring data and another recovered Alaskan oil-spill event.

LTEMP (2005/2006)	Valdez	30-67
	PWS	13-76
	GOA	12-53
1997 *M/V Kuroshima*	2004	25-85
West Coast Mussel Watch (sum of 24 analytes)	average	1,928
	Santa Cruz Island	41
	Elliot Bay	46,700
	Alaska (2001)	53-144

Finally, under the auspices of the EVOS Trustees Program, Long-term Monitoring of Anthropogenic Hydrocarbons in the *Exxon Valdez* Oil Spill Region (050763), ten intertidal sites within the Naked-Knight-Southwest Island complex were examined during the 2005 summer program to measure the extent of buried oil still present 16 years after the spill. At EVOS sites previously designated as heavily oiled, 10 to 50 random pits (depending on the beach width) were excavated to a depth of ~0.5 m to look for residual oil. Where available, mussels were also collected in the proximity of any detected oil. Sediments and mussels were analyzed using LTEMP analytical protocols. The results have been published elsewhere (Short et al., 2007a) but, as part of PWSRCAC efforts,

PAH and SHC sample profiles were included in Appendix E of our 2005/2006 Report (Payne et al., 2008). A separate report is also being prepared by Dr. Jeffrey Short for this survey plus similar studies completed in 2006 and 2007. Briefly, TPAH levels in the oiled pits ranged from a low of 42 ng/g (on Knight Island) to a high of 567,000 ng/g (on Latouche Island) with the oil showing varying states of weathering (from extensively degraded to very fresh – see Appendix E in Payne et al., 2008). The mussel samples collected from these same beaches (but not necessarily immediately adjacent to the oiled pits) showed low (11 to 42 ng/g dry weight) dissolved-phase TPAH signals very similar to those observed at the other ten traditional LTEMP stations. Although there were still persistent buried EVOS residues at a number of the beaches, they are highly sequestered and do not appear to be bioavailable unless disturbed. Rates of disappearance have diminished to an estimated 4% yr^{-1}. If left undisturbed, Short et al. (2007a) predict they will be there for decades.

6 CONCLUSIONS

The LTEMP sites are currently reporting stable, trace-level concentrations of biogenic and petrogenic hydrocarbons whereby any new inputs will appear as an easily detected spike above the near pristine background. Utilizing the reliable, post-1998 portions of the dataset, the station trends suggest that TPAH levels have been decreasing in mussel tissues since 1999 and are now at near all-time lows for the LTEMP sites both within and outside of Port Valdez.

At Alyeska Marine Terminal, mussel tissues continue to indicate the accumulation of seasonally influenced, dissolved- and particulate/oil-phase PAH components from the BWTF, but since October 2002, TPAH concentrations have maintained steady within a range of 52-65 ng/g. Since October 2006, the mussels at the terminal site have exhibited a dominant dissolved-phase signal. Sediment conditions at the Alyeska Terminal site, are also improving. After a one and one-half-year plateau between March 2003 and July 2004 at already low TPAH levels, 167-184 ng/g, subtidal sediments have dropped even lower to 41-86 ng/g since March 2005, but they still show the weathered-ballast-oil signature plus combustion products (which may or may not be related to terminal activities), and the usual biogenic marine and terrestrial components. These trends most likely reflect the decreased ballast-water throughput for the facility as oil flow through the pipeline and subsequent tanker traffic drops and as double-hulled tankers, carrying segregated, oil-free ballast, come into operation.

Mussel tissue loads at GOC had been consistently low (30-116 ng/g) since July 2002, but a diesel spill sometime between July and October 2004 increased the TPAH values to the highest ever observed at that site, 858 ng/g. Diesel residues were still apparent in mussel tissues collected in March 2005 (166 ng/g), but by the following July they were only 51 ng/g, and the diesel signal was no longer apparent. TPAH levels have now dropped to <30 ng/g. TPAH concentrations in GOC sediments are still driven primarily by

combustion products, as has always been the case at this site, but are now at all time lows (12-28 ng/g). There was no evidence of the 2004 diesel spill in the 2005-06 sediment samples at GOC.

Outside Port Valdez, most stations are now showing mussel tissues with less than 60 ng/g TPAH (many with <30 ng/g) and appearing primarily as a dissolved–phase hydrocarbon signal. Based on the regional TPAH trends diminishing to consistently low values, it appears that the final traces of EVOS residues have either stabilized or reached levels that no longer appear in the LTEMP mussel samples (except at Disk Island). From the magnitude and nature of the PAH signal, the bulk of Prince William Sound and the northern Gulf of Alaska reflect only trace background levels of dissolved-phase PAH.

Based on intertidal sediment/seawater partitioning experiments conducted as part of the 2007 field effort, it now appears that sedimentary materials previously believed to only contain sequestered and non-bioavailable PAH, may in fact be contributing to the ubiquitous dissolved-phase signals observed throughout Prince William Sound (Appendix E). This examination of the partitioning behavior was only intended as a scoping experiment, and longer periods of equilibration with different sediment types and other possible particulate sources (airborne particulate soot, smoke, dust, etc.) may provide additional insight on the phenomena and an opportunity to estimate mass balances. As described in Appendix E, additional work should be completed to expand these observations to other conditions.

Using PAH phase-assignments, we have been able to identify temporal and compositional events that characterize three separate regions comprising Port Valdez, central Prince William Sound, and the outer-coastal Gulf of Alaska stations. Highly significant correlations in synchronous phase shifts since July 1998 demonstrate common influences between Knowles Head (KNH) and Sheep Bay (SHB) in PWS. This is further corroborated by regional synchrony of TPAH shifts plus similarity in signatures suggesting that the inner Prince William Sound sites are collectively experiencing one low-level source of hydrocarbons while the outer coastal stations are exposed to a possibly different, common dissolved-phase source. In July/August 2004, both regions showed a dramatic (but below MDL) shift to a common low-level, particulate-PAH source, followed by all stations, except Disk Island, returning to a primarily dissolved-phase signal in 2005 and March 2006. Disk Island is showing recurring trace levels of a particulate signature from activities disturbing EVOS residues buried at the site. The two Port Valdez stations, being mainly influenced by the treated ballast water discharge from the Alyeska Marine Terminal, are trending independently of the regional sites.

7 REFERENCES

Barron, M.G. & Ka'aihue, L. 2001. Potential for photoenhanced toxicity of spilled oil in Prince William Sound and the Gulf of Alaska waters. *Marine Pollution Bulletin* 43: 86-92.

Barron, M.G., Carls, M.G., Heintz, R. & Rice, S.D. 2003. Evaluation of fish early life-stage toxicity models of chronic embryonic exposures to complex polycyclic aromatic hydrocarbon mixtures. *Toxicological Sciences* 78: 60-67.

Baumard, P. H. Budzinski, and P. Garrigues. 1998. Polycyclic aromatic hydrocarbons in sediments and mussels of the Western Mediterranean Sea. *Environmental Toxicology and Chemistry* 17(5):765-776.

Blanchard, Arny L., Howard M. Feder, and David G. Shaw. 2003. Variations in benthic fauna underneath an effluent mixing zone at a marine oil terminal in Port Valdez, Alaska. *Marine Pollution Bulletin* 46: 1583-1589.

Blanchard, A. L., H. M. Feder, and D. G. Shaw. 2005. Environmental Studies in Port Valdez, Alaska: 2004. Final Report to Alyeska Pipeline Service Co., Inst. Of Marine Science, Univ. Alaska Fairbanks, 221 pp.

Blumer, M., M. Mullin, and D.W. Thomas. 1964. Pristane in the Marine Environment, *Helgolander Wissenshcaftliche Meeresuntersuchungen* 10: 187-201.

Boehm, P.D., D.S. Page, W.A. Burns, A.E. Bence, P.J. Mankiewicz and J.S. Brown, 2001. Resolving the Origin of the Petrogenic Hydrocarbon Background in Prince William Sound, Alaska, *Environmental Science and Technology*, 35(3): 471-479.

Boehm, P.D., and J.W. Farrington. 1984. Aspects of the polycyclic aromatic hydrocarbon geochemistry of recent sediments in the Georges Bank Region. *Environmental Science and Technology* 18: 840-845.

Boehm, P.D., J.S. Brown, and T.C. Sauer. 1989. Physical and chemical characterization of San Joaquin Valley crude oil. Final report prepared for ENTRIX, In., Walnut Creek, California.

Boehm, P.D., J.S. Brown, J.M. Neff, D.S. Page, A.W. Maki, W.A. Burns, and A.E. Bence. 2003. The chemical baseline as a key to defining continuing injury and recovery of Prince William Sound. In Proceedings of the 2003 International Oil Spill Conference. API, Washington, D.C. pp 275-283.

Braunstein Geological & Environmental Services, Inc. (BGES). 2007. Prince William Sound RCAC Long Term Environmental Monitoring Program, Preliminary Review. Prepared for the Prince William Sound Regional Citizens' Advisory Council October 2007, 41 pp.

Brown, D.W., L.S. Ramos, M.Y. Friedman, and W.D. MacLeod, Jr. 1980. Ambient temperature extraction of hydrocarbons from marine sediment -- Comparison with boiling solvent extractions. Pages 313-326 in Petroleum in the Marine Environment, L. Petrakis and F.T. Weiss, eds. Advances in Chemistry Series No. 185. American Chemical Society, Washington, D.C.

Brown, J.S. and P.D. Boehm. 1993. The use of double ratio plots of polynuclear aromatic hydrocarbon (PAH) alkyl homologues for petroleum source identification. Pages 799-801 in Proceedings 1993 Oil Spill Conference. American Petroleum Institute, Washington, D.C.

Carls, M.G. 2006. Nonparametric identification of petrogenic and pyrogenic hydrocarbons in aquatic ecosystems. *Environmental Science and Technology* 40: 4233-4239.

Carls, M.G., Short, J.W. & Payne, J. 2006. Accumulation of polycyclic aromatic hydrocarbons by Neocalanus copepods in Port Valdez, Alaska. *Marine Pollution Bulletin* 52(11), 1480-1489.

Colonell, J.M. 1980a. "Ballast Water Dispersal." In Port Valdez, Alaska: Environmental Studies 1976-1979, J.M. Colonell (Ed.), Institute of Marine Science, University of Alaska, Fairbanks, Occasional Publication No. 5. 373 p.

Colonell, J.M. 1980b. "Physical Oceanography". In Port Valdez, Alaska: Environmental Studies 1976-1979, J.M. Colonell (Ed.), Institute of Marine Science, University of Alaska, Fairbanks, Occasional Publication No. 5. 373 p.

Cross, J.N., J.T. Hardy, J.E. Hose, G.P. Hershelman, L.D. Antrim, R.W. Gossett and E.A. Crecelius. 1987. "Contaminant Concentrations and Toxicity of Sea-Surface Microlayer near Los Angeles, California," *Marine Environmental Research* 23: 307-323.

Davis, J.B. 1968, Paraffinic hydrocarbons in the sulfate-reducing bacterium, *Desulfovibrio desulfuricaus*. *Chem. Geol*. 3: 155-160.

Douglas, G.S., A.E. Bence, R.C. Prince, S.J. McMillen, and E.L. Butler. 1996. Environmental stability of selected petroleum hydrocarbon source and weathering ratios. *Environmental Science & Technology* 30(7): 2332-2339.

Driskell, W.B., J.R. Payne, and G. Shigenaka. 2005. Revisiting Source Identification, Weathering Models, and Phase Discrimination for *Exxon Valdez* Oil. In Proceedings of Arctic Marine Oil Spill Conference 2005, Calgary, Alberta, Canada. pp 33-58.

Duesterloh, W., Short, J.W. & Barron, M.G. 2002. Photoenhanced toxicity of weathered Alaska North Slope crude oil to the Calanoid copepods *Calanus marshallae* and *Metridia okhotensis. Environmental Science and Technology* 36: 3953-3959.

Environmental Toxicology and Chemistry (ETC). 1999. Papers from a 1997 American Chemical Society symposium on "The mechanisms and effects of resistant sorption processes of organic compounds in natural particles," *Environmental Toxicology and Chemistry*, 18(8): 1609-1761.

Farrington, J.W., and B.W. Tripp. 1977. Hydrocarbons in western North Atlantic surface sediments. *Geochim. Cosmochim. Acta* 41: 1627-1641.

Federal Register. 1986. Code of Federal Regulations, Title 40, Part 136, Protection of the Environment. (40 CFR 136). U.S. Government Printing Office, Washington, D.C.

Han, J. and M. Calvin. 1969. Hydrocarbon distribution of algae and bacteria and microbiological activity in sediments, pages 436-443. In Proceedings, National Academy of Sciences. Volume 64. Washington, D.C.; NRC 1985).

Hardy, J.T. 1982. "The Sea-Surface Microlayer: Biology, Chemistry and Anthropogenic Enrichment," *Progress in Oceanography* 11: 307-328.

Hardy, J., S. Kiesser, L. Antrim, A. Stubin, R. Kocan and J.A. Strand. 1987a. The sea-surface microlayer of Puget Sound: Part I. Toxic effects on fish eggs and larvae. *Marine Environmental Research* 23: 227-249.

Hardy, J.T., E.A. Crecelius, L.D. Antrim, V.L. Broadhurst, C.W. Apts, J.M. Gurtisen, and T.J. Fortman. 1987b. The sea-surface microlayer of Puget Sound: Part 2. Concentrations of contaminants and relation to toxicity," *Marine Environmental Research* 23: 251-271.

Hardy, J.T., E.A. Crecelius, L.D. Antrim, S.L. Kiesser, V.L. Broadhurst, P.D. Boehm, and W.G. Steinhauer. 1990. Aquatic surface contamination in Chesapeake Bay. *Marine Chemistry* 28: 333-351.

Helton, Doug, Adam Moles, Jeff Short, Jeep Rice 2004. Results of the *M/V Kuroshima* Oil Spill Shellfish Tissue Analysis 1999, 2000 and 2004. Report to the *M/V Kuroshima* Trustee Council. Prepared by NOAA Office of Response and Restoration, Seattle, Washington and NOAA Auke Bay Laboratory, Juneau, Alaska. December 2004, 7 pp.

Karinen, J.F., M.M. Babcock, E.W. Brown, W.D. MacLeod, Jr., L.R. Ramos, and J.W. Short. 1993. Hydrocarbons in intertidal sediments and mussels from Prince William Sound, Alaska, 1977-1980: characterization and probable sources. NOAA (National Oceanic and Atmospheric Administration) Technical Memorandum NMFS (National Marine Fisheries Service) AFSC-9, Seattle.

Kimbrough, K. L., W. E. Johnson, G. G. Lauenstein, J. D. Christensen and D. A. Apeti. 2008. An Assessment of Two Decades of Contaminant Monitoring in the Nation's Coastal Zone. Silver Spring, MD. NOAA Technical Memorandum NOS NCCOS 74. 105 pp.

Kinnetic Laboratories, Inc. (KLI), 2002. 2000-2002 LTEMP Monitoring Report. Prepared for the Prince William Sound Regional Citizens' Advisory Council Long-Term Environmental Monitoring Program. 94 pp. and appendices.

Larsen, M.L. and L.G. Holland 2004. Standard operating procedure for the determination of particle grain size in marine sediments analyzed at the Auke Bay Laboratory. Auke Bay Laboratory, Alaska Fisheries Science Center, National Marine Fisheries Service, NOAA. Juneau, Alaska.

National Research Council (NRC) 1985. *Oil in the Sea: Inputs, Fates, and Effects.* National Academy Press, Washington, D.C. 601 pp.

National Research Council (NRC) 2003. *Oil in the Sea III: Inputs, Fates, and Effects.* National Academy Press, Washington, D.C. 265 pp.

National Research Council (NRC) 2005. *Oil Spill Dispersants: Efficacy and Effects.* National Academy Press, Washington, D.C. 377 pp.

O'Clair, C.E., J.W. Short, and S.D. Rice. 1996. Contamination of intertidal and subtidal sediments by oil from the *Exxon Valdez* in Prince William Sound. Pages 61-93 *in* S.D. Rice, R.B. Spies, D.A. Wolfe, and B.A. Wright (editors). Proceedings of the *Exxon Valdez* oil spill symposium. American Fisheries Society Symposium 18.

O'Connor, T.P. 2002. National distribution of chemical concentrations in mussels and oysters in the USA. *Marine Environmental Research* 53: 117-143

Overton, E.B., J.A. McFall, S.W. Mascarella, C.F. Steele, S.A. Antoine, I.R. Politzer, and J.L. Laseter. 1981. Identification of petroleum residue sources after a fire and oil spill. Proceedings 1981 Oil Spill Conference. American Petroleum Institute, Washington, D.C., pp 541-546.

Page, D., P.D. Boehm, G.S. Douglas, and A.E. Bence. 1993. The natural petroleum hydrocarbon background in subtidal sediments of Prince William Sound, Alaska. Abstract #089 in Ecological Risk Assessment: Lessons Learned. 14th Annual Meeting, Society of Environmental Toxicology and Chemistry (SETAC) 14-18 November 1993, Houston, TX.

Page, D.S., P.D. Boehm, G.S. Douglas, and A.E. Bence. 1995. Identification of hydrocarbon sources in the benthic sediments of Prince William Sound and the Gulf of Alaska following the *Exxon Valdez* oil spill. Pages 41- 83 in Exxon Valdez Oil Spill: Fate and Effects in Alaskan Waters, ASTM STP 1219, Peter G. Wells, James N. Butler, and Jane S. Hughes, Eds., American Society for Testing and Materials, Philadelphia.

Payne, J.R. and W.B. Driskell. 2001. Source characterization and identification of *New Carissa* oil in NRDA environmental samples using a combined statistical and fingerprinting approach. Proceedings of the 2001 Oil Spill Conference, American Petroleum Institute, Washington, D.C., pp. 1403-1409.

Payne, J.R. and W.B. Driskell. 2003. The importance of distinguishing dissolved- versus oil-droplet phases in assessing the fate, transport, and toxic effects of marine oil pollution. Proceedings of the 2003 Oil Spill Conference, American Petroleum Institute, Washington, D.C., pp 771-778.

Payne, J.R., B.E. Kirstein, G.D. McNabb, Jr., J.L. Lambach, R. Redding, R.E. Jordan, W. Hom, C. de Oliveira, G.S. Smith, D.M. Baxter, and R. Geagel. 1984. Multivariate analysis of petroleum weathering in the marine environment - subarctic. Volume I, Technical Results; Volume II, Appendices. In: Final Reports of Principal Investigators, Vol. 21 and 22. February 1984, U.S. Department of Commerce, National Oceanic and Atmospheric Administration, Ocean Assessment Division, Juneau, Alaska. 690 pp. Volume 21 NTIS Accession Number PB85-215796; Volume 22 NTIS Accession Number PB85-215739.

Payne, J.R., J.R. Clayton, Jr., G.D. McNabb, Jr., B.E. Kirstein, C.L. Clary, R.T. Redding, J.S. Evans, E. Reimnitz, and E. Kempema. 1989. Oil-ice sediment interactions during freezeup and breakup. Final Reports of Principal Investigators, U.S. Dept. Commer., NOAA, OCEAP Final Rep. 64, 1-382 (1989). NTIS Accession Number PB-90-156217.

Payne, J.R., W.B. Driskell, and D.C. Lees. 1998. Long Term Environmental Monitoring Program Data Analysis of Hydrocarbons in Intertidal Mussels and Marine Sediments, 1993-1996. Final Report prepared for the Prince William Sound Regional Citizens Advisory Council, Anchorage, Alaska 99501. (PWSRCAC Contract No. 611.98.1). March 16, 1998. 97 pp plus appendices.

Payne, J.R., W.B. Driskell, M.G. Barron, D.C. Lees. 2001. Assessing transport and exposure pathways and potential petroleum toxicity to marine resources in Port Valdez, Alaska. Final Report Prepared for Prince William Sound Regional Citizens' Advisory Council Contract No. 956.02.1. Prepared by Payne Environmental Consultants, Inc., Encinitas, CA. December 21, 2001. 64 pp plus appendices.

Payne, J.R., W.B. Driskell, and J.W. Short. 2003a. 2002-2003 LTEMP Monitoring Report. Final Report prepared to the Prince William Sound Regional Citizens' Advisory Council, Anchorage, Alaska 99051. PWSRCAC Contract No. 951.03.1. Prepared by Payne Environmental Consultants, Inc., Encinitas, CA. Nov. 6, 2003. 107 pp.

Payne, J.R., J.R. Clayton, Jr., and B.E. Kirstein. 2003b. Oil/suspended particulate material interactions and sedimentation. *Spill Science & Technology Bulletin*, 8(2): 201-221.

Payne, J.R., W.B. Driskell, M.G. Barron, J. A. Kalmar, and D.C. Lees. 2003c. Public comment regarding the Draft NPDES Permit for BWTF at Alyeska Marine Terminal. Final Report prepared for the Prince William Sound Regional Citizens' Advisory Council, Anchorage, Alaska 99051. PWSRCAC Contract No. 551.02.01. Prepared by Payne Environmental Consultants, Inc., Encinitas, CA. June 2, 2003, 21 p.

Payne, J.R., W.B. Driskell, M.G. Barron, D.C. Lees, L. Ka'aihue, and J.W. Short. 2003d. Assessing transport and exposure pathways and potential petroleum toxicity to marine resources in Port Valdez, Alaska. Poster No. PT214 presented at the SETAC 24th Annual Meeting in North America. November 9-13, 2003, Austin, Texas.

Payne, J.R., W.B. Driskell, and J.W. Short. 2005a. 2003-2004 LTEMP Monitoring Report. Final Report prepared for the Prince William Sound Regional Citizens' Advisory Council, Anchorage, Alaska 99051. PWSRCAC Contract No. 951.04.1. Prepared by Payne Environmental Consultants, Inc., Encinitas, CA. April 18, 2005. 123 pp.

Payne, J.R., W.B. Driskell, J.F. Braddock, J. Bailey. 2005b. Hydrocarbon biodegradation in the Ballast Water Treatment Facility, Alyeska Marine Terminal. Final Report prepared for the Prince William Sound Regional Citizens' Advisory Council, Anchorage, Alaska 99051. PWSRCAC Contract Numbers 558.04.01 and 560.2004.01. Prepared by Payne Environmental Consultants, Inc., Encinitas, CA. May 2, 2005. 48 pp.

Payne, J.R., W.B. Driskell, J.F. Braddock, J. Bailey, J.W. Short, L. Ka'aihue, T.H. Kuckertz 2005c. From Tankers to Tissues – Tracking the Degradation and Fate of Oil Discharges in Port Valdez, Alaska. Proceedings of Arctic Marine Oil Spill Conference 2005, Calgary, Alberta, Canada. pp 959-991.

Payne, J.R. and W.B. Driskell, M.R. Lindeberg, W. Fournier, M.L. Larsen, J.W. Short, S.D. Rice, and D. Janka. 2005d. Dissolved- and Particulate-Phase Hydrocarbons in Interstitial Water from Prince William Sound Beaches Containing Buried Oil Thirteen Years After the *Exxon Valdez* Oil Spill, Proceedings of the 2005 International Oil Spill Conference, American Petroleum Institute, Washington, D.C., pp. 83-88.

Payne, J.R., W.B. Driskell, J.W. Short, and M.L. Larsen. 2006. 2004-2005 LTEMP Monitoring Report. Final Report prepared for the Prince William Sound Regional Citizens' Advisory Council, Anchorage, Alaska 99051. PWSRCAC Contract No. 951.05.1. (Restoration Project No. 040724). Prepared by Payne Environmental Consultants, Inc., Encinitas, CA. November 2006. 149 pp.

Payne, James R., William B. Driskell, Jeffrey W. Short, Marie L. Larsen. 2008a. Final 2005-2006 LTEMP Oil Monitoring Report, Exxon Valdez Oil Spill Restoration Project Final Report (Restoration Project 050763), Prince William Sound Regional Citizen's Advisory Council, Anchorage, Alaska. 137 pp.

Payne, J.R., W.B. Driskell, J.W. Short and M.L. Larsen. 2008b. Long-term monitoring for oil in the *Exxon Valdez* spill region. *Marine Pollution Bulletin* 56: 2067-2081.

Pelletier, M.C., Burgess, R.M., Ho, K.T., Kuhn, A., McKinney, R.A. & Rybe, S.A. 1997. Phototoxicity of individual polycyclic aromatic hydrocarbons and petroleum to marine invertebrate larvae and juveniles. *Environmental Toxicology and Chemistry* 16: 2190-2199.

Salazar, M., J.W. Short, S.M. Salazar, and J.R. Payne. 2002. Port Valdez Monitoring Report. Prince William Sound Regional Citizens' Advisory Council Contract No. 633.01.1. February 7, 2002. 109 pp plus appendices.

Sauer, T. and P. Boehm. 1991. The use of defensible analytical chemical measurements for oil spill natural resource damage assessment. Proceedings of the 1991 Oil Spill Conference. American Petroleum Institute, Washington, D.C., pp 363-369.

Saupe, Susan 2004. Alaska EMAP coordinator, personal communication.

Savoie, M.A., Savoie, J.M., Trefry, J.H., Semmler, C.M., Woodall, D.W., Trocine, R.P., Brooks, J.M. & McDonald, T. 2006. Port Valdez sediment coring program -- final 2004 monitoring report. Final Report prepared for the Prince William Sound Regional Citizens' Advisory Council, Anchorage, Alaska 99051. (Contract No. 961.04.1) January 2006. 76 pp.

Shaw, D., A.L. Blanchard, and D.L. Hawkins. 2005. Chapter 2 – Hydrocarbon Studies in Environmental Studies in Port Valdez, Alaska: 2004. Final Report to Alyeska Pipeline Service Co., Inst. of Marine Science, Univ. Alaska Fairbanks, 221 pp.

Short, J.W. 2005. Seasonal variability of pristane in mussels (*Mytilus Trossulus*) in Prince William Sound, Alaska. Ph.D. Thesis. University of Alaska, Fairbanks. 204 pp.

Short, J.W. and M.M. Babcock. 1996. Prespill and postspill concentrations of hydrocarbons in mussels and sediments in Prince William Sound. Pages 149-166 *in* S.D. Rice, R.B. Spies, D.A. Wolfe, and B.A. Wright (editors). Proceedings of the *Exxon Valdez* oil spill symposium. American Fisheries Society Symposium 18.

Short, J.W. and K.R. Springman. 2007. Identification of hydrocarbons in biological samples for source determination. Pages 381-403 *in* Oil Spill Environmental Forensics, Z. Wang and S.A. Stout (editors), Elsevier, Inc, Oxford, UK.

Short, J.W., K.A. Kvenvolden, P.R. Carlson, F.D. Hostettler, R.J. Rosenbauer and B.A. Wright. 1999. Natural hydrocarbon background in benthic sediments of Prince William Sound, Alaska: Oil vs. coal, *Environmental Science and Technology*, 33(1): 34-42.

Short, J.W., M.R. Lindeberg, P.A. Harris, J.M. Maselko, J.J. Pella, and S.D. Rice. 2004. An estimate of oil persisting on beaches of Prince William Sound, 12 years after the *Exxon Valdez* oil spill. *Environmental Science & Technology* 38: 19-25

Short, J.W., G.V. Irvine, D.H. Mann, J.M. Maselko, J.J. Pella, M.R. Lindeberg, J.R. Payne, W.B. Driskell, and S.D. Rice. 2007a. Slightly weathered *Exxon Valdez* oil persists in Gulf of Alaska beach sediments after 16 years. *Environmental Science & Technology*. 41(4): 1245-1250.

Short, J.W., J.J. Kolak, J.R. Payne, G.K. Van Kooten. 2007b. An evaluation of petrogenic hydrocarbons in northern Gulf of Alaska continental shelf sediments – The role of coastal oil seep inputs. *Organic Geochemistry* 38(4): 643-670.

Wang, Z. and S.A. Stout. 2007. Oil Spill Environmental Forensics: Fingerprinting and Source Identification. Academic Press, Burlington, MA, USA. 554 pp.

Widdows, J., Donkin, P., Evans, S.V., Page, D.S. & Salkeld, P.N. 1995. Sublethal biological effects and chemical contaminant monitoring of Sullom Voe (Shetland) using mussels (Mytilus edulis). In Proceedings of the Royal Society of Edinburgh103B, 99-112.

Woodward-Clyde Consultants and ENTRIX, Inc. 1987. Ballast water treatment facility effluent plume behavior. A Synthesis of Findings. Prepared for Alyeska Pipeline Service Company. Walnut Creek, California. March 1987.

APPENDIX A LTEMP Oil Primer

This section is included as background material for those readers unfamiliar with oil chemistry or the oil contaminants found in Prince William Sound and central Alaskan coastal regions.

A.1 Regional Sources

In the LTEMP regional environment, oil hydrocarbons arrive from numerous and varied sources. Topping the list would be Alaskan North Slope (ANS) crude including lingering residues from the *Exxon Valdez* oil spill (EVOS); oil products from the Alyeska Marine Terminal (not necessarily ANS); coal, peat and organic-rich shales from vast local and regional deposits; Cook Inlet crude oil; and refined petroleum products that have made their way into the marine environment.

Of primary interest to LTEMP is ANS crude oil. This crude actually consists of a blend of petroleum from the production fields on the Alaskan North Slope, including Prudhoe Bay, Kuparuk, Endicott, and Lisburne, that together exhibit a chemical fingerprint that is quite distinct from that of oil found in other geographic areas. The EVOS of March 1989 consisted of ANS crude, which over time has weathered to produce a significantly different fingerprint than that of fresh ANS crude. Petroleum that originates from organic-rich shales (or hydrocarbon "source rock") and coal deposits in the Gulf of Alaska also contribute significantly to the natural (or “background") hydrocarbons in the study area, and these also exhibit a distinctly different fingerprint. Recent work shows the source rock signature to be particularly widespread in the deep sediments of PWS, and indeed, appears unchanged in coastal sediments from upstream of the Copper River past the Outer Kenai and through Shelikof Straits (unpublished data, Susan Saupe). Fortunately, animals exposed to these sediments do not seem to accumulate higher-molecular-weight components because they are generally not bioavailable. Natural terrestrial oil seeps have also been invoked as hydrocarbon sources, but recent work indicates input from these seeps is insignificant compared with the other sources.

Other petroleum products that may have been introduced into the marine environment in Prince William Sound (PWS) include oil products from source locations other than Alaska. For example, the Great Alaskan Earthquake of 1964 and the resultant tsunamis washed fuel oil and asphalt made from California source oils into Port Valdez, and subsequently into PWS (Kvenvolden et al. 1995). These authors noted that tarballs from these California-sourced products have been found throughout the northern and western parts of PWS. Most recently, hydrocarbons from historic anthropogenic activities (long-abandoned mines, logging operations, camp sites, and fish canneries) in addition to current settlements within PWS have been hypothesized as being additional sources of background hydrocarbon signals (Boehm et al. 2003).

A.2 Oil Chemistry, Source Allocations, and Weathering Behavior

Chemically, oil is a complex mixture of decayed ancient organic matter broken down and modified under geologic heat and pressure. Each deposit is a unique blend but there are commonalities. Hydrocarbons are by far the most abundant compounds in crude oil,

accounting for 50-98% of the volume. And in various proportions, all crude blends contain "lighter fractions" of hydrocarbons (similar to gasoline), "intermediate fractions" like diesel or fuel oil, heavier tars and wax-like hydrocarbons, and ultimately residual materials like asphalt. For purposes of the LTEMP chemical analyses, crude oil is identified by its signature blend of just two compositional hydrocarbon groups, the polycyclic aromatic hydrocarbons (PAH) and the saturated (or aliphatic) hydrocarbons (SHC), also referred to as n-alkanes. These two compositional groups encompass the intermediate, heavier tars, and wax-like fractions. As shown by the plots in Figure 41, we work with approximately 44 PAH compounds and 26 SHC components to identify a hydrocarbon source. (Names and abbreviations of the individual analytes shown in this and all following figures are presented in Table 2 in Section 4.2 - Analytic Methods.) These PAH typically account for 2-5% of petroleum by weight (and about 3% of ANS crude).

For source identifications, it is useful to distinguish between five main families of PAH components. In order from light to heavy (left to right in the plots), they are: naphthalenes (N), fluorenes (F), phenanthrenes/anthracenes (P/A), dibenzothiophenes (D), and chrysenes (C).

The naphthalenes are two-ring aromatics (i.e., two 6-carbon rings linked together) and are less persistent in the environment compared to the other higher-molecular-weight groups. They typically disappear from spilled oil by evaporation and dissolution weathering and as such, they may or may not be present in the plots of oil residues or oil-contaminated mussel and sediment samples. Because they dissolve slowly and to a limited extent in water, they can also be detected moving directly from the water column into exposed organisms. The fluorenes, anthracenes, and phenanthrenes (which are all three-ring aromatics) are each more persistent in the environment, and as such, they can act as markers to help differentiate among different oil sources. The dibenzothiophenes (another three-ring compound that also contains sulfur) are important, because they are substantially more abundant in Alaskan North Slope crude oil than in other oil deposits in the region such as Cook Inlet or Katalla crude oil. Finally, the heavier four- and five-ring aromatics (including, the chrysenes (C) through benzo(g,h,i)perylene (BP)) are important because: 1) they can help distinguish between crude oils and refined products (such as diesel oil) that may have been produced from a particular crude oil; and 2) they are also representative of combustion by-products.

Chemists have developed a nomenclature to distinguish the various members of each family. The simple parent compounds in each of the five PAH families are referred to as "C_0" (e.g., C_0-naphthalene, here abbreviated simply as "N"). Their other family members, known to chemists as alkyl-substituted homologues, are adorned with an alkyl molecule (-CH_3) in a named position around the margin of the PAH ring. These homologues thus become known by their sequence name, e.g., C1-naphthalene (abbreviated as N1), C2-naphthalene (N2), and so on (N3 and N4) (see Figure 41).

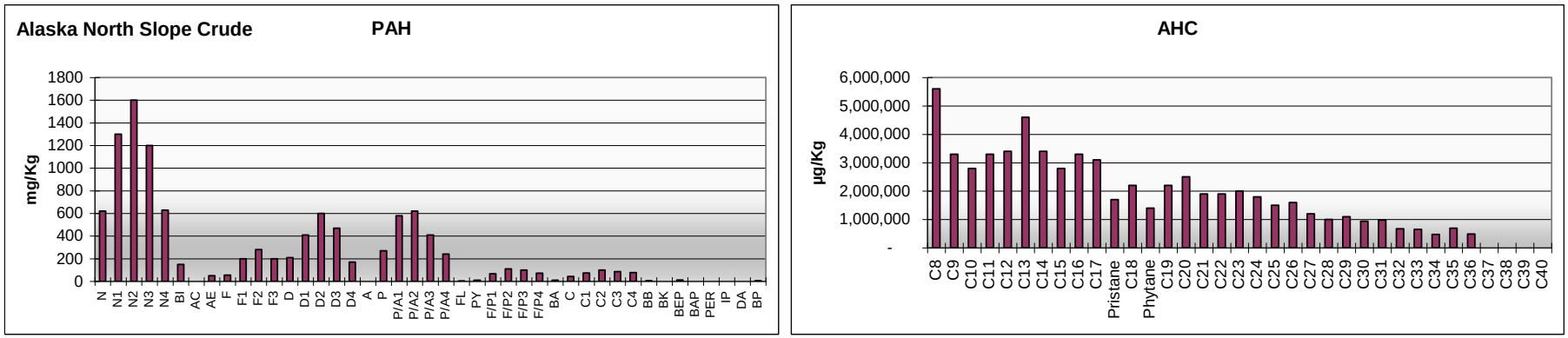

Figure 41 Example plots of ANS PAH and SHC (also referred to as AHC) components.

Regarding the family structure, it is important to note that petrogenic (petroleum-derived) PAHs have a characteristic fingerprint whereby the parent compounds in each of the five PAH families (e.g., the parent C_0-naphthalene, abbreviated as "N") are usually at lower concentrations than their other family members (see Figure 41). With evaporation/ dissolution weathering, these lower-molecular-weight components are more easily eliminated, thus generating a characteristic "water-washed profile" with the levels of $C_0<C_1<C_2<C_3$ within each PAH group. Eventually, with continued weathering, only the most persistent alkylated phenanthrenes/anthracenes, dibenzothiophenes, and chrysenes are seen, and typically at very characteristic, source-specific ratios in the remaining oil residues (Figure 42).

Likewise, in the SHC fraction, the n-alkanes also clearly show the effects of evaporation weathering with losses of all components with molecular weights below n-C_{14} apparent after several weeks (Figure 42). With continued microbial degradation, the remaining n-alkanes will be selectively removed leaving only the branched compounds, pristane and phytane, which are also removed but at a much slower rate over time. Incidentally, phytoplankton make n-C_{15} and n-C_{17} which mussels can accumulate by feeding on the phytoplankton. Substantial concentrations of pristane are also naturally present in some zooplankton; they biosynthesize it from chlorophyll ingested with the phytoplankton they eat. Therefore, all three compounds can show up in mussel and sediment samples as a result of marine biogenic input. In a spring plankton bloom, these natural aliphatic hydrocarbons can easily dominate the SHC fraction. Phytane, on the other hand, is almost exclusively associated with oil, so its presence in samples can also be used as another indicator of petroleum contamination.

Pyrogenic PAHs come from combustion sources including atmospheric fallout and surface runoff from the burning of fossil fuels (diesel, heating oil, gasoline, etc.) and from other pyrogenic sources such as forest fires and camp fires. Creosote, which is used to preserve wood pilings, is also usually included in this category because of a similar PAH profile. Pyrogenic PAHs are characterized by high molecular weight PAHs greater than C_3-dibenzothiophene (D3), and by high concentrations of the <u>parent</u> compounds compared to their alkyl homologues. A typical pattern for pyrogenic PAHs is decreasing concentration with increasing alkyl substitution and molecular weight within a group, i.e., $C_0>C_1>C_2>C_3>C_4$, opposite the trend seen in crude oil and distillate products.

For the aliphatic hydrocarbons, the nomenclature strategy changes. The abbreviation for the aliphatic compound, n-C_{10}, now refers to 10 carbon atoms linked in a straight chain (no cyclic rings). In contrast to the PAHs, aliphatic hydrocarbons can account for more than 70 percent of petroleum by weight. Also, as noted above, aliphatic hydrocarbons can be synthesized by organisms (both planktonic and terrestrial), and may be present as degradation products in some bacteria. As shown in Figure 41, crude petroleum contains a homologous series of n-alkanes ranging from one (methane gas) to more than 30 carbons with odd- and even-numbered n-alkanes present in nearly equal amounts. In contrast, biogenic hydrocarbons (produced by living organisms) preferentially contain specific

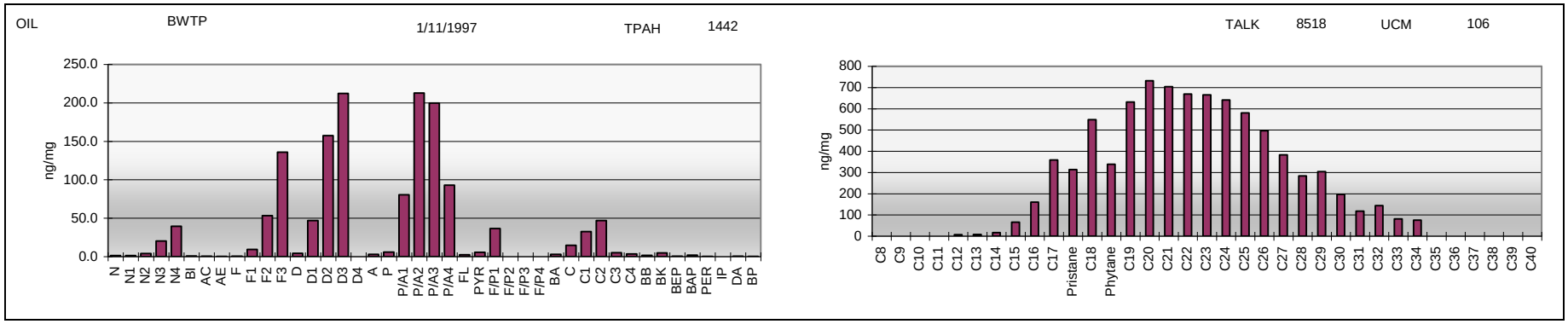

Figure 42 Plot of weathered ANS from LTEMP 11/97.

suites of normal alkanes with mainly odd-numbered carbons between n-C_{15} and n-C_{33}. In addition to the example of n-C_{15}, n-C_{17}, and pristane from marine plankton cited above, terrestrial plants contribute a predominant odd-numbered carbon pattern including n-C_{25}, n-C_{27}, n-C_{29}, n-C_{31}, and n-C_{33}. These so-called "plant waxes" are commonly observed in marine sediments in depositional areas receiving significant amounts of terrestrial runoff.

Petroleum also contains a complex mixture of branched and cyclic compounds generally not found in organisms. This complex mixture can include oxygenated compounds that produce an "unresolved complex mixture" of compounds (the UCM) in the gas chromatographic profiles. The UCM appears proportionally more prominent in analyses as additional oxygenated compounds are introduced to oil by bacterial and photochemical processes. Thus, the presence and amount of the UCM can be a diagnostic indicator of heavily-weathered petroleum contamination.

Once in water, a crude oil signature can be modified by several processes including evaporation and dissolution weathering, and microbial degradation. We've recently identified another twist in tracking an oil source, the dissolved versus particulate fractions. As a droplet of oil enters water, the more readily-dissolvable components, particularly the naphthalenes, are removed from the droplet thus leaving behind a particulate (or oil droplet) fraction with the "water-washed pattern" mentioned above (low on the parent stock). The receiving water then has the dissolved components signature. In essence, one source produces two signatures in water. This process is readily apparent in the discharge into Port Valdez from the Ballast Water Treatment Facility (BWTF) at the Alyeska Marine Terminal.

Figure 43 presents plots of the PAH and SHC associated with this discharge (Payne et al. 2001; Salazar et al. 2002). In this case, the PAH pattern associated with the colloidal/particulate (oil-droplet) phase shows the depletion of naphthalene (N) and methylnaphthalenes (N1) compared to higher alkylated homologues (N2, N3, and N4), and, to a lesser extent, this same "water-washed pattern" is observed for the fluorenes (Fs), dibenzothiophenes (Ds), and phenanthrenes/anthracenes (P/As). The SHC (n-alkane) distribution from the BWTF discharge still shows the presence of minute oil droplets (the water insoluble components that do not dissolve). In addition to evaporation weathering, there is evidence of enhanced microbial degradation from the biological treatment tanks at the BWTF as shown by the depleted concentrations of the n-alkanes compared to pristane and phytane (compare the SHC patterns in Figure 41 and Figure 43).

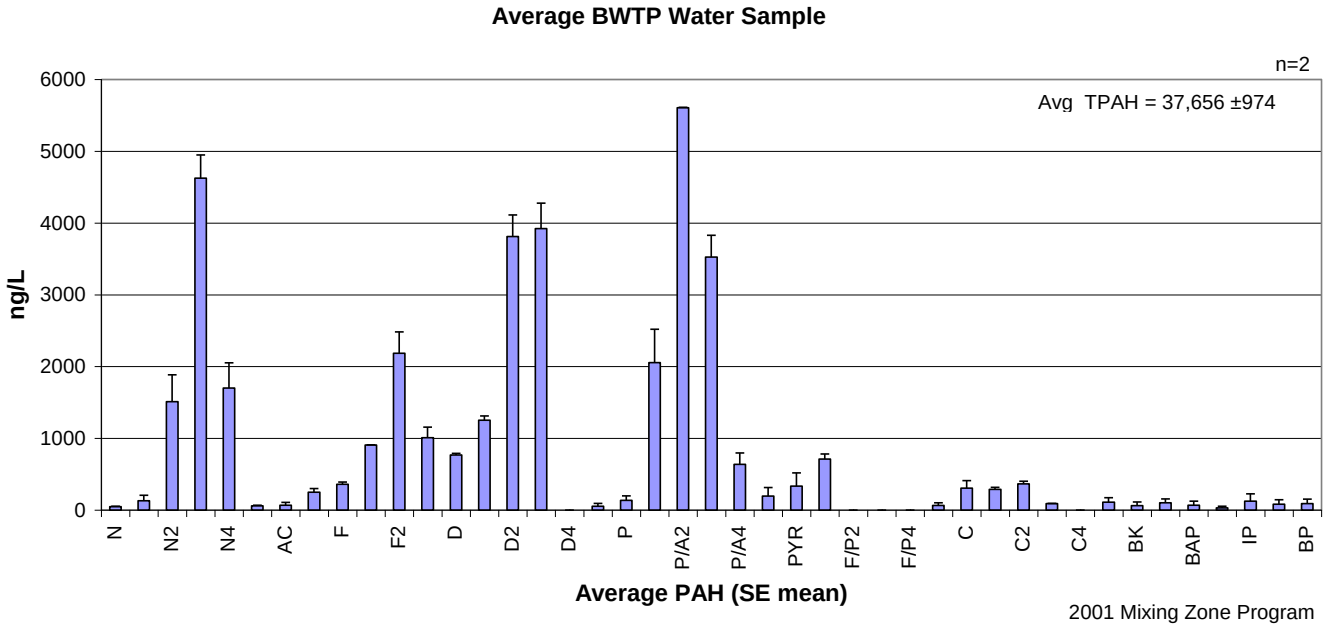

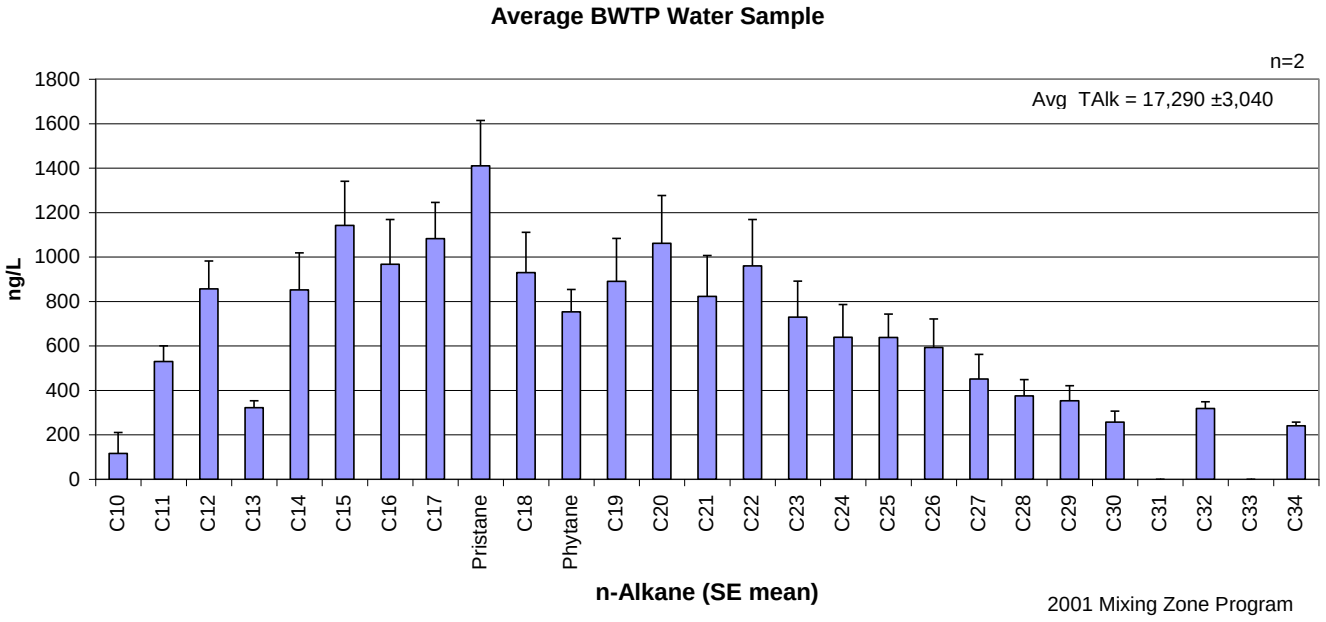

Figure 43 PAH and SHC plots of effluent from the Alyeska Marine Terminal BWTF (from Salazar et al. 2002).

A.3 Mussels as Indicator Organisms

When analyzing the mussel tissue samples collected as part of LTEMP, it is important to recognize that as filter feeders, mussels can accumulate oil from both the dissolved and particulate/oil-droplet phases. Figure 44 (from Payne et al. 2001) presents examples of mussels collected from oiled areas of Cabin Bay, Naked Island in Prince William Sound in May 1989 immediately after the *Exxon Valdez* oil spill and again in May/June in 1990 and 1991. In 1989, the mussels clearly accumulated PAH and aliphatic hydrocarbons from both the dissolved and particulate phases to which they were exposed; however, the particulate (dispersed oil droplet phase) was the predominant source for the accumulated higher-molecular-weight PAH (C_2-dibenzothiophenes (D2) through higher alkylated homologues of the phenanthrenes/anthracenes and chrysenes) and the aliphatics (phytane plus the even distribution of n-alkanes from n-C_{19} through n-C_{34}). As noted above, these higher-molecular-weight components have only limited water solubilities and have long been associated with the whole oil (droplet) phase. In the post-spill 1990 and 1991 data, the mussels accumulated primarily dissolved-phase PAH (at significantly reduced overall concentrations) from the more water-soluble hydrocarbons still leaching from the contaminated intertidal zone. This is manifest in the plots at the bottom of Figure 44 by the predominant naphthalene and alkyl-substituted naphthalene homologues in greater relative abundance compared to the other PAH. Likewise, the SHC profile for the mussel samples in 1990-1991 is characterized primarily by lower molecular weight biogenic components (n-C_{15}, n-C_{17}, and pristane) with little or no contribution of phytane and higher molecular weight n-alkanes from dispersed oil droplets.

These plots are presented as examples of what should be considered in this report and specifically kept in mind when reviewing the data generated during the past 16 years of the LTEMP. The profiles in Figure 44 are particularly important, because they also illustrate typical patterns of oil contamination (from both particulate and dissolved phases) in the absence of other confounding factors, such as lipid interference.

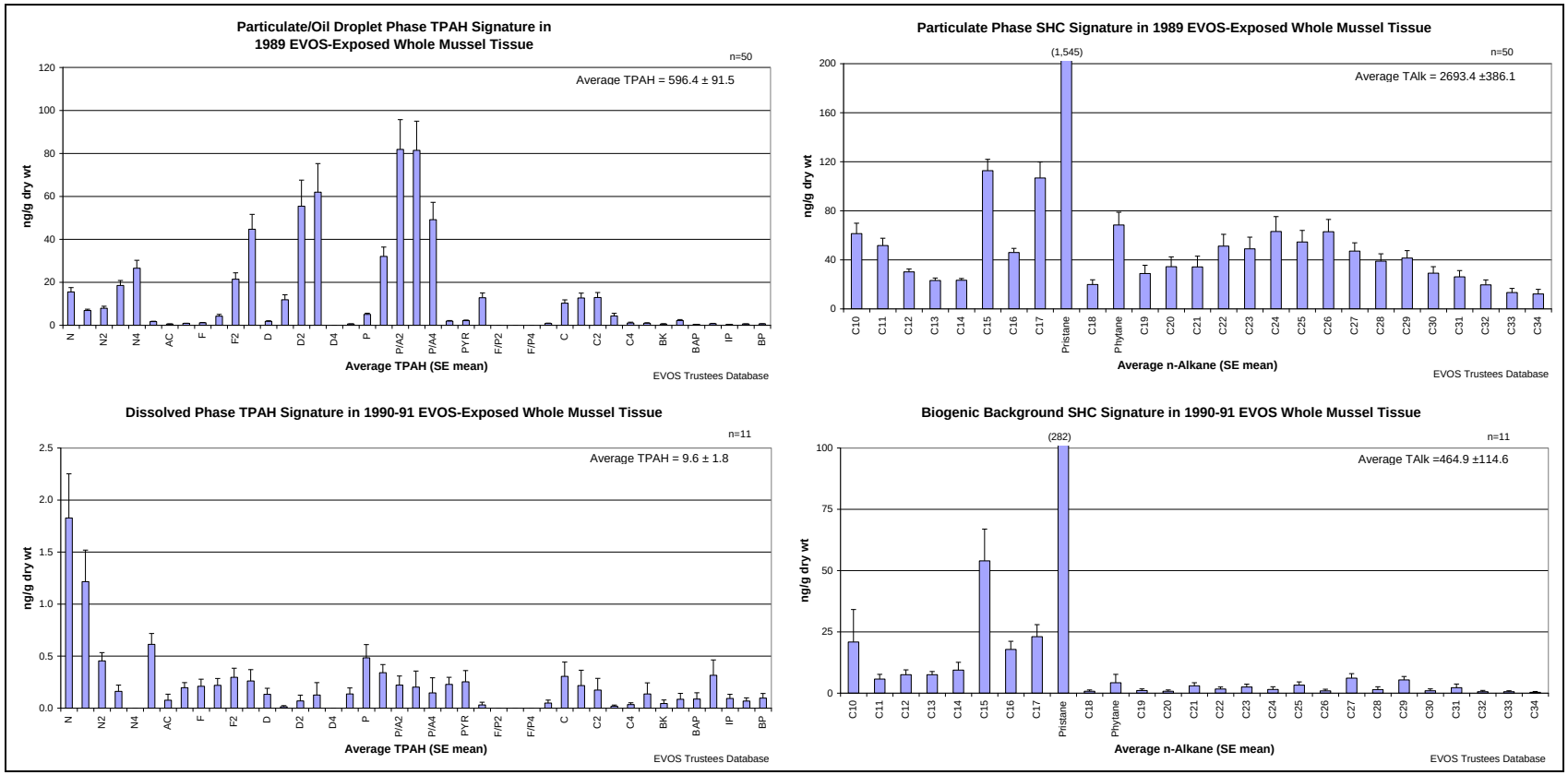

Figure 44 Average PAH and SHC plots of whole mussel extracts from samples collected from oiled areas of Cabin Bay, Naked Island in Prince William Sound in May 1989 after the *Exxon Valdez* oil spill (EVOS) and again in May/June 1990 and 1991. The number of samples contributing to each composite is denoted by "n" (from Payne et al. 2001; data from NOAA EVTHD database).

APPENDIX B LTEMP Sediment TPAH and TSHC Data—All Years

B.1 TPAH and TSHC summary table for Alyeska Marine Terminal, Gold Creek and Constantine Harbor sediment samples, 1993-2007.

Date	Sample ID	Total PAH	Mean	Std Dev	CV	Total SHC	Mean	Std Dev	CV
Alyeska Marine Terminal Subtidal Sediments (AMT-S)									
3-Apr-93	PWS93PAT0040	1868				196			
3-Apr-93	PWS93PAT0041	2533				341			
3-Apr-93	PWS93PAT0042	1873	2091	383	18.3	191	243	85	35.1
16-Jul-93	PWS93PAT0043	1164				146			
16-Jul-93	PWS93PAT0044	3183				198			
16-Jul-93	PWS93PAT0045	1707	2018	1045	51.8	394	246	131	53.2
26-Mar-94	PWS94PAT0025	1047				202			
26-Mar-94	PWS94PAT0026	1698				167			
26-Mar-94	PWS94PAT0027	1675	1473	369	25.1	239	203	36	17.8
20-Jul-94	PWS94PAT0031	1425				174			
20-Jul-94	PWS94PAT0032	1242				230			
20-Jul-94	PWS94PAT0033	1922	1530	352	23	389	264	112	42.2
3-Apr-95	PWS95PAT0022	1291				206			
3-Apr-95	PWS95PAT0023	1093				244			
3-Apr-95	PWS95PAT0024	1785	1390	356	25.6	186	212	29	13.9
11-Jul-95	PWS95PAT0028	2189				1650			
11-Jul-95	PWS95PAT0029	1872				362			
11-Jul-95	PWS95PAT0030	2763	2275	452	19.9	629	880	680	77.2
16-Mar-96	PWS96PAT0004	1109				160			
16-Mar-96	PWS96PAT0005	1578				311			
16-Mar-96	PWS96PAT0006	1100	1262	273	21.7	135	202	95	47.1
12-Jul-96	PWS96PAT0025	2265				326			
12-Jul-96	PWS96PAT0026	1782				201			
12-Jul-96	PWS96PAT0027	1602	1883	343	18.2	381	303	92	30.5
6-Mar-97	PWS97PAT0001	2203				417			
6-Mar-97	PWS97PAT0002	1980				449			
6-Mar-97	PWS97PAT0003	2929	2371	496	20.9	388	418	31	7.3
17-Jul-97	PWS97PAT0029	1124				246			
17-Jul-97	PWS97PAT0030	1477				377			
17-Jul-97	PWS97PAT0031	1892	1498	384	25.7	288	303	67	22
29-Mar-98	PWS98PAT0016	1112				120			
29-Mar-98	PWS98PAT0017	1668				451			
29-Mar-98	PWS98PAT0018	972	1251	368	29.4	144	238	185	77.6
5-Apr-00	PWS00PAT0004	1465				313			
5-Apr-00	PWS00PAT0005	1575				335			
5-Apr-00	PWS00PAT0006	1568	1536	62	4	412	353	52	14.7
21-Jul-00	PWS00PAT0010	2080				392			
21-Jul-00	PWS00PAT0011	3016				452			

21-Jul-00	PWS00PAT0012	2107	2401	533	22.2	571	472	91	19.4
28-Mar-01	PWS01PAT0001	2987				814			
28-Mar-01	PWS01PAT0002	1803				465			
28-Mar-01	PWS01PAT0003	2659	2483	611	24.6	564	614	180	29.3
22-Jul-01	PWS01PAT0010	1044				160			
22-Jul-01	PWS01PAT0011	1276				536			
22-Jul-01	PWS01PAT0012	1969	1429	481	33.7	311	335	189	56.4
15-Mar-02	PWS02PAT0004	2508				10			
15-Mar-02	PWS02PAT0005	2452				68			
15-Mar-02	PWS02PAT0006	3514	2825	598	21.2	149	76	70	92.2
10-Jul-02	AMT-S-02-2-1	473				192			
10-Jul-02	AMT-S-02-2-2	504				158			
10-Jul-02	AMT-S-02-2-3	551	509	39	7.7	1089	480	528	110.2
18-Mar-03	AMT-S-03-1-1	654				134			
18-Mar-03	AMT-S-03-1-2	694				271			
18-Mar-03	AMT-S-03-1-3	594	648	51	7.8	131	179	80	44.7
27-Jul-03	AMT-S-03-2-1P	604				199			
27-Jul-03	AMT-S-03-2-2P	564				132			
27-Jul-03	AMT-S-03-2-3P	522	563	41	7.3	109	147	47	31.7
27-Jul-03	AMT-S-03-2-1A	791				230			
27-Jul-03	AMT-S-03-2-2A	701				286			
27-Jul-03	AMT-S-03-2-3A	496	663	151	22.8	144	220	71	32.4
23-Mar-04	AMT-S-04-1-1	451				128			
23-Mar-04	AMT-S-04-1-2	417				231			
23-Mar-04	AMT-S-04-1-3	352	407	50	12.3	142	167	56	33.6
13-Oct-04	AMT-S-04-2-1	629				93			
13-Oct-04	AMT-S-04-2-2	703				329			
13-Oct-04	AMT-S-04-2-3	402	578	157	27.1	103	175	133	76.3
4-Mar-04	AMT-S-05-1-1	243				65			
4-Mar-04	AMT-S-05-1-2	337				47			
4-Mar-04	AMT-S-05-1-3	350	310	58	18.8	41	51	12	24.5
28-Jul-04	AMT-S-04-2-1	870				93			
28-Jul-04	AMT-S-04-2-2	943				329			
28-Jul-04	AMT-S-04-2-3	608	807	176	0.22	103	175	133	0.76
4-Mar-05	AMT-S-05-1-1	367				65			
4-Mar-05	AMT-S-05-1-2	491				47			
4-Mar-05	AMT-S-05-1-3	455	438	64	0.15	41	51	12	0.24
25-Jul-05	AMT-S-05-2-1	731				106			
25-Jul-05	AMT-S-05-2-2	535				61			
25-Jul-05	AMT-S-05-2-3	677	648	59	15.7	92	86	13	26.9
2-Mar-06	AMT-S-06-1-1	419				48			
2-Mar-06	AMT-S-06-1-2	388				49			
2-Mar-06	AMT-S-06-1-3	670	492	89	31.4	64	54	5	17.1
15-Jul-06	AMT-S-06-2-1	83				687			
15-Jul-06	AMT-S-06-2-2	44				348			
15-Jul-06	AMT-S-06-2-3	68	65	11	30.2	358	464	112	41.6
5-Apr-07	AMT-S-07-1-1	40				253			

5-Apr-07	AMT-S-07-1-2	36				289			
5-Apr-07	AMT-S-07-1-3	48	41	4	15.0	473	338	68	34.9
10-Jul-07	AMT-S-07-2-1	72				609			
10-Jul-07	AMT-S-07-2-2	66				590			
10-Jul-07	AMT-S-07-2-3	75	71	3	6.9	751	650	51	13.6
Gold Coast Subtidal Sediments (GOC-S)									
19-Mar-93	PWS93PAT0001	47				941			
19-Mar-93	PWS93PAT0002	36				436			
19-Mar-93	PWS93PAT0003	58	47	11	23.4	1460	946	512	54.1
25-Jul-93	PWS93PAT0071	57				1036			
25-Jul-93	PWS93PAT0072	31				408			
25-Jul-93	PWS93PAT0073	25	38	17	45.2	256	567	413	73
26-Mar-94	PWS94PAT0022	60				1429			
26-Mar-94	PWS94PAT0023	45				571			
26-Mar-94	PWS94PAT0024	106	70	32	45.2	638	879	477	54.3
19-Jul-94	PWS94PAT0028	47				385			
19-Jul-94	PWS94PAT0029	18				378			
19-Jul-94	PWS94PAT0030	68	44	25	56.6	737	500	205	41.1
3-Apr-95	PWS95PAT0019	57				463			
3-Apr-95	PWS95PAT0020	34				322			
3-Apr-95	PWS95PAT0021	31	41	14	35	528	438	105	24.1
11-Jul-95	PWS95PAT0025	67				750			
11-Jul-95	PWS95PAT0026	59				598			
11-Jul-95	PWS95PAT0027	31	52	19	36.1	444	597	153	25.6
16-Mar-96	PWS96PAT0001	78				588			
16-Mar-96	PWS96PAT0002	156				470			
16-Mar-96	PWS96PAT0003	33	89	62	69.9	523	527	59	11.2
12-Jul-96	PWS96PAT0028	56				541			
12-Jul-96	PWS96PAT0029	45				440			
12-Jul-96	PWS96PAT0030	52	51	6	10.9	629	537	95	17.6
6-Mar-97	PWS97PAT0004	54				624			
6-Mar-97	PWS97PAT0005	39				431			
6-Mar-97	PWS97PAT0006	40	44	8	18.9	441	499	109	21.8
17-Jul-97	PWS97PAT0026	53				514			
17-Jul-97	PWS97PAT0027	55				788			
17-Jul-97	PWS97PAT0028	60	56	3	5.7	552	618	148	24
29-Mar-98	PWS98PAT0013	42				341			
29-Mar-98	PWS98PAT0014	48				301			
29-Mar-98	PWS98PAT0015	38	43	5	11.6	352	331	27	8.1
5-Apr-00	PWS00PAT0001	126				590			
5-Apr-00	PWS00PAT0002	81				668			
5-Apr-00	PWS00PAT0003	126	111	26	23.4	918	725	171	23.6
20-Jul-00	PWS00PAT0007	105				966			
20-Jul-00	PWS00PAT0008	111				753			
21-Jul-00	PWS00PAT0009	92	103	10	9.3	912	877	111	12.7
28-Mar-01	PWS01PAT0004	125				904			
28-Mar-01	PWS01PAT0005	131				833			

28-Mar-01	PWS01PAT0006	120	126	5	4.2	901	879	40	4.6
21-Jul-01	PWS01PAT0007	40				311			
21-Jul-01	PWS01PAT0008	59				506			
21-Jul-01	PWS01PAT0009	108	69	35	50.8	2993	1270	1495	117.8
15-Mar-02	PWS02PAT0002	91				1568			
15-Mar-02	PWS02PAT0003	33				1165			
15-Mar-02	PWS02PAT0007	134	86	51	59.1	1407	1380	203	14.7
10-Jul-02	GOC-S-02-2-1	42				188			
10-Jul-02	GOC-S-02-2-2	46				147			
10-Jul-02	GOC-S-02-2-3	29	39	9	22.4	117	151	36	23.9
18-Mar-03	GOC-S-03-1-1	31				291			
18-Mar-03	GOC-S-03-1-2	52				368			
18-Mar-03	GOC-S-03-1-3	45	43	11	24.7	280	313	48	15.4
27-Jul-03	GOC-S-03-2-1P	31				203			
27-Jul-03	GOC-S-03-2-2P	26				179			
27-Jul-03	GOC-S-03-2-3P	115	57	50	87.9	225	202	23	11.4
27-Jul-03	GOC-S-03-2-1A	32				283			
27-Jul-03	GOC-S-03-2-2A	31				306			
27-Jul-03	GOC-S-03-2-3A	33	32	1	2.1	219	269	45	16.8
23-Mar-04	GOC-S-04-1-1	33				193			
23-Mar-04	GOC-S-04-1-2	16				316			
23-Mar-04	GOC-S-04-1-3	36	28	11	38.7	132	214	94	43.8
28-Jul-04	GOC-S-04-2-1	22				353			
28-Jul-04	GOC-S-04-2-2	28				261			
28-Jul-04	GOC-S-04-2-3	22	24	3	14.0	150	254	102	40.0
4-Mar-05	GOC-S-05-1-1	17				189			
4-Mar-05	GOC-S-05-1-2	22				224			
4-Mar-05	GOC-S-05-1-3	18	19	3	13.0	271	228	41	18.0
25-Jul-05	GOC-S-05-2-1	32				210			
25-Jul-05	GOC-S-05-2-2	23				189			
25-Jul-05	GOC-S-05-2-3	30	28	3	15.5	148	182	18	17.4
2-Mar-06	GOC-S-06-1-1	20				157			
2-Mar-06	GOC-S-06-1-2	23				201			
2-Mar-06	GOC-S-06-1-3	21	21	1	6.6	250	203	27	23.1
15-Jul-06	GOC-S-06-2-1	17				192			
15-Jul-06	GOC-S-06-2-2	17				125			
15-Jul-06	GOC-S-06-2-3	27	21	3	28.4	168	162	20	21.2
5-Apr-07	GOC-S-07-1-1	8				366			
5-Apr-07	GOC-S-07-1-2	18				348			
5-Apr-07	GOC-S-07-1-3	13	13	3	40.8	448	387	31	13.7
10-Jul-07	GOC-S-07-2-1	11				391			
10-Jul-07	GOC-S-07-2-2	18				204			
10-Jul-07	GOC-S-07-2-3	8	12	3	41.2	296	297	54	31.5
Constantine Harbor Sediments COH-S									
19-Jul-05	COH-S-05-2-1	36				166			
19-Jul-05	COH-S-05-2-2	61				187			
19-Jul-05	COH-S-05-2-3	58	52	8	26.1	289	214	38	30.9

4-Mar-06	COH-S-06-1-1	81				263			
4-Mar-06	COH-S-06-1-2	70				233			
4-Mar-06	COH-S-06-1-3	78	76	3	7.8	283	260	15	9.7
27-Jul-06	COH-S-06-2-1	45				168			
27-Jul-06	COH-S-06-2-2	54				215			
27-Jul-06	COH-S-06-2-3	61	53	5	14.8	222	202	17	14.4
12-Jul-07	COH-S-07-2-1	53				356			
12-Jul-07	COH-S-07-2-2	86				679			
12-Jul-07	COH-S-07-2-3	30	56	16	50.3	160	398	151	65.8

B.2 Summary of Sediment TPAH and Phase Component Fractions, 1993-2007

			Dissolved		Particulate		Pyrogenic			TPAH	
Sample ID	Sample Date	TPAH	ng/g	portion	ng/g	portion	ng/g	portion	Analytic Lab	Mean	SE mean
Alyeska Marine Terminal Sediments (AMT-S)											
PWS93PAT0040	4/3/1993	196	0	0	171.2	0.88	22.5	0.12	GERG		
PWS93PAT0041	4/3/1993	341	43.6	0.13	269.5	0.8	23.9	0.07	GERG		
PWS93PAT0042	4/3/1993	191	0	0	175.3	0.93	13.9	0.07	GERG	243	49
PWS93PAT0043	7/16/1993	145	0	0	125.9	0.87	18.2	0.13	GERG		
PWS93PAT0044	7/16/1993	198	0	0	179.9	0.92	16.3	0.08	GERG		
PWS93PAT0045	7/16/1993	394	33.4	0.09	49.5	0.13	306.4	0.79	GERG	246	76
PWS94PAT0025	3/26/1994	202	0	0	142.8	0.71	57.3	0.29	GERG		
PWS94PAT0026	3/26/1994	167	0	0	151.1	0.92	13.9	0.08	GERG		
PWS94PAT0027	3/26/1994	239	0	0	174.3	0.74	62.6	0.26	GERG	203	21
PWS94PAT0031	7/20/1994	175	0	0	156.2	0.9	16.8	0.1	GERG		
PWS94PAT0032	7/20/1994	230	0	0	204.2	0.9	23.4	0.1	GERG		
PWS94PAT0033	7/20/1994	389	0	0	336.7	0.87	50.2	0.13	GERG	265	64
PWS95PAT0022	4/3/1995	206	0	0	162.2	0.8	41.7	0.2	GERG		
PWS95PAT0023	4/3/1995	244	0	0	193.3	0.8	48.9	0.2	GERG		
PWS95PAT0024	4/3/1995	187	0	0	164.5	0.89	20.4	0.11	GERG	212	17
PWS95PAT0028	7/11/1995	1,650	0	0	526.9	0.32	1108.8	0.68	GERG		
PWS95PAT0029	7/11/1995	362	0	0	339.6	0.95	18.8	0.06	GERG		
PWS95PAT0030	7/11/1995	630	0	0	607.6	0.97	19.5	0.03	GERG	881	392
PWS96PAT0004	3/16/1996	160	0	0	136.8	0.86	21.5	0.14	GERG		
PWS96PAT0006	3/16/1996	311	0	0	297.4	0.96	11.7	0.04	GERG		
PWS96PAT0006	3/16/1996	135	0	0	119.9	0.9	13.6	0.1	GERG	202	55
PWS96PAT0025	7/12/1996	326	0	0	306.2	0.94	19	0.06	GERG		
PWS96PAT0026	7/12/1996	201	0	0	188.3	0.94	11.4	0.06	GERG		
PWS96PAT0027	7/12/1996	381	0	0	110.7	0.31	251.2	0.69	GERG	303	53
PWS97PAT0001	3/6/1997	417	0	0	377	0.91	36.4	0.09	GERG		
PWS97PAT0002	3/6/1997	449	0	0	416.2	0.93	29.3	0.07	GERG		

PWS97PAT0003	3/6/1997	388	0	0	342.4	0.89	43.2	0.11	GERG	418	18
PWS97PAT0029	7/17/1997	246	0	0	223.5	0.92	18.8	0.08	GERG		
PWS97PAT0030	7/17/1997	377	0	0	341.1	0.92	31.6	0.08	GERG		
PWS97PAT0031	7/17/1997	288	0	0	268.5	0.95	15.4	0.06	GERG	303	39
PWS98PAT0016	3/29/1998	120	0	0	108.9	0.93	8.8	0.07	GERG		
PWS98PAT0017	3/29/1998	451	0	0	210.8	0.47	233.6	0.53	GERG		
PWS98PAT0018	3/29/1998	144	0	0	129.1	0.91	12.1	0.09	GERG	238	107
PWS00PAT0004	4/5/2000	313	0	0	222.7	0.72	86.8	0.28	GERG		
PWS00PAT0006	4/5/2000	335	0	0	303.3	0.91	28.5	0.09	GERG		
PWS00PAT0006	4/5/2000	412	0	0	374.9	0.92	34.2	0.08	GERG	353	30
PWS00PAT0010	7/21/2000	392	0	0	333.5	0.86	54.1	0.14	GERG		
PWS00PAT0011	7/21/2000	452	0	0	397.3	0.89	50.8	0.11	GERG		
PWS00PAT0012	7/21/2000	571	54.5	0.1	147.8	0.26	356.4	0.64	GERG	472	53
PWS01PAT0001	3/28/2001	814	0	0	725.8	0.9	79	0.1	GERG		
PWS01PAT0002	3/28/2001	465	0	0	406.1	0.88	53.9	0.12	GERG		
PWS01PAT0003	3/28/2001	564	43.5	0.08	445.5	0.8	66.9	0.12	GERG	614	104
PWS01PAT0010	7/22/2001	160	20.5	0.13	74.2	0.48	61.5	0.39	GERG		
PWS01PAT0011	7/22/2001	536	51.2	0.1	58.1	0.11	408.9	0.79	GERG		
PWS01PAT0012	7/22/2001	311	0	0	287	0.94	19.4	0.06	GERG	335	109
PWS02PAT0004	3/15/2002	10	4.9	0.53	2.4	0.26	2	0.22	GERG		
PWS02PAT0006	3/15/2002	68	0	0	59	0.88	8	0.12	GERG		
PWS02PAT0006	3/15/2002	149	0	0	94	0.65	51.4	0.35	GERG	76	40
AMT-S-02-2-1	7/10/2002	1,068	0	0	1033	0.98	25.2	0.02	ABL		
AMT-S-02-2-2	7/10/2002	183	23	0.13	98.6	0.55	58.7	0.33	ABL		
AMT-S-02-2-3	7/10/2002	148	21.4	0.15	84.9	0.58	39.8	0.27	ABL	466	301
AMT-S-03-1-1	3/18/2003	127	0	0	94.1	0.75	31.7	0.25	ABL		
AMT-S-03-1-2	3/18/2003	260	0	0	171.7	0.66	87.2	0.34	ABL		
AMT-S-03-1-3	3/18/2003	123	0	0	114.6	0.94	7.2	0.06	ABL	170	45
AMT-S-03-2-1P	7/27/2003	165	14.5	0.09	133.8	0.82	14.1	0.09	ABL		
AMT-S-03-2-2P	7/27/2003	118	12	0.1	58.3	0.5	45.3	0.39	ABL		
AMT-S-03-2-3P	7/27/2003	93	10.1	0.11	75.1	0.82	6.2	0.07	ABL	125	21
AMT-S-03-2-1A	7/27/2003	195	23	0.12	157.6	0.82	11.2	0.06	ABL		

AMT-S-03-2-2A	7/27/2003	265	23.9	0.09	2.9	0.01	232.3	0.9	ABL		
AMT-S-03-2-3A	7/27/2003	126	16.9	0.14	95	0.77	11.2	0.09	ABL	195	40
AMT-S-04-1-1	3/23/2004	121	0	0	21.2	0.18	98.1	0.82	ABL		
AMT-S-04-1-2	3/23/2004	225	30.6	0.14	3.6	0.02	185	0.84	ABL		
AMT-S-04-1-3	3/23/2004	134	0	0	44.9	0.34	85.8	0.66	ABL	160	33
AMT-S-04-2-1	7/28/2004	89	0	0	12.4	0.14	74.7	0.86	ABL		
AMT-S-04-2-2	7/28/2004	321	28.7	0.09	3.4	0.01	280.3	0.9	ABL		
AMT-S-04-2-3	7/28/2004	91	0	0	44.4	0.5	44.7	0.5	ABL	167	77
AMT-S-05-1-1	3/4/2005	106	1.6	0.76	41.8	0.12	4	0.12	ABL		
AMT-S-05-1-2	3/4/2005	61	23.2	0.79	0	0.17	12.3	0.04	ABL		
AMT-S-05-1-3	3/4/2005	92	1.3	0.79	44.3	0.16	1.9	0.05	ABL	86	13
AMT-S-05-2-1	7/25/2005	48	40.9	0.56	12	0.2	3.8	0.24	ABL		
AMT-S-05-2-2	7/25/2005	49	33.2	0.72	10.4	0.2	2.1	0.08	ABL		
AMT-S-05-2-3	7/25/2005	64	34.1	0.74	14.5	0.2	3.6	0.06	ABL	54	5
AMT-S-06-1-1	3/3/2006	61	7.8	0.13	1.1	0.02	50.5	0.85	ABL		
AMT-S-06-1-2	3/3/2006	42	7.6	0.18	23.1	0.56	10.7	0.26	ABL		
AMT-S-06-1-3	3/3/2006	37	0	0	25.5	0.73	9.7	0.27	ABL	47	7
AMT-S-06-2-1	7/15/2006	83	35.2	0.4	13.6	0.17	35.8	0.45	ABL		
AMT-S-06-2-2	7/15/2006	44	32.2	0.8	10.0	0.24	1.6	0.04	ABL		
AMT-S-06-2-3	7/15/2006	68	35.7	0.6	12.2	0.19	20.6	0.32	ABL	65	11
AMT-S-07-1-1	4/5/2007	40	37.2	1.0	0.0	0.00	3.7	0.10	ABL		
AMT-S-07-1-2	4/5/2007	36	24.7	0.7	8.7	0.26	2.9	0.08	ABL		
AMT-S-07-1-3	4/5/2007	48	32.6	0.7	0.0	0.00	15.2	0.34	ABL	41	4
AMT-S-07-2-1	7/10/2007	72	50.2	0.7	15.8	0.22	8.7	0.12	ABL		
AMT-S-07-2-2	7/10/2007	66	47.0	0.7	12.0	0.19	8.8	0.14	ABL		
AMT-S-07-2-3	7/10/2007	75	55.4	0.7	14.8	0.20	9.2	0.12	ABL	71	3
Gold Creek Sediments (GOC-S)											
PWS93PAT0001	3/19/1993	47	0	0	16.3	0.35	29.8	0.65	GERG		
PWS93PAT0002	3/19/1993	36	0	0	12.5	0.35	23	0.65	GERG		
PWS93PAT0003	3/19/1993	58	0	0	25	0.44	31.8	0.56	GERG	47	6
PWS93PAT0071	7/25/1993	57	0	0	15.4	0.28	40.5	0.72	GERG		
PWS93PAT0072	7/25/1993	31	0	0	8.3	0.27	22	0.73	GERG		

PWS93PAT0073	7/25/1993	25	0	0	8.7	0.35	15.9	0.65	GERG	38	10
PWS94PAT0022	3/26/1994	61	0	0	49.1	0.83	10.2	0.17	GERG		
PWS94PAT0023	3/26/1994	46	0	0	27.9	0.63	16.4	0.37	GERG		
PWS94PAT0024	3/26/1994	106	0	0	19.9	0.19	84.9	0.81	GERG	71	18
PWS94PAT0028	7/19/1994	47	0	0	26.7	0.59	18.9	0.41	GERG		
PWS94PAT0029	7/19/1994	18	0	0	12.3	0.7	5.2	0.3	GERG		
PWS94PAT0030	7/19/1994	69	0	0	13.6	0.2	53.6	0.8	GERG	44	15
PWS95PAT0019	4/3/1995	57	8.2	0.15	2.6	0.06	45.3	0.81	GERG		
PWS95PAT0020	4/3/1995	34	0	0	10.9	0.33	22.4	0.67	GERG		
PWS95PAT0021	4/3/1995	31	0	0	13.5	0.45	16.8	0.55	GERG	41	8
PWS95PAT0025	7/11/1995	67	0	0	45.6	0.7	19.9	0.3	GERG		
PWS95PAT0026	7/11/1995	59	0	0	28.9	0.51	28.1	0.49	GERG		
PWS95PAT0027	7/11/1995	31	0	0	23	0.79	6.2	0.21	GERG	52	11
PWS96PAT0001	3/16/1996	78	0	0	12.2	0.16	63.7	0.84	GERG		
PWS96PAT0002	3/16/1996	156	11.8	0.08	0	0	140.5	0.92	GERG		
PWS96PAT0003	3/16/1996	33	9.7	0.31	9.1	0.29	12.8	0.41	GERG	89	36
PWS96PAT0028	7/12/1996	56	0	0	26	0.48	28.6	0.52	GERG		
PWS96PAT0029	7/12/1996	46	0	0	23	0.52	21.4	0.48	GERG		
PWS96PAT0030	7/12/1996	53	0	0	25.9	0.5	25.4	0.5	GERG	51	3
PWS97PAT0004	3/6/1997	54	0	0	24.3	0.46	28.1	0.54	GERG		
PWS97PAT0006	3/6/1997	39	0	0	23.8	0.63	14.2	0.37	GERG		
PWS97PAT0006	3/6/1997	40	0	0	17	0.43	22.3	0.57	GERG	44	5
PWS97PAT0026	7/17/1997	53	14.3	0.28	9.7	0.19	27.8	0.54	GERG		
PWS97PAT0027	7/17/1997	55	12.6	0.24	11.4	0.22	28.7	0.54	GERG		
PWS97PAT0028	7/17/1997	60	13	0.23	11.6	0.2	32.8	0.57	GERG	56	2
PWS98PAT0013	3/29/1998	42	14.3	0.35	23.3	0.58	2.8	0.07	GERG		
PWS98PAT0014	3/29/1998	48	0	0	24.8	0.54	20.9	0.46	GERG		
PWS98PAT0015	3/29/1998	38	14.9	0.41	19.4	0.53	2.1	0.06	GERG	43	3
PWS00PAT0001	4/5/2000	127	0	0	32.9	0.27	90.8	0.73	GERG		
PWS00PAT0002	4/5/2000	81	0	0	29.9	0.38	48.5	0.62	GERG		
PWS00PAT0003	4/5/2000	126	0	0	44	0.36	79.1	0.64	GERG	111	15
PWS00PAT0007	7/20/2000	106	26.4	0.26	7.5	0.07	68.1	0.67	GERG		

PWS00PAT0008	7/20/2000	111	32	0.3	10.5	0.1	65.2	0.61	GERG		
PWS00PAT0009	7/21/2000	92	24.8	0.28	8.5	0.1	55.9	0.63	GERG	103	6
PWS01PAT0004	3/28/2001	125	25.2	0.21	10.4	0.09	86	0.71	GERG		
PWS01PAT0006	3/28/2001	131	30.7	0.24	10.8	0.09	84.8	0.67	GERG		
PWS01PAT0006	3/28/2001	120	28.6	0.25	11.8	0.1	76	0.65	GERG	126	3
PWS01PAT0007	7/21/2001	40	0	0	15.7	0.42	21.6	0.58	GERG		
PWS01PAT0008	7/21/2001	59	21.7	0.39	3.1	0.06	31.3	0.56	GERG		
PWS01PAT0009	7/21/2001	108	17.5	0.17	3.1	0.03	83.9	0.8	GERG	69	20
PWS02PAT0002	3/15/2002	91	0	0	38.2	0.43	50.3	0.57	GERG		
PWS02PAT0003	3/15/2002	33	12.3	0.4	1.5	0.06	17.2	0.55	GERG		
PWS02PAT0007	3/15/2002	134	0	0	36.4	0.28	95.2	0.72	GERG	86	29
GOC-S-02-2-1	7/10/2002	42	0	0	19.2	0.48	20.9	0.52	ABL		
GOC-S-02-2-2	7/10/2002	46	16.7	0.38	1.5	0.03	26.2	0.59	ABL		
GOC-S-02-2-3	7/10/2002	29	13.9	0.5	0.7	0.02	13.1	0.47	ABL	39	5
GOC-S-03-1-1	3/18/2003	31	0	0	13.9	0.46	16.4	0.54	ABL		
GOC-S-03-1-2	3/18/2003	52	0	0	23	0.46	27.2	0.54	ABL		
GOC-S-03-1-3	3/18/2003	45	0	0	20.2	0.47	22.5	0.53	ABL	43	6
GOC-S-03-2-1A	7/27/2003	32	13.9	0.47	3.4	0.11	12.5	0.42	ABL		
GOC-S-03-2-2A	7/27/2003	31	11.3	0.38	0.8	0.03	17.6	0.59	ABL		
GOC-S-03-2-3A	7/27/2003	33	12.3	0.41	4.4	0.15	13.4	0.44	ABL	32	0
GOC-S-03-2-1P	7/27/2003	31	13.2	0.46	3.5	0.12	12	0.42	ABL		
GOC-S-03-2-2P	7/27/2003	26	10.6	0.45	2.4	0.1	10.4	0.44	ABL		
GOC-S-03-2-3P	7/27/2003	115	0	0	22	0.19	91.2	0.81	ABL	57	29
GOC-S-04-1-1	3/23/2004	33	14.3	0.45	1.1	0.03	16.1	0.51	ABL		
GOC-S-04-1-2	3/23/2004	16	7.2	0.49	0.6	0.04	7	0.47	ABL		
GOC-S-04-1-3	3/23/2004	36	14.5	0.43	1	0.03	18.2	0.54	ABL	28	6
GOC-S-04-2-1	7/28/2004	22	0	0	8.4	0.41	11.9	0.59	ABL		
GOC-S-04-2-2	7/28/2004	28	0	0	7.5	0.29	18.1	0.71	ABL		
GOC-S-04-2-3	7/28/2004	22	7.5	0.37	0.2	0.01	12.7	0.62	ABL	24	2
GOC-S-05-1-1	3/4/2005	17	0	0	6.8	0.44	8.6	0.56	ABL		
GOC-S-05-1-2	3/4/2005	22	8.8	0.42	0.4	0.02	11.8	0.56	ABL		
GOC-S-05-1-3	3/4/2005	18	7.1	0.41	0.3	0.02	9.7	0.57	ABL	19	2

GOC-S-05-2-1	7/25/2005	32	69.5	0.03	11.1	0.39	10.8	0.58	ABL		
GOC-S-05-2-2	7/25/2005	23	43.1	0.03	9.4	0.43	2.4	0.54	ABL		
GOC-S-05-2-3	7/25/2005	30	63.5	0.02	12.7	0.33	4.4	0.65	ABL	28	3
GOC-S-06-1-1	3/2/2006	20	23.6	0.03	8.6	0.47	10.3	0.5	ABL		
GOC-S-06-1-2	3/2/2006	23	31.6	0.02	8.8	0.45	3.5	0.52	ABL		
GOC-S-06-1-3	3/2/2006	21	42.5	0.02	11.7	0.42	3.3	0.56	ABL	21	1
GOC-S-06-2-1	7/15/2006	17	7.7	0.5	0.0	0.00	8.8	0.56	ABL		
GOC-S-06-2-2	7/15/2006	17	7.8	0.5	0.0	0.00	8.5	0.53	ABL		
GOC-S-06-2-3	7/15/2006	27	7.9	0.3	0.0	0.00	18.9	0.73	ABL	21	3
GOC-S-07-1-1	4/5/2007	8	3.5	0.5	0.0	0.00	3.5	0.53	ABL		
GOC-S-07-1-2	4/5/2007	18	7.5	0.5	0.0	0.00	10.1	0.61	ABL		
GOC-S-07-1-3	4/5/2007	13	4.8	0.4	0.0	0.00	7.0	0.63	ABL	13	3
GOC-S-07-2-1	7/10/2007	11	0.2	0.0	3.8	0.39	6.2	0.64	ABL		
GOC-S-07-2-2	7/10/2007	18	0.3	0.0	6.1	0.39	9.9	0.63	ABL		
GOC-S-07-2-3	7/10/2007	8	0.1	0.0	3.1	0.46	3.7	0.56	ABL	12	3
Constantine Harbor Sediments COH-S											
COH-S-05-2-1	7/19/2005	36	32.7	0.92	0	0	2.05	0.06	ABL		
COH-S-05-2-2	7/19/2005	61	28.4	0.47	26	0.43	4.26	0.07	ABL		
COH-S-05-2-3	7/19/2005	58	29.1	0.5	23.2	0.4	4.24	0.07	ABL	7.8	
COH-S-06-1-1	3/4/2006	81	35.7	0.45	37.9	0.48	5.27	0.07	ABL		
COH-S-06-1-2	3/4/2006	70	30.6	0.44	32.3	0.47	4.12	0.06	ABL		
COH-S-06-1-3	3/4/2006	78	33.4	0.43	37.4	0.49	4.28	0.06	ABL	3.5	
COH-S-05-2-1	7/19/2005	36	32.7	0.9	0.0	0.00	2.0	0.06	ABL		
COH-S-05-2-2	7/19/2005	61	28.4	0.5	26.0	0.43	4.3	0.07	ABL		
COH-S-05-2-3	7/19/2005	58	29.1	0.5	23.2	0.40	4.2	0.07	ABL	52	8
COH-S-06-1-1	3/4/2006	81	35.7	0.5	37.9	0.48	5.3	0.07	ABL		
COH-S-06-1-2	3/4/2006	70	30.6	0.4	32.3	0.47	4.1	0.06	ABL		
COH-S-06-1-3	3/4/2006	78	33.4	0.4	37.4	0.49	4.3	0.06	ABL	76	3
COH-S-06-2-1	7/27/2006	45	42.4	1.0	0.0	0.00	3.2	0.07	ABL		
COH-S-06-2-2	7/27/2006	54	50.6	1.0	0.0	0.00	3.3	0.06	ABL		
COH-S-06-2-3	7/27/2006	61	57.7	1.0	0.0	0.00	3.9	0.07	ABL	53	5
COH-S-07-2-1	7/12/2007	53	48.6	1.0	0.0	0.00	5.6	0.11	ABL		

COH-S-07-2-2	7/12/2007	86	79.5	1.0	0.0	0.00	8.3	0.10	ABL		
COH-S-07-2-3	7/12/2007	30	26.9	1.0	0.0	0.00	3.0	0.11	ABL	56	16

APPENDIX C Tissue TPAH and TSHC summary for LTEMP 2006-2007.

		TPAH			TSHC			Particulate		Dissolved		Pyrogenic	
Sample ID	Sample Date	ng/g dw	Mean	SE Mean	ng/g dw	Mean	SE Mean	ng/g	portion	ng/g	portion	ng/g	portion
AIB-B-06-2-1	7/27/2006	37			2310			6.4	0.18	30.7	0.85	0.0	0.00
AIB-B-06-2-2		16			2270			0.0	0.00	14.9	1.00	0.0	0.00
AIB-B-06-2-3		9	21	9	2763	2448	158	0.0	0.00	8.3	1.00	0.0	0.00
AIB-B-07-1-1	4/17/2007	19			877			3.4	0.19	15.4	0.85	0.0	0.00
AIB-B-07-1-2		61			2235			34.7	0.61	0.0	0.00	23.4	0.41
AIB-B-07-1-3		64	48	14	2269	1794	458	35.1	0.58	0.0	0.00	27.8	0.46
AIB-B-07-2-1	7/28/2007	14			3092			2.7	0.19	11.3	0.81	0.0	0.00
AIB-B-07-2-2		12			1975			0.0	0.00	11.3	0.96	0.5	0.04
AIB-B-07-2-3		10	12	1	1811	2293	403	9.0	0.98	0.0	0.00	0.2	0.02
AMT-B-06-2-1	7/15/2006	39			623			37.5	0.98	0.0	0.00	2.6	0.07
AMT-B-06-2-2		63			1219			65.3	1.05	0.0	0.00	0.7	0.01
AMT-B-06-2-3		37	46	8	854	899	173	37.0	1.04	0.0	0.00	0.7	0.02
AMT-B-06-3-1	10/6/2006	57			1502			9.6	0.17	54.2	0.97	1.9	0.03
AMT-B-06-3-2		79			2279			39.6	0.62	0.0	0.00	24.0	0.38
AMT-B-06-3-3		61	66	7	1915	1899	224	12.4	0.21	56.2	0.97	1.8	0.03
AMT-B-07-1-1	4/5/2007	47			632			22.0	0.46	0.0	0.00	26.9	0.57
AMT-B-07-1-2		60			385			10.9	0.18	50.8	0.85	0.0	0.00
AMT-B-07-1-3		53	54	4	317	445	96	3.3	0.06	44.6	0.87	3.2	0.06
AMT-B-07-2-1	7/10/2007	69			2317			41.5	0.64	0.0	0.00	24.4	0.38
AMT-B-07-2-2		52			1938			1.3	0.03	46.7	0.92	4.0	0.08
AMT-B-07-2-3		53			2034			1.4	0.03	47.4	0.92	4.2	0.08
AMT-B-07-2-3D		46	57	6	2271	2136	110	0.0	0.00	38.7	0.93	2.9	0.07
AMT-B-07-3-1	10/27/2007	25			241			10.7	0.44	0.0	0.00	13.7	0.56
AMT-B-07-3-2		32			218			14.3	0.46	0.0	0.00	17.1	0.54
AMT-B-07-3-3		98	52	23	178	212	18	3.7	0.04	88.4	0.93	6.2	0.07
COH-B-06-2-1	7/27/2006	33			754			0.7	0.02	30.0	0.94	1.2	0.04

COH-B-06-2-2		45			1336			1.3	0.03	40.9	0.96	0.3	0.01
COH-B-06-2-3		46	41	4	1020	1037	168	0.9	0.02	43.3	0.97	0.2	0.01
COH-B-07-2-1	7/12/2007	28			968			14.0	0.51	0.0	0.00	14.4	0.52
COH-B-07-2-2		31			1017			3.0	0.10	28.4	0.90	0.7	0.02
COH-B-07-2-3		26	28	2	1018	1001	17	2.2	0.09	22.8	0.88	0.8	0.03
DII-B-06-2-1	7/27/2006	43			599			4.9	0.12	38.4	0.91	0.0	0.00
DII-B-06-2-2		69			464			45.7	0.67	23.9	0.35	0.0	0.00
DII-B-06-2-3		23	45	13	575	546	41	22.7	1.00	0.0	0.00	0.0	0.00
DII-B-07-1-1	4/17/2007	28			1708			1.4	0.05	27.2	0.98	0.0	0.00
DII-B-07-1-2		50			1159			45.0	0.92	0.0	0.00	4.1	0.08
DII-B-07-1-3		33	37	6	1686	1518	179	32.9	1.03	0.0	0.00	0.0	0.00
DII-B-07-2-1	7/17/2007	35			2815			20.3	0.59	0.0	0.00	14.2	0.41
DII-B-07-2-2		15			2374			8.4	0.57	0.0	0.00	6.3	0.43
DII-B-07-2-3		19	23	6	2244	2478	173	11.2	0.60	0.0	0.00	9.2	0.50
GOC-B-06-2-1	7/15/2006	47			1139			20.8	0.47	0.0	0.00	24.2	0.54
GOC-B-06-2-2		41			666			37.8	0.99	0.0	0.00	4.1	0.11
GOC-B-06-2-3		46	45	2	651	819	160	36.3	0.82	0.0	0.00	8.8	0.20
GOC-B-06-3-1	10/6/2006	41			1151			22.3	0.60	0.0	0.00	21.4	0.57
GOC-B-06-3-2		43			1075			5.0	0.13	33.6	0.89	4.2	0.11
GOC-B-06-3-3		41	42	1	763	996	119	27.0	0.68	0.0	0.00	18.2	0.46
GOC-B-07-1-1	4/5/2007	92			327			46.8	0.59	0.0	0.00	32.0	0.41
GOC-B-07-1-2		58			405			25.4	0.44	0.0	0.00	33.1	0.58
GOC-B-07-1-3		75	75	10	536	423	61	32.8	0.45	0.0	0.00	42.8	0.58
GOC-B-07-2-1	7/10/2007	62			1810			1.7	0.03	54.7	0.89	6.5	0.11
GOC-B-07-2-2		65			1650			26.6	0.42	0.0	0.00	39.1	0.61
GOC-B-07-2-3		74	67	3	1579	1680	68	38.4	0.53	0.0	0.00	36.0	0.50
GOC-B-07-3-1	10/27/2007	45			263			25.5	0.65	0.0	0.00	17.2	0.44
GOC-B-07-3-2		25			291			0.0	0.00	22.5	0.92	1.8	0.08
GOC-B-07-3-3		22	30	7	218	257	21	14.7	0.69	0.0	0.00	6.6	0.31
KNH-B-06-2-1	7/7/2006	44			886			0.0	0.00	40.9	0.97	1.2	0.03
KNH-B-06-2-2		29			1122			18.7	0.67	0.0	0.00	9.1	0.33
KNH-B-06-2-3		26			771			0.6	0.03	23.9	0.96	0.9	0.04

KNH-B-06-2-4		25	31	4	1168	987	95	0.6	0.03	23.4	0.95	1.3	0.05
KNH-B-07-1-1	4/6/2007	32			685			1.5	0.06	25.7	0.97	0.8	0.03
KNH-B-07-1-2		26			656			1.9	0.07	24.4	0.95	0.3	0.01
KNH-B-07-1-3		23	27	3	470	604	67	0.0	0.00	20.4	0.94	1.3	0.06
KNH-B-07-2-1	7/11/2007	31			1074			0.6	0.02	28.9	0.95	1.6	0.05
KNH-B-07-2-2		32			1011			0.5	0.01	31.3	0.99	0.5	0.01
KNH-B-07-2-3		19	27	4	1268	1118	78	11.4	0.62	0.0	0.00	7.0	0.38
SHB-B-06-2-1	7/27/2006	29			819			0.0	0.00	27.6	0.99	0.4	0.01
SHB-B-06-2-2		82			630			0.0	0.00	80.0	0.99	0.7	0.01
SHB-B-06-2-3		27	46	18	626	692	64	0.0	0.00	25.7	0.97	0.7	0.03
SHB-B-07-1-1	4/6/2007	30			154			1.3	0.04	27.7	0.93	0.6	0.02
SHB-B-07-1-2		29			201			1.2	0.04	26.3	0.94	0.6	0.02
SHB-B-07-1-3		22	27	3	114	156	25	0.0	0.00	20.5	0.96	0.9	0.04
SHB-B-07-2-1	7/11/2007	68			3416			0.0	0.00	48.0	0.71	20.0	0.29
SHB-B-07-2-2		19			2785			0.0	0.00	17.8	0.95	0.9	0.05
SHB-B-07-2-3		18	35	17	2357	2853	308	1.1	0.06	16.8	0.96	0.0	0.00
SHH-B-06-2-1	7/26/2006	29			2978			7.9	0.28	19.4	0.69	1.2	0.04
SHH-B-06-2-2		22			1877			5.9	0.28	13.9	0.65	2.4	0.11
SHH-B-06-2-3		108	53	28	1871	2242	368	5.2	0.05	102.0	0.94	1.6	0.01
SHH-B-07-1-1	4/17/2007	19			368			0.8	0.20	0.0	0.00	4.0	1.00
SHH-B-07-1-2		31			0			0.0	0.00	19.9	1.00	0.0	0.00
SHH-B-07-1-3		33	28	4	0	123	123	1.5	0.06	24.0	1.00	0.0	0.00
SHH-B-07-2-1	7/28/2007	6			3637			1.1	0.17	5.1	0.80	0.1	0.02
SHH-B-07-2-2		7			2965			0.0	0.00	6.4	0.90	0.7	0.10
SHH-B-07-2-2D		6			2402			0.0	0.00	5.7	0.98	0.1	0.02
SHH-B-07-2-3		5	6	0	1774	2699	538	3.4	0.66	0.0	0.00	1.8	0.34
SLB-B-06-2-1	7/11/2006	18			1703			0.3	0.02	14.6	0.92	1.2	0.08
SLB-B-06-2-2		26			1483			1.2	0.05	22.7	0.88	3.1	0.12
SLB-B-06-2-3		22	22	2	1403	1530	90	0.0	0.00	20.1	0.95	1.1	0.05
SLB-B-07-1-1	4/17/2007	20			1208			13.2	0.70	0.0	0.00	5.7	0.30
SLB-B-07-1-2		30			1827			0.4	0.01	29.5	1.00	0.0	0.00
SLB-B-07-1-3		19	23	4	1646	1560	184	0.4	0.02	18.6	1.00	0.0	0.00

SLB-B-07-2-1	7/14/2007	19			1120			12.8	0.67	0.0	0.00	6.3	0.33
SLB-B-07-2-2		14			1557			7.3	0.54	0.0	0.00	6.3	0.46
SLB-B-07-2-3		15	16	2	2606	1761	441	9.4	0.63	0.0	0.00	5.6	0.37
WIB-B-06-2-1	7/25/2006	19			1324			7.8	0.42	11.0	0.60	0.2	0.01
WIB-B-06-2-2		23			1400			10.5	0.48	11.1	0.51	1.9	0.09
WIB-B-06-2-3		25	22	2	1100	1274	90	24.2	0.98	0.0	0.00	1.7	0.07
WIB-B-07-1-1	4/17/2007	22			452			0.6	0.03	21.5	1.00	0.0	0.00
WIB-B-07-1-2		25			275			4.4	0.18	20.2	0.82	0.5	0.02
WIB-B-07-1-3		28	25	2	1441	723	363	1.1	0.04	27.1	0.99	0.4	0.01
WIB-B-07-2-1	7/28/2007	9			2086			1.6	0.19	6.9	0.78	0.3	0.03
WIB-B-07-2-2		9			2201			0.0	0.00	8.6	0.99	0.1	0.01
WIB-B-07-2-3		8	9	0	1651	1979	168	0.0	0.00	7.1	0.95	0.4	0.05
ZAB-B-06-2-1	7/27/2006	28			748			0.0	0.00	23.2	0.94	1.4	0.06
ZAB-B-06-2-2		25			1025			0.0	0.00	23.7	0.98	0.5	0.02
ZAB-B-06-2-3		22	25	2	715	829	98	0.0	0.00	21.1	0.98	0.4	0.02
ZAB-B-07-1-1	4/17/2007	24			351			0.0	0.00	23.2	1.00	0.0	0.00
ZAB-B-07-1-2		26			484			0.1	0.01	25.5	1.00	0.0	0.00
ZAB-B-07-1-3		37	29	4	125	320	105	0.0	0.00	36.6	1.00	0.0	0.00
ZAB-B-07-2-1	7/12/2007	12			1109			11.9	1.00	0.0	0.00	0.0	0.00
ZAB-B-07-2-1D		11			868			0.0	0.00	11.0	0.97	0.3	0.03
ZAB-B-07-2-3		198			1402			65.5	0.33	142.3	0.72	1.3	0.01
ZAB-B-07-2-2		18	76	61	1342	1244	129	0.0	0.00	16.8	0.96	0.7	0.04

APPENDIX D PAH and SHC plots from the 2006-2008 Program (through October 2007)

Plots are in alphabetic order:

Aialik Bay (AIB)

Alyeska Marine Terminal (AMT, tissue & sediment)

Constantine Harbor (COH, tissue & sediment)

Disk Island (DII)

Gold Creek (GOC, tissue & sediment)

Knowles Head (KNH)

Sheep Bay (SHB)

Shuyak Harbor (SHH)

Sleepy Bay (SLB)

Windy Bay (WIB)

Zaikof Bay (ZAB)

Each plot represents a triplicate sample for the site and date. Samples with "D" prefix are lab duplicates of like-numbered samples reanalyzed for QA purposes. Sample ids are coded by site-matrix-year-cruise-rep.

Tissue
27-Jul-06

AIB-B-06-2-1

85, 18, 0% diss, part, pyro

37 TPAH

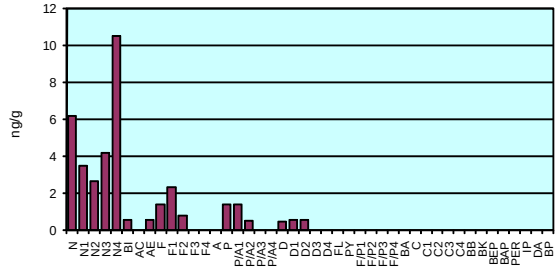

1701907
27-Jul-06

AIB-B-06-2-1

2310 **TSHC**

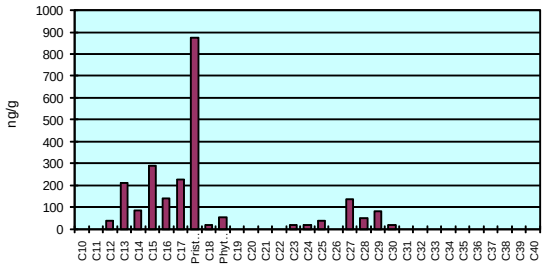

Tissue
27-Jul-06

AIB-B-06-2-2

100, 0, 0% diss, part, pyro

16 TPAH

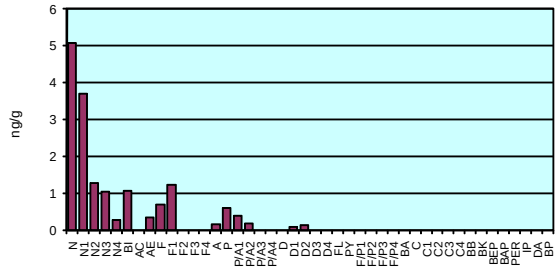

1701908
27-Jul-06

AIB-B-06-2-2

2270 **TSHC**

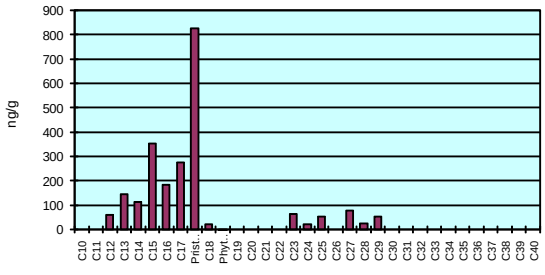

Tissue
27-Jul-06

AIB-B-06-2-3

100, 0, 0% diss, part, pyro

9 TPAH

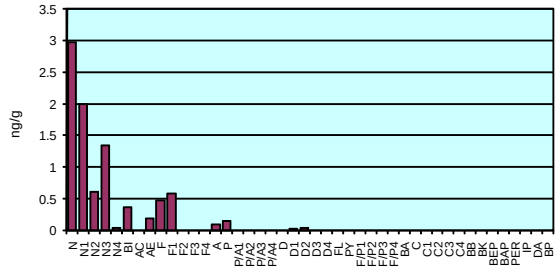

1701909
27-Jul-06

AIB-B-06-2-3

2763 **TSHC**

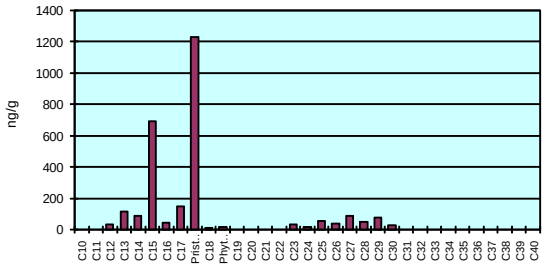

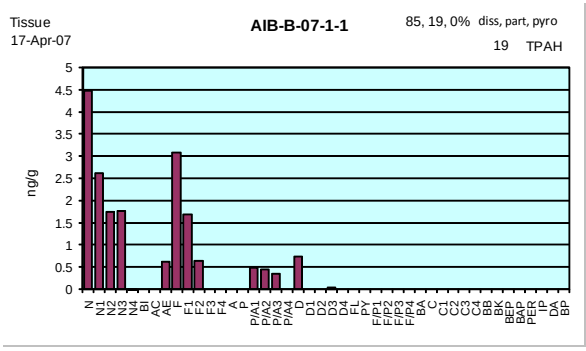
Tissue
17-Apr-07
AIB-B-07-1-1
85, 19, 0% diss, part, pyro
19 TPAH
ng/g

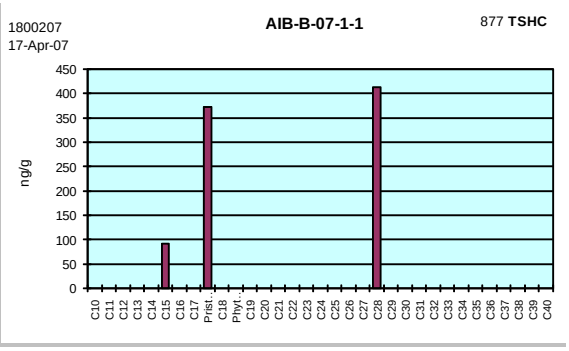
1800207
17-Apr-07
AIB-B-07-1-1
877 TSHC
ng/g

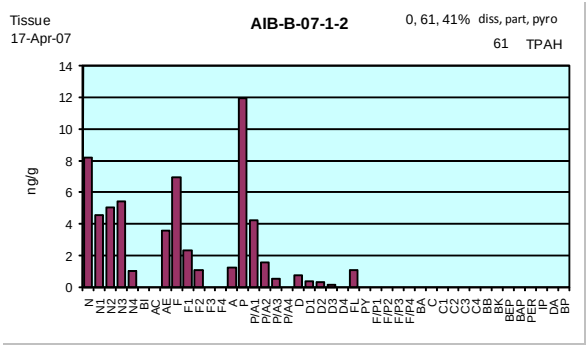
Tissue
17-Apr-07
AIB-B-07-1-2
0, 61, 41% diss, part, pyro
61 TPAH
ng/g

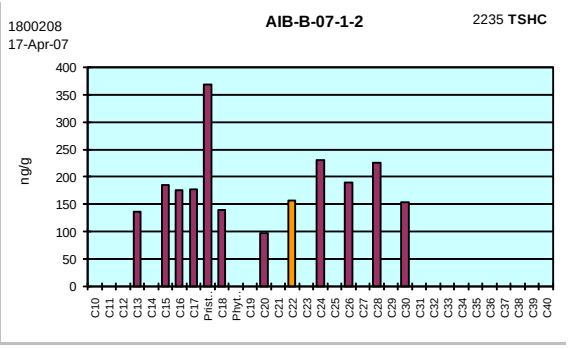
1800208
17-Apr-07
AIB-B-07-1-2
2235 TSHC
ng/g

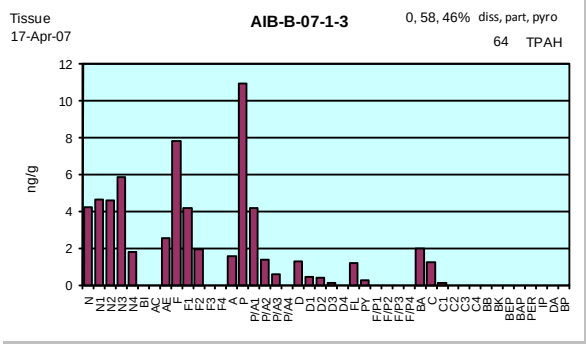
Tissue
17-Apr-07
AIB-B-07-1-3
0, 58, 46% diss, part, pyro
64 TPAH
ng/g

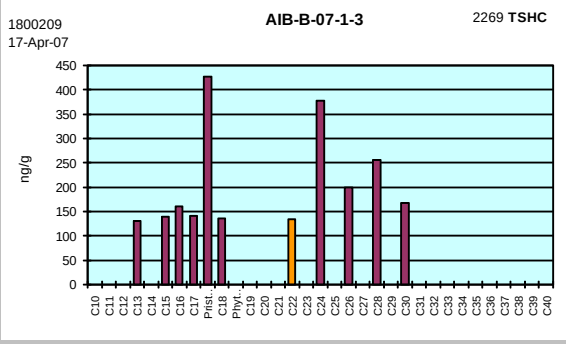
1800209
17-Apr-07
AIB-B-07-1-3
2269 TSHC
ng/g

Tissue
28-Jul-07

AIB-B-07-2-1

81, 19, 0% diss, part, pyro

14 TPAH

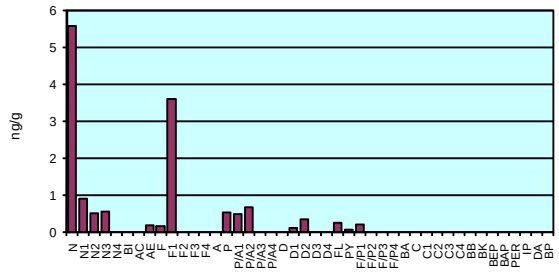

1801207
28-Jul-07

AIB-B-07-2-1

3092 **TSHC**

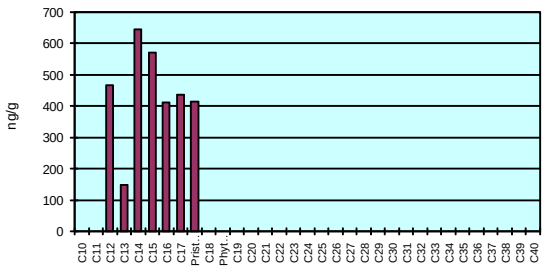

Tissue
28-Jul-07

AIB-B-07-2-2

96, 0, 4% diss, part, pyro

12 TPAH

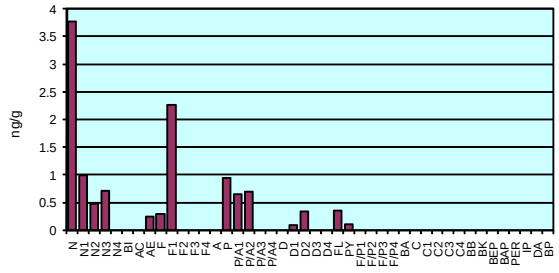

1801208
28-Jul-07

AIB-B-07-2-2

1975 **TSHC**

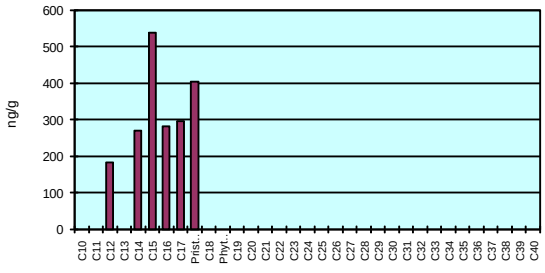

Tissue
28-Jul-07

AIB-B-07-2-3

0, 98, 2% diss, part, pyro

10 TPAH

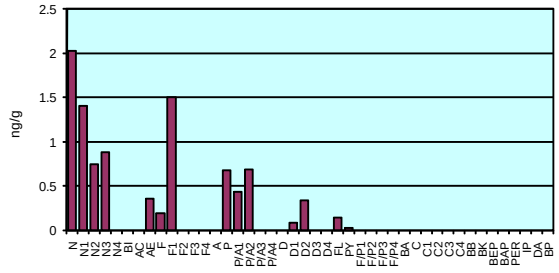

1801209
28-Jul-07

AIB-B-07-2-3

1811 **TSHC**

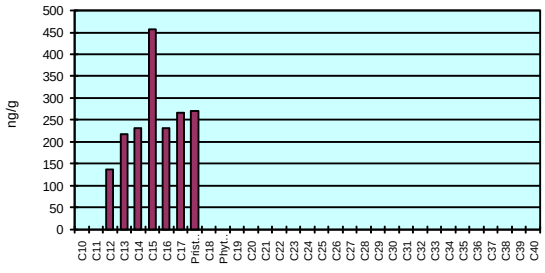

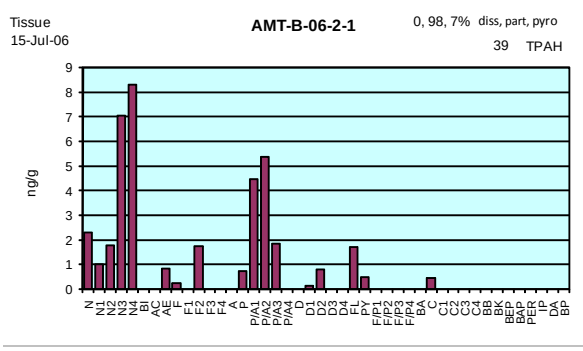
Tissue
15-Jul-06
AMT-B-06-2-1
0, 98, 7% diss, part, pyro
39 TPAH
ng/g

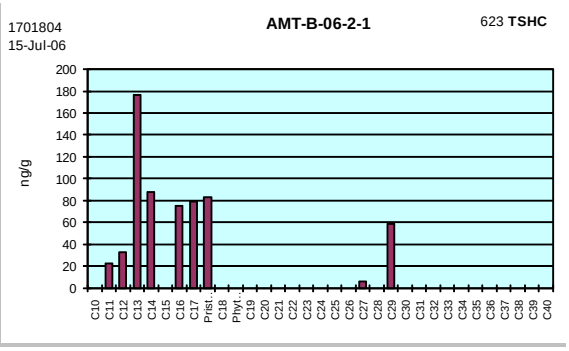
1701804
15-Jul-06
AMT-B-06-2-1
623 TSHC
ng/g

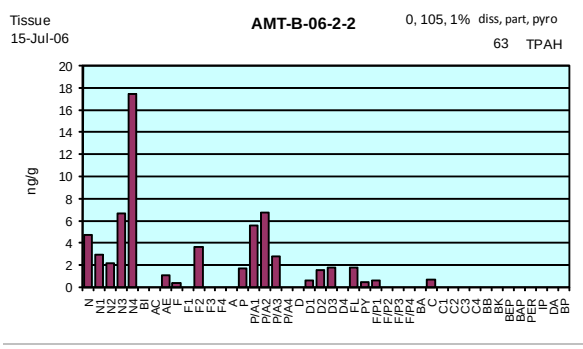
Tissue
15-Jul-06
AMT-B-06-2-2
0, 105, 1% diss, part, pyro
63 TPAH
ng/g

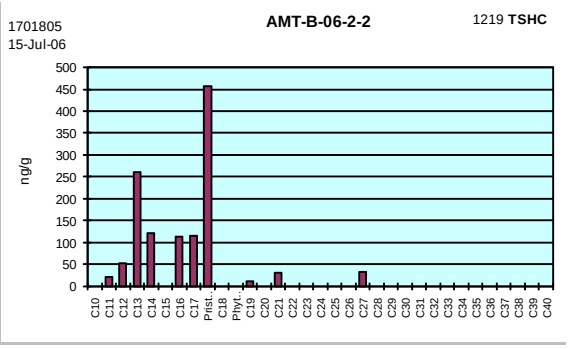
1701805
15-Jul-06
AMT-B-06-2-2
1219 TSHC
ng/g

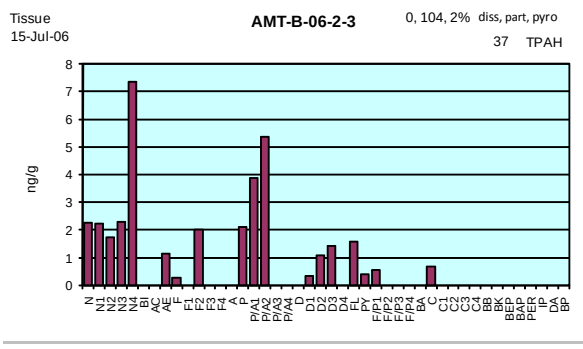
Tissue
15-Jul-06
AMT-B-06-2-3
0, 104, 2% diss, part, pyro
37 TPAH
ng/g

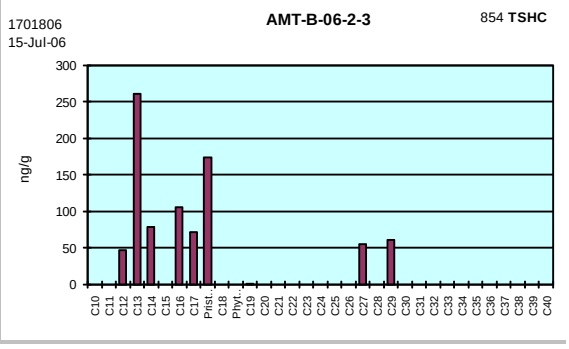
1701806
15-Jul-06
AMT-B-06-2-3
854 TSHC
ng/g

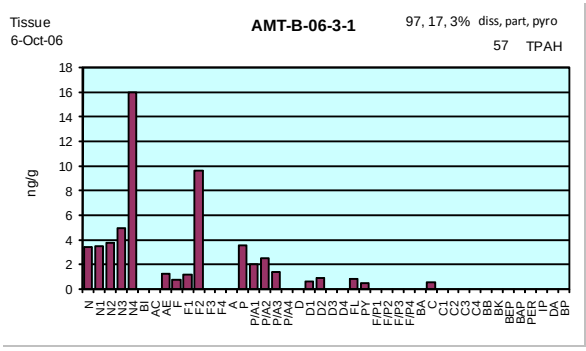
Tissue
6-Oct-06
AMT-B-06-3-1
97, 17, 3% diss, part, pyro
57 TPAH
ng/g

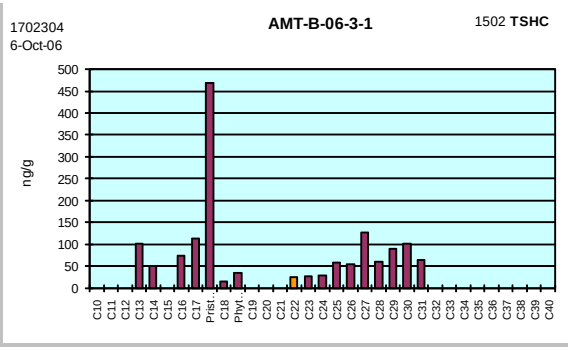
1702304
6-Oct-06
AMT-B-06-3-1
1502 TSHC
ng/g
Prist.
Phyt.

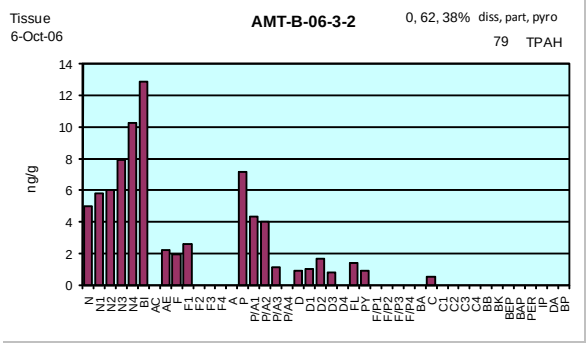
Tissue
6-Oct-06
AMT-B-06-3-2
0, 62, 38% diss, part, pyro
79 TPAH
ng/g

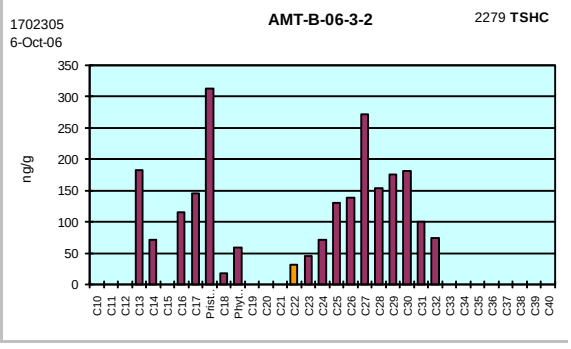
1702305
6-Oct-06
AMT-B-06-3-2
2279 TSHC
ng/g
Prist.
Phyt.

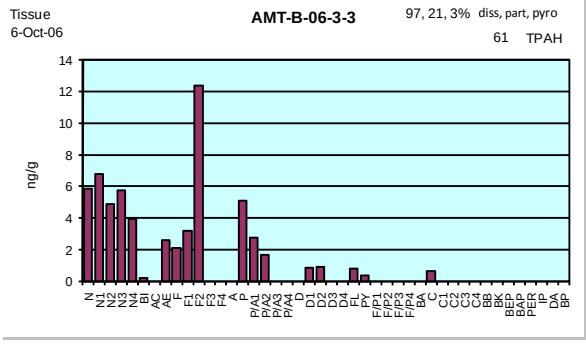
Tissue
6-Oct-06
AMT-B-06-3-3
97, 21, 3% diss, part, pyro
61 TPAH
ng/g

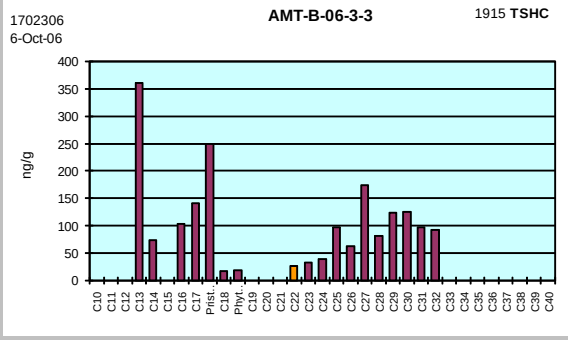
1702306
6-Oct-06
AMT-B-06-3-3
1915 TSHC
ng/g
Prist.
Phyt.

Tissue
5-Apr-07

AMT-B-07-1-1

0, 46, 57% diss, part, pyro

47 TPAH

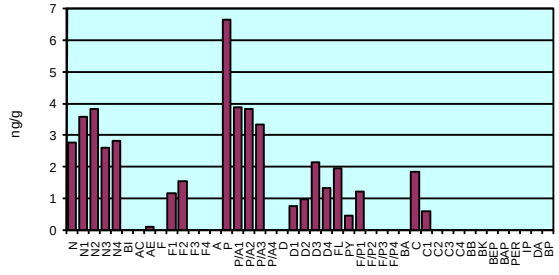

1800104
5-Apr-07

AMT-B-07-1-1

632 **TSHC**

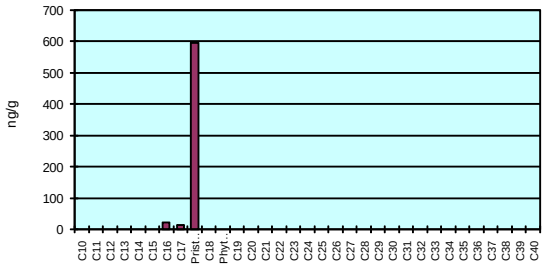

Tissue
5-Apr-07

AMT-B-07-1-2

85, 18, 0% diss, part, pyro

60 TPAH

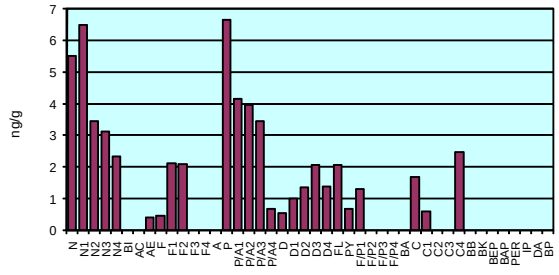

1800105
5-Apr-07

AMT-B-07-1-2

385 **TSHC**

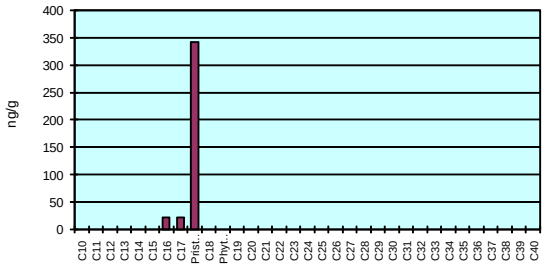

Tissue
5-Apr-07

AMT-B-07-1-3

87, 6, 6% diss, part, pyro

53 TPAH

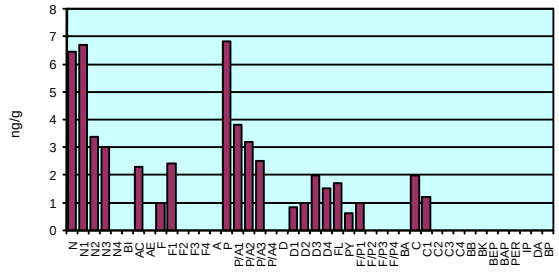

1800106
5-Apr-07

AMT-B-07-1-3

317 **TSHC**

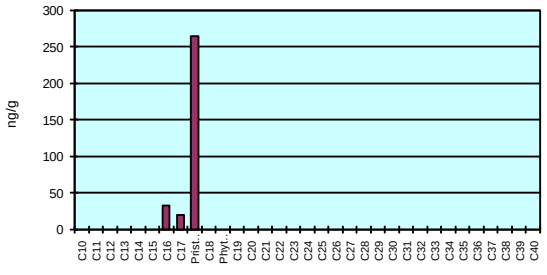

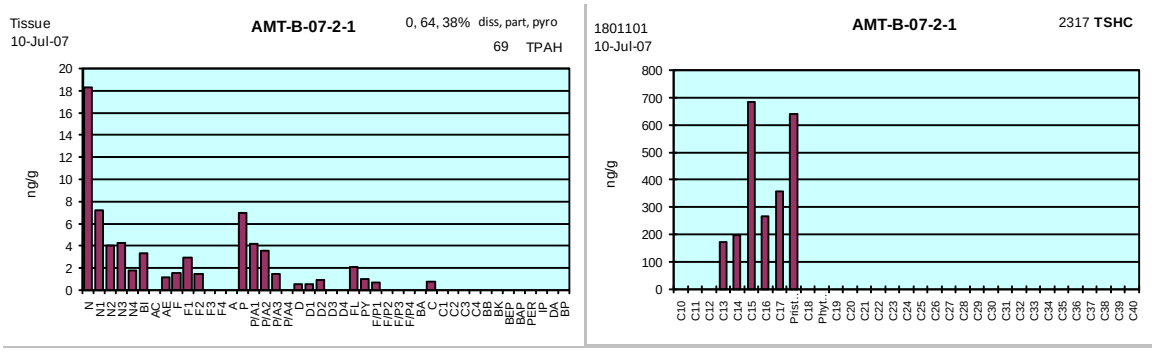
Tissue
10-Jul-07
AMT-B-07-2-1
0, 64, 38% diss, part, pyro
69 TPAH
ng/g
1801101
10-Jul-07
AMT-B-07-2-1
2317 TSHC
ng/g

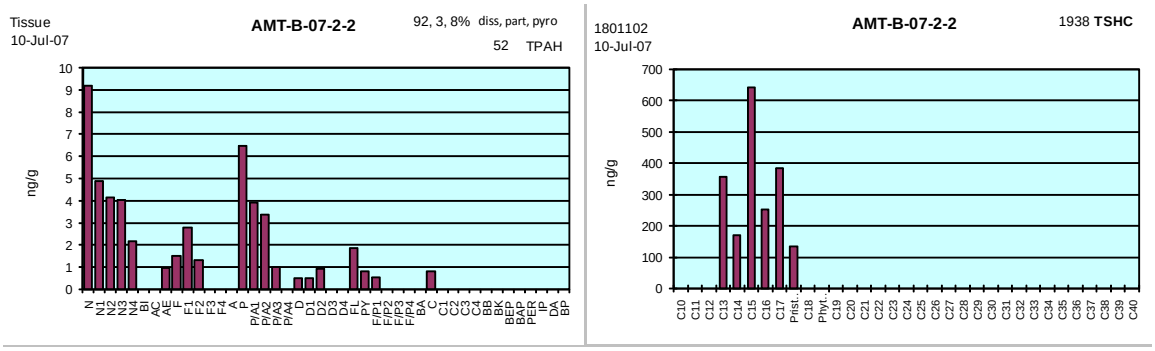
Tissue
10-Jul-07
AMT-B-07-2-2
92, 3, 8% diss, part, pyro
52 TPAH
ng/g
1801102
10-Jul-07
AMT-B-07-2-2
1938 TSHC
ng/g

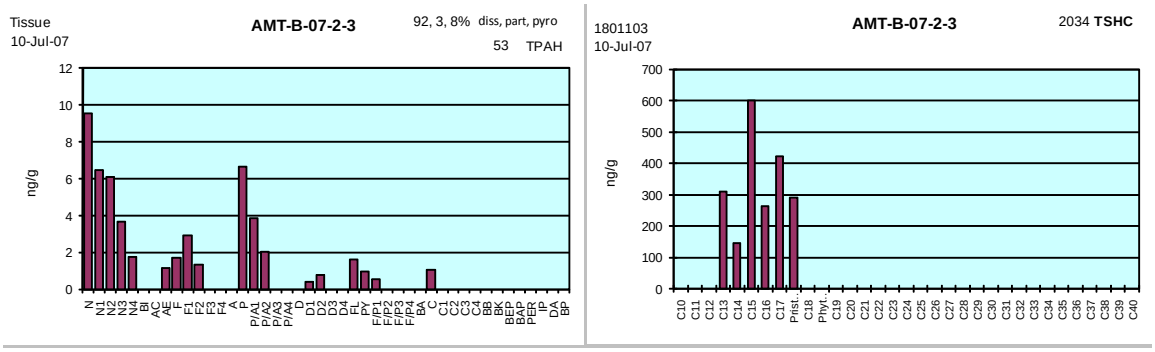
Tissue
10-Jul-07
AMT-B-07-2-3
92, 3, 8% diss, part, pyro
53 TPAH
ng/g
1801103
10-Jul-07
AMT-B-07-2-3
2034 TSHC
ng/g

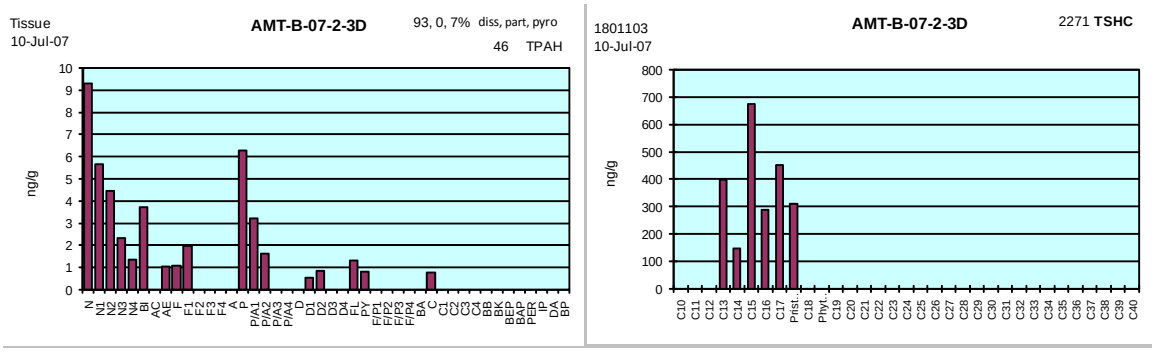
Tissue
10-Jul-07
AMT-B-07-2-3D
93, 0, 7% diss, part, pyro
46 TPAH
ng/g
1801103
10-Jul-07
AMT-B-07-2-3D
2271 TSHC
ng/g

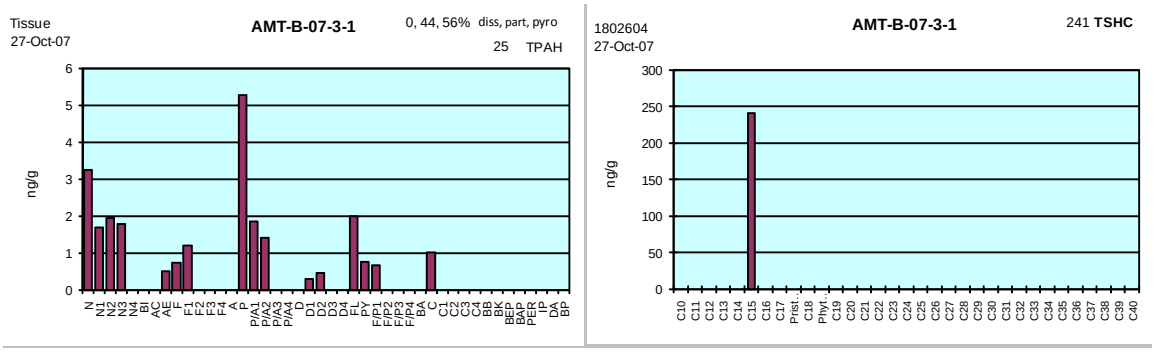
Tissue
27-Oct-07
AMT-B-07-3-1
0, 44, 56% diss, part, pyro
25 TPAH
ng/g
1802604
27-Oct-07
AMT-B-07-3-1
241 TSHC
ng/g

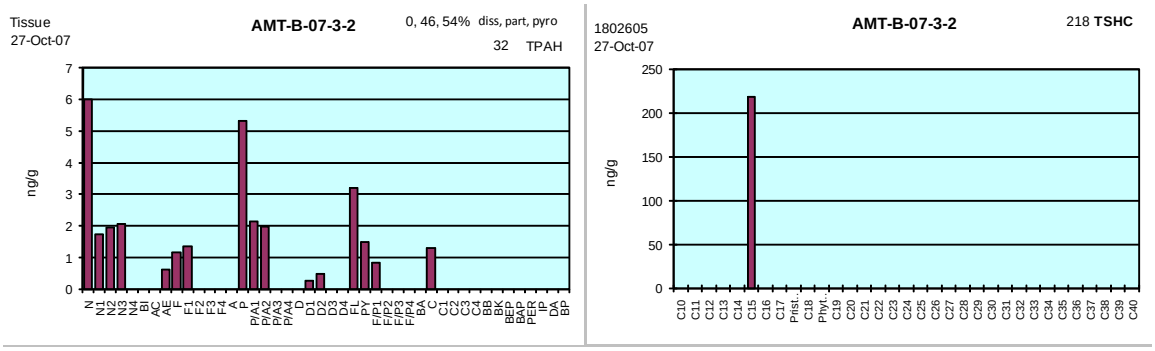
Tissue
27-Oct-07
AMT-B-07-3-2
0, 46, 54% diss, part, pyro
32 TPAH
ng/g
1802605
27-Oct-07
AMT-B-07-3-2
218 TSHC
ng/g

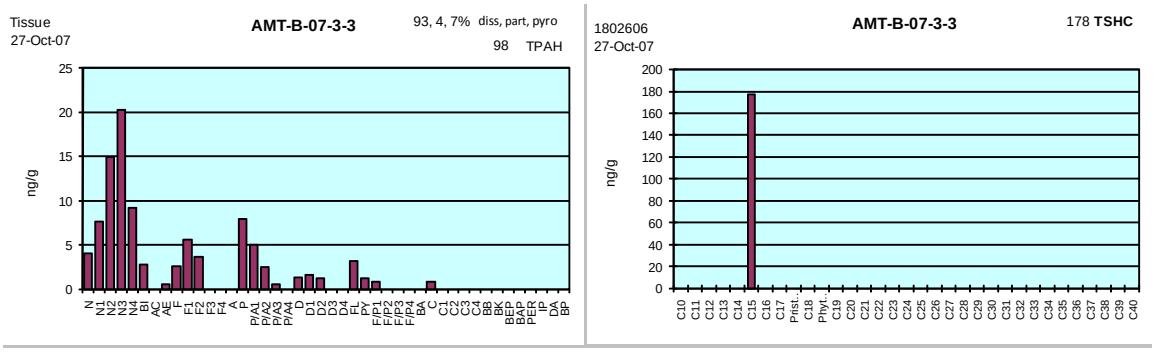
Tissue
27-Oct-07
AMT-B-07-3-3
93, 4, 7% diss, part, pyro
98 TPAH
ng/g
1802606
27-Oct-07
AMT-B-07-3-3
178 TSHC
ng/g

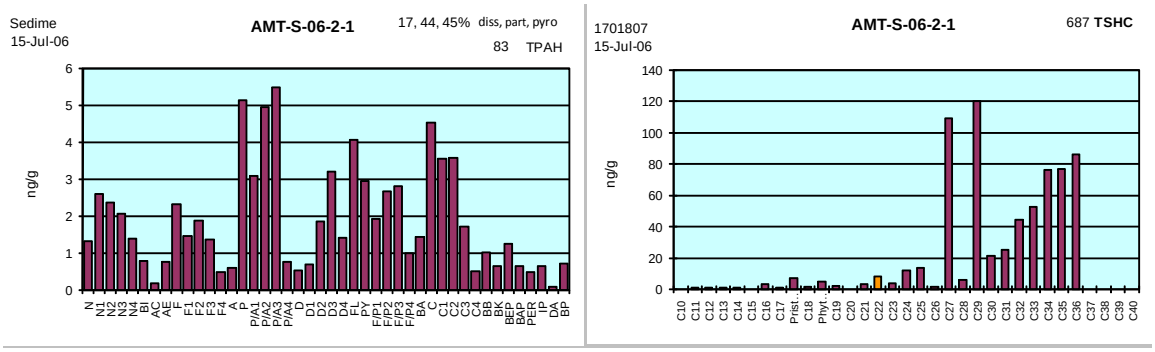
Sedime
15-Jul-06
AMT-S-06-2-1
17, 44, 45% diss, part, pyro
83 TPAH
ng/g
1701807
15-Jul-06
AMT-S-06-2-1
687 TSHC
ng/g

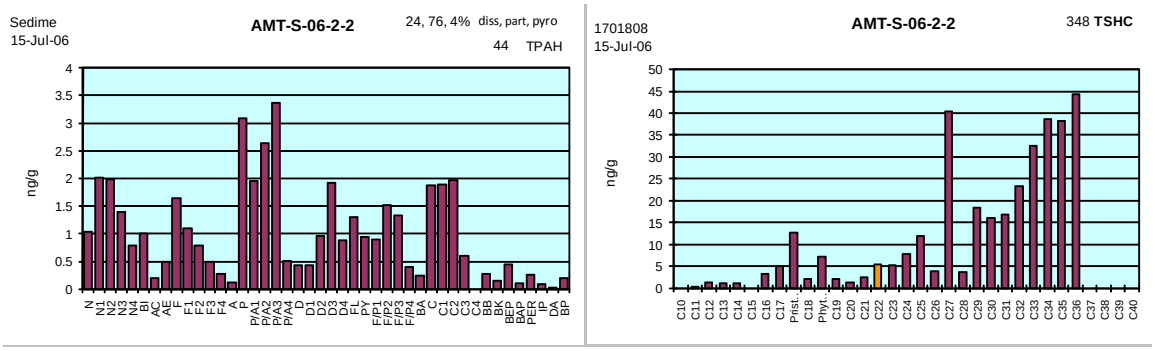
Sedime
15-Jul-06
AMT-S-06-2-2
24, 76, 4% diss, part, pyro
44 TPAH
ng/g
1701808
15-Jul-06
AMT-S-06-2-2
348 TSHC
ng/g

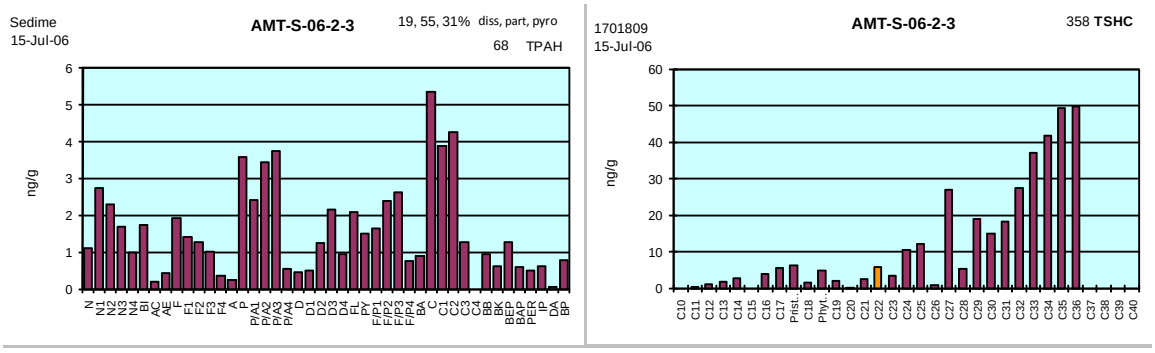
Sedime
15-Jul-06
AMT-S-06-2-3
19, 55, 31% diss, part, pyro
68 TPAH
ng/g
1701809
15-Jul-06
AMT-S-06-2-3
358 TSHC
ng/g

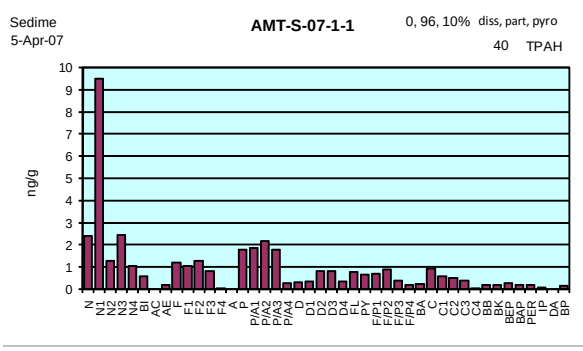
Sedime
5-Apr-07
AMT-S-07-1-1
0, 96, 10% diss, part, pyro
40 TPAH
ng/g

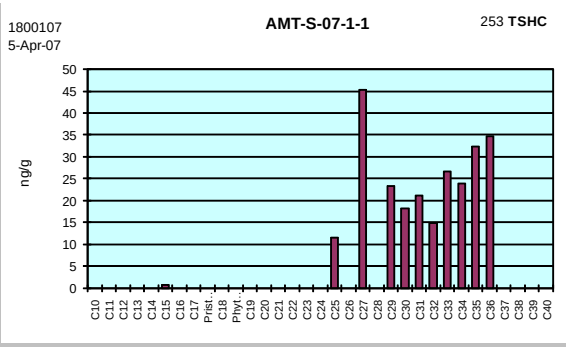
1800107
5-Apr-07
AMT-S-07-1-1
253 TSHC
ng/g

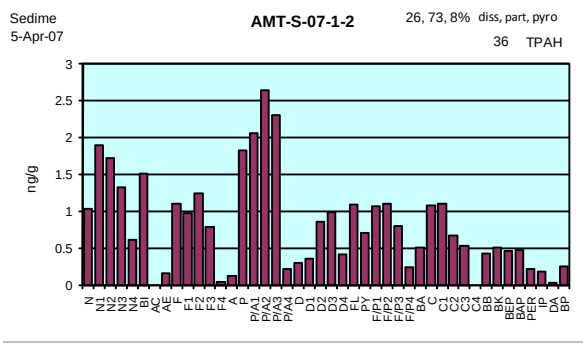
Sedime
5-Apr-07
AMT-S-07-1-2
26, 73, 8% diss, part, pyro
36 TPAH
ng/g

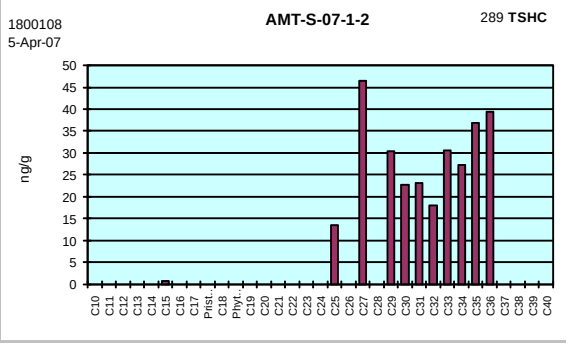
1800108
5-Apr-07
AMT-S-07-1-2
289 TSHC
ng/g

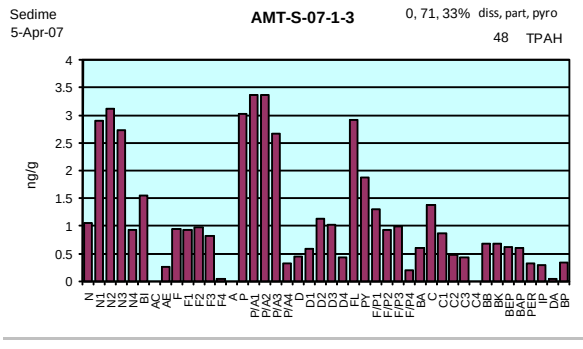
Sedime
5-Apr-07
AMT-S-07-1-3
0, 71, 33% diss, part, pyro
48 TPAH
ng/g

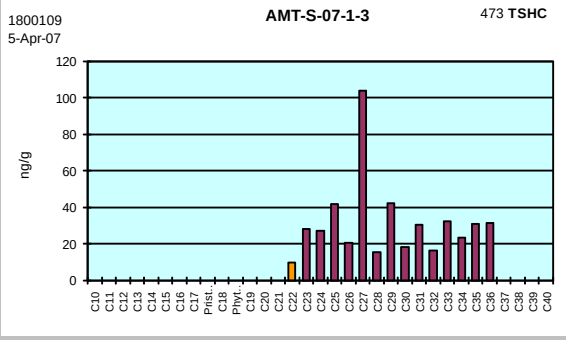
1800109
5-Apr-07
AMT-S-07-1-3
473 TSHC
ng/g

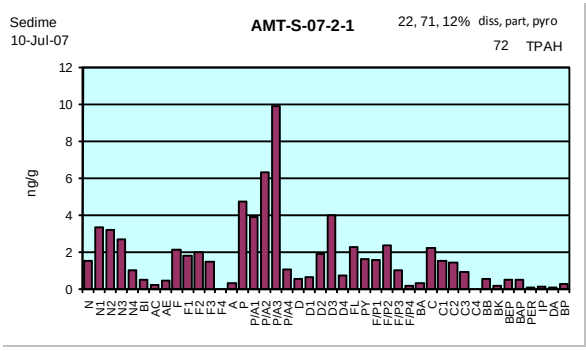
Sedime
10-Jul-07
AMT-S-07-2-1
22, 71, 12% diss, part, pyro
72 TPAH
ng/g
N N1 N2 N3 N4 Bl AC AE F F1 F2 F3 F4 A P P/A1 P/A2 P/A3 P/A4 D D1 D2 D3 D4 FL PY F/P1 F/P2 F/P3 F/P4 BA C C1 C2 C3 C4 BB BK BEP BAP PER IP DA BP

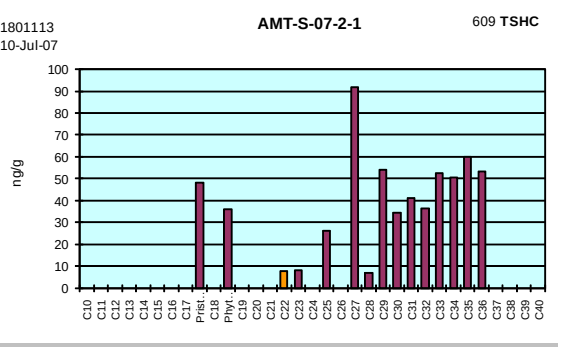
1801113
10-Jul-07
AMT-S-07-2-1
609 TSHC
ng/g
C10 C11 C12 C13 C14 C15 C16 C17 Pris. C18 Phyt. C19 C20 C21 C22 C23 C24 C25 C26 C27 C28 C29 C30 C31 C32 C33 C34 C35 C36 C37 C38 C39 C40

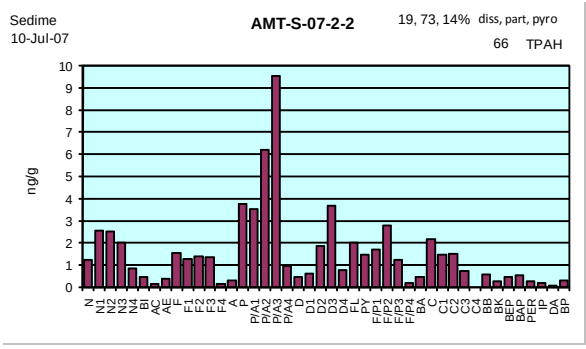
Sedime
10-Jul-07
AMT-S-07-2-2
19, 73, 14% diss, part, pyro
66 TPAH
ng/g
N N1 N2 N3 N4 Bl AC AE F F1 F2 F3 F4 A P P/A1 P/A2 P/A3 P/A4 D D1 D2 D3 D4 FL PY F/P1 F/P2 F/P3 F/P4 BA C C1 C2 C3 C4 BB BK BEP BAP PER IP DA BP

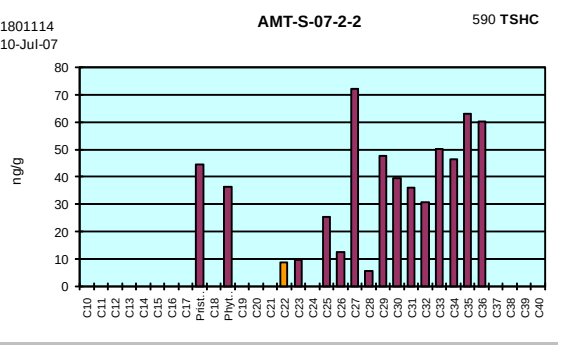
1801114
10-Jul-07
AMT-S-07-2-2
590 TSHC
ng/g
C10 C11 C12 C13 C14 C15 C16 C17 Pris. C18 Phyt. C19 C20 C21 C22 C23 C24 C25 C26 C27 C28 C29 C30 C31 C32 C33 C34 C35 C36 C37 C38 C39 C40

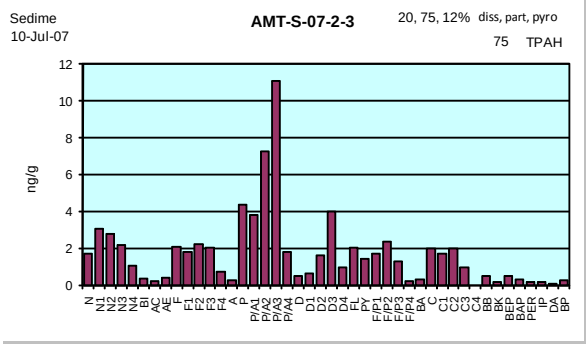
Sedime
10-Jul-07
AMT-S-07-2-3
20, 75, 12% diss, part, pyro
75 TPAH
ng/g
N N1 N2 N3 N4 Bl AC AE F F1 F2 F3 F4 A P P/A1 P/A2 P/A3 P/A4 D D1 D2 D3 D4 FL PY F/P1 F/P2 F/P3 F/P4 BA C C1 C2 C3 C4 BB BK BEP BAP PER IP DA BP

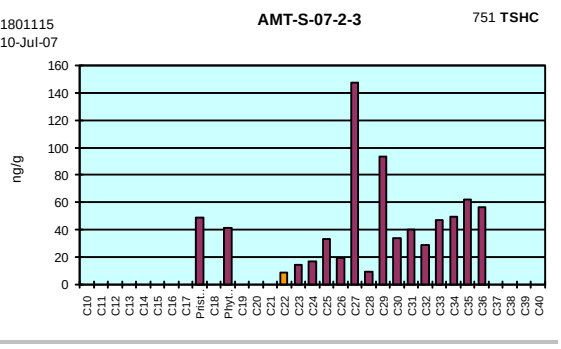
1801115
10-Jul-07
AMT-S-07-2-3
751 TSHC
ng/g
C10 C11 C12 C13 C14 C15 C16 C17 Pris. C18 Phyt. C19 C20 C21 C22 C23 C24 C25 C26 C27 C28 C29 C30 C31 C32 C33 C34 C35 C36 C37 C38 C39 C40

Tissue
27-Jul-06

COH-B-06-2-1

94, 2, 4% diss, part, pyro

33 TPAH

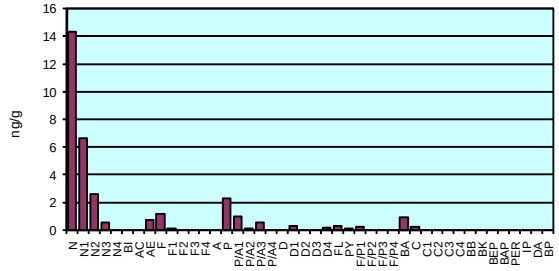

1701919
27-Jul-06

COH-B-06-2-1

754 **TSHC**

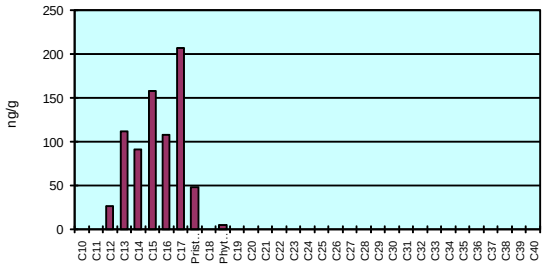

Tissue
27-Jul-06

COH-B-06-2-2

92, 3, 1% diss, part, pyro

45 TPAH

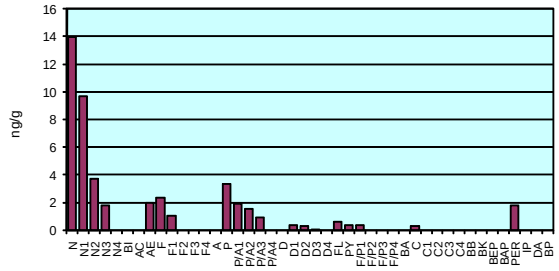

1701920
27-Jul-06

COH-B-06-2-2

1336 **TSHC**

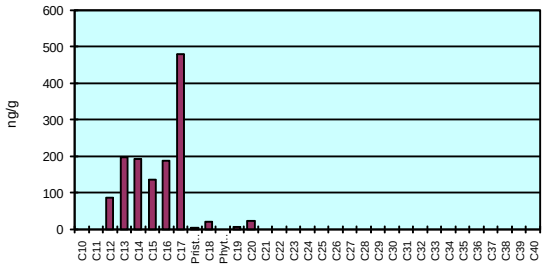

Tissue
27-Jul-06

COH-B-06-2-3

94, 2, 1% diss, part, pyro

46 TPAH

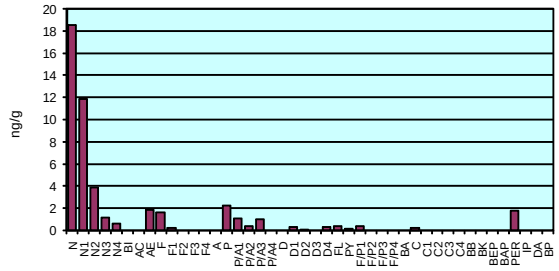

1701921
27-Jul-06

COH-B-06-2-3

1020 **TSHC**

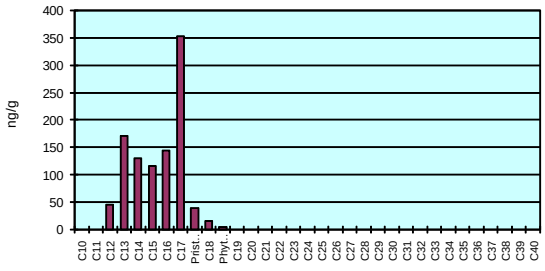

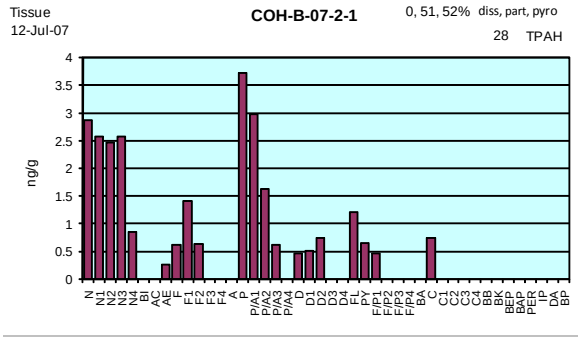
Tissue
12-Jul-07
COH-B-07-2-1
0, 51, 52% diss, part, pyro
28 TPAH
ng/g

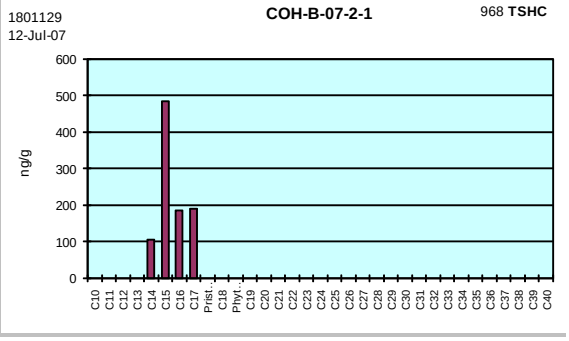
1801129
12-Jul-07
COH-B-07-2-1
968 TSHC
ng/g

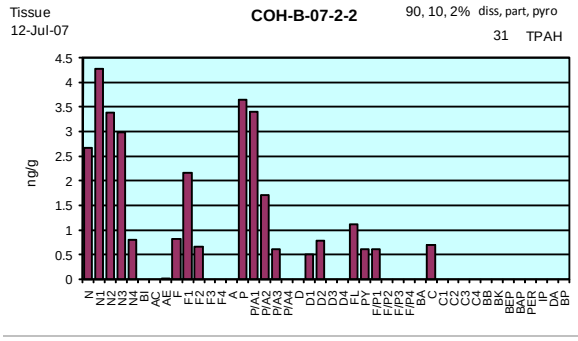
Tissue
12-Jul-07
COH-B-07-2-2
90, 10, 2% diss, part, pyro
31 TPAH
ng/g

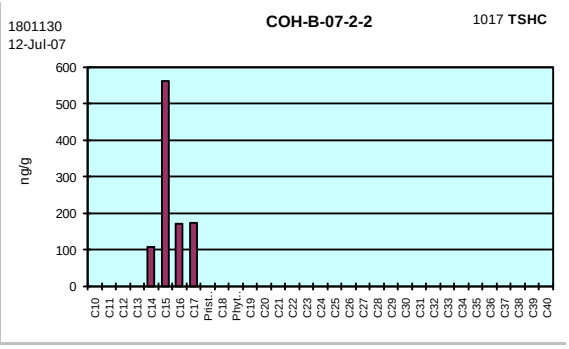
1801130
12-Jul-07
COH-B-07-2-2
1017 TSHC
ng/g

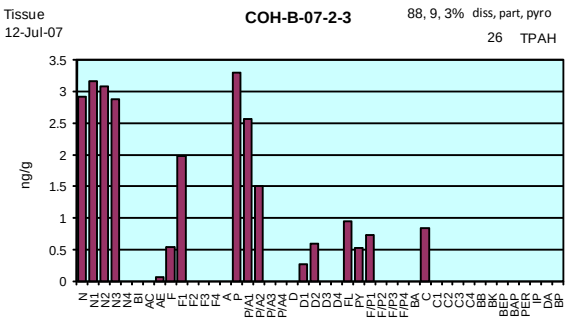
Tissue
12-Jul-07
COH-B-07-2-3
88, 9, 3% diss, part, pyro
26 TPAH
ng/g

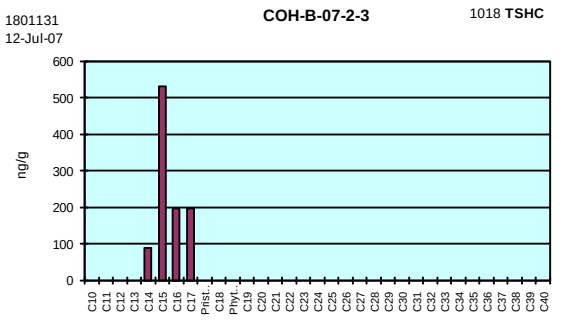
1801131
12-Jul-07
COH-B-07-2-3
1018 TSHC
ng/g

Sedime
27-Jul-06

COH-S-06-2-1

0, 95, 7% diss, part, pyro

45 TPAH

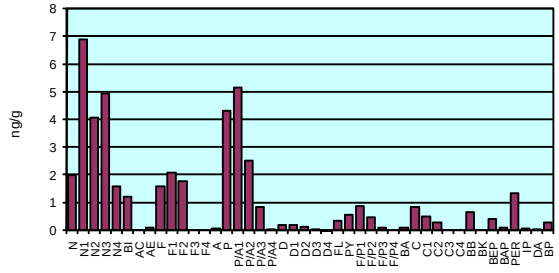

1701922
27-Jul-06

COH-S-06-2-1

168 **TSHC**

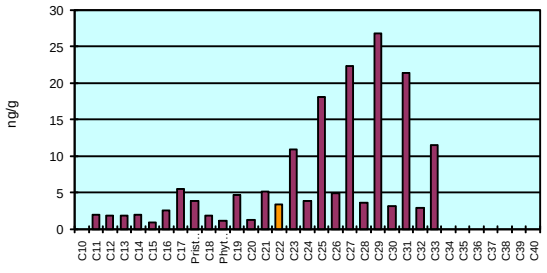

Sedime
27-Jul-06

COH-S-06-2-2

0, 95, 6% diss, part, pyro

54 TPAH

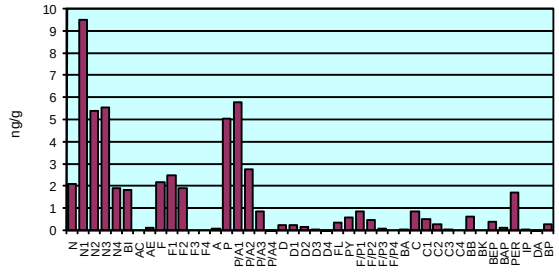

1701923
27-Jul-06

COH-S-06-2-2

215 **TSHC**

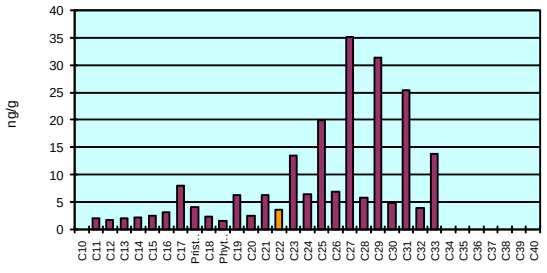

Sedime
27-Jul-06

COH-S-06-2-3

0, 96, 6% diss, part, pyro

61 TPAH

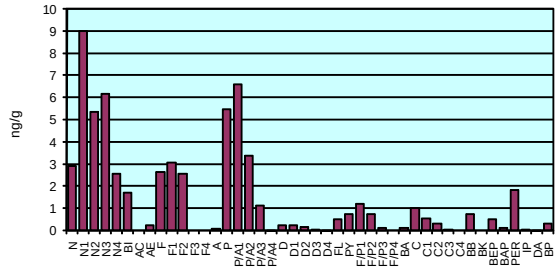

1701924
27-Jul-06

COH-S-06-2-3

222 **TSHC**

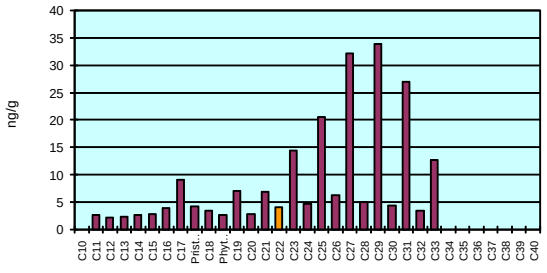

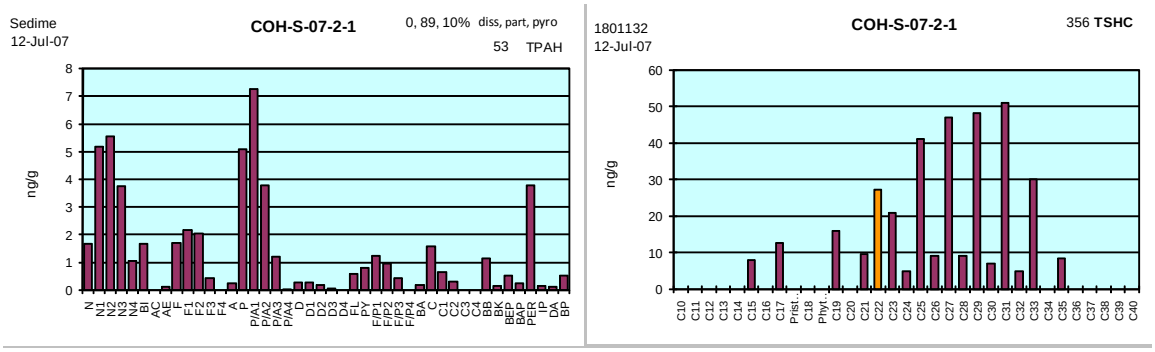
Sedime
12-Jul-07
COH-S-07-2-1
0, 89, 10% diss, part, pyro
53 TPAH
ng/g
1801132
12-Jul-07
COH-S-07-2-1
356 TSHC
ng/g

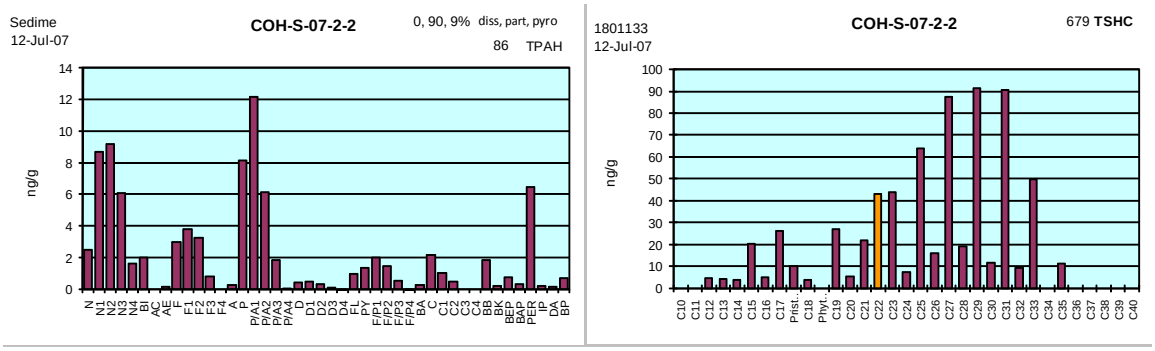
Sedime
12-Jul-07
COH-S-07-2-2
0, 90, 9% diss, part, pyro
86 TPAH
ng/g
1801133
12-Jul-07
COH-S-07-2-2
679 TSHC
ng/g

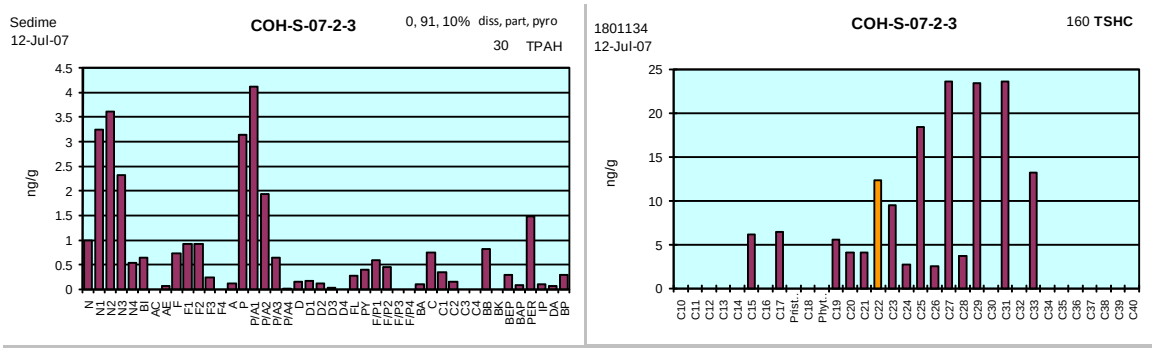
Sedime
12-Jul-07
COH-S-07-2-3
0, 91, 10% diss, part, pyro
30 TPAH
ng/g
1801134
12-Jul-07
COH-S-07-2-3
160 TSHC
ng/g

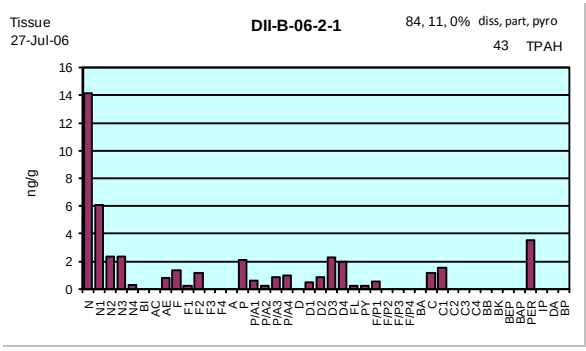
Tissue
27-Jul-06
DII-B-06-2-1
84, 11, 0% diss, part, pyro
43 TPAH
ng/g

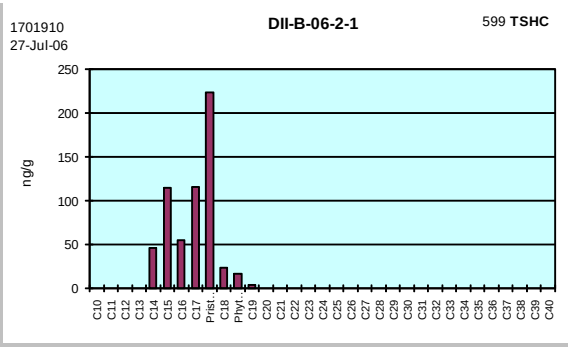
1701910
27-Jul-06
DII-B-06-2-1
599 TSHC
ng/g
Prist.
Phyt.

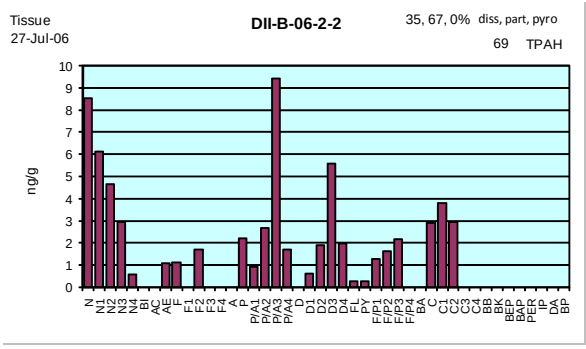
Tissue
27-Jul-06
DII-B-06-2-2
35, 67, 0% diss, part, pyro
69 TPAH
ng/g

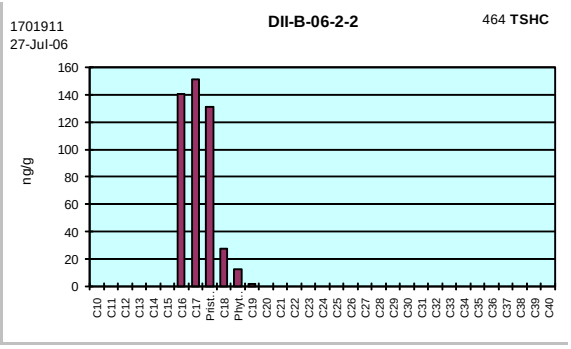
1701911
27-Jul-06
DII-B-06-2-2
464 TSHC
ng/g
Prist.
Phyt.

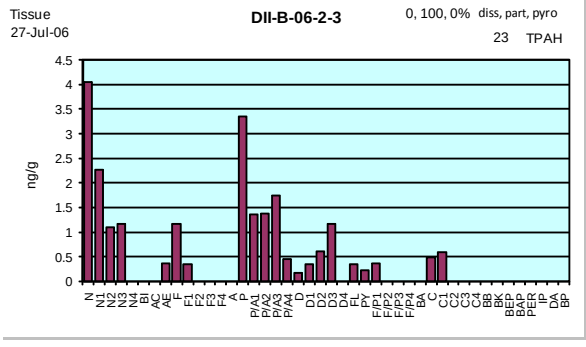
Tissue
27-Jul-06
DII-B-06-2-3
0, 100, 0% diss, part, pyro
23 TPAH
ng/g

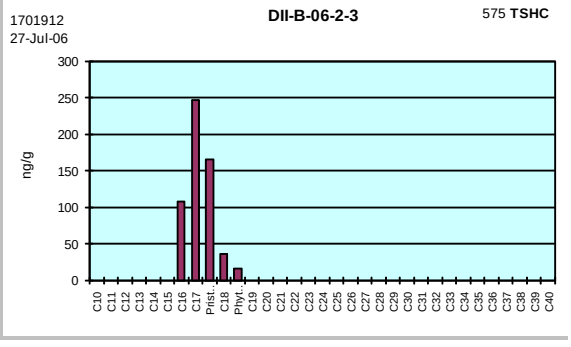
1701912
27-Jul-06
DII-B-06-2-3
575 TSHC
ng/g
Prist.
Phyt.

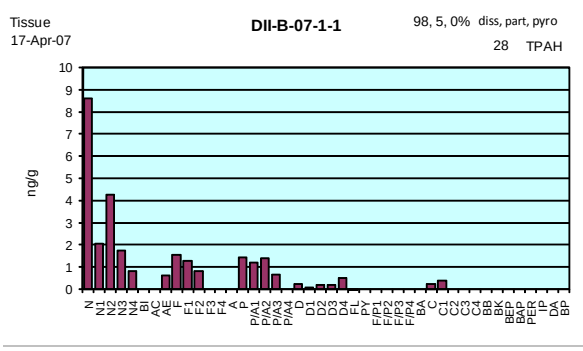
Tissue
17-Apr-07
DII-B-07-1-1
98, 5, 0% diss, part, pyro
28 TPAH
ng/g

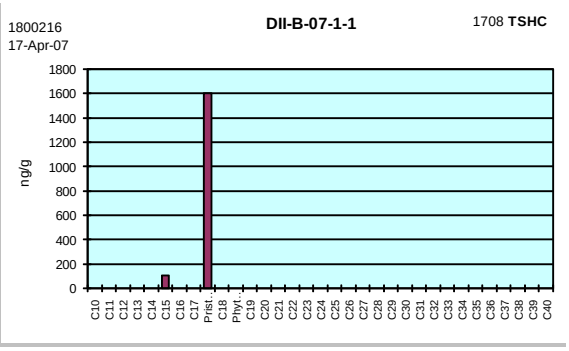
1800216
17-Apr-07
DII-B-07-1-1
1708 TSHC
ng/g

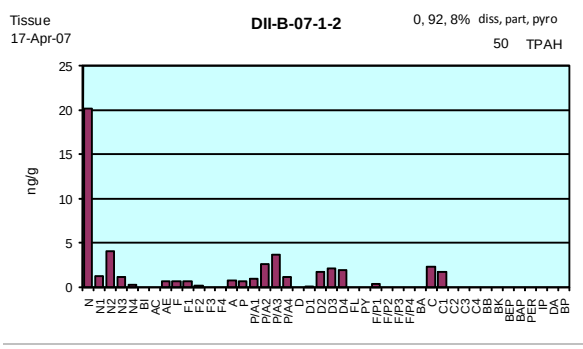
Tissue
17-Apr-07
DII-B-07-1-2
0, 92, 8% diss, part, pyro
50 TPAH
ng/g

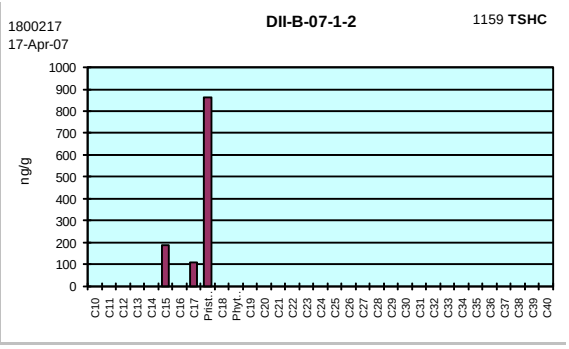
1800217
17-Apr-07
DII-B-07-1-2
1159 TSHC
ng/g

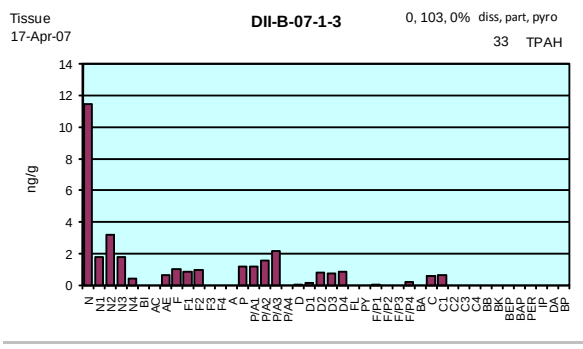
Tissue
17-Apr-07
DII-B-07-1-3
0, 103, 0% diss, part, pyro
33 TPAH
ng/g

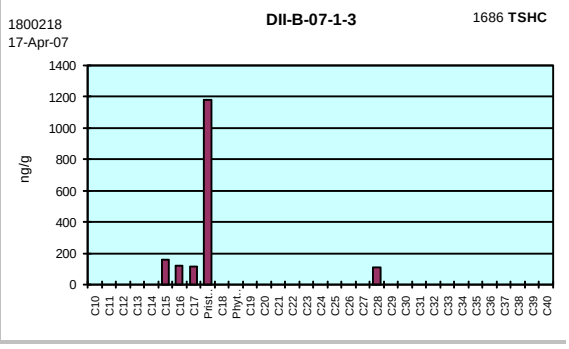
1800218
17-Apr-07
DII-B-07-1-3
1686 TSHC
ng/g

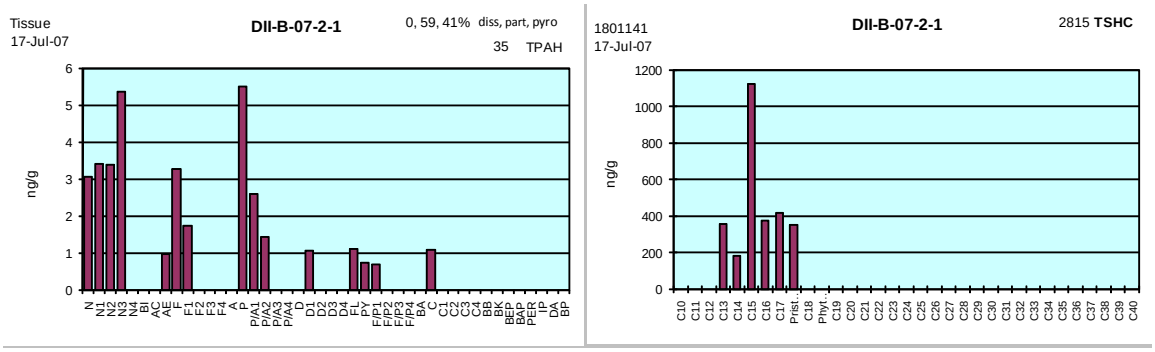
Tissue
17-Jul-07
DII-B-07-2-1
0, 59, 41% diss, part, pyro
35 TPAH
ng/g
1801141
17-Jul-07
DII-B-07-2-1
2815 TSHC
ng/g

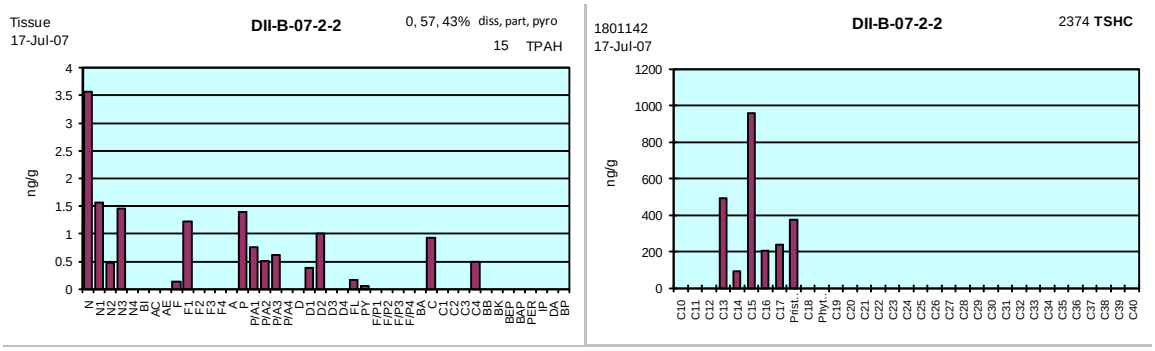
Tissue
17-Jul-07
DII-B-07-2-2
0, 57, 43% diss, part, pyro
15 TPAH
ng/g
1801142
17-Jul-07
DII-B-07-2-2
2374 TSHC
ng/g

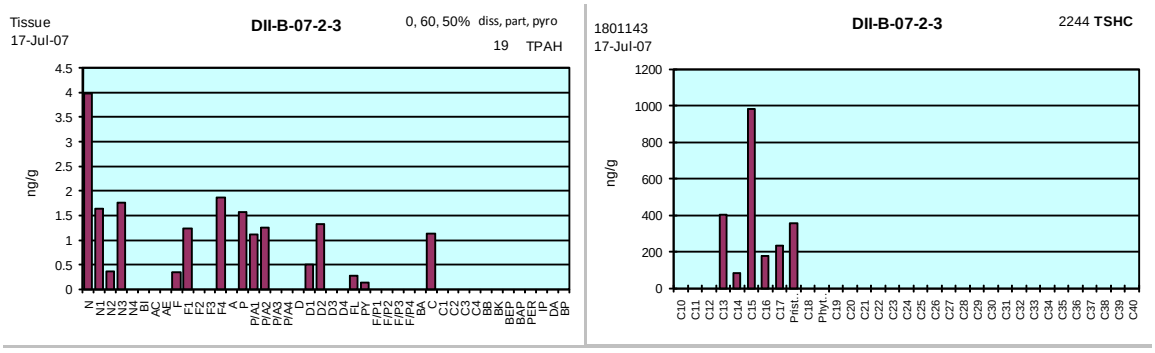
Tissue
17-Jul-07
DII-B-07-2-3
0, 60, 50% diss, part, pyro
19 TPAH
ng/g
1801143
17-Jul-07
DII-B-07-2-3
2244 TSHC
ng/g

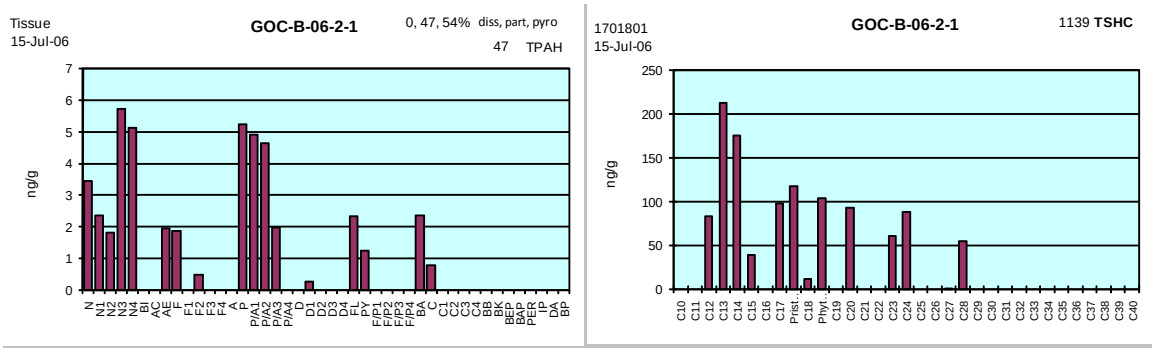
Tissue
15-Jul-06
GOC-B-06-2-1
0, 47, 54% diss, part, pyro
47 TPAH
ng/g
1701801
15-Jul-06
GOC-B-06-2-1
1139 TSHC
ng/g

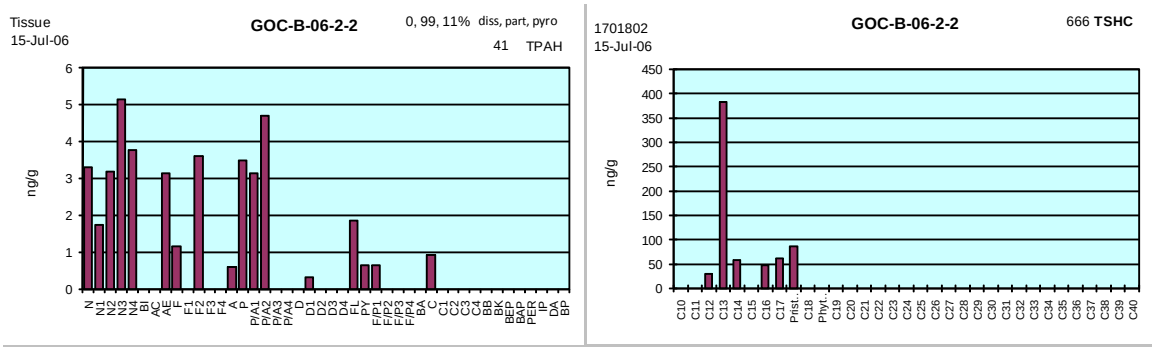
Tissue
15-Jul-06
GOC-B-06-2-2
0, 99, 11% diss, part, pyro
41 TPAH
ng/g
1701802
15-Jul-06
GOC-B-06-2-2
666 TSHC
ng/g

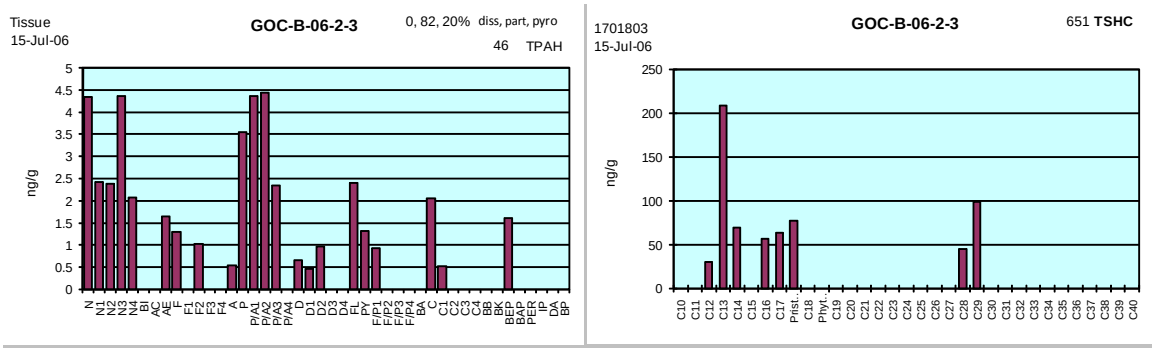
Tissue
15-Jul-06
GOC-B-06-2-3
0, 82, 20% diss, part, pyro
46 TPAH
ng/g
1701803
15-Jul-06
GOC-B-06-2-3
651 TSHC
ng/g

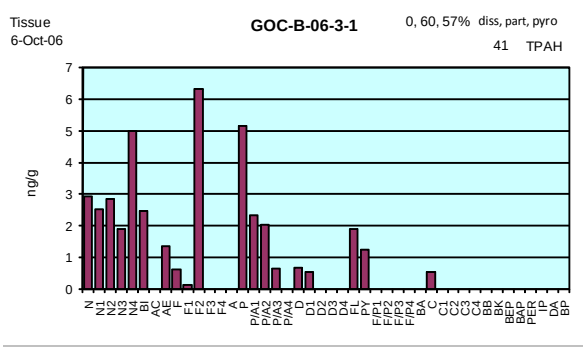
Tissue
6-Oct-06
GOC-B-06-3-1
0, 60, 57% diss, part, pyro
41 TPAH
ng/g

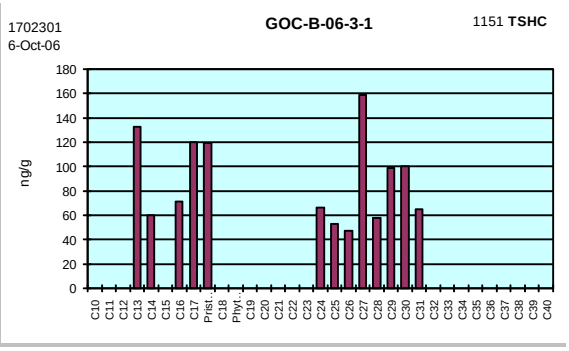
1702301
6-Oct-06
GOC-B-06-3-1
1151 TSHC
ng/g

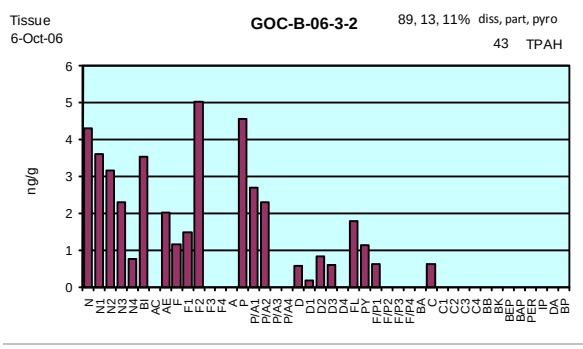
Tissue
6-Oct-06
GOC-B-06-3-2
89, 13, 11% diss, part, pyro
43 TPAH
ng/g

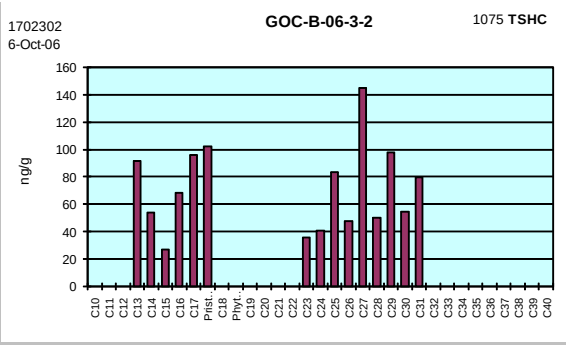
1702302
6-Oct-06
GOC-B-06-3-2
1075 TSHC
ng/g

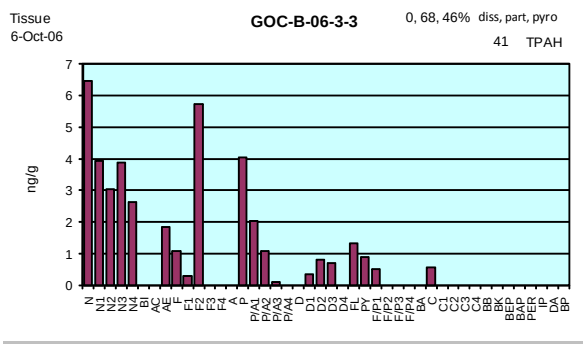
Tissue
6-Oct-06
GOC-B-06-3-3
0, 68, 46% diss, part, pyro
41 TPAH
ng/g

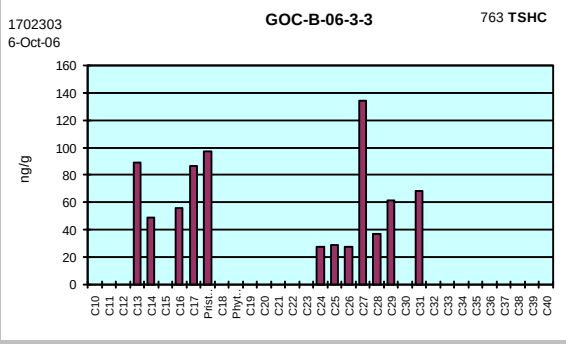
1702303
6-Oct-06
GOC-B-06-3-3
763 TSHC
ng/g

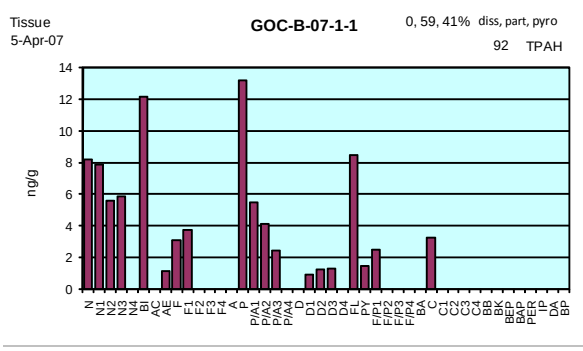
Tissue
5-Apr-07
GOC-B-07-1-1
0, 59, 41% diss, part, pyro
92 TPAH
ng/g

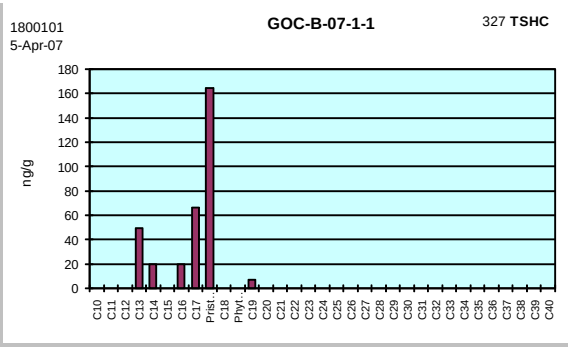
1800101
5-Apr-07
GOC-B-07-1-1
327 TSHC
ng/g

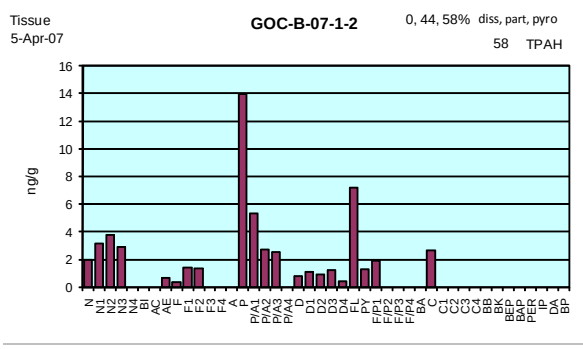
Tissue
5-Apr-07
GOC-B-07-1-2
0, 44, 58% diss, part, pyro
58 TPAH
ng/g

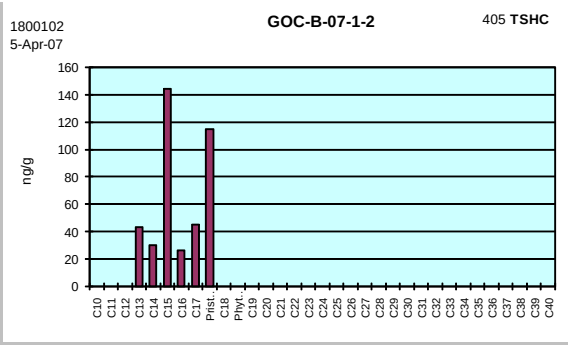
1800102
5-Apr-07
GOC-B-07-1-2
405 TSHC
ng/g

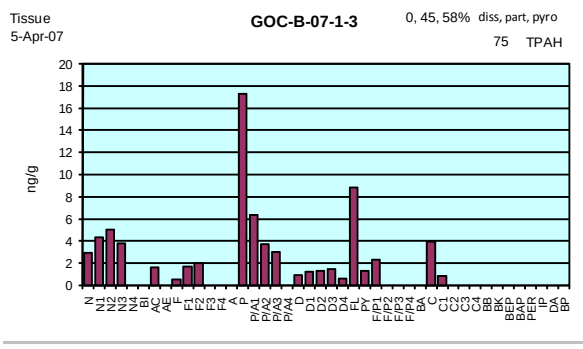
Tissue
5-Apr-07
GOC-B-07-1-3
0, 45, 58% diss, part, pyro
75 TPAH
ng/g

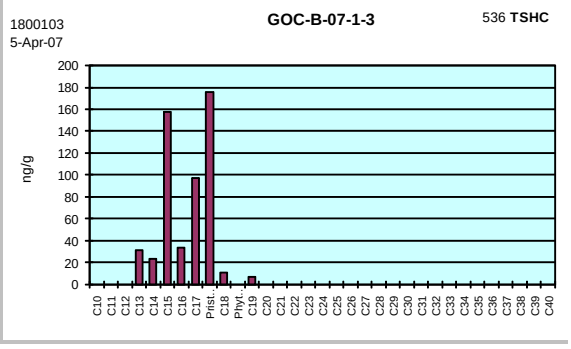
1800103
5-Apr-07
GOC-B-07-1-3
536 TSHC
ng/g

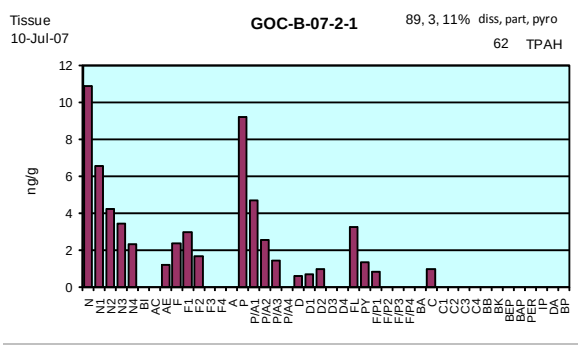
Tissue
10-Jul-07
GOC-B-07-2-1
89, 3, 11% diss, part, pyro
62 TPAH
ng/g

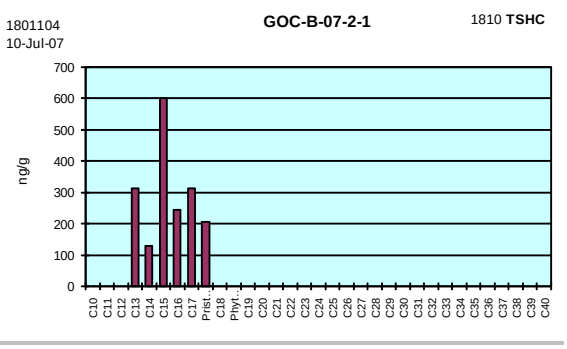
1801104
10-Jul-07
GOC-B-07-2-1
1810 TSHC
ng/g

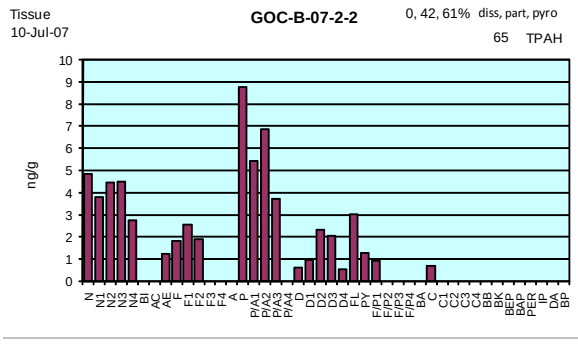
Tissue
10-Jul-07
GOC-B-07-2-2
0, 42, 61% diss, part, pyro
65 TPAH
ng/g

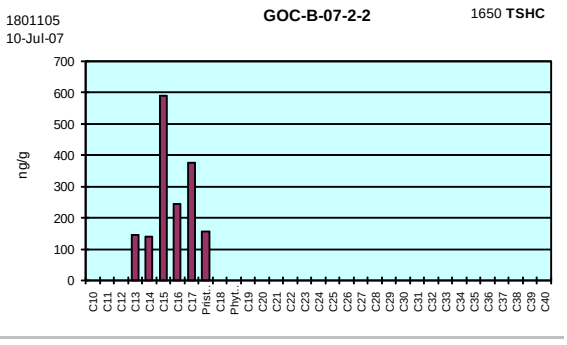
1801105
10-Jul-07
GOC-B-07-2-2
1650 TSHC
ng/g

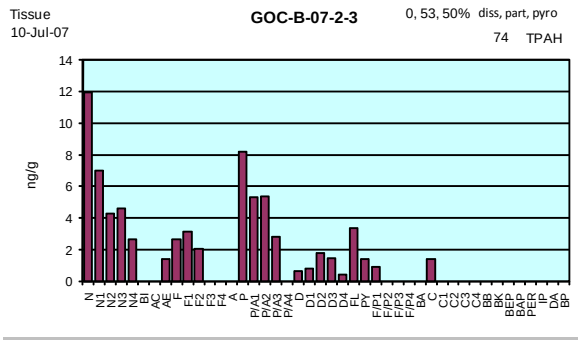
Tissue
10-Jul-07
GOC-B-07-2-3
0, 53, 50% diss, part, pyro
74 TPAH
ng/g

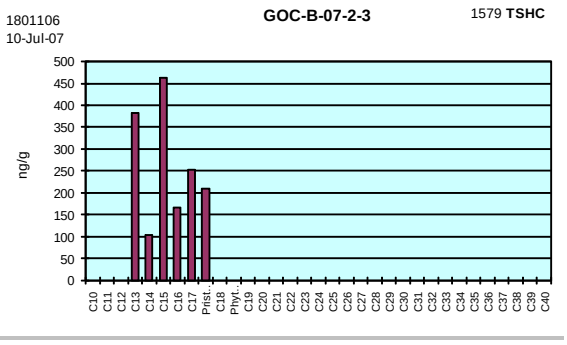
1801106
10-Jul-07
GOC-B-07-2-3
1579 TSHC
ng/g

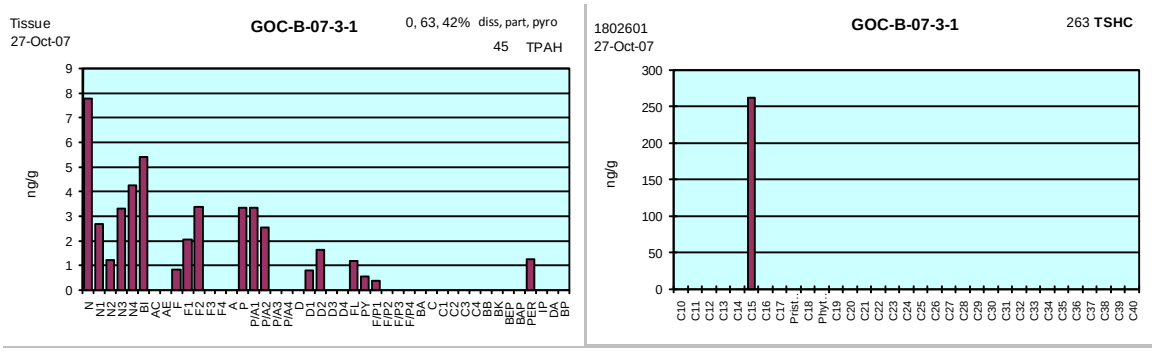
Tissue
27-Oct-07
GOC-B-07-3-1
0, 63, 42% diss, part, pyro
45 TPAH
ng/g
1802601
27-Oct-07
GOC-B-07-3-1
263 TSHC
ng/g

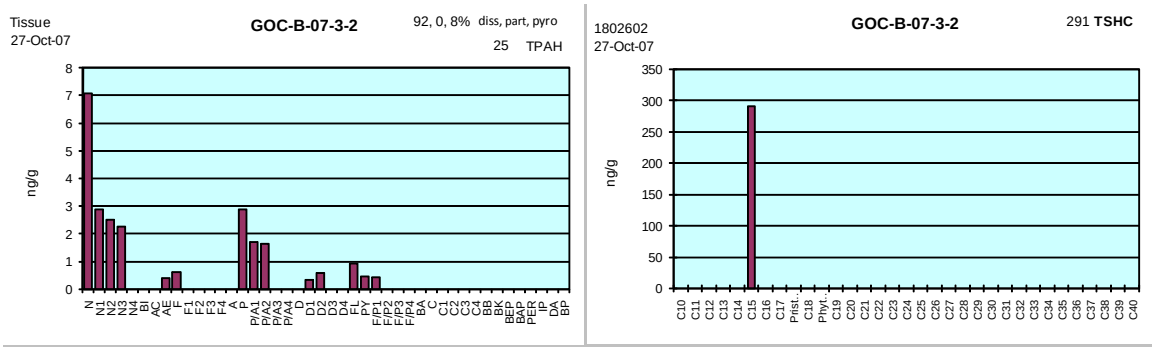
Tissue
27-Oct-07
GOC-B-07-3-2
92, 0, 8% diss, part, pyro
25 TPAH
ng/g
1802602
27-Oct-07
GOC-B-07-3-2
291 TSHC
ng/g

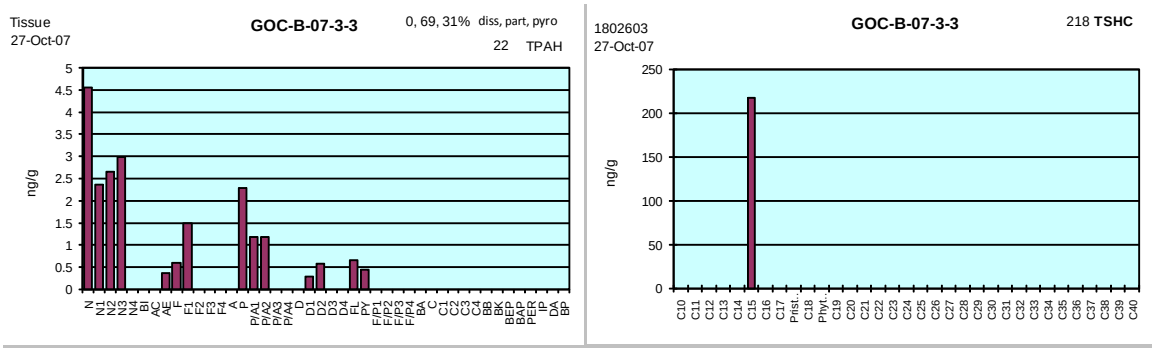
Tissue
27-Oct-07
GOC-B-07-3-3
0, 69, 31% diss, part, pyro
22 TPAH
ng/g
1802603
27-Oct-07
GOC-B-07-3-3
218 TSHC
ng/g

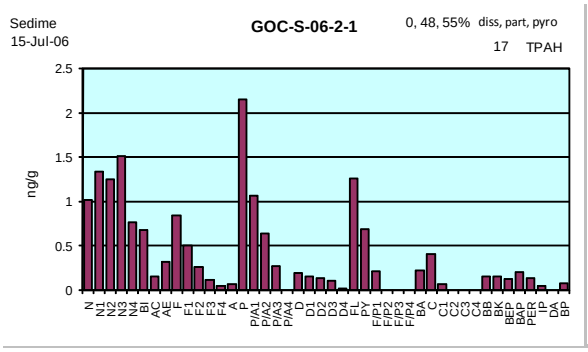
Sedime
15-Jul-06
GOC-S-06-2-1
0, 48, 55% diss, part, pyro
17 TPAH
ng/g
N N1 N2 N3 N4 BI AC AE F F1 F2 F3 F4 A P P/A1 P/A2 P/A3 P/A4 D D1 D2 D3 D4 FL PY F/P1 F/P2 F/P3 F/P4 BA C C1 C2 C3 C4 BB BK BEP BAP PER IP DA BP

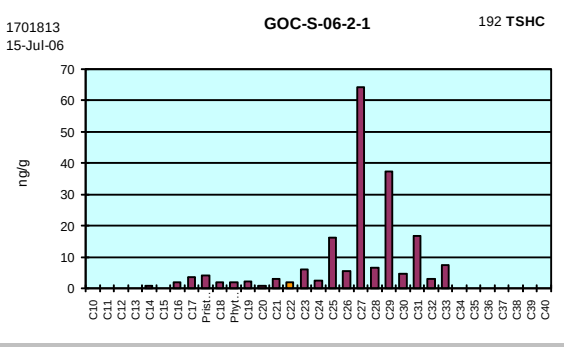
1701813
15-Jul-06
GOC-S-06-2-1
192 TSHC
ng/g
C10 C11 C12 C13 C14 C15 C16 C17 Prist. C18 Phyt. C19 C20 C21 C22 C23 C24 C25 C26 C27 C28 C29 C30 C31 C32 C33 C34 C35 C36 C37 C38 C39 C40

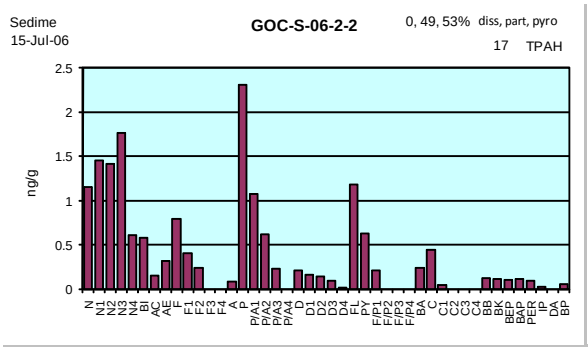
Sedime
15-Jul-06
GOC-S-06-2-2
0, 49, 53% diss, part, pyro
17 TPAH
ng/g
N N1 N2 N3 N4 BI AC AE F F1 F2 F3 F4 A P P/A1 P/A2 P/A3 P/A4 D D1 D2 D3 D4 FL PY F/P1 F/P2 F/P3 F/P4 BA C C1 C2 C3 C4 BB BK BEP BAP PER IP DA BP

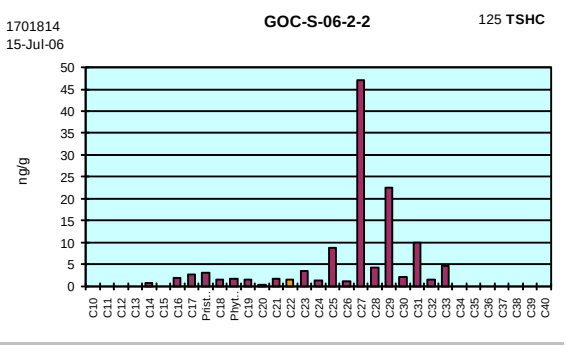
1701814
15-Jul-06
GOC-S-06-2-2
125 TSHC
ng/g
C10 C11 C12 C13 C14 C15 C16 C17 Prist. C18 Phyt. C19 C20 C21 C22 C23 C24 C25 C26 C27 C28 C29 C30 C31 C32 C33 C34 C35 C36 C37 C38 C39 C40

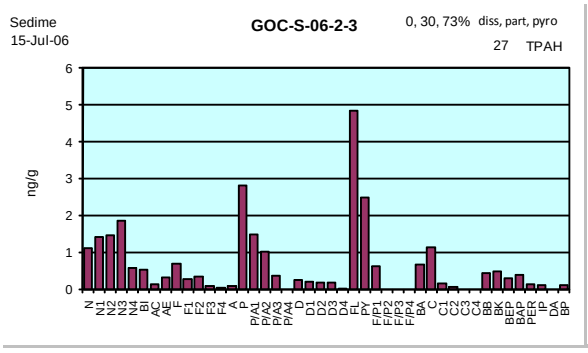
Sedime
15-Jul-06
GOC-S-06-2-3
0, 30, 73% diss, part, pyro
27 TPAH
ng/g
N N1 N2 N3 N4 BI AC AE F F1 F2 F3 F4 A P P/A1 P/A2 P/A3 P/A4 D D1 D2 D3 D4 FL PY F/P1 F/P2 F/P3 F/P4 BA C C1 C2 C3 C4 BB BK BEP BAP PER IP DA BP

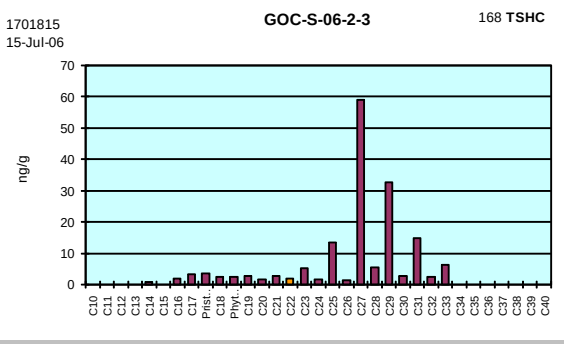
1701815
15-Jul-06
GOC-S-06-2-3
168 TSHC
ng/g
C10 C11 C12 C13 C14 C15 C16 C17 Prist. C18 Phyt. C19 C20 C21 C22 C23 C24 C25 C26 C27 C28 C29 C30 C31 C32 C33 C34 C35 C36 C37 C38 C39 C40

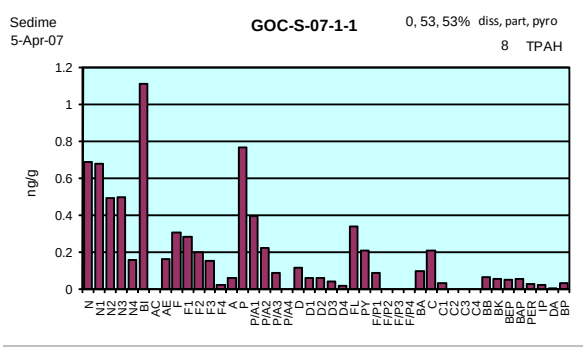
Sedime
5-Apr-07
GOC-S-07-1-1
0, 53, 53% diss, part, pyro
8 TPAH
ng/g
N N1 N2 N3 N4 BI AC AE F F1 F2 F3 F4 A P P/A1 P/A2 P/A3 P/A4 D D1 D2 D3 D4 FL PY F/P1 F/P2 F/P3 F/P4 BA C C1 C2 C3 C4 BB BK BEP BAP PER IP DA BP

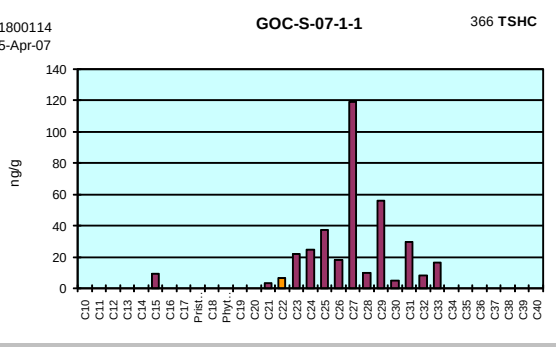
1800114
5-Apr-07
GOC-S-07-1-1
366 TSHC
ng/g
C10 C11 C12 C13 C14 C15 C16 C17 Prist. C18 Phyt. C19 C20 C21 C22 C23 C24 C25 C26 C27 C28 C29 C30 C31 C32 C33 C34 C35 C36 C37 C38 C39 C40

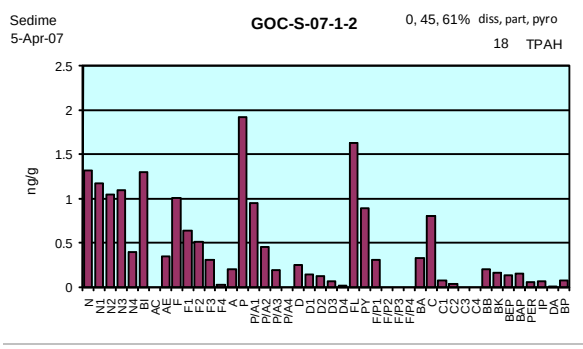
Sedime
5-Apr-07
GOC-S-07-1-2
0, 45, 61% diss, part, pyro
18 TPAH
ng/g
N N1 N2 N3 N4 BI AC AE F F1 F2 F3 F4 A P P/A1 P/A2 P/A3 P/A4 D D1 D2 D3 D4 FL PY F/P1 F/P2 F/P3 F/P4 BA C C1 C2 C3 C4 BB BK BEP BAP PER IP DA BP

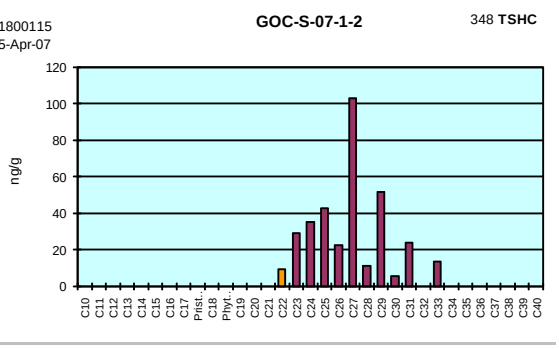
1800115
5-Apr-07
GOC-S-07-1-2
348 TSHC
ng/g
C10 C11 C12 C13 C14 C15 C16 C17 Prist. C18 Phyt. C19 C20 C21 C22 C23 C24 C25 C26 C27 C28 C29 C30 C31 C32 C33 C34 C35 C36 C37 C38 C39 C40

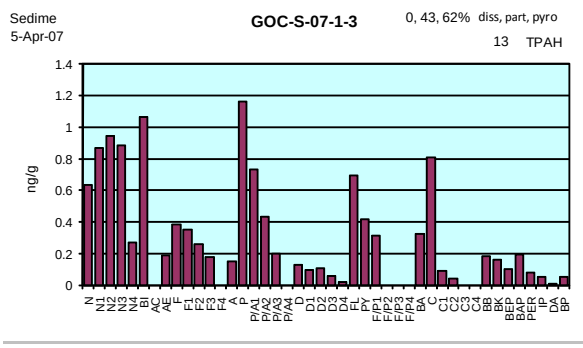
Sedime
5-Apr-07
GOC-S-07-1-3
0, 43, 62% diss, part, pyro
13 TPAH
ng/g
N N1 N2 N3 N4 BI AC AE F F1 F2 F3 F4 A P P/A1 P/A2 P/A3 P/A4 D D1 D2 D3 D4 FL PY F/P1 F/P2 F/P3 F/P4 BA C C1 C2 C3 C4 BB BK BEP BAP PER IP DA BP

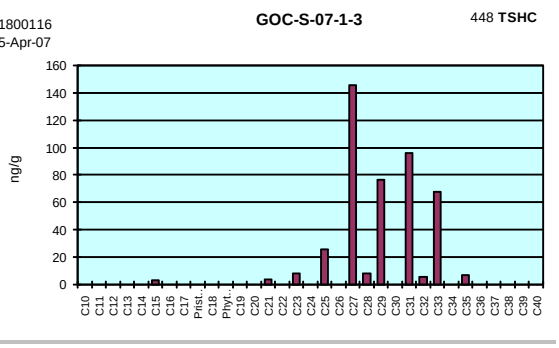
1800116
5-Apr-07
GOC-S-07-1-3
448 TSHC
ng/g
C10 C11 C12 C13 C14 C15 C16 C17 Prist. C18 Phyt. C19 C20 C21 C22 C23 C24 C25 C26 C27 C28 C29 C30 C31 C32 C33 C34 C35 C36 C37 C38 C39 C40

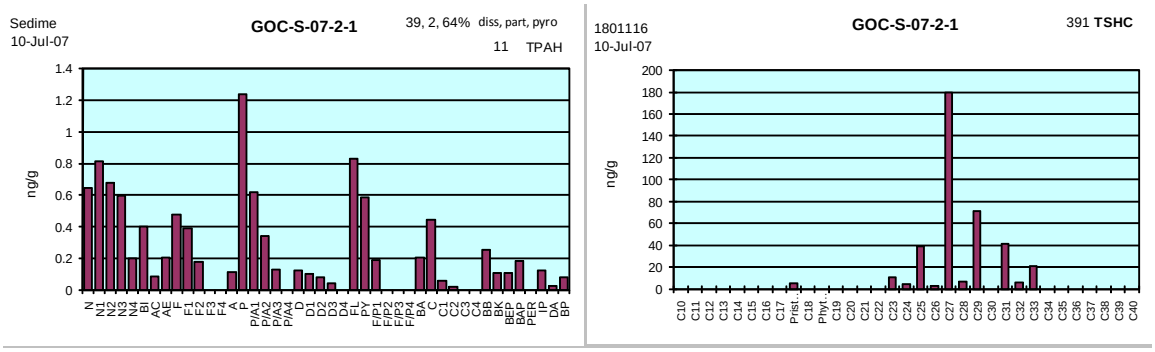
Sedime
10-Jul-07
GOC-S-07-2-1
39, 2, 64% diss, part, pyro
11 TPAH
ng/g
1801116
10-Jul-07
GOC-S-07-2-1
391 TSHC
ng/g

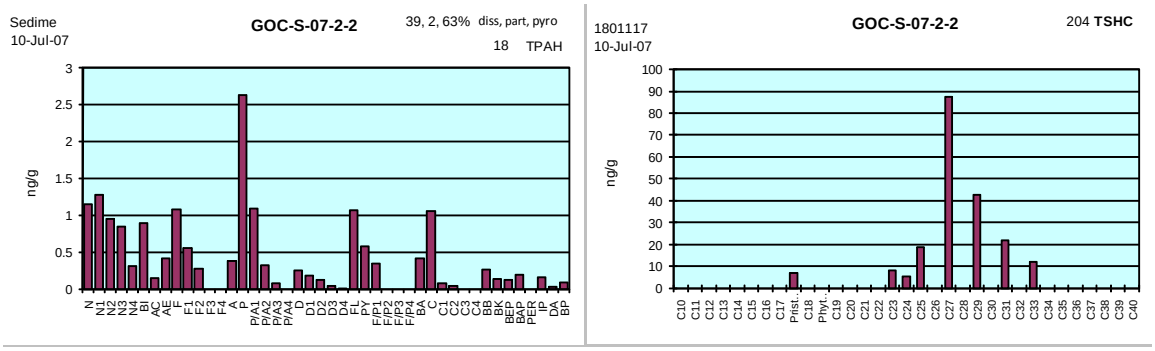
Sedime
10-Jul-07
GOC-S-07-2-2
39, 2, 63% diss, part, pyro
18 TPAH
ng/g
1801117
10-Jul-07
GOC-S-07-2-2
204 TSHC
ng/g

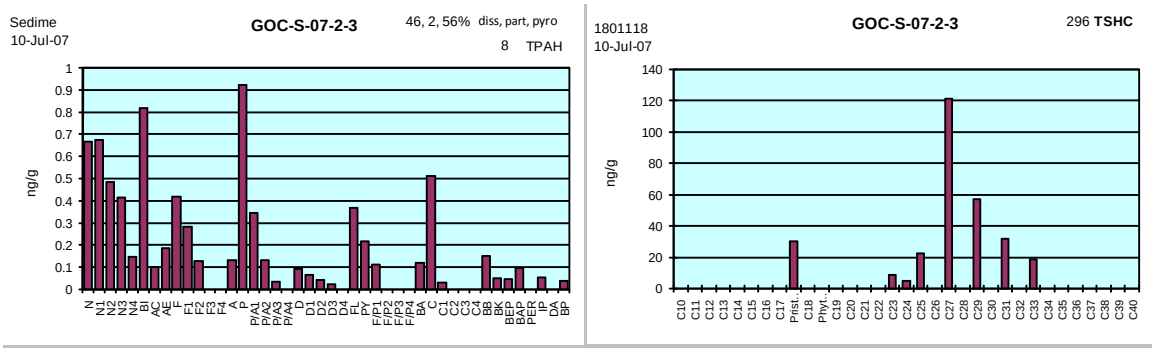
Sedime
10-Jul-07
GOC-S-07-2-3
46, 2, 56% diss, part, pyro
8 TPAH
ng/g
1801118
10-Jul-07
GOC-S-07-2-3
296 TSHC
ng/g

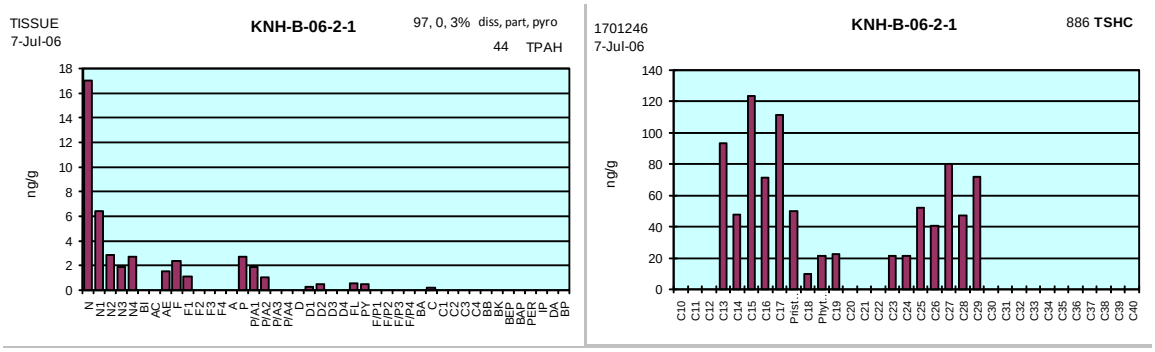
TISSUE
7-Jul-06
KNH-B-06-2-1
97, 0, 3% diss, part, pyro
44 TPAH
ng/g
1701246
7-Jul-06
KNH-B-06-2-1
886 TSHC
ng/g

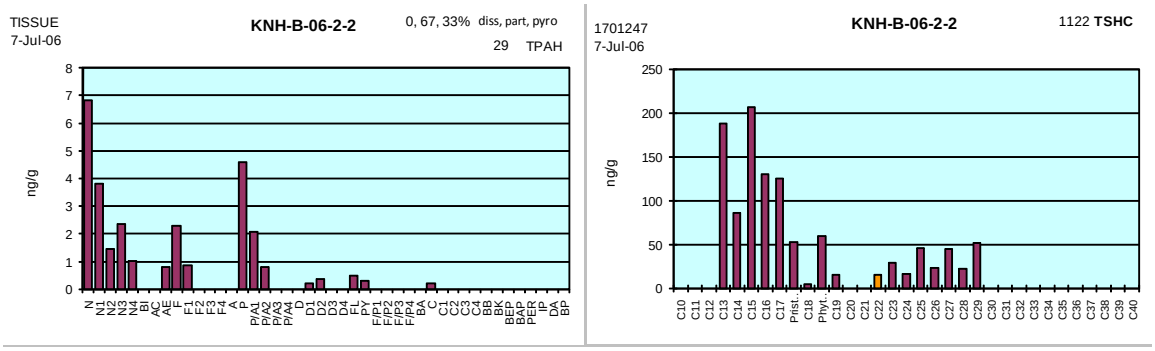
TISSUE
7-Jul-06
KNH-B-06-2-2
0, 67, 33% diss, part, pyro
29 TPAH
ng/g
1701247
7-Jul-06
KNH-B-06-2-2
1122 TSHC
ng/g

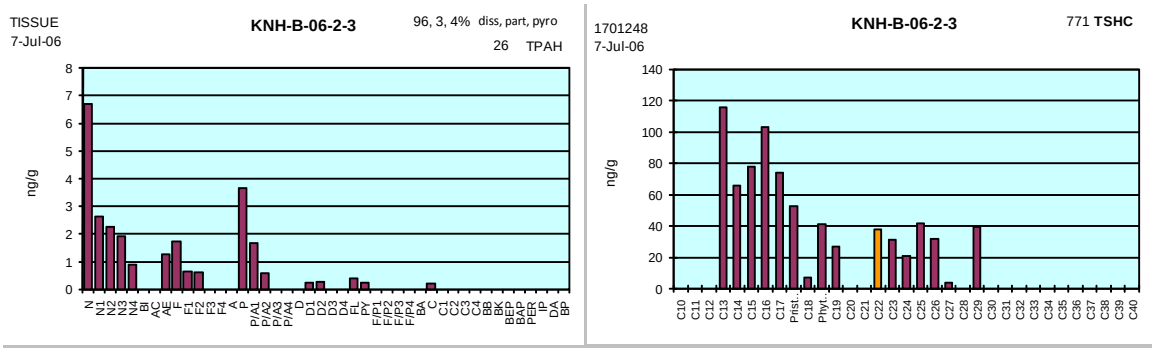
TISSUE
7-Jul-06
KNH-B-06-2-3
96, 3, 4% diss, part, pyro
26 TPAH
ng/g
1701248
7-Jul-06
KNH-B-06-2-3
771 TSHC
ng/g

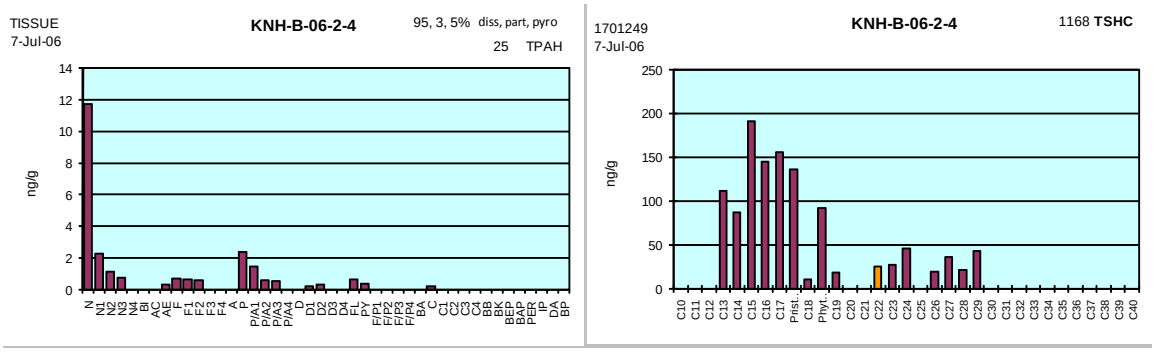
TISSUE
7-Jul-06
KNH-B-06-2-4
95, 3, 5% diss, part, pyro
25 TPAH
ng/g
1701249
7-Jul-06
KNH-B-06-2-4
1168 TSHC
ng/g

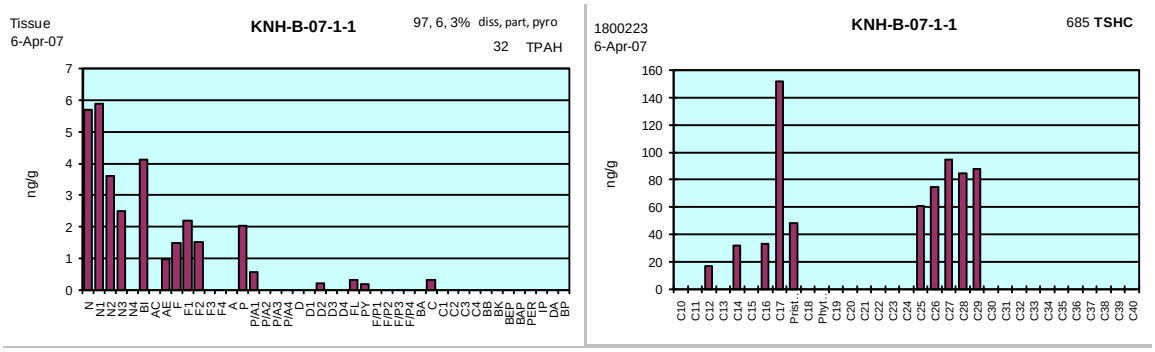
Tissue
6-Apr-07
KNH-B-07-1-1
97, 6, 3% diss, part, pyro
32 TPAH
ng/g
1800223
6-Apr-07
KNH-B-07-1-1
685 TSHC
ng/g

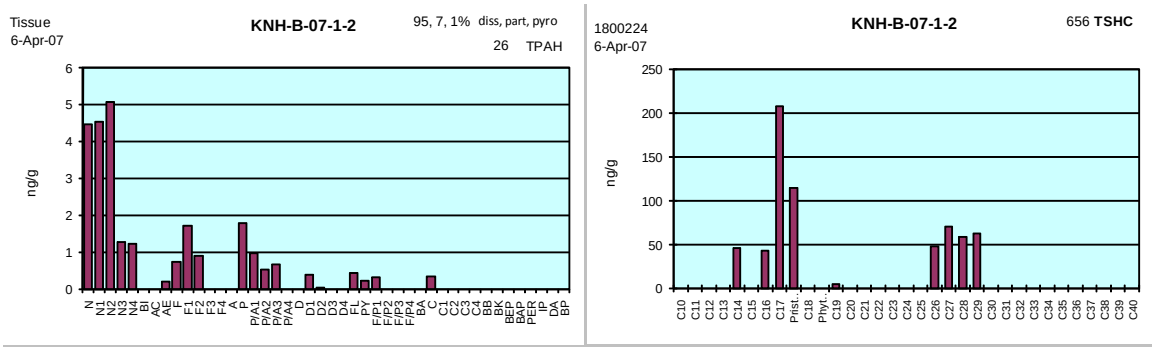
Tissue
6-Apr-07
KNH-B-07-1-2
95, 7, 1% diss, part, pyro
26 TPAH
ng/g
1800224
6-Apr-07
KNH-B-07-1-2
656 TSHC
ng/g

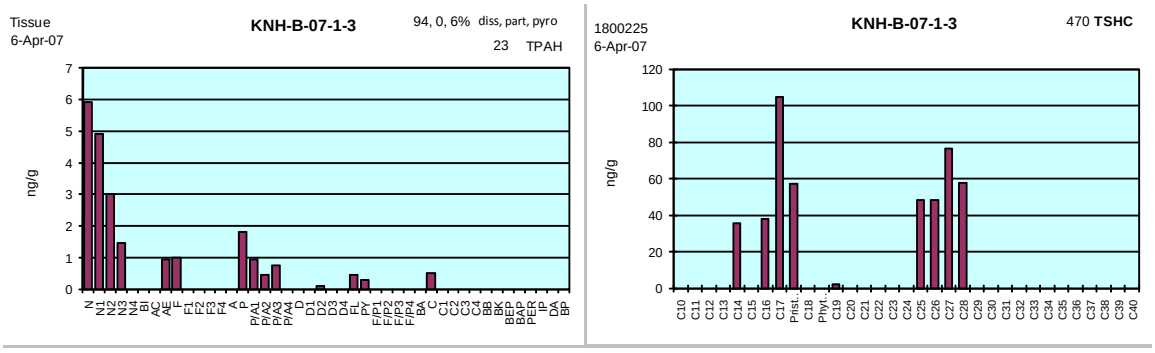
Tissue
6-Apr-07
KNH-B-07-1-3
94, 0, 6% diss, part, pyro
23 TPAH
ng/g
1800225
6-Apr-07
KNH-B-07-1-3
470 TSHC
ng/g

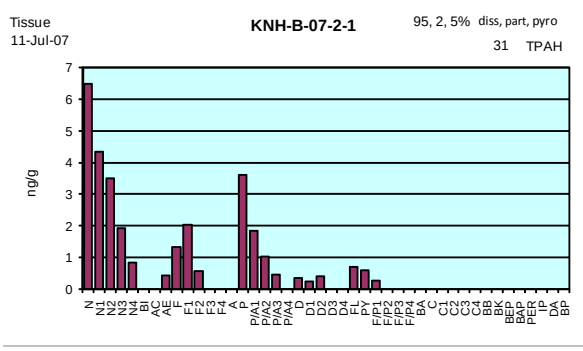
Tissue
11-Jul-07
KNH-B-07-2-1
95, 2, 5% diss, part, pyro
31 TPAH
ng/g

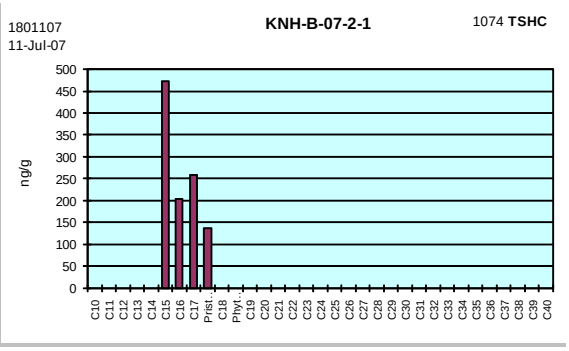
1801107
11-Jul-07
KNH-B-07-2-1
1074 TSHC
ng/g

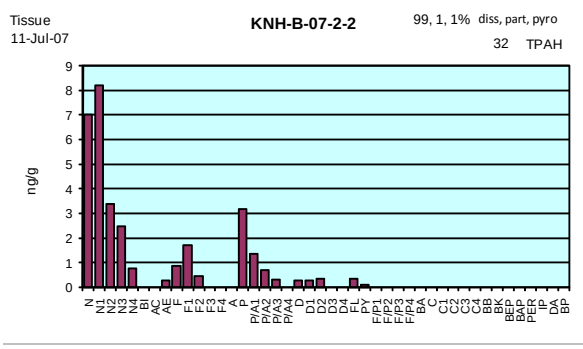
Tissue
11-Jul-07
KNH-B-07-2-2
99, 1, 1% diss, part, pyro
32 TPAH
ng/g

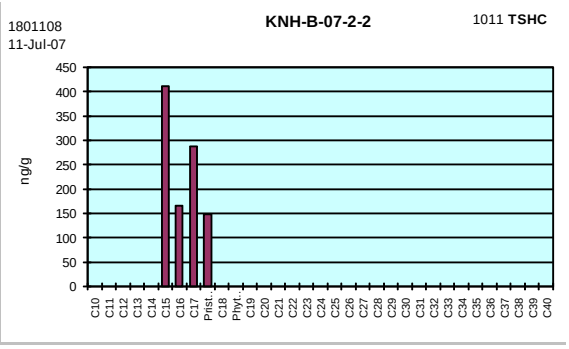
1801108
11-Jul-07
KNH-B-07-2-2
1011 TSHC
ng/g

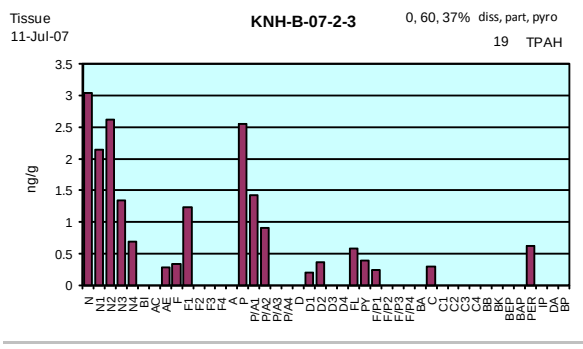
Tissue
11-Jul-07
KNH-B-07-2-3
0, 60, 37% diss, part, pyro
19 TPAH
ng/g

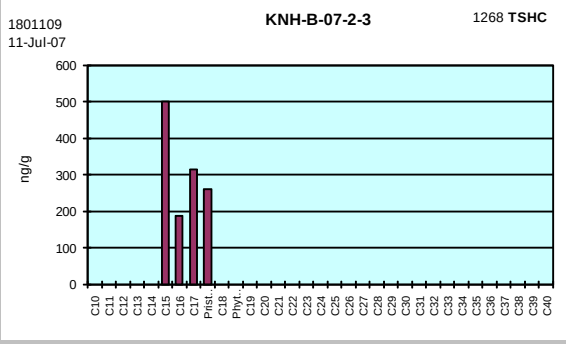
1801109
11-Jul-07
KNH-B-07-2-3
1268 TSHC
ng/g

Tissue
27-Jul-06

SHB-B-06-2-1

99, 0, 1% diss, part, pyro

29 TPAH

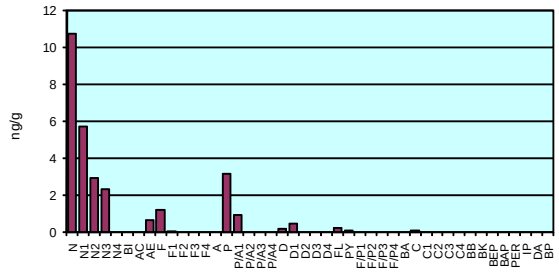

1701913
27-Jul-06

SHB-B-06-2-1

819 **TSHC**

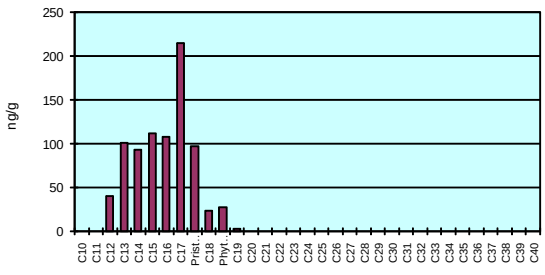

Tissue
27-Jul-06

SHB-B-06-2-2

95, 0, 1% diss, part, pyro

82 TPAH

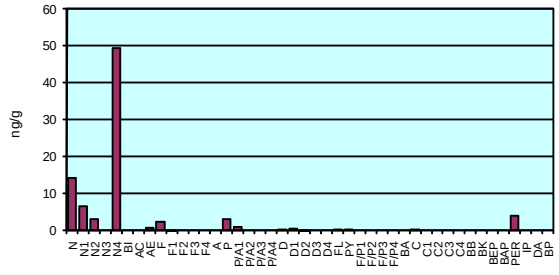

1701914
27-Jul-06

SHB-B-06-2-2

630 **TSHC**

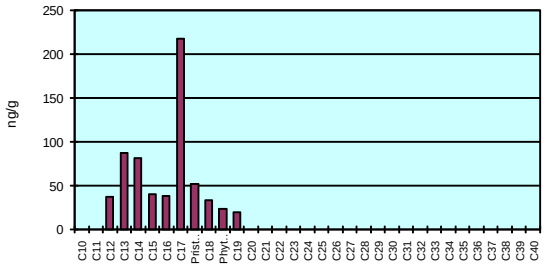

Tissue
27-Jul-06

SHB-B-06-2-3

97, 0, 3% diss, part, pyro

27 TPAH

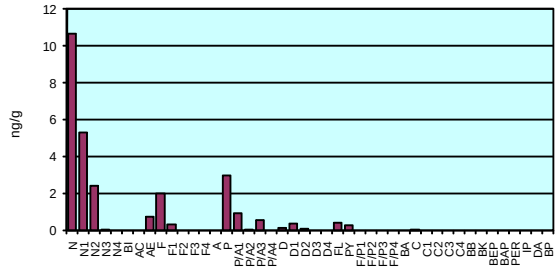

1701915
27-Jul-06

SHB-B-06-2-3

626 **TSHC**

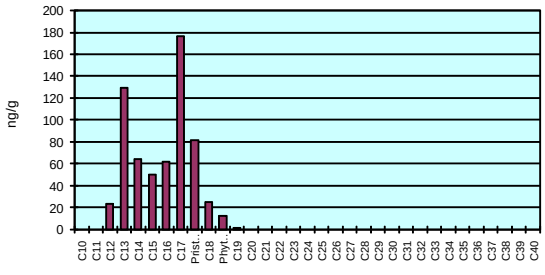

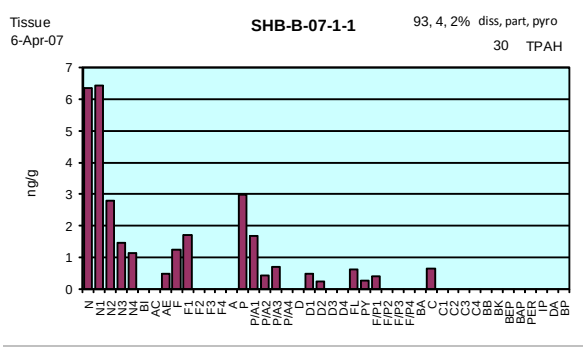
Tissue
6-Apr-07
SHB-B-07-1-1
93, 4, 2% diss, part, pyro
30 TPAH
ng/g
N N1 N2 N3 N4 BI AC AE F F1 F2 F3 F4 A P P/A1 P/A2 P/A3 P/A4 D D1 D2 D3 D4 FL PY F/P1 F/P2 F/P3 F/P4 BA C C1 C2 C3 C4 BB BK BEP BAP PER IP DA BP

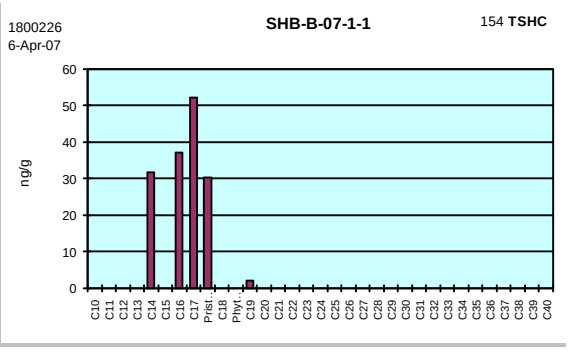
1800226
6-Apr-07
SHB-B-07-1-1
154 TSHC
ng/g
C10 C11 C12 C13 C14 C15 C16 C17 Prist. C18 Phyt. C19 C20 C21 C22 C23 C24 C25 C26 C27 C28 C29 C30 C31 C32 C33 C34 C35 C36 C37 C38 C39 C40

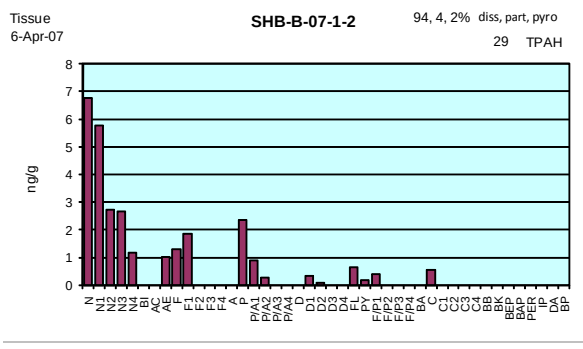
Tissue
6-Apr-07
SHB-B-07-1-2
94, 4, 2% diss, part, pyro
29 TPAH
ng/g
N N1 N2 N3 N4 BI AC AE F F1 F2 F3 F4 A P P/A1 P/A2 P/A3 P/A4 D D1 D2 D3 D4 FL PY F/P1 F/P2 F/P3 F/P4 BA C C1 C2 C3 C4 BB BK BEP BAP PER IP DA BP

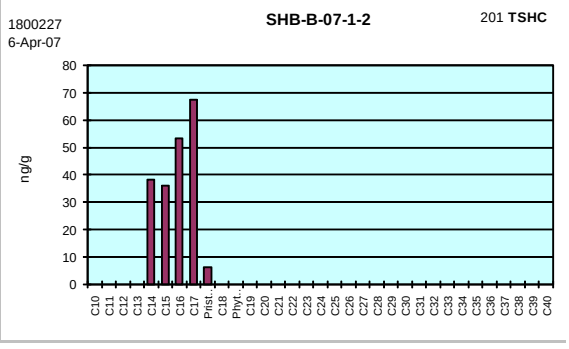
1800227
6-Apr-07
SHB-B-07-1-2
201 TSHC
ng/g
C10 C11 C12 C13 C14 C15 C16 C17 Prist. C18 Phyt. C19 C20 C21 C22 C23 C24 C25 C26 C27 C28 C29 C30 C31 C32 C33 C34 C35 C36 C37 C38 C39 C40

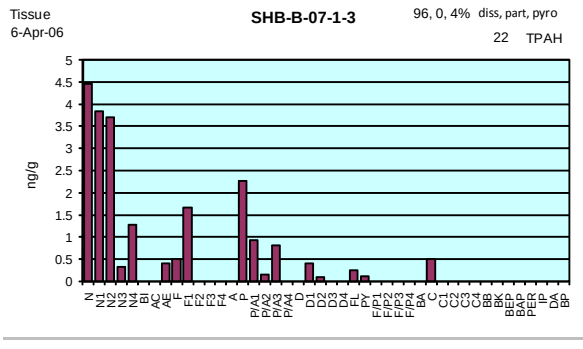
Tissue
6-Apr-06
SHB-B-07-1-3
96, 0, 4% diss, part, pyro
22 TPAH
ng/g
N N1 N2 N3 N4 BI AC AE F F1 F2 F3 F4 A P P/A1 P/A2 P/A3 P/A4 D D1 D2 D3 D4 FL PY F/P1 F/P2 F/P3 F/P4 BA C C1 C2 C3 C4 BB BK BEP BAP PER IP DA BP

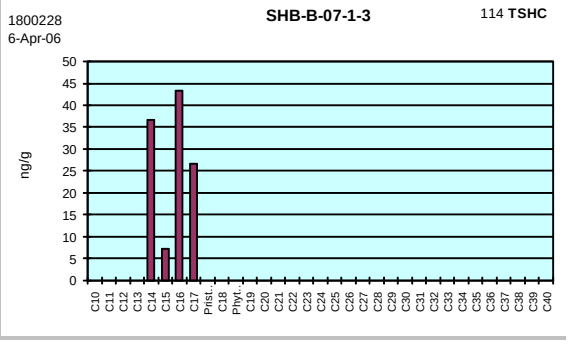
1800228
6-Apr-06
SHB-B-07-1-3
114 TSHC
ng/g
C10 C11 C12 C13 C14 C15 C16 C17 Prist. C18 Phyt. C19 C20 C21 C22 C23 C24 C25 C26 C27 C28 C29 C30 C31 C32 C33 C34 C35 C36 C37 C38 C39 C40

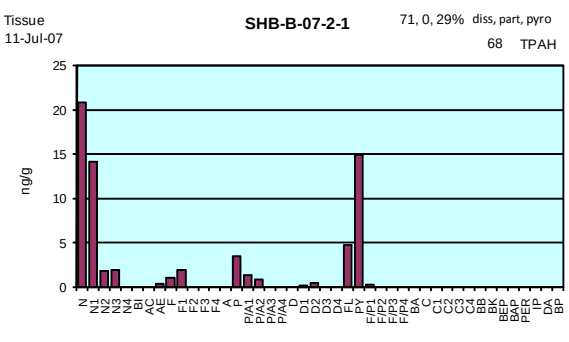
Tissue
11-Jul-07
SHB-B-07-2-1
71, 0, 29% diss, part, pyro
68 TPAH
ng/g

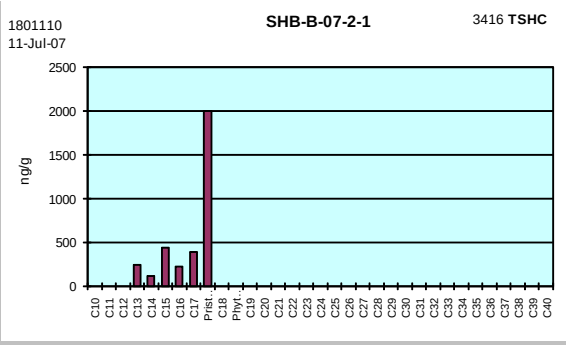
1801110
11-Jul-07
SHB-B-07-2-1
3416 TSHC
ng/g

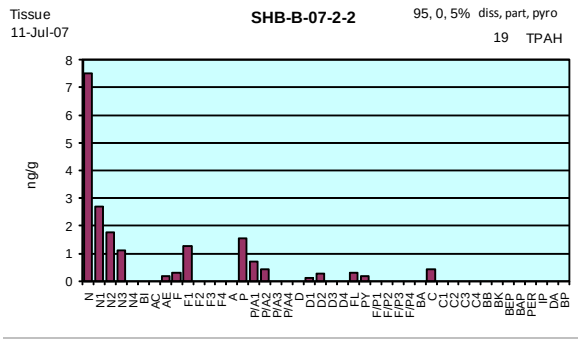
Tissue
11-Jul-07
SHB-B-07-2-2
95, 0, 5% diss, part, pyro
19 TPAH
ng/g

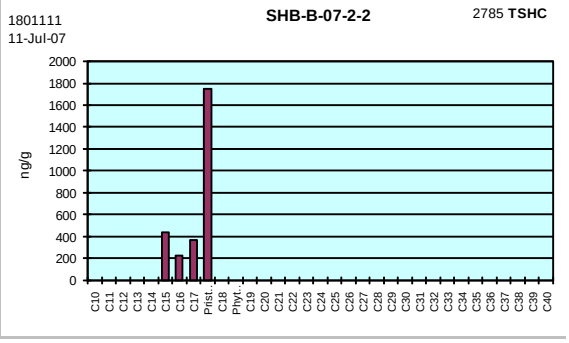
1801111
11-Jul-07
SHB-B-07-2-2
2785 TSHC
ng/g

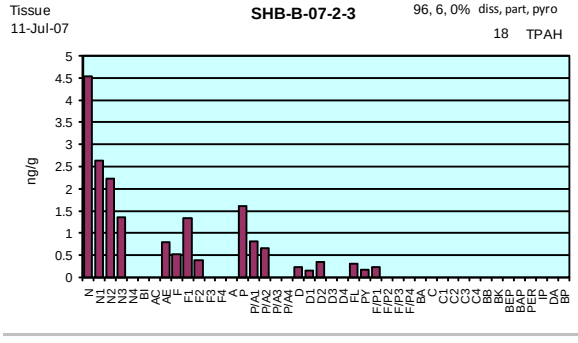
Tissue
11-Jul-07
SHB-B-07-2-3
96, 6, 0% diss, part, pyro
18 TPAH
ng/g

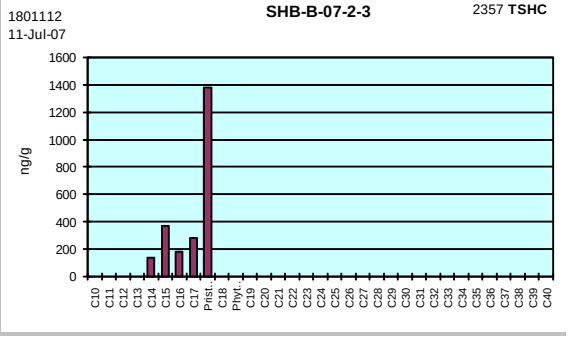
1801112
11-Jul-07
SHB-B-07-2-3
2357 TSHC
ng/g

Tissue
26-Jul-06

SHH-B-06-2-1

69, 28, 4% diss, part, pyro

29 TPAH

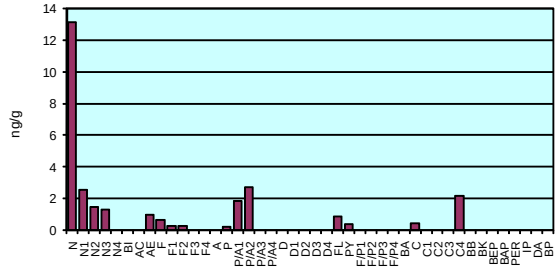

1701904
26-Jul-06

SHH-B-06-2-1

2978 **TSHC**

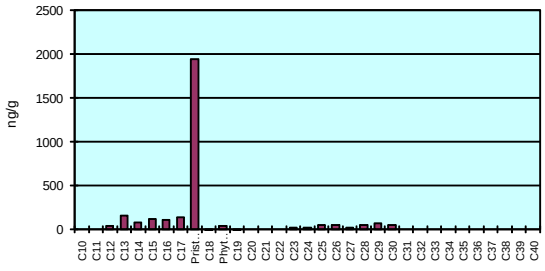

Tissue
26-Jul-06

SHH-B-06-2-2

65, 28, 11% diss, part, pyro

22 TPAH

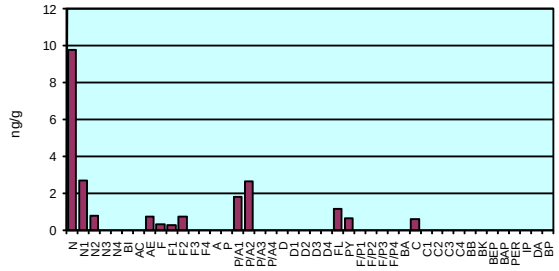

1701905
26-Jul-06

SHH-B-06-2-2

1877 **TSHC**

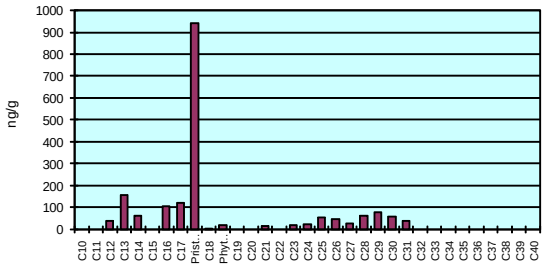

Tissue
26-Jul-06

SHH-B-06-2-3

94, 5, 1% diss, part, pyro

108 TPAH

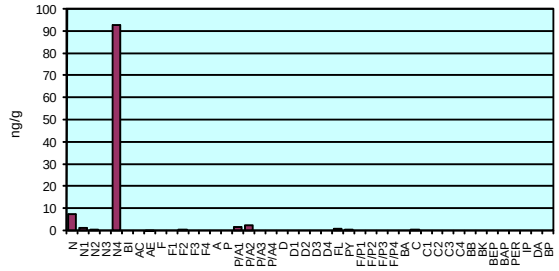

1701906
26-Jul-06

SHH-B-06-2-3

1871 **TSHC**

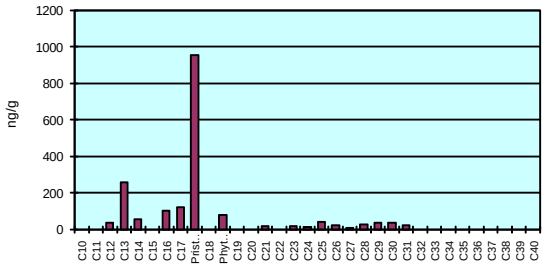

Tissue
17-Apr-07

SHH-B-07-1-1 0, 13, 68% diss, part, pyro

19 TPAH

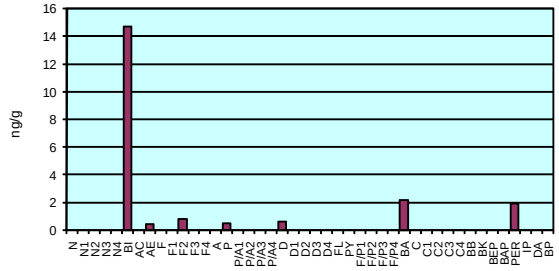

1800201
17-Apr-07

SHH-B-07-1-1 368 **TSHC**

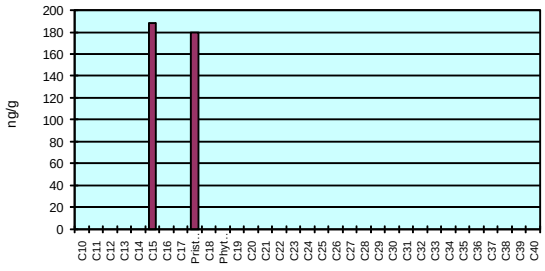

Tissue
17-Apr-07

SHH-B-07-1-2 100, 0, 0% diss, part, pyro

31 TPAH

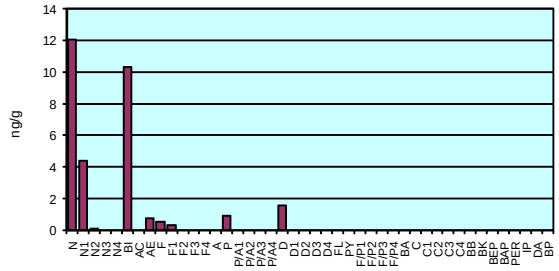

1800202
17-Apr-07

SHH-B-07-1-2 0 **TSHC**

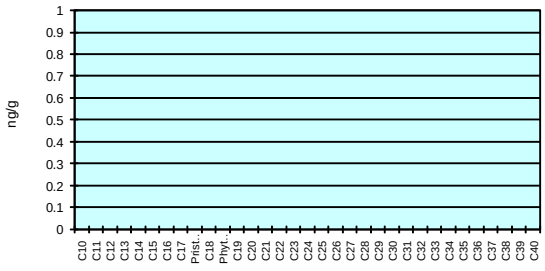

Tissue
17-Apr-07

SHH-B-07-1-3 100, 6, 0% diss, part, pyro

33 TPAH

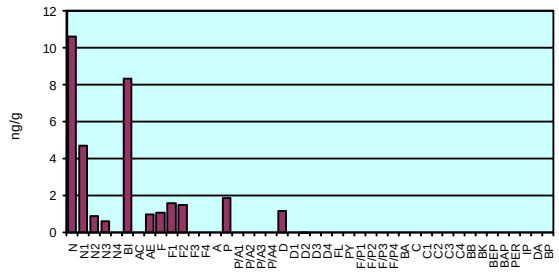

1800203
17-Apr-07

SHH-B-07-1-3 0 **TSHC**

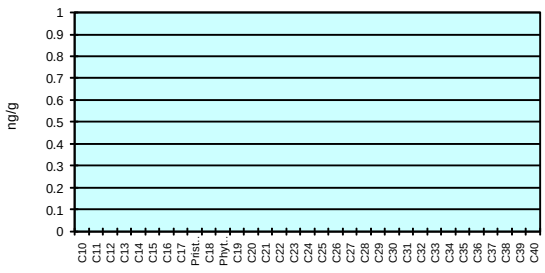

Tissue
28-Jul-07

SHH-B-07-2-1

80, 17, 2% diss, part, pyro

6 TPAH

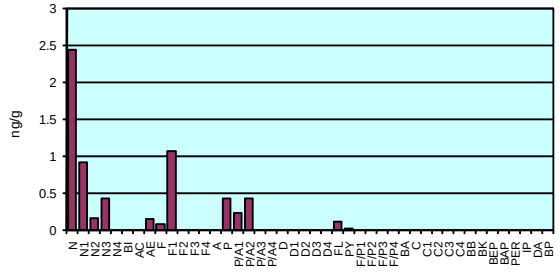

1801201
28-Jul-07

SHH-B-07-2-1

3637 **TSHC**

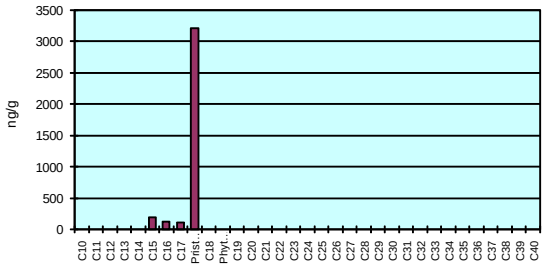

Tissue
28-Jul-07

SHH-B-07-2-2

90, 0, 10% diss, part, pyro

7 TPAH

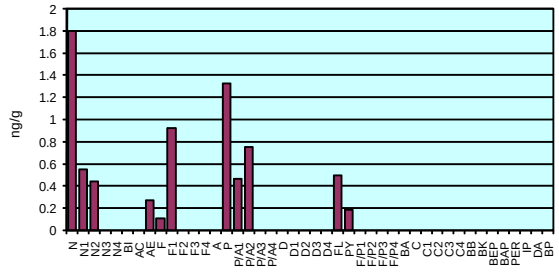

1801202
28-Jul-07

SHH-B-07-2-2

2965 **TSHC**

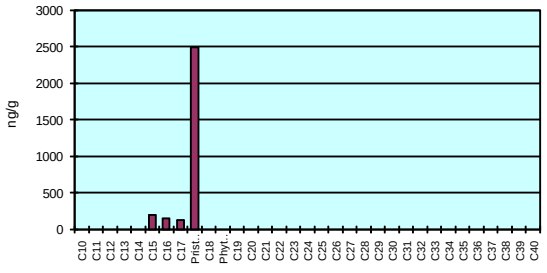

Tissue
28-Jul-07

SHH-B-07-2-2D

98, 0, 2% diss, part, pyro

6 TPAH

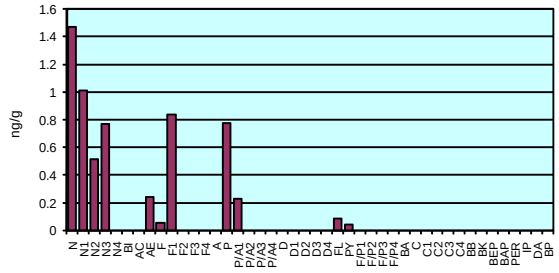

1801202
28-Jul-07

SHH-B-07-2-2D

2402 **TSHC**

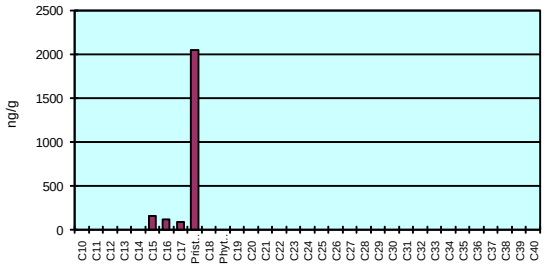

Tissue
28-Jul-07

SHH-B-07-2-3

0, 66, 34% diss, part, pyro

5 TPAH

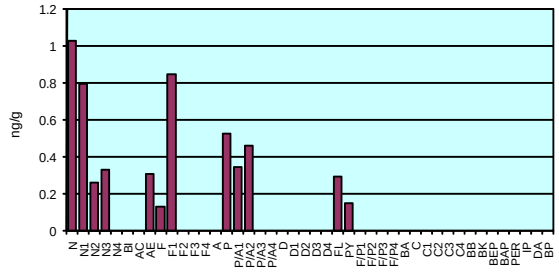

1801203
28-Jul-07

SHH-B-07-2-3

1774 **TSHC**

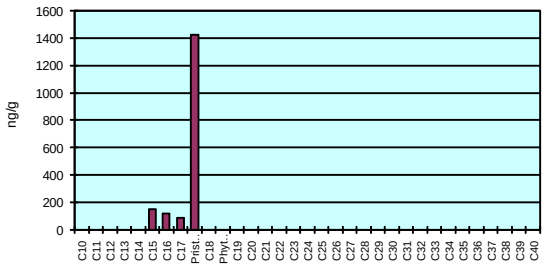

TISSUE
11-Jul-06

SLB-B-06-2-1

80, 2, 7% diss, part, pyro

18 TPAH

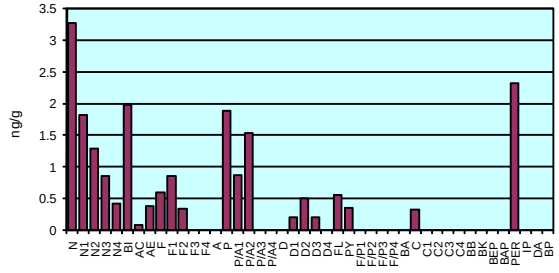

1701225
11-Jul-06

SLB-B-06-2-1

1703 **TSHC**

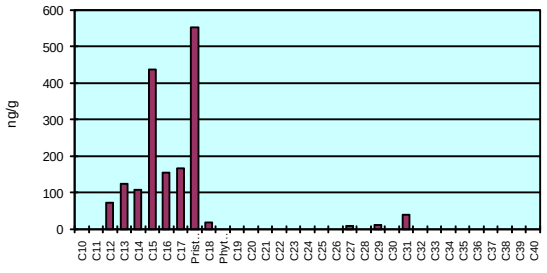

TISSUE
11-Jul-06

SLB-B-06-2-2

86, 5, 12% diss, part, pyro

26 TPAH

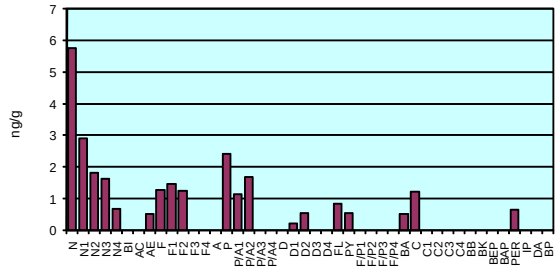

1701226
11-Jul-06

SLB-B-06-2-2

1483 **TSHC**

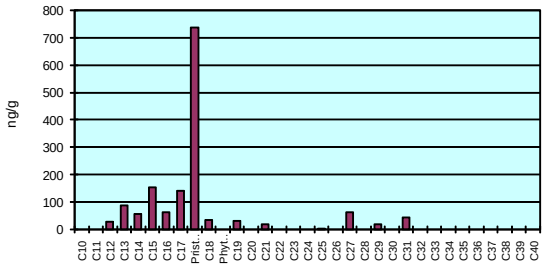

TISSUE
11-Jul-06

SLB-B-06-2-3

95, 0, 5% diss, part, pyro

22 TPAH

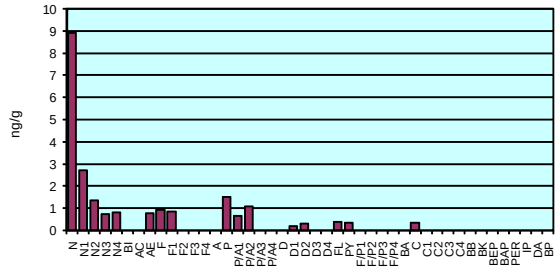

1701227
11-Jul-06

SLB-B-06-2-3

1403 **TSHC**

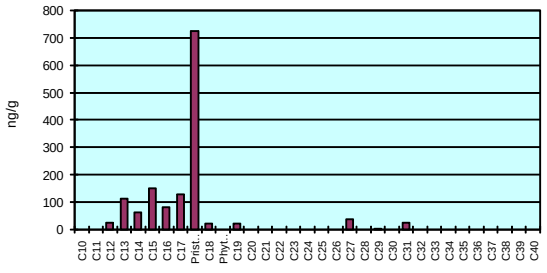

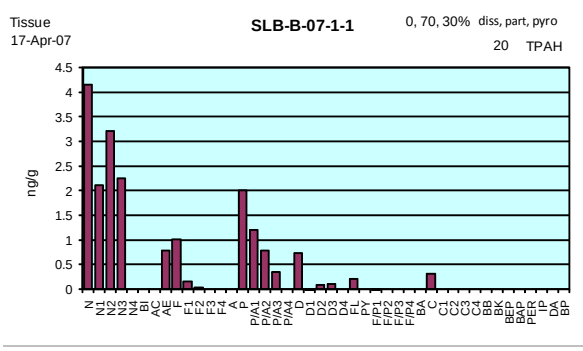
Tissue
17-Apr-07
SLB-B-07-1-1
0, 70, 30% diss, part, pyro
20 TPAH
ng/g

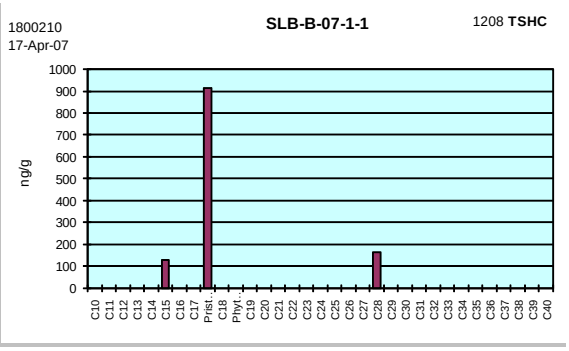
1800210
17-Apr-07
SLB-B-07-1-1
1208 TSHC
ng/g
Prist.
Phyt.

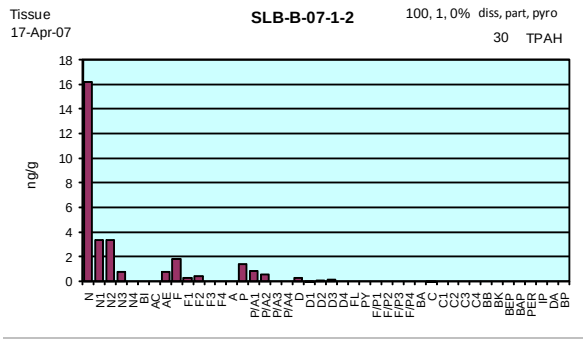
Tissue
17-Apr-07
SLB-B-07-1-2
100, 1, 0% diss, part, pyro
30 TPAH
ng/g

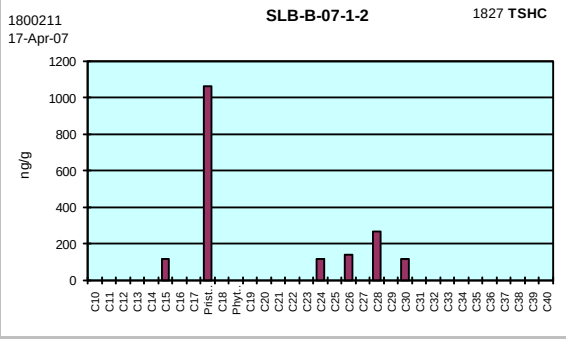
1800211
17-Apr-07
SLB-B-07-1-2
1827 TSHC
ng/g
Prist.
Phyt.

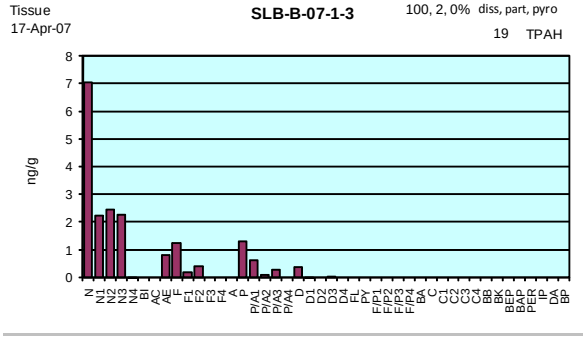
Tissue
17-Apr-07
SLB-B-07-1-3
100, 2, 0% diss, part, pyro
19 TPAH
ng/g

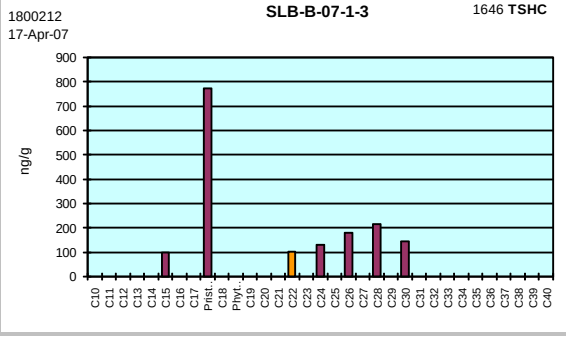
1800212
17-Apr-07
SLB-B-07-1-3
1646 TSHC
ng/g
Prist.
Phyt.

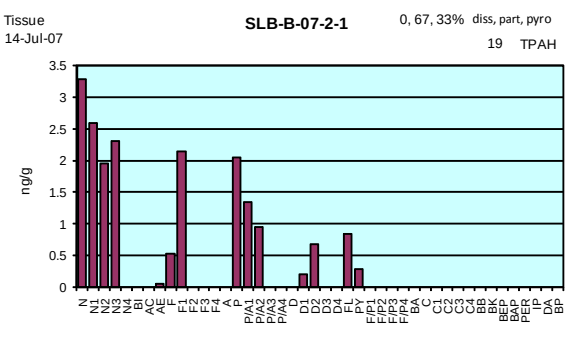
Tissue
14-Jul-07
SLB-B-07-2-1
0, 67, 33% diss, part, pyro
19 TPAH
ng/g

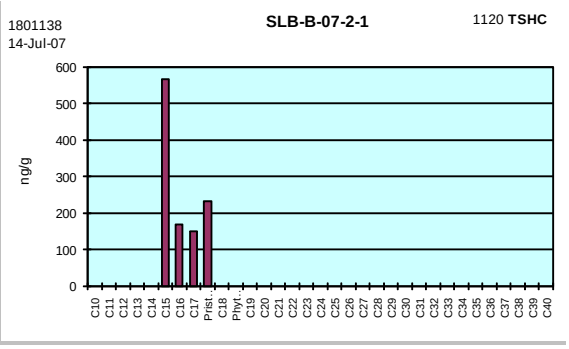
1801138
14-Jul-07
SLB-B-07-2-1
1120 TSHC
ng/g

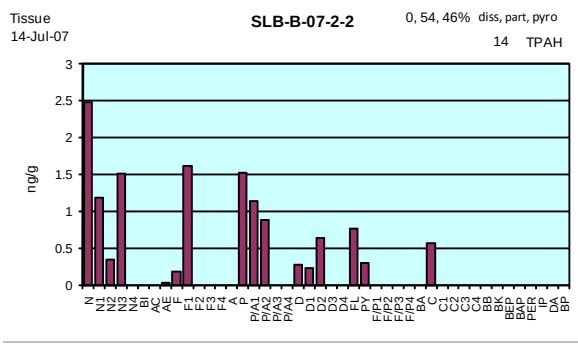
Tissue
14-Jul-07
SLB-B-07-2-2
0, 54, 46% diss, part, pyro
14 TPAH
ng/g

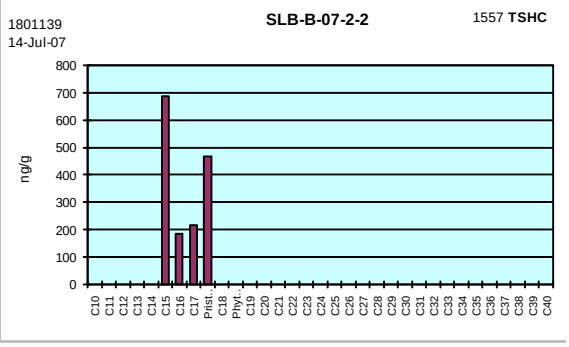
1801139
14-Jul-07
SLB-B-07-2-2
1557 TSHC
ng/g

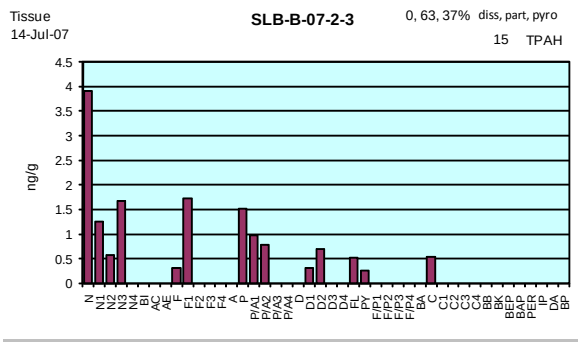
Tissue
14-Jul-07
SLB-B-07-2-3
0, 63, 37% diss, part, pyro
15 TPAH
ng/g

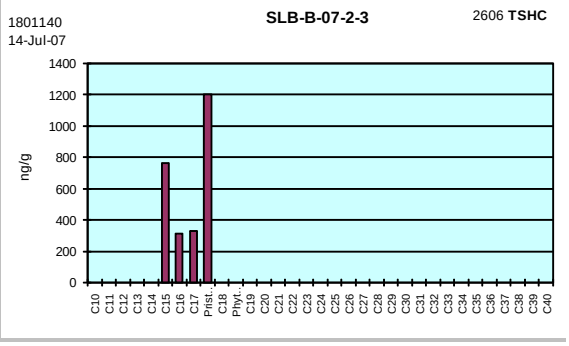
1801140
14-Jul-07
SLB-B-07-2-3
2606 TSHC
ng/g

Tissue
25-Jul-06

WIB-B-06-2-1

60, 42, 1% diss, part, pyro

19 TPAH

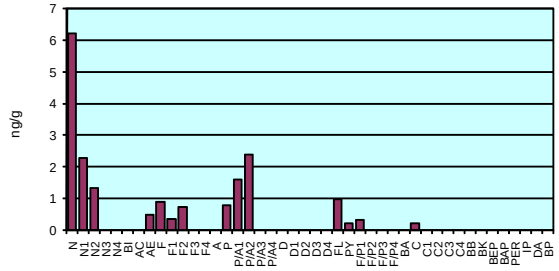

1701901
25-Jul-06

WIB-B-06-2-1

1324 **TSHC**

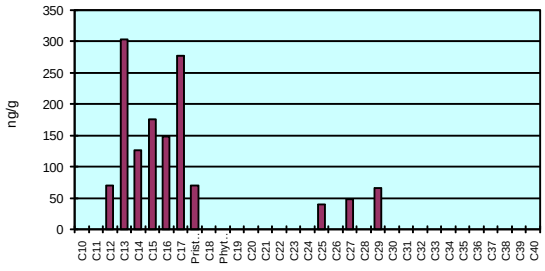

Tissue
25-Jul-06

WIB-B-06-2-2

51, 48, 9% diss, part, pyro

23 TPAH

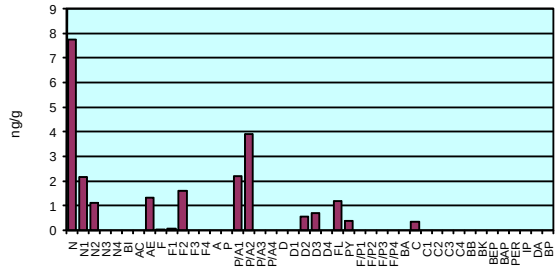

1701902
25-Jul-06

WIB-B-06-2-2

1400 **TSHC**

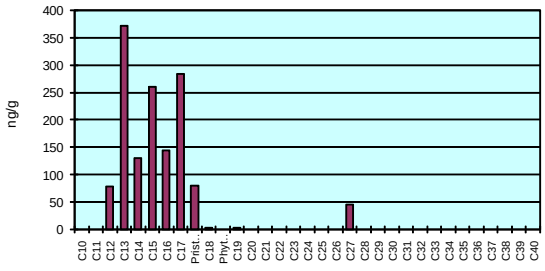

Tissue
25-Jul-06

WIB-B-06-2-3

0, 98, 7% diss, part, pyro

25 TPAH

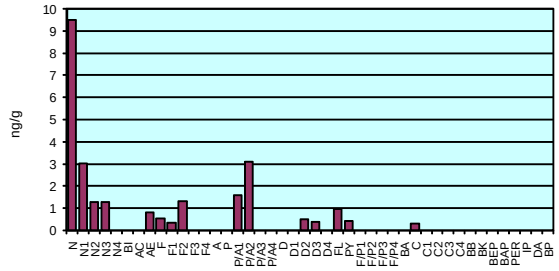

1701903
25-Jul-06

WIB-B-06-2-3

1100 **TSHC**

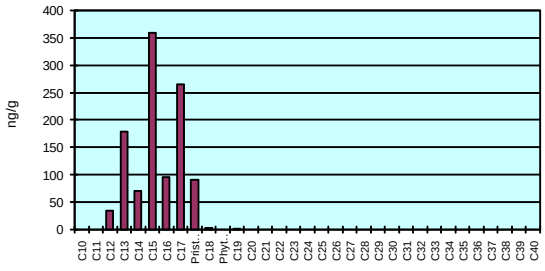

Tissue
17-Apr-07

WIB-B-07-1-1

100, 3, 0% diss, part, pyro

22 TPAH

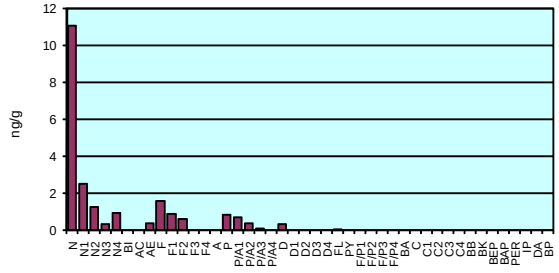

1800204
17-Apr-07

WIB-B-07-1-1

452 **TSHC**

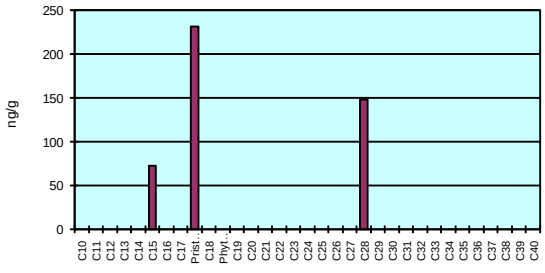

Tissue
17-Apr-07

WIB-B-07-1-2

82, 18, 2% diss, part, pyro

25 TPAH

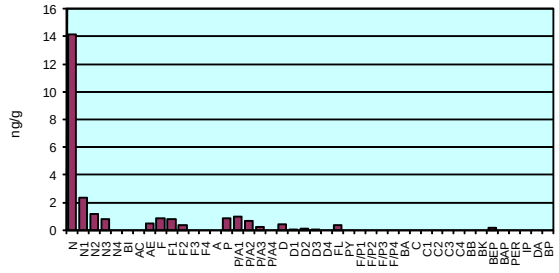

1800205
17-Apr-07

WIB-B-07-1-2

275 **TSHC**

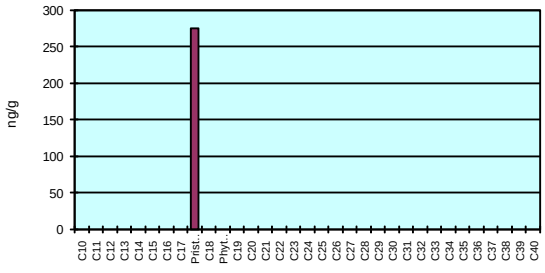

Tissue
17-Apr-07

WIB-B-07-1-3

99, 4, 1% diss, part, pyro

28 TPAH

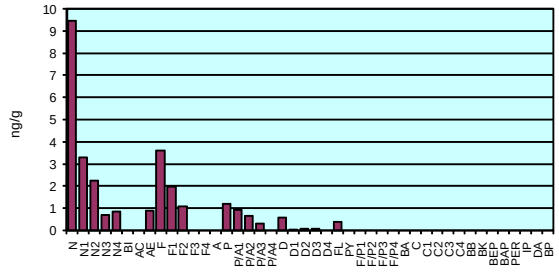

1800206
17-Apr-07

WIB-B-07-1-3

1441 **TSHC**

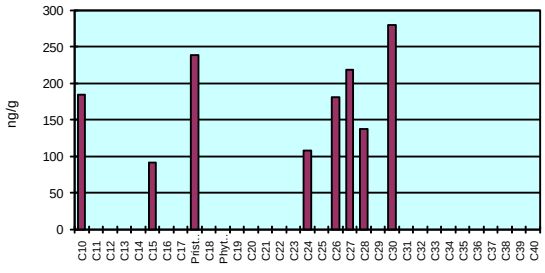

Tissue
28-Jul-07

WIB-B-07-2-1

78, 19, 3% diss, part, pyro

9 TPAH

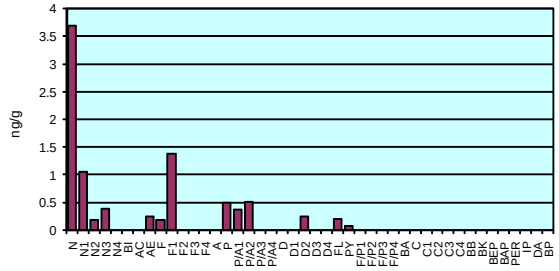

1801204
28-Jul-07

WIB-B-07-2-1

2086 **TSHC**

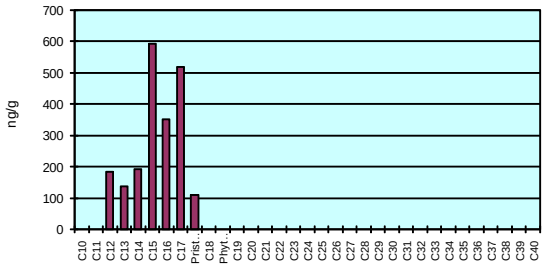

Tissue
28-Jul-07

WIB-B-07-2-2

99, 0, 1% diss, part, pyro

9 TPAH

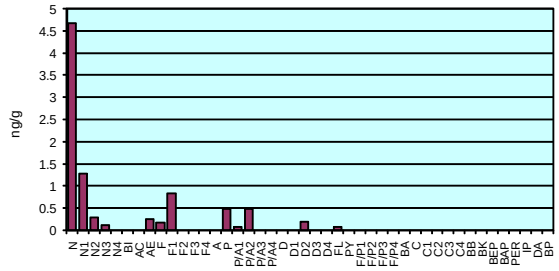

1801205
28-Jul-07

WIB-B-07-2-2

2201 **TSHC**

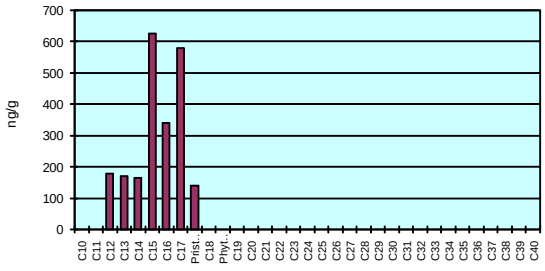

Tissue
28-Jul-07

WIB-B-07-2-3

95, 0, 5% diss, part, pyro

8 TPAH

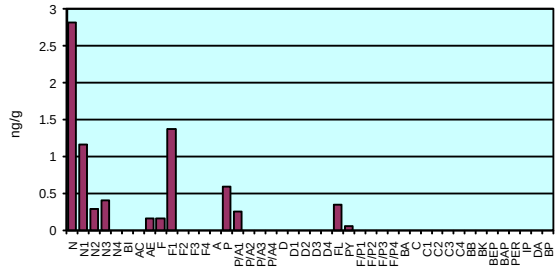

1801206
28-Jul-07

WIB-B-07-2-3

1651 **TSHC**

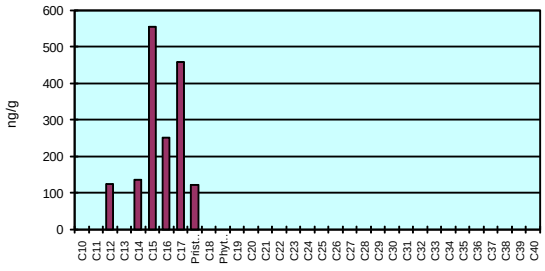

Tissue
27-Jul-06

ZAB-B-06-2-1

84, 0, 5% diss, part, pyro

28 TPAH

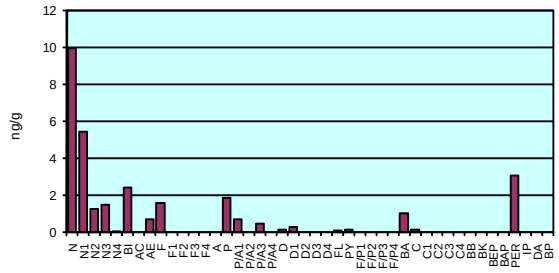

1701916
27-Jul-06

ZAB-B-06-2-1

748 **TSHC**

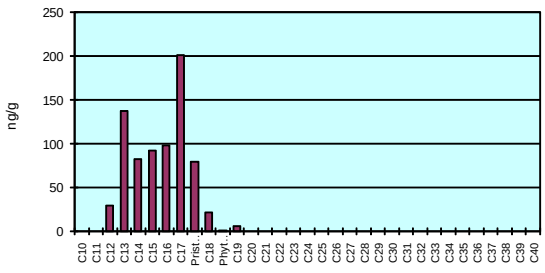

Tissue
27-Jul-06

ZAB-B-06-2-2

98, 0, 2% diss, part, pyro

25 TPAH

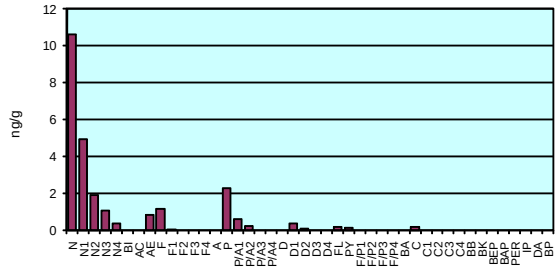

1701917
27-Jul-06

ZAB-B-06-2-2

1025 **TSHC**

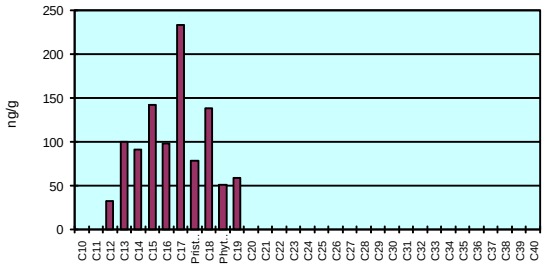

Tissue
27-Jul-06

ZAB-B-06-2-3

98, 0, 2% diss, part, pyro

22 TPAH

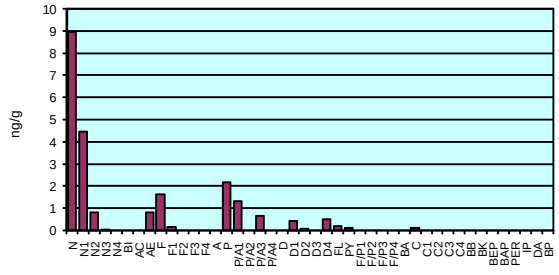

1701918
27-Jul-06

ZAB-B-06-2-3

715 **TSHC**

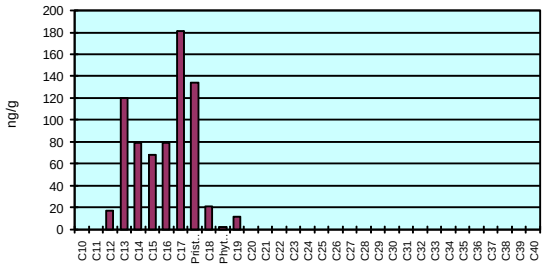

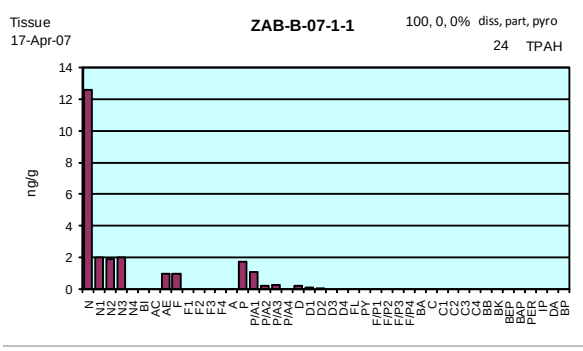
Tissue
17-Apr-07
ZAB-B-07-1-1
100, 0, 0% diss, part, pyro
24 TPAH
ng/g

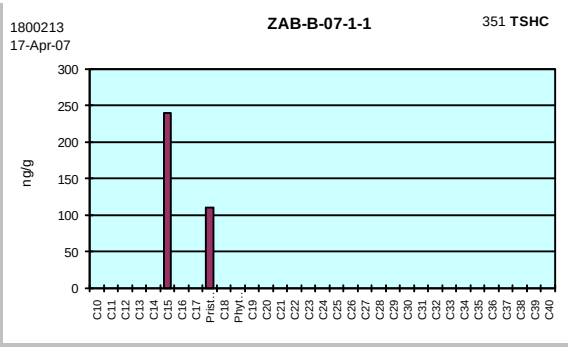
1800213
17-Apr-07
ZAB-B-07-1-1
351 TSHC
ng/g

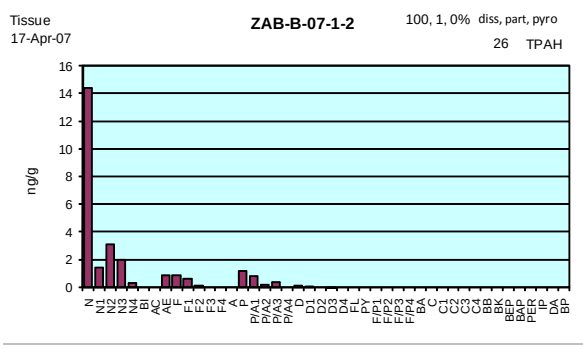
Tissue
17-Apr-07
ZAB-B-07-1-2
100, 1, 0% diss, part, pyro
26 TPAH
ng/g

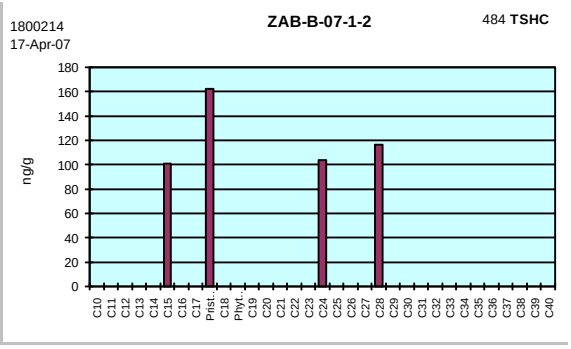
1800214
17-Apr-07
ZAB-B-07-1-2
484 TSHC
ng/g

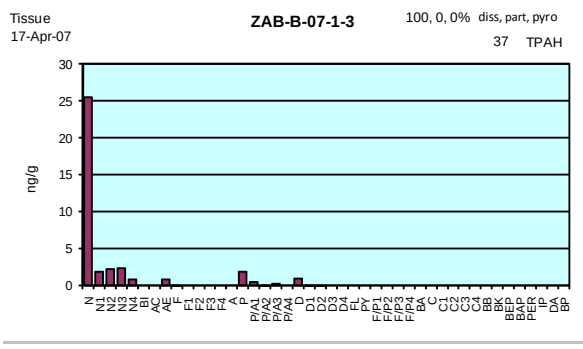
Tissue
17-Apr-07
ZAB-B-07-1-3
100, 0, 0% diss, part, pyro
37 TPAH
ng/g

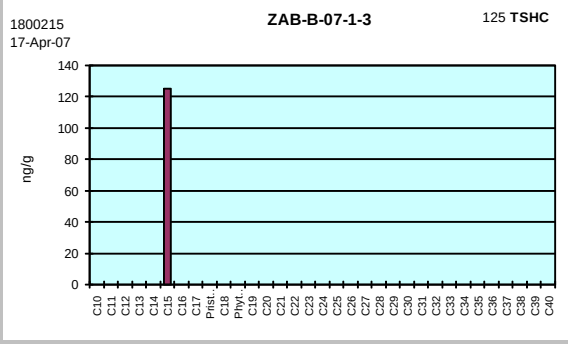
1800215
17-Apr-07
ZAB-B-07-1-3
125 TSHC
ng/g

Tissue
12-Jul-07

ZAB-B-07-2-1

0, 100, 0% diss, part, pyro

12 TPAH

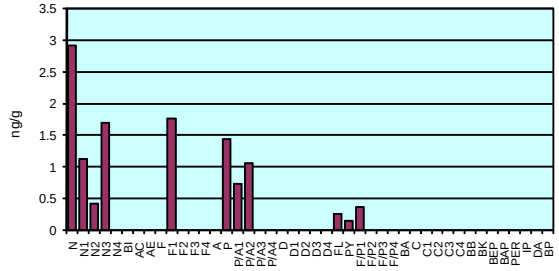

1801135
12-Jul-07

ZAB-B-07-2-1

1109 **TSHC**

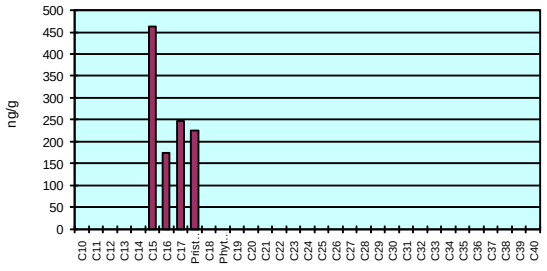

Tissue
12-Jul-07

ZAB-B-07-2-1D

97, 0, 3% diss, part, pyro

11 TPAH

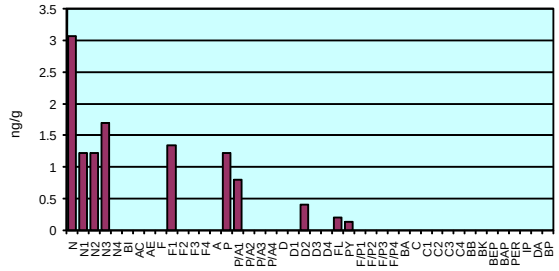

1801135
12-Jul-07

ZAB-B-07-2-1D

868 **TSHC**

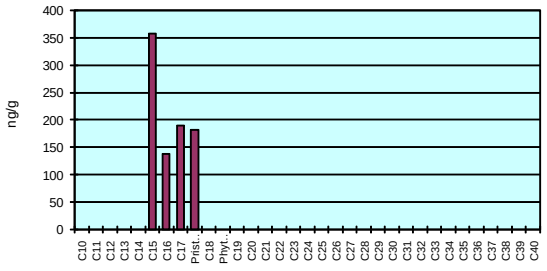

Tissue
12-Jul-07

ZAB-B-07-2-2

96, 0, 4% diss, part, pyro

18 TPAH

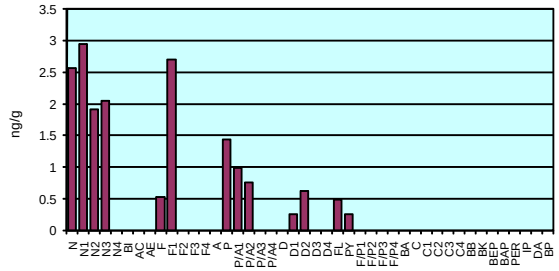

1801136
12-Jul-07

ZAB-B-07-2-2

1342 **TSHC**

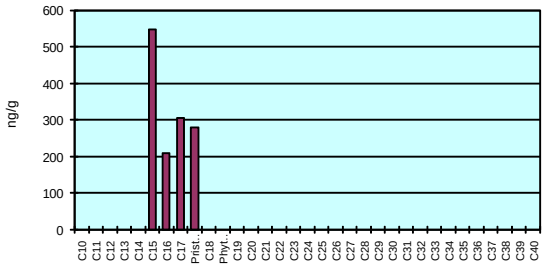

Tissue
12-Jul-07

ZAB-B-07-2-3

72, 33, 1% diss, part, pyro

198 TPAH

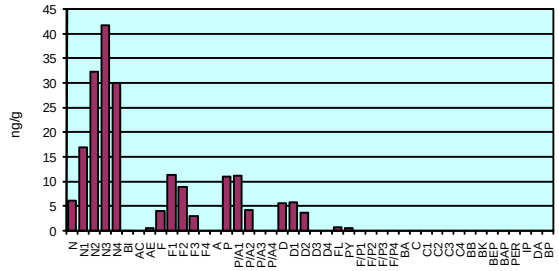

1801137
12-Jul-07

ZAB-B-07-2-3

1402 **TSHC**

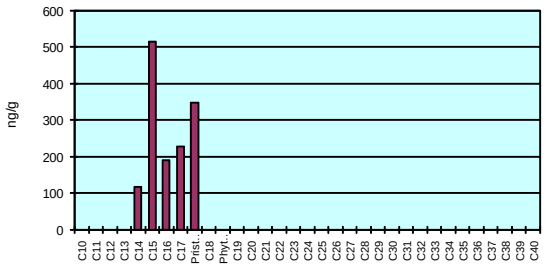

APPENDIX E Investigations into a Possible Source for the Dissolved-Phase Signals Observed in LTEMP Mytilus Samples

Introduction and Objectives

Over the sixteen years of monitoring PAH and SHC contaminants in *Mytilus* samples as part of the LTEMP effort, several specific oil-spill events (e.g., the 1994 *Eastern Lion* oil spill at the Alyeska Marine Terminal, the 1997 Ballast Water Treatment Facility sheening event, and the 2004 mystery diesel spill at Gold Creek), as well as the gradual recovery from *Exxon Valdez* Oil Spill (EVOS) impacts at Disk Island and Sleepy Bay, have all been well documented. At many station locations, however, a ubiquitous background signal of dissolved-phase lower-molecular-weight components (e.g., naphthalenes, biphenyl, fluorenes, and phenanthrenes/anthracenes) has been observed, and it has become more dominant as PAH signals from EVOS and other sources have decreased over time.

The source of the ubiquitous dissolved-phase PAH signal has remained a mystery, although possibilities include atmospheric deposition of dust and soot, forest fires, leaching of water-soluble constituents from the pervasive source-rock (oil shale or coal that constitutes much of the suspended sediments being transported through the region), some upwelling/climate-driven events, residues leaching from buried EVOS oil in Prince William Sound, and on a more localized scale harbor operations, wastewater discharges, and small oil and diesel spills. Leaching from buried EVOS residues, while demonstrated on local scales (Payne et al., 2005a,b), would not explain the region-wide observations in areas that were not impacted by the spill and the fact that the dissolved-phase signal was observed before EVOS (Karinen et al., 1993). Likewise, the other localized sources listed would not be expected to contribute to a region-wide signal.

The sources of PAH in Gulf of Alaska and Prince William Sound sediments have been the subject of intense and hotly debated research for over 15 years (Page et al., 1993, 1995; Short and Babcock 1996; Short, et al., 1999; Boehm, et al., 2001; Short, et al., 2007). It is now generally accepted that sediment bound PAH can be attributed to input from suspended particulate material (SPM) derived from eroded source-rock, coal, and organic material (e.g., kerogen) along with several natural oil seeps that drain into the glacial rivers and streams that feed into the Alaska Coastal Current along the Gulf of Alaska coastline southeast of the Sound (Figure 45). In addition to water-borne sources of suspended particulate material, aeolian input of fine particulate material from the Copper River drainage has also been documented (Figure 46). Other sources of particulate PAH to the sediments include atmospheric dust, smoke and haze from forest fires, oil spills (including buried EVOS residues within Prince William Sound), earthquake related spills, terminal and tanker operations, discharges from commercial-, fishing-, and recreational-boating activities, and other anthropogenic and natural sources from localized harbor operations and historic human habitation sites. Up to this time, however, these particulate/sediment-bound PAH have not been generally considered to be bioavailable, and they were not believed to be a possible source for the dissolved-phase components observed in the mussels.

In an effort to evaluate the possibility that water soluble constituents may be leaching from the water-borne sedimentary materials themselves, a modest experiment was conducted as part of the EVOS Trustees-sponsored SCAT VII Program in July 2007.

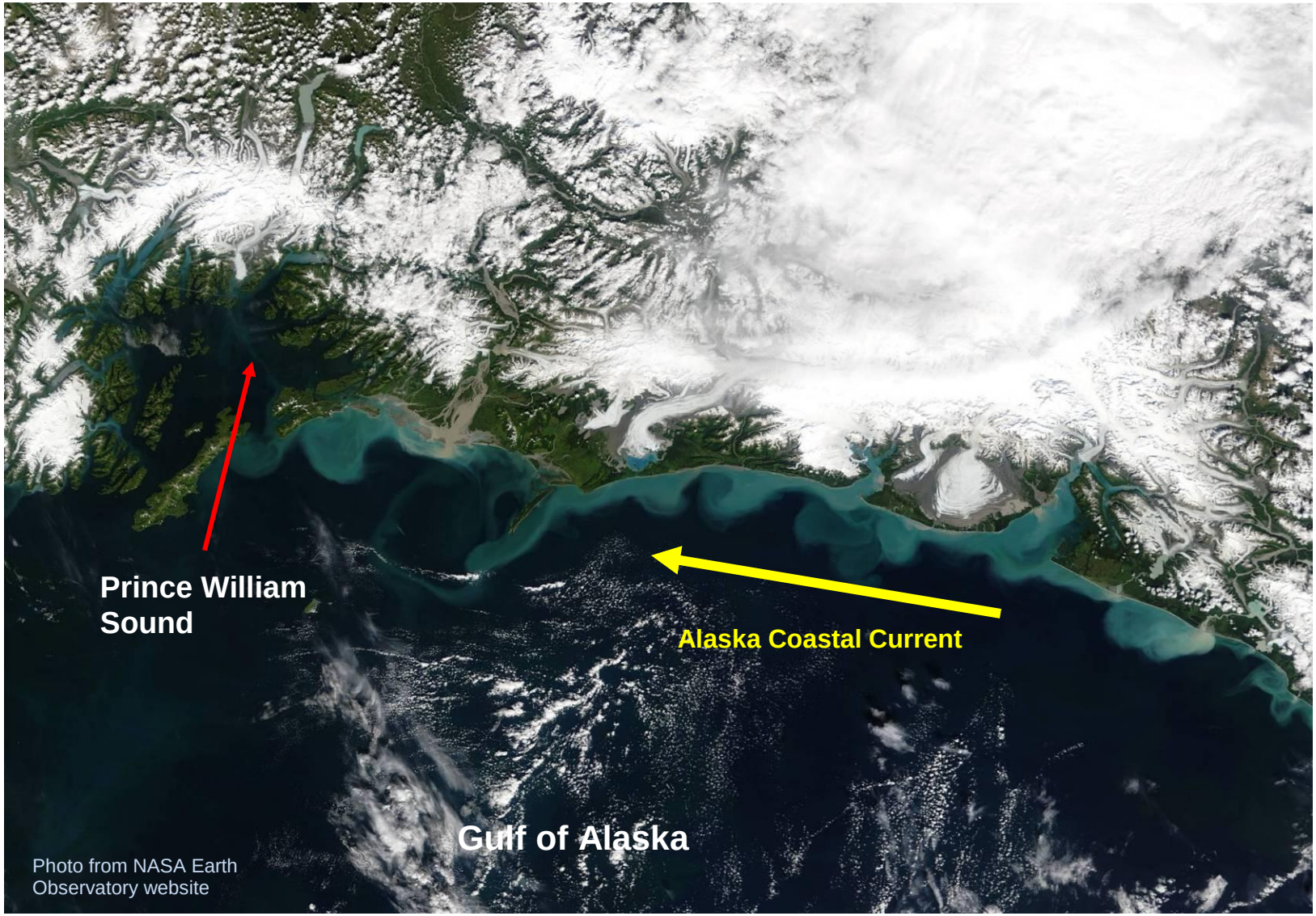

Figure 45 Satellite image showing glacial and Copper River borne sediment plumes introduced into the Alaska Coastal Current, August 2003.

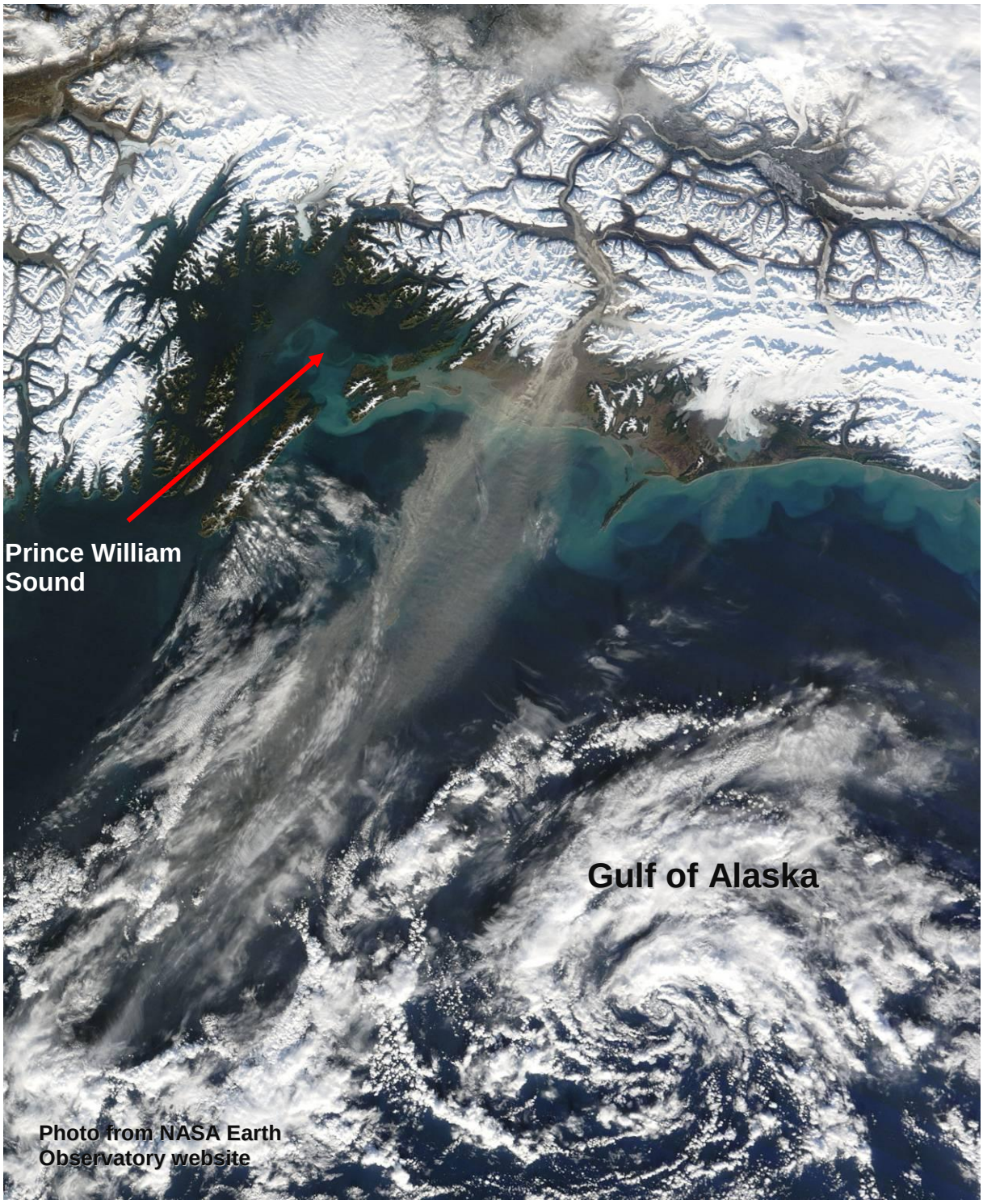

Figure 46 Satellite image of Copper River silt and clay (light gray color) transported during a strong offshore wind event on October 30, 2009. Water-borne sediment plumes are also seen along the shoreline carried by the Alaska Coastal Current.

We have known that Constantine Harbor receives PAH bearing sedimentary deposits from SPM introduced to Prince William Sound by the Alaska Coastal Current sweeping the Gulf of Alaska coastline southeast of the Sound (Short and Babcock 1996), and yet the mussel collections from this site reflect only the background dissolved-phase PAH signal and biogenic saturated hydrocarbons (SHC) from marine and terrestrial sources observed at other non-EVOS impacted sites (Figure 47; Payne et al., 2008b).

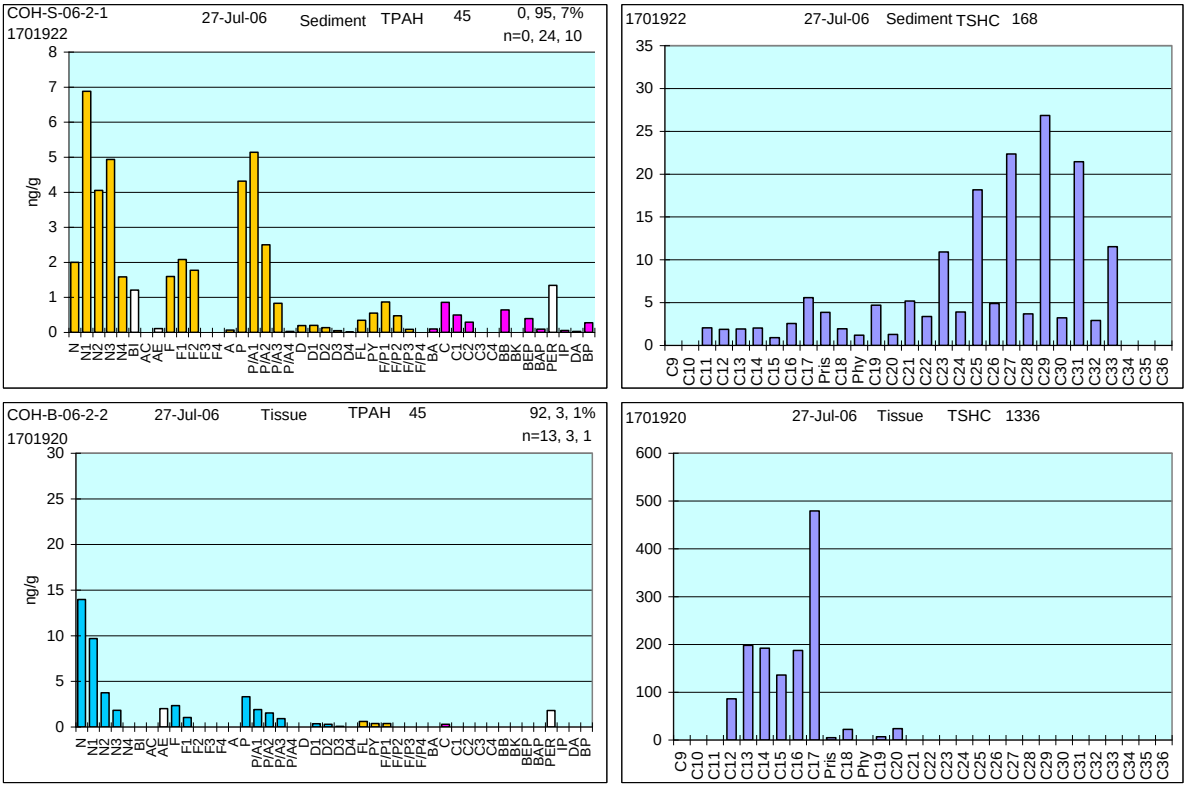

Figure 47 PAH and SHC histograms of collocated Constantine Harbor intertidal sediment and mussel samples collected in July 2006.

The sediments (upper graphs) show the background Alaska Coastal Current-derived petrogenic PAH and a mixture of marine- and terrestrial-sourced biogenic SHC, while the mussels (lower graphs) show only the pervasive dissolved-phase PAH and marine biogenic-sourced SHC signals (Figure 47). The mussels are clearly not directly contaminated by the sediments. Based on these observations, a pilot experiment was designed to determine if the intertidal sediments from this location would leach dissolved-phase components like those observed in the mussels throughout Prince William Sound.

Methods

The experimental approach for the partitioning/equilibration experiment consisted of first filling five one-gallon (3.8 L) amber glass jugs with "clean" seawater from the Hinchinbrook Entrance between Hinchinbrook and Montague Islands, the primary ocean entrance to PWS. The seawater samples were collected with a 4-L GoFlo Bottle® (Figure 48) designed to pass through the air-sea interface while closed to avoid possible contamination by surface microfilms. After collection, the seawater samples were directly transferred into the I-Chem Certified-Clean® amber glass jugs and stored in the dark below deck in the forward cabin of the *M/V Auklet*.

The next morning, the LTEMP station in Constantine Harbor on Hinchinbrook Island was occupied approximately one-hour before low tide (Figure 49); however, before any other sampling was undertaken, PECI's Portable Large Volume Water Sampling System (PLVWSS) was set up adjacent to the water's edge, and a near-shore water sample was collected (Figure 50 and Figure 51). The PLVWSS is designed to allow filtration of a water sample through a 0.7-µm glass fiber filter at the time of collection to provide separate dissolved- and particulate-phase samples (Payne et al., 1999; 2005a,b). After collection, the filtered water sample (contained in an I-Chem 3.8 L amber-glass jug) was stored in the dark until extraction (see below), and the filter (containing the particulate fraction) was placed in an I-Chem Certified-Clean® wide-mouth jar and frozen.

After the near-shore water sample was collected, a shallow pit (~ 20 cm deep) was excavated on-shore just above the water-line, and interstitial water was allowed to percolate into the excavation. The first interstitial water to fill the hole was carefully scooped out to remove the bulk of suspended sediments generated by digging, and additional interstitial water was allowed to percolate into the excavation over a 20-minute period. The PLVWSS was again utilized to collect a filtered sample of the freshly infiltrated interstitial water and associated SPM (see Payne et al., 2005a,b for details). While these activities were being completed, bulk intertidal sediments for the sediment/seawater partitioning experiments and the LTEMP mussels from several gravel/*Fucus* zones on the beach were collected (both operations up-wind of the portable generator used for the PLVWSS vacuum pump).

Upon returning to the *M/V Auklet*, different amounts of intertidal sediment were added to each bottle to assess the effect of sediment loading on PAH partitioning (Table 8, Figure 52 and Figure 53). The nine amber-glass jugs (treatments) were stored in the dark and shaken end-over-end twice each day for 30 seconds until the experiment was completed four days later. Random agitation was also provided by the moving vessel.

Figure 48 Seawater collection from the *M/V Auklet* using a 4-L GoFlo Bottle®.

Figure 49 LTEMP station at Constantine Harbor, Hinchinbrook Island. Note the otter foraging pits in the foreground.

Figure 50. Portable Large Volume Water Sampling System (PLVWSS) set up adjacent to the water's edge. The filter unit is on top of the cruise box in the middle left side of the photograph. The portable generator for the vacuum unit (connected by the orange extension cord) was ~ 25 m downwind from the sampling station.

Figure 51 Wand and vacuum tubing used to collect a near-shore surface water sample.

Figure 52 Weighing sediments for each treatment.

Figure 53 Adding sediment to the jug of seawater.

After four days, the jug mixtures were processed on the back deck of the *M/V Auklet* with the PLVWSS to separate the dissolved-phase and particulate/SPM-bound components. Starting with the cleanest samples (i.e. background seawater, near-shore water, 4.2 g-sediment loading, 16.8 g-sediment loading, 31.3 g-sediment loading, 148.6-g sediment loading, and interstitial pore-water from the intertidal pit), the samples were sequentially agitated for two minutes, and the contents vacuum filtered through the PLVWSS (Figure 54 through Figure 57).

After filtration, the SPM fractions on the glass-fiber filters were placed in wide-mouth I-Chem jars and frozen for later transport to the NOAA Auke Bay Laboratory. The filtered seawater samples in new amber-glass jugs were then spiked with a NOAA surrogate recovery standard (Payne et al., 2005a,b), and starting with the cleanest samples, they were sequentially extracted with methylene chloride on the rear deck of the *M/V Auklet* (Figure 58 and Figure 59) using NOAA's Interstitial Water Field Extraction Protocol (Payne et al., 2005a,b). The methylene chloride extracts were stored in amber 250 mL I-Chem narrow-neck bottles in a freezer until they were later transferred to the NOAA Auke Bay Laboratory.

Table 8. Extracted Sample Volumes and Notes for Seawater, Sediment, and SPM Fractions Collected During 2007 EVOS SCAT VII Program.

ABL COC No.	Sample ID	Extracted Seawater Volume (L)	Comments
1801310	Jug # 1 (SW Blank) – field extracted	3.55	DCM extract of Seawater (SW) poured directly into amber jug from GoFlo® Bottle
1801311	Jug # 6 (Hardware Blank)) – field extracted	3.66	DCM extract of SW through PLVWSS[2] but no filter
1801312	Jug # 7 (PLVWSS System Blank)) – field extracted	3.93	DCM extract of SW through PLVWSS with filter (Dissolved PLVWSS system blank)
1801301	Filter # 1 (SW exposed Filter Blank)	3.93	Frozen SPM/filter from Jug # 7 (Particulate PLVWSS system blank)
1801313	Jug # 8) – field extracted	3.99	DCM extract of Constantine HBR nearshore water
1801302	Filter # 2	3.99	Frozen SPM/filter from Jug # 8
1801314	Jug # 2) – field extracted	3.07	DCM extract of SW w 4.2 g Constantine HBR Sediment suspended and agitated 2x per day for 4 days
1801306	Filter # 4	3.07	Frozen SPM/filter from Jug # 2
1801315	Jug # 3) – field extracted	2.90	DCM extract of SW w 16.8 g Constantine HBR Sediment suspended and agitated 2x per day for 4 days
1801307	Filter # 5	2.90	Frozen SPM/filter from Jug # 3
1801316	Jug # 4) – field extracted	2.90	DCM extract of SW w 31.3 g Constantine HBR Sediment suspended and agitated 2x per day for 4 days
1801308	Filter # 6	2.90	Frozen SPM/filter from Jug # 4
1801317	Jug # 5) – field extracted	3.03	DCM extract of SW w 148.6 g Constantine HBR Sediment suspended and agitated 2x per day for 4 days
1801309	Filter # 7	3.03	Frozen SPM/filter from Jug # 5
1801318	Jug # 9) – field extracted	3.27	DCM extract of interstitial water pumped from intertidal pit on Constantine HBR shoreline
1801303	Filter # 3	3.27	Frozen SPM/filter from Jug # 9
1801304	CNST SPK SED	n.a.	Constantine HBR intertidal sediment used for SW equilibration experiments (analyze for PAH and SHC)
1801305	CNST SPK SED (pgs)	n.a.	Constantine HBR intertidal sediment used for SW equilibration experiments (analyze for PGS)

Note: All seawater (SW) samples were spiked with 500 uL of "Surrogate Water Spike" (p 99 PWS-342) before being extracted onboard the *Auklet*. The associated SPM samples were not spiked, but simply frozen on the glass-fiber filter used to separate them.

Figure 54 Placing a clean 0.7 µm glass fiber filter into the PLVWSS before sediment/ seawater sample processing.

Figure 55 Vacuum filtration of a sediment/seawater sample after four days of mixing.

Figure 56 Vacuum filtration collecting the dissolved phase from a sample.

Figure 57 Removal of the filter showing the isolated suspended sediment portion of the sample.

Figure 58 Filtered seawater samples before surrogate spiking and extraction on the rear deck of the *M/V Auklet*.

Figure 59 Separatory-funnel extraction of the filtered seawater samples.

All of the dissolved-phase (filtered) sample extracts were analyzed by Selected Ion Monitoring GC/MS at the Auke Bay Laboratory utilizing the protocols described in Payne et al., (2008). Results are surrogate-recovery corrected and are reported on a per-liter of seawater-extracted basis (Table 8). The frozen glass fiber filters containing the separated SPM phase were spiked with surrogate recovery standards at the NOAA Auke Bay Laboratory and extracted with the same protocols used for LTEMP sediments. Concentrations of PAH and SHC on the filters are surrogate-recovery corrected and, like their corresponding water samples, are reported on a per-liter of seawater-extracted basis (Table 8).

Results and Discussion

The unfiltered background seawater sample collected from Hinchinbrook Entrance (Figure 60, top panel) shows low-level dissolved- and particulate-phase PAH components associated with the trace levels of glacially derived suspended particulate material (SPM) from the Alaska Coastal Current. When this seawater was partitioned against increasing amounts of intertidal sediment and then filtered through the 0.7-µm glass fiber filters in the PLVWSS, increased concentrations of dissolved-phase naphthalene, C1-naphthalene, and biphenyl were seen (Figure 60, second and third panels). At the highest sediment loading (148 ng/g wet weight), the PAH profile is essentially identical to the one obtained from the interstitial water collected from the shallow pit excavated in the intertidal zone at Constantine Harbor (Figure 60, third and fourth panels). Other PAH components present in the starting seawater are still observed, but as will be discussed below, increasing SPM loads appear to remove the higher-molecular-weight constituents by adsorption and physical sequestering during filtration.

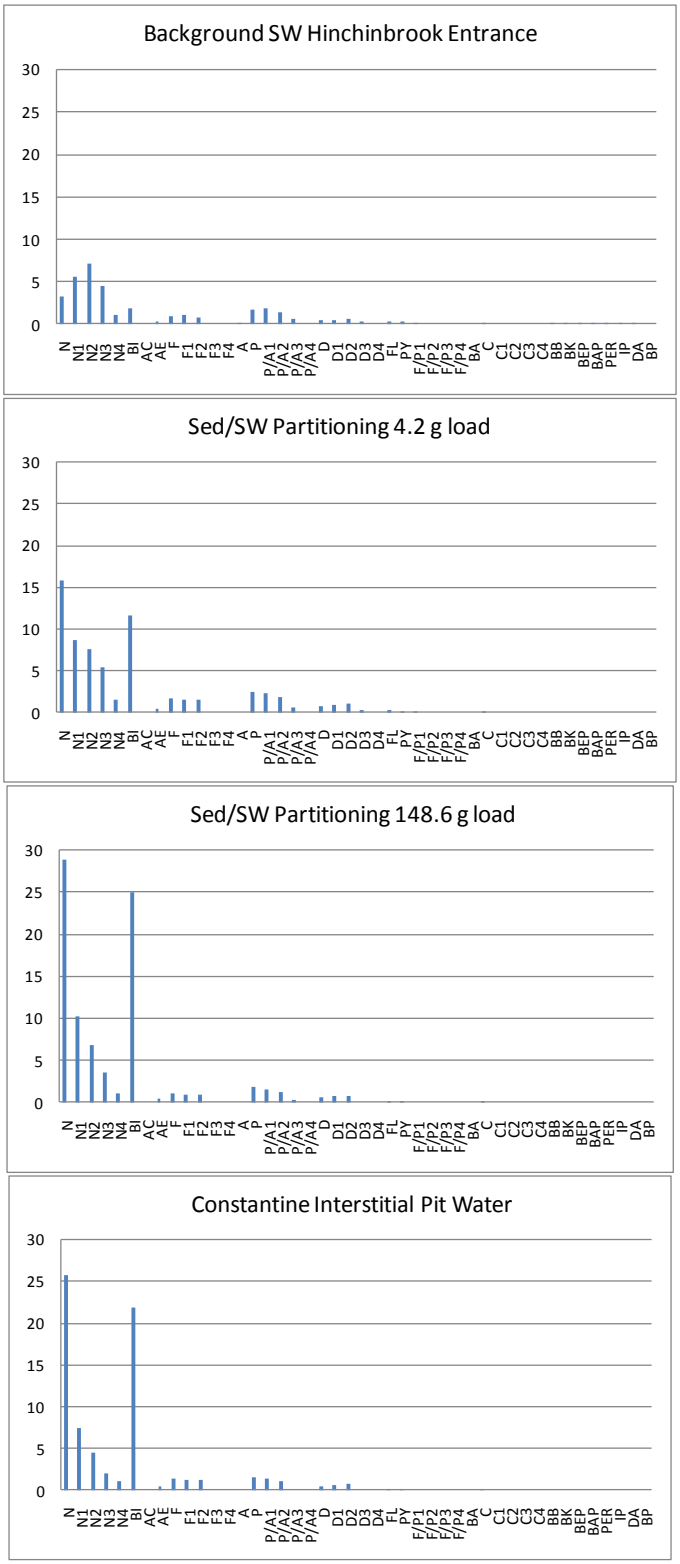

Figure 60 PAH Seawater extracts from sediment partitioning experiments. Background seawater from the Hinchinbrook Entrance, two filtered samples with different sediment loadings, and filtered interstitial water from the intertidal pit in Constantine Harbor. All concentrations are in ng/L.

The effect of the intertidal sediment loading on dissolved-phase PAH concentrations is even more apparent when the concentrations in the filtered-seawater samples are plotted against the nominal intertidal sediment loading (Figure 61). In the case of naphthalene, C1-naphthalene, and biphenyl, there is a strong correlation between the measured dissolved-phase concentration and the amount of intertidal sediment placed in the amber-glass jug for the partitioning experiment. For these three most water-soluble constituents (with the lowest octanol-water partitioning coefficients [K_{ow}], Table 9), the dissolved-phase concentrations increase with increasing sediment load. As the log K_{ow} values for the higher alkylated two-ring naphthalenes and the three-ring PAH increase, however, the effect of the increased SPM load is to remove the dissolved-phase components (Figure 61 and Figure 62) as the molecular weight and degree of alkylation increase. This trend follows accepted increased particulate adsorption behavior of dissolved components (for a general review see, American Chemical Society (ACS) 1997 and for oil/SPM interactions see Payne et al., 2003, and references therein).

To ensure that the observed increases in two ring PAH concentrations in the dissolved phase seawater extracts were not due to breakthrough of particulate-phase components through the 0.7 µm glass fiber filters, the PAH profile of the SPM phase on those filters was also examined (Figure 63). In this instance, there are a number of higher-molecular-weight PAH (dibenzothiophenes, fluoranthene/pyrenes, and chrysenes) observed that are not present in the filtered seawater extracts (Figure 60). Had breakthrough of the particulate-phase occurred, these components would have been observed in the filtered seawater extracts, and the very characteristic relative abundance patterns of the alkylated naphthalenes, fluorenes, phenanthrenes/anthracenes, and dibenzothiophenes from the particulate phase (Figure 63) would have been dominant. Clearly, they are not, and instead, the filtered water samples (Figure 60) contain only the dissolved-phase (parent PAH > C1 > C2 > C3 homologue) pattern for the naphthalenes, fluorenes, and phenanthrene/anthracenes, similar to the patterns observed in many mussel samples examined in LTEMP.

Finally, to confirm that the nominal sediment/SPM additions used in these experiments were indeed providing increasing individual and total PAH loadings as desired, the individual PAH and TPAH measured on the SPM trapped on each of the filters was examined as a function of initial sediment loading. Only the data for the TPAH vs. sediment loading are presented here (Figure 64), but the same trend was observed for each of the individual PAH and the TPAH shown in the figure. The data show that the PAH exposure ranged over nearly an order of magnitude, and that there was a strong correlation with the nominal sediment loading.

Based on these initial measurements, we feel that additional research should focus on this partitioning behavior with a wider variety of sediment types, and that these studies might incorporate exposed mussel populations to filtered and unfiltered seawater generated from the partitioning experiments under controlled laboratory conditions. We believe that it is clear from these initial scoping experiments, however, that the dissolved-phase

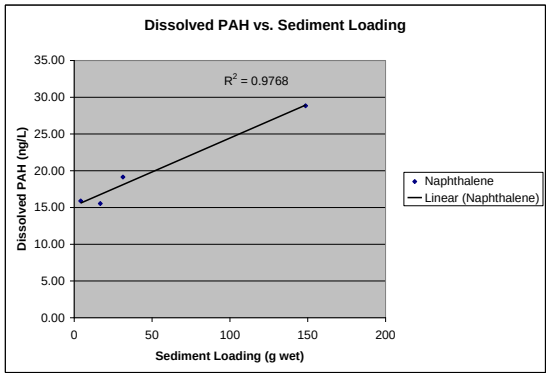

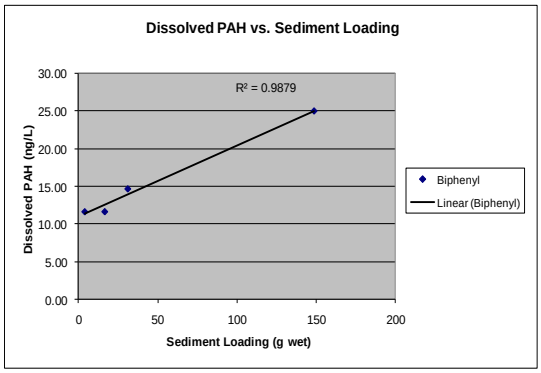

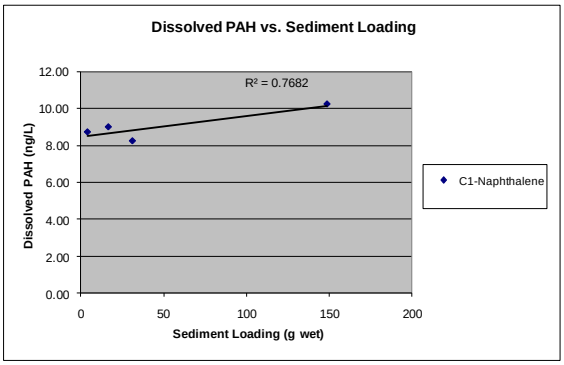

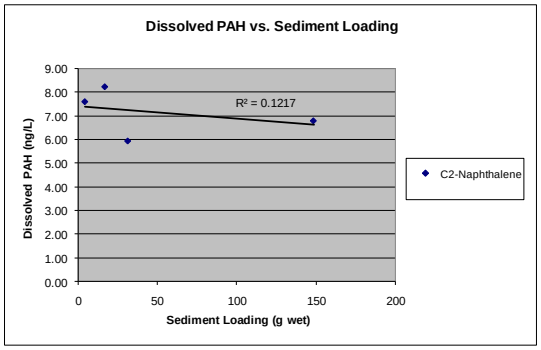

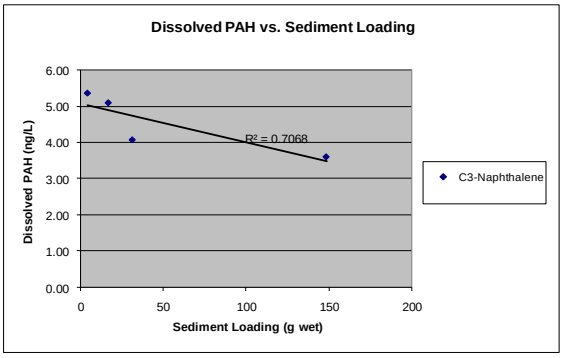

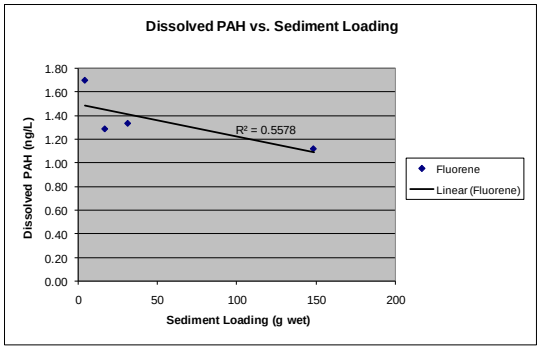

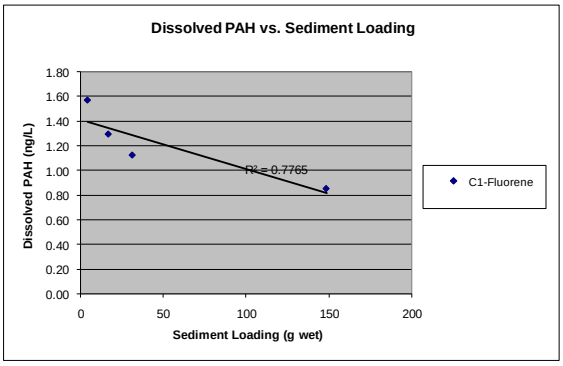

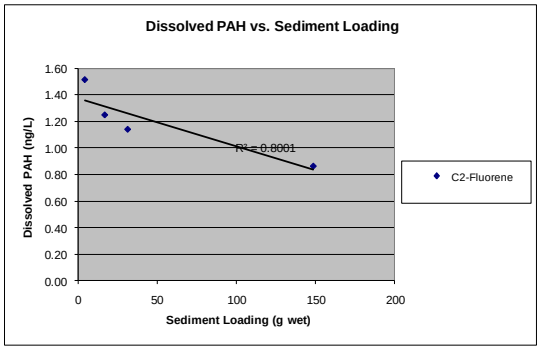

Figure 61 Dissolved-phase (filtered sample) concentrations of naphthalene, biphenyl, and fluorene homologues vs. Constantine Harbor intertidal sediment loading after four days of equilibration/partitioning.

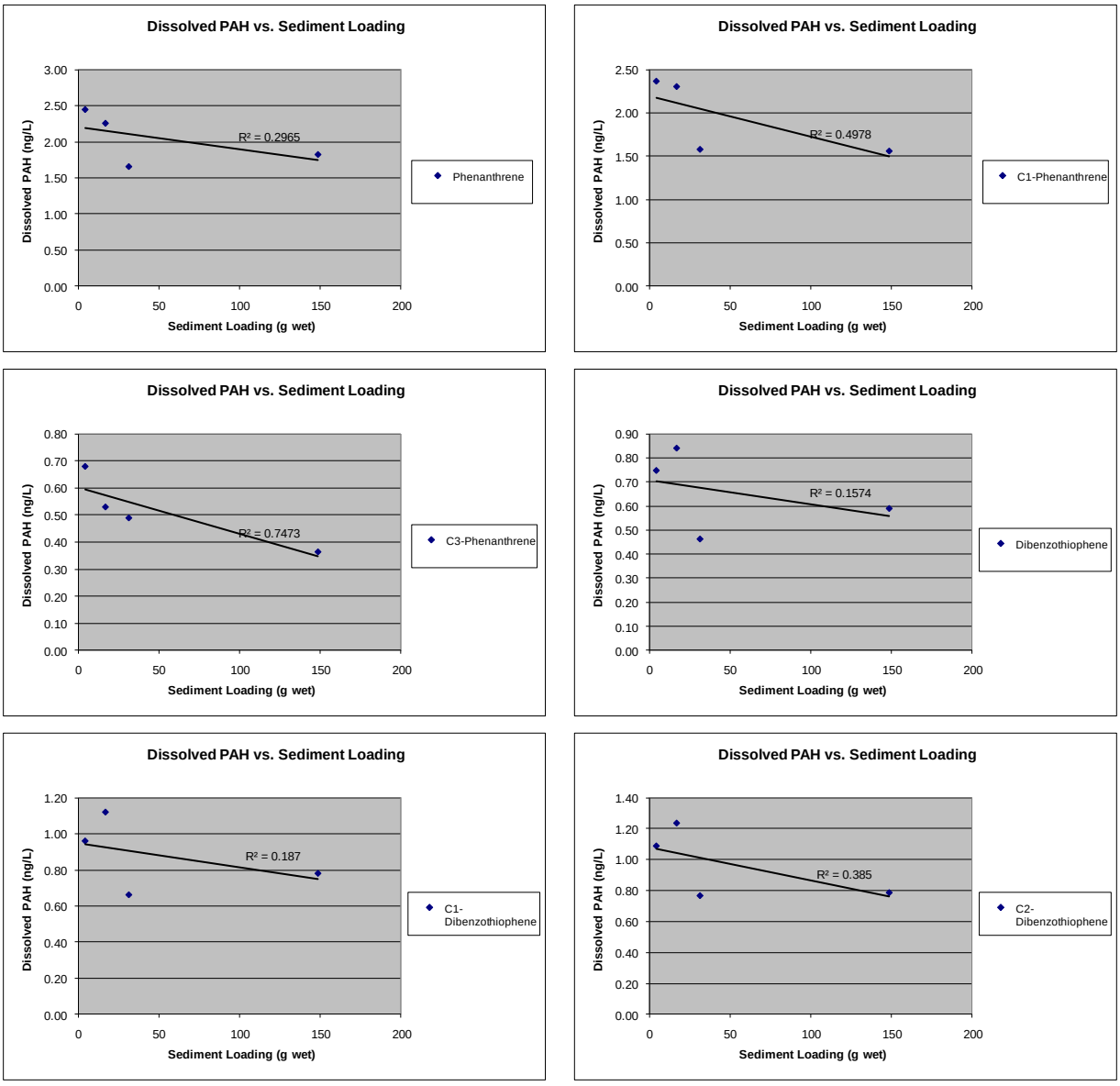

Figure 62 Dissolved-phase (filtered sample) concentrations of phenanthrene and dibenzothiophene homologues vs. Constantine Harbor intertidal sediment loading after four days of equilibration/partitioning.

Table 9 Log K_{ow} (Octanol-Water Partition Coefficients) used for modeling monoaromatic and polycyclic aromatic hydrocarbon dissolution behavior
(from Lee et al., 1992; Mackay et al., 1992a,b; and French-McCay 2001, 2002).

PAH	Mol. Wt. g/mol	Log Kow	Model Cut #	
benzene	78	2.13	1	
Toluene	92	2.69	1	
Ethylbenzene	106	3.13	1	
o-Xylene	106	3.15	1	
p-Xylene	106	3.18	1	
m-Xylene	106	3.2	1	
Xylenes	106	3.18	1	
styrene	104	3.05	1	
methylstyrenes	118	3.35	1	
1,2,3-Trimethylbenzene	120	3.55	1	
1,2,4-Trimethylbenzene	120	3.6	1	
1,3,4-Trimethylbenzene	120	3.6	1	
1,3,5-Trimethylbenzene	120	3.58	1	
Trimethylbenzenes	120	3.58	1	
n-propylbenzene	120	3.69	1	
iso-propylbenzene	120	3.63	1	
ethyl-methylbenzenes	120	3.63	1	
iso-propyl-4-methylbenzene	134	4.10	2	
butylbenzenes	134	4.12	2	
tetramethylbenzenes	134	4.01	2	
tetralin	132	3.83	2	
diphenylmethane	168	4.14	2	
naphthalene	128	3.37	2	
C1-naphthalenes	142	3.87	2	
C2-naphthalenes	156	4.37	2	
C3-naphthalenes	170	5.00	3	
C4-naphthalenes	185	5.55	3	
acenaphthylene	152	4.07	3	
acenaphthene	154	3.92	3	
biphenyls	154	3.9	2	
dibenzofuran	168	4.31	3	
Fluorene	166	4.18	3	
C1-fluorenes	181	4.97	3	
C2-fluorenes	196	5.20	3	
C3-fluorenes	211	5.50	3	
anthracene	178	4.54	3	
phenanthrene	178	4.57	3	
C1-phenanthrenes/anthracenes	192	5.14	3	
C2-phenanthrenes/anthracenes	207	5.25	3	
C3-phenanthrenes/anthracenes	222	**6.00**	4	
C4-phenanthrenes/anthracenes	237	**6.51**	4	
dibenzothiophene	184	4.49	3	
C1-dibenzothiophene	199	4.86	3	
C2-dibenzothiophene	214	5.50	3	
C3-dibenzothiophene	228	**5.73**	4	
fluoranthene	202	5.22	3	
pyrene	202	5.18	3	

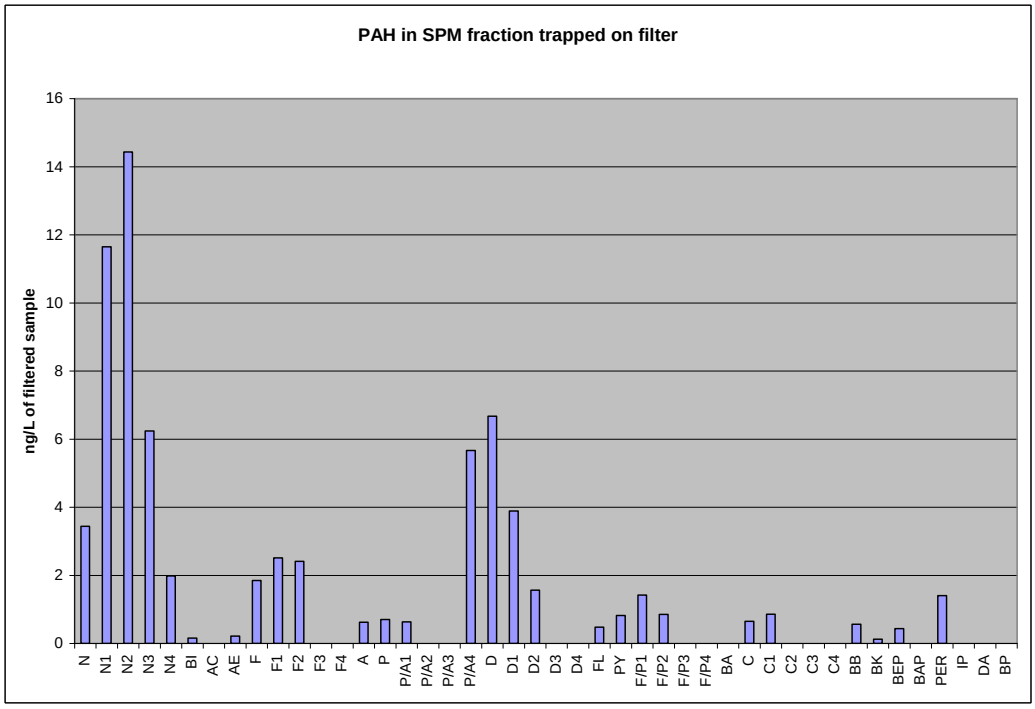

Figure 63 PAH profile from suspended intertidal sediment load trapped on 0.7 µm glass fiber filter after 4 days of equilibrium partitioning.

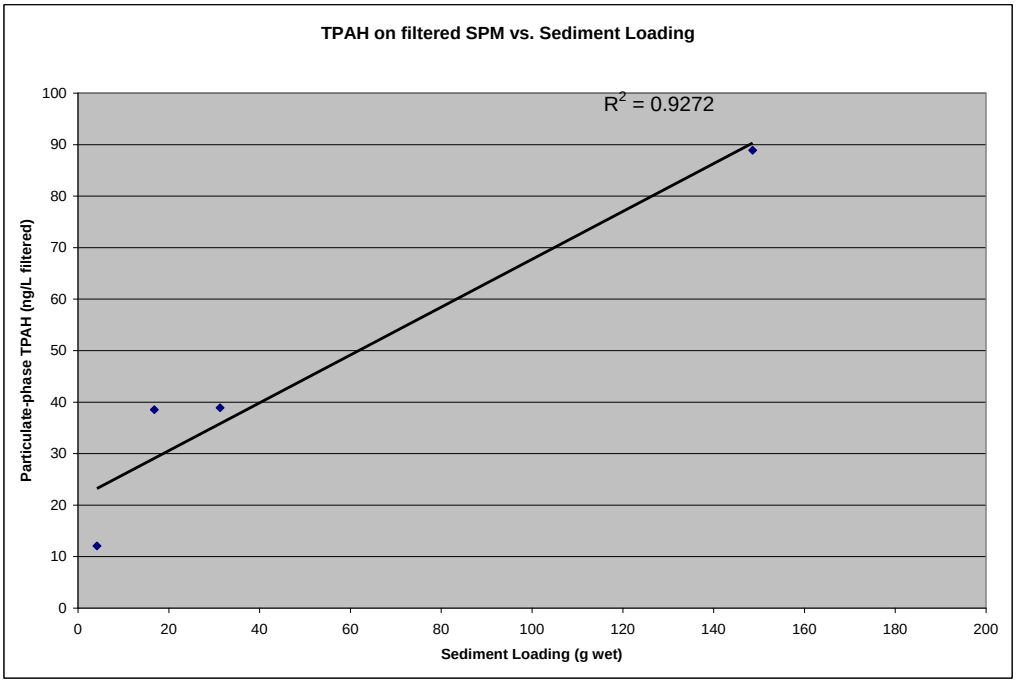

Figure 64 TPAH on suspended sediment trapped on 0.7-µm glass fiber filter vs. initial intertidal sediment loading (g wet) added to the bottled seawater.

pattern observed in many of the mussel samples examined in the LTEMP effort to date, could be derived from selective partitioning and dissolution of lower-molecular weight PAH from natural suspended particulate material introduced from glacial and riverine erosion of PAH-laden terrestrial sediments surrounding the region.

But if the plume of coastal sediments is leaching dissolved phase PAHs, why don't the sediments have the typical water-washed pattern with decreased naphthalenes, etc.? The lack of the water-washed profile is likely due to the nature of the leaching process itself. We postulate that the leaching of the water soluble constituents would be limited to the outer-most surface of the suspended particulate material, as migration of these PAH (which are themselves solids under most environmental conditions) from inside the sediment particles would be diffusion controlled within the solid phase. As such, only the thinnest outside surface of each particulate fragment would be subject to aqueous leaching. This would be analogous to the initial dissolution of the outside color coating on an M&M® candy, except in the case of the candy the inside chocolate also eventually gets dissolved. Given the current state-of-the-art in analytical chemistry, it is almost impossible to measure this outside surface of suspended sedimentary material without picking up or entraining some of the inside of each particle where higher concentrations of non-leached PAH would reside. So measuring the effect on fine SPM has eluded our efforts to date. On the other hand, when a bulk sediment sample is subject to chemical analyses in the laboratory, it is extracted with methylene chloride (a much more aggressive solvent for removing hydrocarbons compared to seawater), and sonication is used to further break up the sample and provide solvent access to the interstices, cracks, and fissures within the sediment matrix. The resultant extract contains a mixture of PAH that reflects the entire sample, and any evidence of leaching from the outside particle surfaces would be masked by the bulk of the PAH signal from the interior of the particles.

In an analogous sense, we struggled for years to document this phenomenon of enhanced evaporation and dissolution behavior from the outside surface of tarballs and oil droplets with diffusion controlled liberation of materials from the interior of such matrices (Payne et al., 1991). It was only after a –30 degree Centigrade cold room incident where oil was spread out as a thin wedge from < 1 mm to approximately 1 cm in thickness on a slab of sea ice inclined at a 20 degree angle that we were able to accurately document evaporation weathering as a function of oil-film thickness. Prior to that, all attempts to sample oil droplets or tarballs as a function of depth met with failure in our efforts to quantify diffusion controlled behavior within the oil phase.

Conclusions

The monotonic increase in dissolved-phase naphthalene, C1-naphthalene, and biphenyl concentrations as the suspended sediment load and concomitant PAH exposure was increased suggests that the sediments themselves were the source of these three more water-soluble PAH in the filtered seawater extracts. Then, as the log K_{ow} increases for

higher molecular weight PAH, the suspended sediment acts as a scavenger or sink for the previously existing trace-level dissolved- and particulate-phase PAH, and they are removed with the particulate-phase trapped by filtration.

This examination of the partitioning behavior was only intended as a scoping experiment, and longer periods of equilibration with different sediment types and other possible particulate sources (airborne particulate soot, smoke, dust, etc.) may provide additional insight on the phenomena and an opportunity to estimate mass balances. Longer SPM/seawater partitioning times, varying total organic carbon loading, and varying particulate size ranges and number densities may provide data on the partitioning behavior for the higher-alkylated naphthalenes and fluorenes observed in the LTEMP mussel tissues but not liberated into the dissolved-phase in this four-day experiment. Clearly, these data support the hypothesis that sedimentary materials previously believed to only contain sequestered and non-bioavailable PAH, may in fact be contributing to the ubiquitous dissolved-phase signals observed throughout Prince William Sound, but additional work should be completed to expand these observations to other conditions.

References

American Chemical Society (ACS) 1997. The mechanisms and effects of resistant sorption processes of organic compounds in natural particles. Special issue of *Environmental Toxicology and Chemistry* 18(8) 1999.

Boehm, P.D., D.S. Page, W.A. Burns, A.E. Bence, P.J. Mankiewicz and J.S. Brown, 2001. Resolving the origin of the petrogenic hydrocarbon background in Prince William Sound, Alaska, *Environmental Science and Technology*, 35(3): 471-479.

French-McCay, D.P. 2001. Development and application of an oil toxicity and exposure model, OilToxEx. Report prepared for the National Oceanic and Atmospheric Administration, Damage Assessment Center. National Oceanic and Atmospheric Administration, Silver Spring, Maryland.

French-McCay, D.P. 2002. Development and application of an oil toxicity and exposure model, OilToxEx. *Journal of Environmental Toxicology and Chemistry* 21:2080-2094.

Karinen, J.F., M.M. Babcock, E.W. Brown, W.D. MacLeod, Jr., L.R. Ramos, and J.W. Short. 1993. Hydrocarbons in intertidal sediments and mussels from Prince William Sound, Alaska, 1977-1980: characterization and probable sources. NOAA (National Oceanic and Atmospheric Administration) Technical Memorandum NMFS (National Marine Fisheries Service) AFSC-9, Seattle.

Lee, L.S., M. Hagwall, J.J. Delfino, and P.S.C. Rao, 1992. Partitioning of polycyclic aromatic hydrocarbons from diesel fuel into water, *Environmental Science and Technology* 26: 2104-2110.

Mackay, D., W.Y. Shiu, and K.C. Ma, 1992a. Illustrated Handbook of Physical-Chemical Properties and Environmental Fate for Organic Chemicals, Vol. I, Monoaromatic Hydrocarbons, Chlorobenzenes, and PCBs. Lewis Publ., Chelsea, Michigan, 668p.

Mackay, D., W.Y. Shiu, and K.C. Ma, 1992b. Illustrated Handbook of Physical-Chemical Properties and Environmental Fate for Organic Chemicals, Vol. II, Polynuclear Aromatic Hydrocarbons, Polychlorinated Dioxins, and Dibenzofurans. Lewis Publ., Chelsea, Michigan, 566p.

Page, D., P.D. Boehm, G.S. Douglas, and A.E. Bence. 1993. The natural petroleum hydrocarbon background in subtidal sediments of Prince William Sound, Alaska. Abstract #089 in Ecological Risk Assessment: Lessons Learned. 14th Annual Meeting, Society of Environmental Toxicology and Chemistry (SETAC) 14-18 November 1993, Houston, TX.

Page, D.S., P.D. Boehm, G.S. Douglas, and A.E. Bence. 1995. Identification of hydrocarbon sources in the benthic sediments of Prince William Sound and the Gulf of Alaska following the *Exxon Valdez* oil spill. Pages 41- 83 in Exxon Valdez Oil Spill: Fate and Effects in Alaskan Waters, ASTM STP 1219, Peter G. Wells, James N. Butler, and Jane S. Hughes, Eds., American Society for Testing and Materials, Philadelphia.

Payne, J.R., G.D. McNabb, Jr., and J.R. Clayton, Jr. Oil-weathering behavior in arctic environments. *Polar Research* 10(2), 631-662 (1991).

Payne, J.R., T.J. Reilly, and D.P. French. 1999. Fabrication of a portable large-volume water sampling system to support oil spill NRDA efforts. Proceedings of the 1999 Oil Spill Conference, American Petroleum Institute, Washington, D.C., 1179-1184.

Payne, J.R., J.R. Clayton, Jr., and B.E. Kirstein. 2003. Oil/suspended particulate material interactions and sedimentation. *Spill Science & Technology Bulletin*, 8(2): 201-221.

Payne, J.R., W.B. Driskell, M.R. Lindeberg, W. Fournier, M.L. Larsen, J.W. Short, S.D. Rice, and D. Janka. 2005a. Dissolved- and particulate-phase hydrocarbons in interstitial water from Prince William Sound beaches containing buried oil thirteen years after the *Exxon Valdez* Oil Spill. Prepared for National Oceanic and Atmospheric Administration, National Marine Fisheries Service, Auke Bay, AK, February 7, 2005.

Payne, J.R. and W.B. Driskell, M.R. Lindeberg, W. Fournier, M.L. Larsen, J.W. Short, S.D. Rice, and D. Janka. 2005b. Dissolved- and Particulate-Phase Hydrocarbons in Interstitial Water from Prince William Sound Beaches Containing Buried Oil Thirteen Years After the *Exxon Valdez* Oil Spill, Proceedings of the 2005 International Oil Spill Conference, American Petroleum Institute, Washington, D.C., pp. 83-88.

Payne, J.R., W.B. Driskell, J.W. Short, M.L. Larsen. 2008a. Long term monitoring for oil in the *Exxon Valdez* spill region. *Marine Pollution Bulletin* 56:2067-2081.

Payne, James R., William B. Driskell, Jeffrey W. Short, Marie L. Larsen. 2008b. Final 2005-2006 LTEMP Oil Monitoring Report, *Exxon Valdez* Oil Spill Restoration Project Final Report (Restoration Project 050763), Prince William Sound Regional Citizen's Advisory Council, Anchorage, Alaska. 137 pp.

Short, J.W. and M.M. Babcock. 1996. Prespill and postspill concentrations of hydrocarbons in mussels and sediments in Prince William Sound. Pages 149-166 *in* S.D. Rice, R.B. Spies, D.A. Wolfe, and B.A. Wright (editors). Proceedings of the *Exxon Valdez* oil spill Symposium. American Fisheries Society Symposium 18.

Short, J.W., K.A. Kvenvolden, P.R. Carlson, F.D. Hostettler, R.J. Rosenbauer and B.A. Wright. 1999. Natural hydrocarbon background in benthic sediments of Prince William Sound, Alaska: Oil vs. coal, *Environmental Science and Technology*, 33(1): 34-42.

Short, J.W., J.J. Kolak, J.R. Payne, G.K. Van Kooten. 2007. An evaluation of petrogenic hydrocarbons in northern Gulf of Alaska continental shelf sediments – The role of coastal oil seep inputs. *Organic Geochemistry* 38(4), pp. 643-670.

APPENDIX F Comparison of Selected Statistical Methods

This appendix comprises a review of analytic approaches to the project along with evaluating some exploratory methods to further understand the complete dataset. Most of the single-perspective indices used in early LTEMP reports (Table 10) and recently proposed by the SAC for upcoming reports contain only the sparsest of information useful for identifying oil signatures. Excepting our CRUDE index, they each regard a single characteristic of the signal that fails to provide the relevant discrimination for identifying an ANS-source sample (a prime objective of LTEMP). Furthermore, when we formulated the CRUDE index (combining the pertinent indices into a single value which would emphasize petrogenic sources), it was specifically to resolve our frustrations with the mental gymnastics of integrating multiple indices as an assessment approach. CRUDE accomplishes that goal in some fashion but still discards a lot of information about the signal pattern, including the ability to discriminate the source, i.e., a diesel spill will look similar to an ANS crude spill using just these indices.

Table 10 Single-perspective hydrocarbon indices used in early LTEMP reports.

Parameter	Relevance
TPAH (mussel tissue and sediments)	Total PAH as determined by high resolution GC/MS with quantification by selected ion monitoring; defined as the sum of 2 to 5-ring polycyclic aromatic hydrocarbons: Naphthalene + fluorene + dibenzothiophene + phenanthrene/anthracene + chrysene, and their alkyl homologues + other PAHs (excluding perylene); useful for determining TPAH contamination and the relative contribution of petrogenic, pyrogenic, and diagenic sources
FFPI	The fossil fuel pollution index is the ratio of fossil-derived PAH to TPAH and is defined as follows: FFPI = (N+F+P+D)/TPAH x 100, where: N (Naphthalene series) = C0-N + C1-N + C2-N + C3-N + C4-N F (Fluorene series) = C0-F + C1-F + C2-F + C3-F P (Phenanthrene/Anthracene series) = C0-A + C0-P + C1-P + C2-P + C3-P + C4-P D (Dibenzothiophene series) = C0-D + C1-D + C2-D + C3-D FFPI is near 100 for petrogenic PAH; FFPI for pyrogenic PAH is near 0 (Boehm and Farrington, 1984).
UCM (sediments)	Unresolved Complex Mixture – petroleum compounds represented by the GC-FID signal for total resolved peaks plus unresolved area minus the total area of the resolved peaks quantified with valley-to-valley baseline integration; a characteristic of some fresh oils and most weathered oils.
TSHC (sediments)	Total Saturated Hydrocarbons quantifies the total n-alkanes (n-C_{10} to n-C_{34}) + pristane and phytane; represents the total resolved hydrocarbons and unresolved complex mixture (UCM) as determined by high resolution gas chromatography with flame ionization detection (GC/FID); includes both petrogenic and biogenic sources.
Total resolved aliphatic hydrocarbons (TRAHC)	A mixture of hydrocarbons defined and undefined by gas chromatographic techniques, that represents the total resolved area of the GC run determined by valley-to-valley baseline integration. Includes the AHC analyte list and other compounds.
CPI	The carbon preference index represents the relative amounts of odd and even chain alkanes within a specific boiling range and is defined as follows: CPI = 2(C27+C29)/(C26+2C28+C30) Odd and even numbered n-alkanes are equally abundant in petroleum but have an odd numbered preference in biological material; a CPI close to 1 is an indication of petroleum and higher values indicate biogenic input (Farrington and Tripp, 1997).
CRUDE Index (sediments)	A summation of TPAH, TSHC and UCM weighted to assess the petrogenic fractions (derived from FFPI and CPI indices) (Payne et al., 1998). $CRUDE = (TPAH \times FFPI/100) + (TSHC/CPI^2) + UCM$

So, for heuristic purposes, let's examine a couple of data sets using the these indices. Below are the index plots for Gold Creek, selected especially for the diesel spill event detected in Oct 2004, and Disk Island, selected for its on-going trace contamination from residual EVOS oil.

For those readers familiar with Gold Creek history, early spill events such as the *T/V Eastern Lion* oil spill in May 1994 and the BWTF spill/sheening event in January 1997 precede the plotted time series (Figure 65) but there are spikes in July 1999 and Oct 2001 that similarly reflect elevated PAH levels at AMT (mostly due to fluorine anomalies from the lab). The most visible *confirmed* event is the diesel spill in Oct 2004. These events exemplify the ambiguity of reporting just indices. In July 1999, when a weathered ANS oil signal was present (albeit exaggerated by lab issues), there was no confirming UCM, the SHC was tainted by lipid interference, FFPI was static, CPI was uninformative, and therefore, CRUDE barely blipped. In Oct 2004, the diesel spill tripped three of the five indices and thus, also spiked on the CRUDE index. But without examining the samples' actual PAH patterns, the source would not be identified.

From Disk Island (Figure 66), where a persistent trace of residual EVOS oil still leaks from the sediments, the signal, according to these indices, is enigmatic. Simply examining these values would never reveal the true source or scenario.

Rather than using the generic indices which only suggest the presence of oil, other indices can be used to match samples to known oils. Most common are double-ratio plots using homologue ratios of phenanthrene to dibenzothiophene and, more specifically, D2/P2 and D3/P3. Because these two compounds tend to weather at similar rates, the ratios tend to remain stable within a linear range. In the following D/P plot of Disk Island samples (Figure 67), recent samples tend to remain within a linear (weathering) group extending from the origin towards the upper right. The few pre-2002 samples tend to form in an outlier pattern intersecting from the upper left to lower right and clustered near the origin. The timing may suggest a delayed appearance of the oil signal at Disk and/or analytic issues. Although ratio conformation is not an absolute validation, a sample with ratio values falling with the range strongly suggests a matching signal. To increase certainty of matching, a suite of various conservative double ratios may be used. We've used this as one approach for damage assessment proceedings for the 2008 *Cosco Busan* spill in San Francisco.

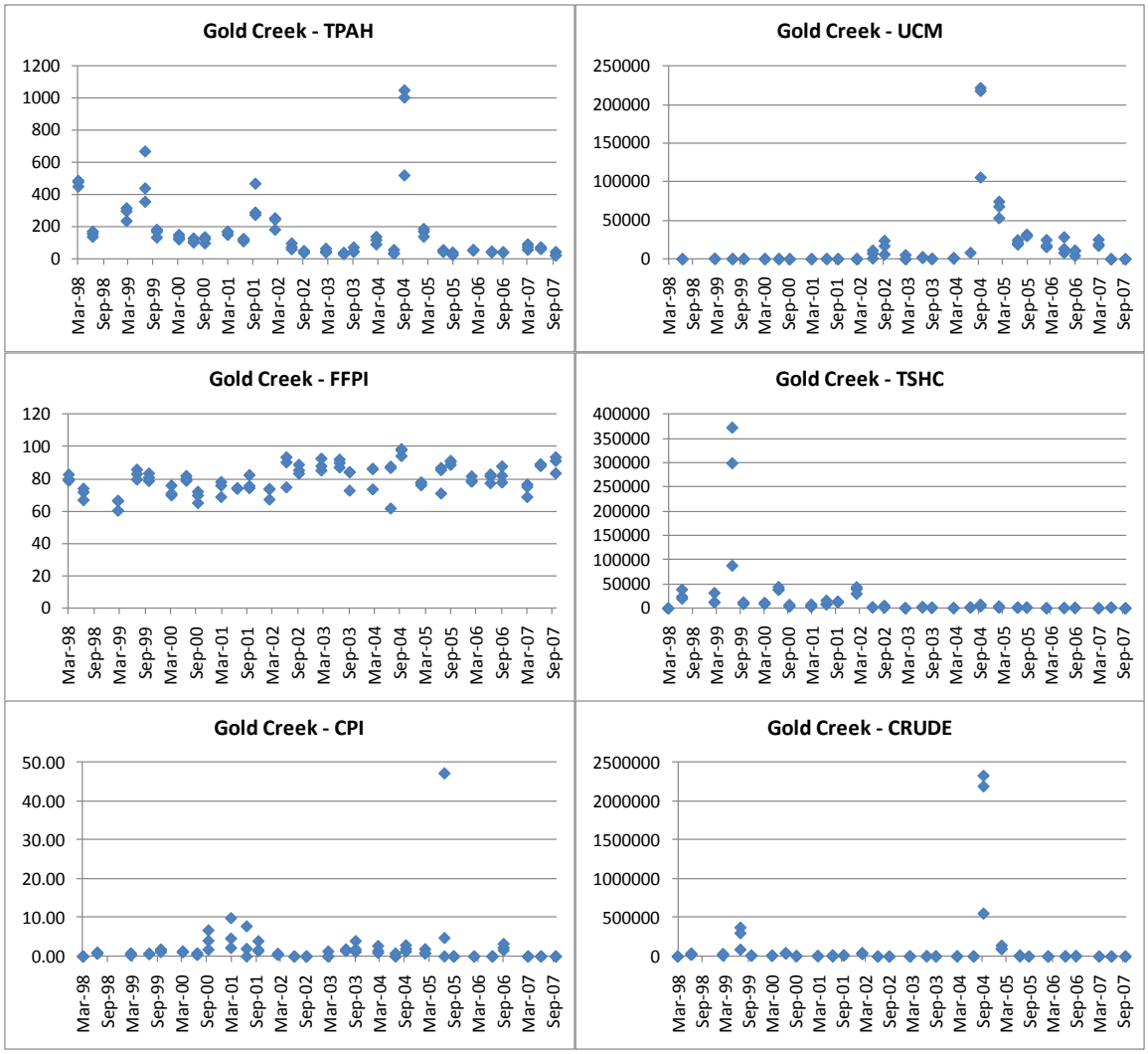

Figure 65 Time series of summary indices from Gold Creek mussels, 1998-2007.

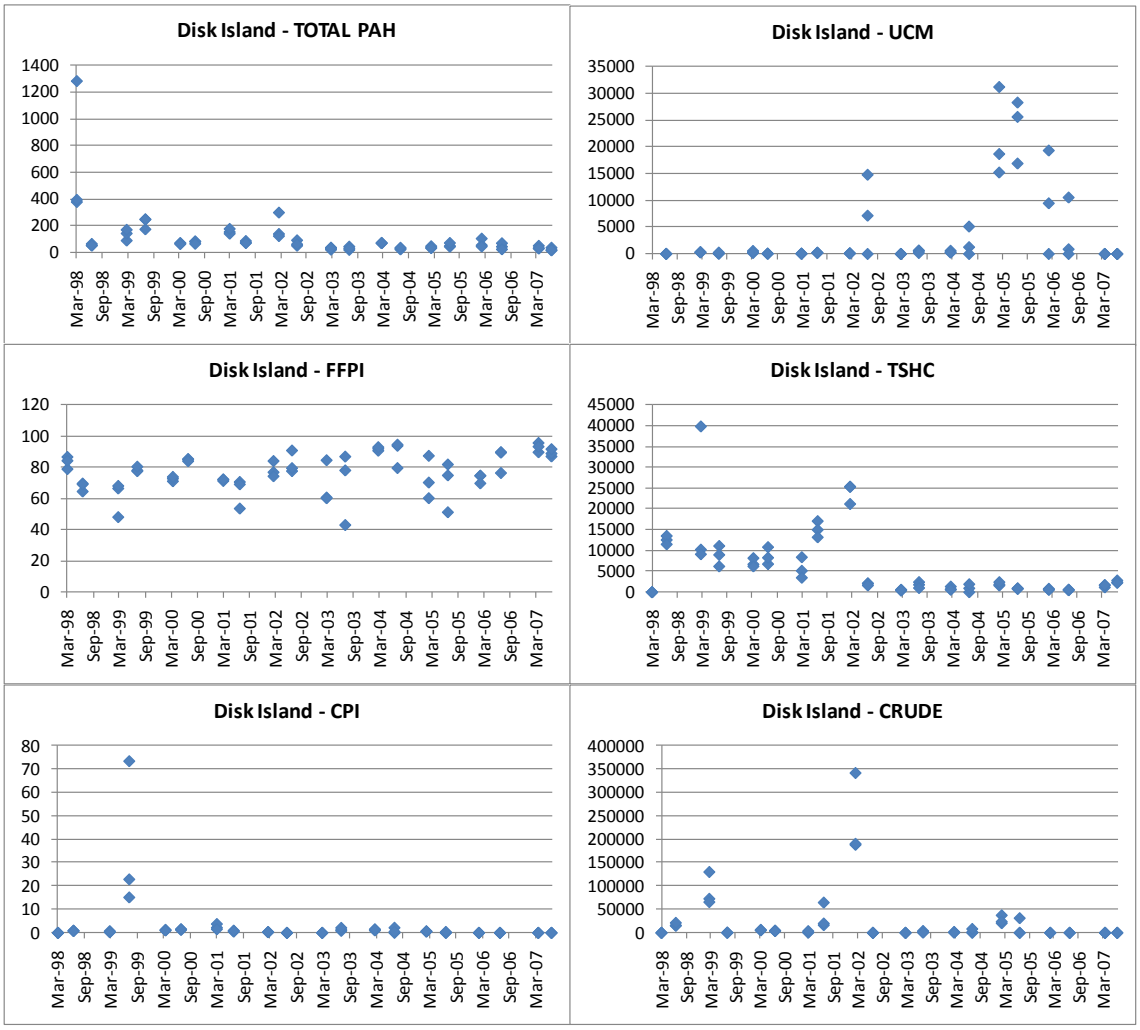

Figure 66 Time series of summary indices from Disk Island mussels, 1998-2007.

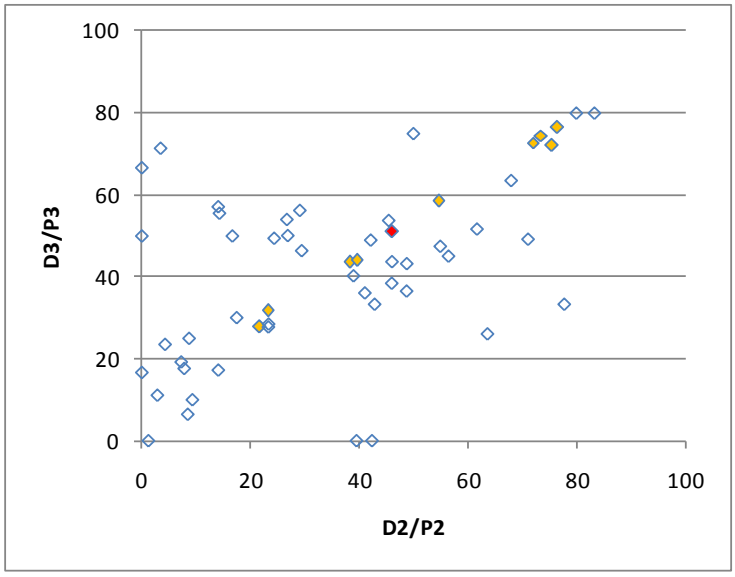

Figure 67 Double-ratio plot of Disk Island mussels, 1998-2007. Red symbol represents ANS reference oil, gold for 2005-07 samples.

During our work on the *New Carissa* spill (Payne and Driskell, 2001), we identified a dissolved-phase, spill-source signal in some species but not others based on their feeding modes (crabs vs. oysters). This was a breakthrough in injury assessment, to be able to identify and attribute exposure from a dissolved rather than just the whole oil signal. As a result, we later developed and published a phase-assignment algorithm (partially described in section 4.7.1, pg 19) and began to use it with some success on LTEMP data. Summarizing our LTEMP findings since 2002, the data are mostly comprised of low level concentrations usually of a dissolved-phase signal and likely representing chronic background contamination. In one sense, this statement alone would be sufficient to meet the goals of the LTEMP program. However, there is still more information left on the table. As we examined the data series, it became apparent that there were synchronous regional trends. We began to track these using various correlation and regression techniques. But as the signal has diminished into ultra-trace levels, the phase algorithm has become sensitive to small variations in the signal. For example, a tissue sample with TPAH with less than 20 ng/g dry weight may easily flip between being reported as fully dissolved or fully particulate based on 1 ng difference in a naphthalene homologue. Since 1 ng could easily be within analytic error, there is high uncertainty with these marginal assignments at the ultra-trace concentrations currently being measured.

In exploring the algorithm's sensitivity, we tried alternative methods of calculating each site's average phase assignments. Traditionally, we have averaged the phases after they have been calculated for each triplicate sample at a given site. Thus, if one sample were reported as primarily dissolved and the other two replicates were primarily particulate, the average would be somewhat particulate, i.e., the mean of the portions. But another approach would be to first combine or average the replicate data and then calculate the

phases, a statistically acceptable approach but one that may cause problems by hybridizing disparate profiles. One combining method would be to simply average the individual PAH concentrations (ng/g dry weight) from each sample (equivalent to mass compositing 3 samples) and then calculate the phases. For a second method, each PAH analyte would be standardized to the sample's total PAH (TPAH for just the constituents of interest) and then averaged and phase calculated, i.e., averaging the signals rather than the individual component concentrations.

If all three replicates had similar patterns, it follows that the phase results of each method would be similar. In effect, the second method, compositing individual PAH concentrations for all three replicates, gives statistical weight to the highest concentration replicate. The third method eliminates the concentration bias but blends potentially disparate profiles into a mixed-hybrid profile. The traditional method (utilized in this and our previous reports) emphasizes the uniqueness of each profile and their phases. None of the methods are "incorrect," just different. We are particularly interested in comparing the traditional approach to the TPAH-standardized (3^{rd}) method because it tends to desensitize the algorithm to the small critical differences in individual component (e.g., N1, N2 and N3) concentrations.

As mentioned above, the more similar the patterns between replicates, the less will be the difference in the results from the three methods. Applying these methods and looking at just the dissolved phase assignments in the LTEMP data, we see a range of effects (Figure 68). The overlaid results from Knowles Head show very little difference (excepting July 04) in contrast to several samples at Gold Creek in the 2003-05 period. Again, there is no "right" answer or "right" way to calculate phase assignments, only different perspectives on the data. For future analyses, we would favor both the phase average and TPAH standardized average methods to address our questions. We would also tend to avoid classifying low concentration samples where the algorithm is sensitive to small absolute differences in individual component concentrations.

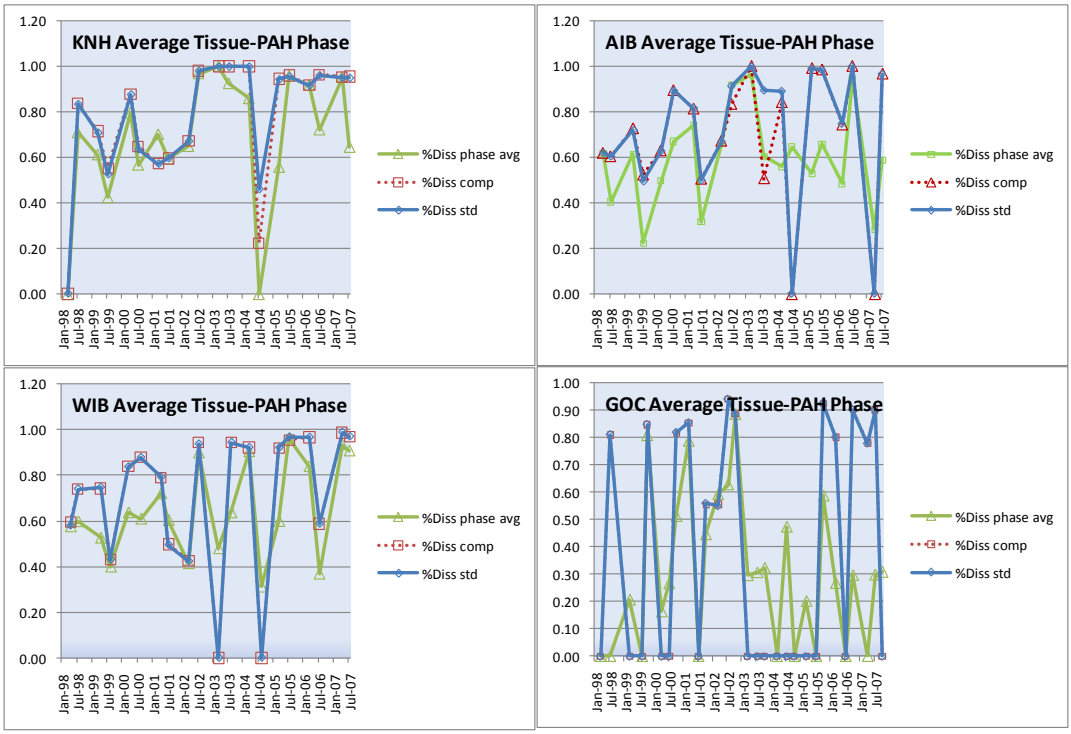

Figure 68 Comparison of dissolved phase assignments for selected stations using three methods for combining triplicate samples. Green = traditional average of individual sample phase assignments; Red = raw average of individual component concentrations; Blue = average of the normalized individual component contributions to the TPAH.

Although LTEMP phase patterns had greatly boosted our understanding of oil transport and exposure, we have still relied on directly evaluating each sample's signature to assess their similarities and sources. This year, we explored using a multivariate statistical approach (PCA or MDS) in which more information about the signal is incorporated into the parameter set. The utility of introducing multivariates at this point in the program is that the signals, being from indeterminate sources, are not always easily qualified into patterns or trends. Furthermore, multivariate methods present an overview of the entire data set (or data subsets) looking at all the information (rather than just a single-characteristic index) and reducing the commonalities into smaller dimensions (factors).

One statistical dead end we have seen in other oil-PCA analyses that we wanted to avoid, was simply plugging in the raw data and letting the model establish irrelevant, unintelligible groupings. Since we were mainly interested in the subtleties of signal patterns rather than concentrations or dominance of individual analytes, the data were converted to the relative proportion of each homologue within their respective PAH groups. This later step included various attempts to discriminate the relative analyte proportions between and within PAH "families" (N, F, P, D, FP, C), factors that we know to be germane to oil patterns. Thus, we worked with a subset of TPAH, excluding various minor non-alkylated PAH and the 5-6 ringed pyrogenic compounds. This approach begins to mimic the expert judgment of forensic pattern analysis.

The resulting 3-D plots are then examined in an exploratory mode for correlations with other parameters (e.g., station, date, phase, TPAH, region, etc.) to tease out relevant patterns. For this exercise, the data manipulation was done in Excel, the PCA was run with XLSTAT software and the results examined using Miner3D to visually explore data groupings against various parameters. Associated individual PCA data points (samples) were then polled for the analytes determining group affinities, i.e., the most relevant factors. For additional validation, we ran the dataset through PATN software using a hybrid MDS-style model.

We are aware of other multivariate methods, e.g., canonical correspondence analysis, which accomplishes a similar task but we felt we should first understand the data set and its weaknesses before subjecting it to higher statistical horsepower. In the end, although multivariate techniques are very efficient in clustering similar samples for discerning patterns and differences, it still requires expert knowledge to translate the patterns back to the data set to interpret the common profiles and assign probable sources and effects.

In viewing each of LTEMP's three regional data groupings (PWS, GOA and Port Valdez), a couple of points become obvious. The shifts noted in TPAH and phase plots are also nicely reflected in the three-dimensional, PCA factor plots. Secondly, the suggestion of synchrony between certain sites at certain times (discussed above) also appears in the multivariate placements (plot groupings). In Port Valdez, there are loose seasonal groupings of samples as suggested in the phase plots. Finally, even after discarding the anomalous fluorine data from pre-2002, there is still indication of systematic analytic differences between the contract labs.

Looking at just the six PWS stations (Figure 69, Figure 70, and Figure 71), the samples generally intermix except for the Disk samples (dark green in Figure 69) spreading out along the F2 axis. These samples, of course, reflect the trace EVOS particulate signal while the other stations have become more dissolved in character. In the next figure from the same PCA run but color coded for sampling dates, samplings from pre-2002 (blue and dark green) strongly cluster behind the post-2002 samplings (mostly hidden here in Figure 70). This positioning reflects both the differences in analytic labs and possibly, continued transitions in the environmental signals. The final data representation (Figure 71) depicts corroboration of the phase assignments; samples on the right "branch" of the cluster are more dissolved (red) than on the left (i.e., the Disk Island particulate EVOS signal).

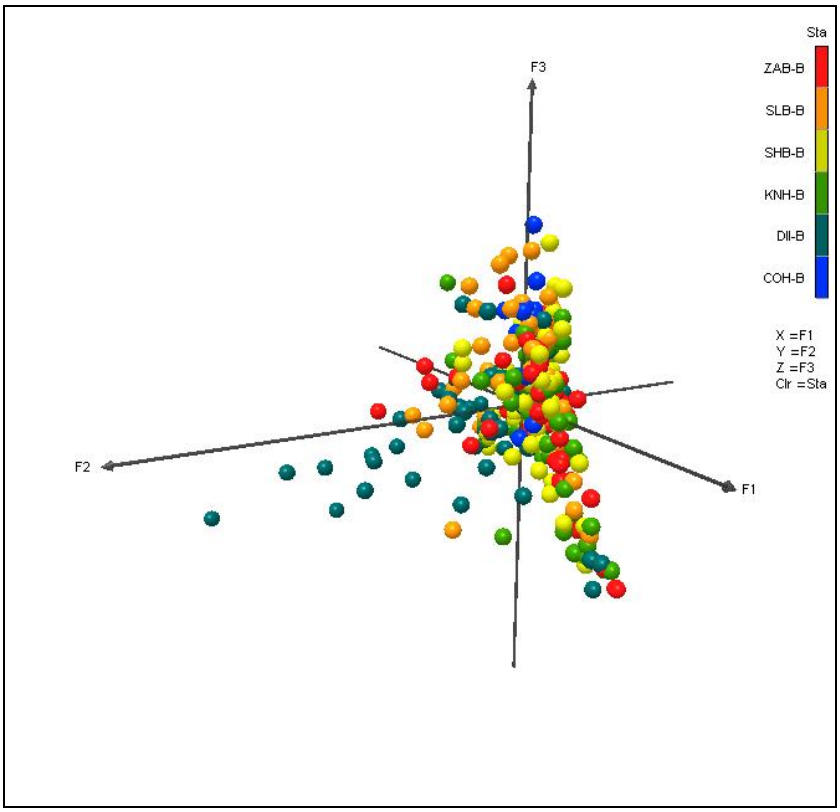

Figure 69 Three dimensional PCA plots of PWS stations highlighting clustering by stations.

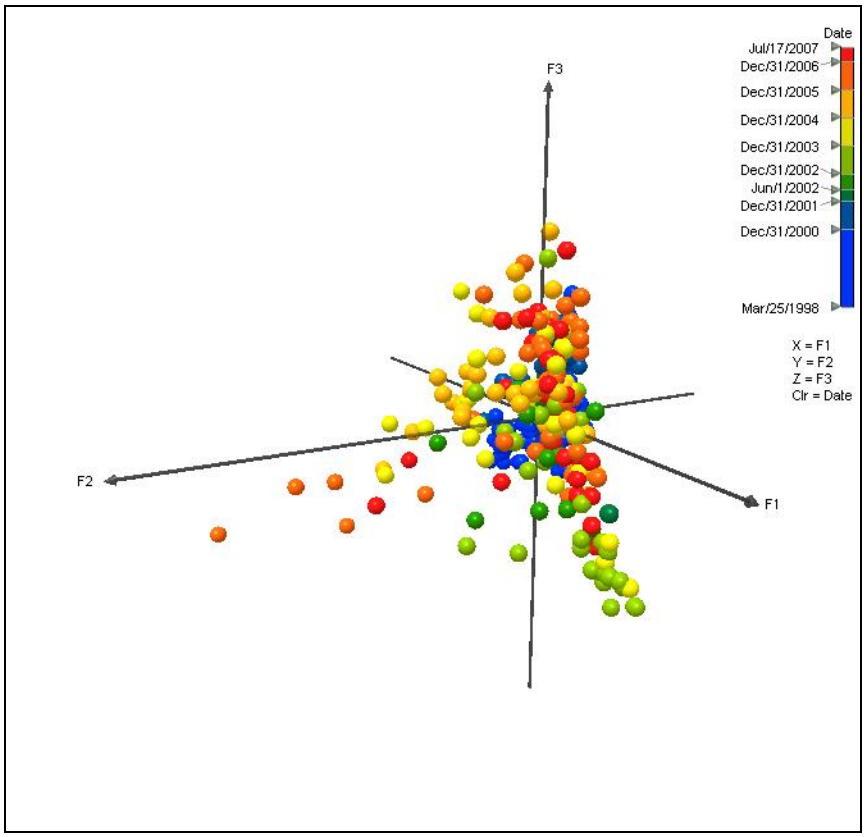

Figure 70 Three dimensional PCA plots of PWS stations highlighting clustering by collection date.

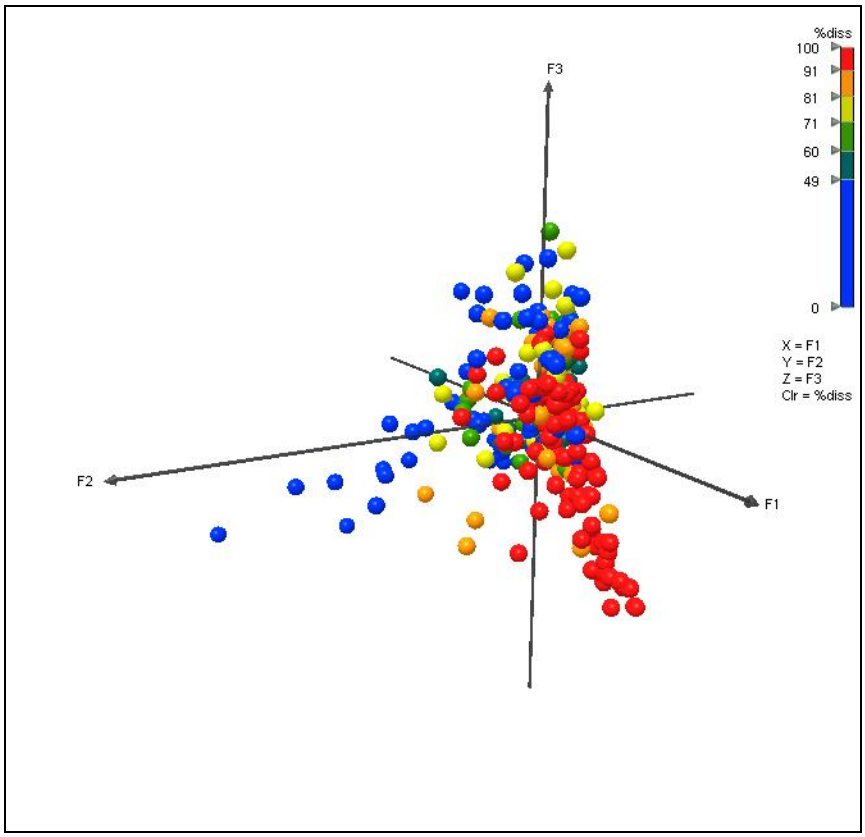

Figure 71 Three dimensional PCA plots of PWS stations highlighting clustering by dissolved-phase portion.

After spending some effort on this multivariate approach, we attempted to validate the trends by looking at underlying pattern similarities for the data groupings to sort out exactly what was driving the groupings. To our disappointment, although the overall multivariate patterns nicely portray what we know and expected about the samples and trends, the PCA had discriminated on analyte differences that expert knowledge would consider less relevant, differences we would ignore or consider less important than obvious patterns suggesting weathering or discriminating sources. We noted this same flaw in work of other EVOS chemistry researchers where the statistical approach was blind to the underlying processes. We ran some additional analyses incorporating other clever data transforms and manipulations but were unable to create a dataset whereby the analysis would discriminate primarily on components germane to the known physical processes. Realizing the approach would take much greater development effort and was beyond the scope of this project, we shelved the task without reaching a conclusive model.

In summary, other than TPAH, we find little to no utility in the single-characteristic indices tabled above. At best, they only produce summary totals or suggest whether a signal may be petrogenic. Since historically, the LTEMP program has only seen particulate ANS oil, diesel, and unknown dissolved or pyrogenic signals, the current analytic methods (double ratio plots, phase assignments, and eventually, multivariates)

incorporate significantly more information and are much better at identifying and tracking these sources. And, as much as we would all like to simplify, automate and "objectify" the process, all of these statistical methods merely assist in classifying the samples; the final interpretation falls ultimately to expert pattern recognition.

APPENDIX G Human Habitation Sites Occupied as part of the EVOS Trustees SCAT VI and VII Programs

Under the auspices of the EVOS Trustees Program, Long-term Monitoring of Anthropogenic Hydrocarbons in the *Exxon Valdez* Oil Spill Region (050763), ten intertidal sites within the Naked-Knight-Southwest Island complex were examined during the 2005 summer program to measure the extent of buried oil still present 16 years after the spill. At EVOS sites previously designated as heavily oiled, a number of random-stratified pits were dug to a depth of ~0.5 m to look for residual oil. Where available, mussels were also collected. Sediments and mussels were analyzed using LTEMP analytical protocols. The results have been published (Short et al., 2007a) and a separate analysis will be reported by Dr. Jeffrey Short for this survey plus the continuation studies completed in 2006 and 2007. As part of PWSRCAC efforts, PAH and SHC sample profiles for the 2005 mussels and sediments were included in Appendix E of the 2005/2006 report (Payne et al., 2008). Briefly, TPAH levels in the oiled pits ranged from a low of 42 ng/g (on Knight Island) to a high of 567,000 ng/g (on Latouche Island) with the buried oil showing varying states of weathering (from extensively degraded to very fresh). The mussel samples collected from these same beaches (but not necessarily immediately adjacent to the oiled pits) showed low (11 to 42 ng/g dry weight) dissolved-phase TPAH signals very similar to those observed at the traditional LTEMP stations but dissimilar to the buried oil. Although there were still persistent buried EVOS residues at a number of the beaches, they are highly sequestered and do not appear to be bioavailable unless disturbed. Rates of disappearance have diminished to an estimated 4% yr^{-1}. If left undisturbed, Short et al. predict they will be there for decades.

During the LTEMP 2006/2007 and 2007/2008 project years, the EVOS Trustees component of the summer field efforts included excavation of stratified random pits at eleven current or past human habitation sites at the stations identified below (Table 11).

Table 11 Human habitation station locations for the 2006/2007 SCAT VI & VII surveys.

Location	EVOS Segment Number	length	Lat (NAD 27)	Long (NAD 27)
Thumb bay	4	100	60.206044	147.818671
Sawmill bay	27	100	60.056975	148.054013
Latouche	32	100	60.061845	147.891803
Latouche	26	100	60.061845	147.891803
Sawmill bay	40	100	60.060235	148.045645
Latouche	3	100	60.061845	147.891803
Sawmill bay	72	100	60.069952	148.003354
Sawmill bay	45	100	60.063089	148.037465
Sawmill bay	47	100	60.063619	148.034187
Latouche	23	100	60.061845	147.891803
Barnes cove	2	100	60.312488	147.780959

During the 2006 summer program stations were completed at Sawmill Bay (Crab Bay EV 72), Latouche Island (LA 26); Latouche Island (LA 32); Sawmill Bay (EV40); Sawmill Bay (EV45); and Sawmill Bay (EV47). During the 2007 summer program, stations were re-occupied at Sawmill Bay (EV40, EV45, and EV72) due to a sighting error in 2006, and new stations were completed at Barns Cove (EV2); Latouche (EV3 and EV23); and Thumb Bay (EV4). No visual evidence of any buried oil was observed in any of the 50 pits dug at each of the sites examined in the 2006 and 2007 field programs. Additional interpretations of these activities will be reported by Dr. Short.